Characterization of stripe rust resistance and yield-related traits in an ‘Overley’ x ‘Overland’ population

by

Wardah K. Mustahsan

B.S., Xavier University of Louisiana, 2013
M.S., Texas A&M University, 2018

AN ABSTRACT OF A DISSERTATION

submitted in partial fulfillment of the requirements for the degree

DOCTOR OF PHILOSOPHY

Department of Agronomy
College of Agriculture

KANSAS STATE UNIVERSITY
Manhattan, Kansas

2022

Abstract

Wheat is a vital cereal crop, providing 20 % of the daily nutritional requirements for consumers worldwide. Although there has been a substantial increase in production and yield gains, food demands will still be on the rise in future decades, and wheat yields must continue to increase rapidly to meet these demands. Grain yield can be inhibited by biotic factors (pathogens), which require the development of resistant varieties against pathogens. Stripe (yellow) rust produces massive yield losses in wheat production, and ample resistance against stripe rust is achieved by pyramiding multiple resistant genes together. Yield also can be improved by characterizing the underlying mechanisms that define yield and yield-related traits. We used breeding technology tools to dissect the genetic architecture of yield-related traits, yield, and stripe rust resistance to identify genomic regions that can improve these traits in wheat germplasm and broaden the genetic resources available for breeders to develop robust breeding germplasm that can improve the profitability and resilience of wheat production.

Stripe (yellow) rust, caused by *Puccinia striiformis* (*Pst*), is a devastating disease of wheat worldwide. In commercial production, stripe rust reduces forage yield, grain yield and grain quality. Yield losses caused by stripe rust range from 10% to 70%. This study was conducted using two different wheat reference genomes (IWGSC v2.1(‘Chinese Spring’) and ‘Jagger’) to identify quantitative trait loci (QTL) associated with adult plant field resistance to stripe rust in the hard winter wheat RIL population, ‘Overley’ x ‘Overland’ to provide breeders with identified genomic regions associated with quantitative field resistance. Our QTL analysis identified genomic regions on 2AS ($2N^{v}S$ translocation), 2BS, 2BL, and 2DL using two different mapping methods (Inclusive Composite Interval Mapping and Multi-Environmental Trial Analysis) that were associated with stripe rust resistance for both infection type and severity

using genetic maps from both genomes. There were no meaningful differences in interpreting the data from the two maps. Overley contributed the resistance alleles at the 2AS and 2BL QTLs. Overland contributed the resistance alleles at the 2BS and 2DL QTLs. The 2DL QTL (*QYr.hwwg-2D)* will be further refined due its environmental stability for resistance. We designed PCR-based SNP marker assays to efficiently identify these genomic regions in breeding populations.

Yield improvement can be facilitated by a deeper understanding of the underlying infrastructure of components that determine grain yield. We performed a QTL analysis on the population Overley x Overland, to identify genomic regions in our population can explain the variation in yield and its components in field trials using the two different reference maps. We identified major QTLs in both reference maps for yield (3BL), single kernel weight (4AL), plant height (6AS), grains per spike (4AL), thousand grain weight (4AL), and physiological maturity (2BS). The Jagger map identified more QTLs (40 QTLs) than the IWGSCv2.1 map (30 QTLs). The future direction of these studies will be marker development to utilize these QTLs in yield-improvement breeding programs.

Characterization of stripe rust resistance and yield-related traits in an ‘Overley’ x ‘Overland’ population

by
Wardah K. Mustahsan

B.S., Xavier University of Louisiana, 2013
M.S., Texas A&M University, 2018

A DISSERTATION
submitted in partial fulfillment of the requirements for the degree

DOCTOR OF PHILOSOPHY

Department of Agronomy
College of Agriculture

KANSAS STATE UNIVERSITY
Manhattan, Kansas

2022

Approved by:

Co-Major Professor
Dr. Romullo Lollato

Approved by:

Co-Major Professor
Dr. Mary Guttieri

Copyright

Abstract

Wheat is a vital cereal crop, providing 20 % of the daily nutritional requirements for consumers worldwide. Although there has been a substantial increase in production and yield gains, food demands will still be on the rise in future decades, and wheat yields must continue to increase rapidly to meet these demands. Grain yield can be inhibited by biotic factors (pathogens), which require the development of resistant varieties against pathogens. Stripe (yellow) rust produces massive yield losses in wheat production, and ample resistance against stripe rust is achieved by pyramiding multiple resistant genes together. Yield also can be improved by characterizing the underlying mechanisms that define yield and yield-related traits. We used breeding technology tools to dissect the genetic architecture of yield-related traits, yield, and stripe rust resistance to identify genomic regions that can improve these traits in wheat germplasm and broaden the genetic resources available for breeders to develop robust breeding germplasm that can improve the profitability and resilience of wheat production.

Stripe (yellow) rust, caused by *Puccinia striiformis* (*Pst*), is a devastating disease of wheat worldwide. In commercial production, stripe rust reduces forage yield, grain yield and grain quality. Yield losses caused by stripe rust range from 10% to 70%. This study was conducted using two different wheat reference genomes (IWGSC v2.1(‘Chinese Spring’) and ‘Jagger’) to identify quantitative trait loci (QTL) associated with adult plant field resistance to stripe rust in the hard winter wheat RIL population, ‘Overley’ x ‘Overland’ to provide breeders with identified genomic regions associated with quantitative field resistance. Our QTL analysis identified genomic regions on 2AS (2N^{v}S translocation), 2BS, 2BL, and 2DL using two different mapping methods (Inclusive Composite Interval Mapping and Multi-Environmental Trial Analysis) that were associated with stripe rust resistance for both infection type and severity

using genetic maps from both genomes. There were no meaningful differences in interpreting the data from the two maps. Overley contributed the resistance alleles at the 2AS and 2BL QTLs. Overland contributed the resistance alleles at the 2BS and 2DL QTLs. The 2DL QTL (*QYr.hwwg-2D)* will be further refined due its environmental stability for resistance. We designed PCR-based SNP marker assays to efficiently identify these genomic regions in breeding populations.

Yield improvement can be facilitated by a deeper understanding of the underlying infrastructure of components that determine grain yield. We performed a QTL analysis on the population Overley x Overland, to identify genomic regions in our population can explain the variation in yield and its components in field trials using the two different reference maps. We identified major QTLs in both reference maps for yield (3BL), single kernel weight (4AL), plant height (6AS), grains per spike (4AL), thousand grain weight (4AL), and physiological maturity (2BS). The Jagger map identified more QTLs (40 QTLs) than the IWGSCv2.1 map (30 QTLs). The future direction of these studies will be marker development to utilize these QTLs in yield-improvement breeding programs.

Table of Contents

List of Figures

List of Tables

List of Abbreviations

Abbreviation	Description
CG	Candidate Gene
DPA	Days Post-Anthesis is
Eps	Earliness Per Se Gene
FT	Flowering Time Gene
FZP	Frizzy Panicle Gene
GWAS	Genome-wide Association Study
GA	Gibberellic Acid
GDM	Grain Diameter
GN	Grain Number
GN1	Grain Number Increase 1 Gene
GNS	Grain Number/Spike
GS	Grain Size
GWP	Grain Weight Potential
GWT	Grain Weight
GWS	Grain Weight per Spike
GY	Grain Yield
ICIM	Interval Composite Interval Mapping
LOD	Logarithmic Odds Ratio
LD	Long-Day
MTA	Marker Trait Association
MQTL	Meta Quantitative Trait Loci
MAGIC	Multiparent Advanced Generation Intercross
NIL	Near-Isogenic Line
PVE	Phenotypic Variation Explained
Ppd	Photoperiod Gene
PMAT	Physiological Maturity
PCD	Plant Cell Death
PHT	Plant Height
PRR	Pseudo-Response Regulator
QRC	QTL-rich Cluster
QTL	Quantitative Trait Loci
RIL	Recombinant Inbred Line
Rht	Reducing Height Gene
SD	Short-Day
SNP	Single Nucleotide Polymorphism
SN	Spike Number per square meter
SNS	Spikelet Number/Spike
TB	Teosinte Branched 1Gene
TGW	Thousand Grain Weight
TF	Transcription Factor
T6P	Trehalose-6-Phosphate
Vrn	Vernalization Gene
YLD	Yield
YTC	Yield-Trait Component

Acknowledgments

I am pleased to acknowledge the Wheat Coordinated Agricultural Project (TCAP) and NIFA-USDA for sponsoring my Ph.D. program at Kansas State University. I sincerely appreciate the support and guidance received from the faculty and staff of the Agronomy Department and USDA-ARS HWW unit. I would like to extend my sincerest gratitude to my co-major professor Dr. Mary Guttieri, who has mentored me throughout my program and given me the privilege to be a part of her research group. I appreciate all the time she has invested in giving me guidance, knowledge, and techniques to become a better scientist throughout my Ph.D. journey. I would also like to thank my co-major professors, Dr. Romullo Lollato and Dr. Guorong Zhang, as well as my thesis committee members, Dr. Guihai Bai and Dr. Harold Trick, for their continuous encouragement, time, and effort invested in reviewing this dissertation. Their expertise, comments, and suggestions have been invaluable to expanding my knowledge while writing this dissertation. Without the constant support of my co-major professors and committee members, completing my Ph.D. program would not be possible.

I would also like to thank current and former members of Dr. Guttieri's and Dr. Bai's lab. From Dr. Bai's lab, I would like to express my gratitude to Dr. Paul St. Amand and Dr. Amy Bernado for preparing GBS libraries and managing other genotyping projects associated with my dissertation. From Dr. Guttieri's lab, I would like to thank Bill Bickmer, Tara Wilson, Alexandra Dominguez, Nick Schuh, Kyle Wicker, Abigail Tucker, Emma Pruvis, and undergraduate students who have helped tremendously with all field-related, greenhouse, and lab activities. With coding-related activities, I would like to express my gratitude to Dr. Emily Delorean, Dr. Paula Silva, and Marshall Clinesmith. I would also like to thank Dr. Guorang Zhang and his team for managing my field trials in Hays and Dr. Robert Bowden for his aid in managing my

stripe rust trials and engaging in educational discussions about stripe rust. Lastly, I thank my family for their unconditional love and support throughout this journey.

Dedication

This dissertation is dedicated to my family, Mohammad Mustahsan Ansary, Syedda Ghazala Mustahsan, Kashif Mohammad Mustahsan, and all colleagues involved in my professional educational journey.

Chapter 1 - Mapping the Quantitative Field Resistance to Stripe Rust in a Hard Winter Wheat Population 'Overley' x 'Overland'

Introduction

Stripe (yellow) rust, caused by the fungus *Puccinia striiformis* Westend. f. sp. *tritici* Erikss (*Pst*) is among the most harmful diseases in wheat. The pathogen typically infects the green plant tissues of cereal crops and grasses. In wheat, infection occurs at all growth stages (Chen, 2005), with varied infection rates depending on plant resistance levels and moisture and temperature conditions during the infection. Symptoms can appear about one week after infection, and sporulation starts about two weeks after infection. The pathogen produces yellow-orange rust pustules (uredia), and each uredium contains thousands of urediniospores, which make the characteristic orange stripes. The pathogen uses water and nutrients from the host plant to spread infection (Chen, 2005). In commercial wheat production, stripe rust reduces forage yield, grain yield, and quality of seeds. If stripe rust occurs very early and continues its progression throughout the growing season, it can cause a 100% yield loss (Chen, 2005). Wheat-producing regions commonly have losses caused by stripe rust ranging from 10% to 70%. The severity of yield (YLD) loss depends on infection timing, rate of disease progression, disease duration, and wheat cultivar susceptibility (Chen, 2005). Before 2000, stripe rust epidemics had commonly occurred in the western U.S. wheat-producing States, including California, Washington, Idaho, and Oregon. Stripe rust has since become more prominent in the Great Plains (Kansas, Colorado, Nebraska, Missouri, Oklahoma, Texas, and South Dakota) and southern wheat-producing states (Louisiana, Mississippi, Texas, and Arkansas) after 2000. In

Kansas, the largest wheat-producing state in the United States, crop losses to stripe rust have been episodic, with an average of 7.6% from 2015 to 2019, ranging from 0.3% in 2018 to 15.4% in 2015 (https://agriculture.ks.gov/docs/default-source/pp-disease-reports-2012/wheat-disease-report-2019.pdf?sfvrsn=4ef189c1_0; Accessed 7/23/20). Fungicide applications and resistant cultivars are used to reduce YLD losses from this disease (Chen, 2005; Cruppe et al., 2021; Jaenisch et al., 2019). Yield loss underestimates the total economic cost of stripe rust as it does not incorporate the cost of fungicide applications made to control the disease, or potential losses in grain and seed quality resulting from severe infections.

Wheat host plant resistance to stripe rust is broadly categorized into two types: all-stage resistance (ASR), also known as seedling resistance, and adult-plant resistance (APR). All-stage resistance is typically effective from the seedling stage through all wheat growth stages, and ASR generally is race-specific (Chen, 2013). All-stage resistance is mainly controlled by major-effect single genes. Wheat genotypes with APR typically are susceptible to stripe rust as seedlings but become more resistant at adult growth stages. Some APR is race non-specific and has been durable, while other APR is race-specific. Adult plant resistance (APR) may also increase in effectiveness under high temperatures (high-temperature adult-plant resistance, HTAP) (Chen, 2013; Kumar et al., 2020). Adult plant resistance genes often provide partial, additive resistance. Large-effect APR genes have been identified (e.g., *Lr34/Yr18/Sr57/Pm58/Ltn1*, *Lr46/Yr29/Sr58/Pm39/Ltn2*, *Sr2/Yr30*) and have been used by breeders for decades (Krattinger et al., 2009; Singh et al., 2011; William et al., 2003). However, other unnamed genes have also provided durable resistance. Genetic rust resistance can be improved by stacking multiple resistance genes together in wheat cultivars (Singh et al., 2000; Singh et al., 2005). For example, field trials in Mexico evaluated susceptible seedlings that

demonstrated durable resistance expressed in *Yr* gene complexes (known *Yr* genes and unknown genes) that contributed to adult plant resistance. These *Yr* gene complexes included *Lr34/Yr18* plus four unknown genes, *Lr46/Yr29, Sr2/Yr30*, and one unknown gene. *Lr34/Yr18*, together with other unnamed slow rusting genes, is involved in the durable resistance of 'Frontana' and other wheat lines (Singh et al., 1992). *Lr46/Yr29* and unnamed genes provided durable resistance in 'Pavon76' (Singh et al., 1998). Due to the continuous rise in genetic variation of the pathogens, the durable stacking strategy of combining effective race-specific and non-race-specific resistance genes is needed (Maccaferri et al., 2015). Genetic markers can facilitate the construction of these durable stacks for the partial resistance genes in the germplasm pool because ASR genes mask the presence of partial resistance genes in phenotypic screening.

The *Yr17* stripe resistance gene has been commercially important in the Great Plains. *Yr17* entered the cultivated hexaploid bread wheat germplasm pool through the French cultivar, 'VPM1,' derived from a bridge cross of *Aegilops ventricosa* Tausch, *T. persicum*, and *T. aestivum* (Bayles et al., 2000). As chronicled in Carter et al. (2020), this breeding lineage was initially developed for eyespot resistance rather than rust resistance. The USDA-ARS breeding program in Pullman, WA, led by Dr. Robert Allan, received two VPM1 derivatives from France in 1973 and used these as parents in crossing. The VPM1-derived parents provided rust resistance with three named genes: *Yr17*, leaf rust (caused by *P. recondita* Rob. Ex. Desm. f. sp. *tritici*) resistance gene *Lr37*, and stem rust (caused by *P. graminis* subsp. *graminis* Pers.:Pers) resistance gene *Sr38*. Bariana and McIntosh (1993) subsequently demonstrated that the rust resistance from VPM1 was carried on a $2N^{v}S/2AS$ translocation, which is distinct from the $7D^{v}/7DL$ translocation that confers eyespot resistance. The VPM1-derived winter wheat germplasm from the USDA-ARS Pullman breeding program was broadly used by Great Plains

breeding programs, leading to the development of commercially important *Yr17/Lr37/Sr38*-carrying cultivars such as 'Jagger' (Gao et al., 2020; Sears et al., 1997). *Yr17* is highly prevalent in Great Plains hard winter wheat (HWW) germplasm. A recent survey of regional breeding nurseries (Mu et al. 2020) identified *Yr17* in over 60% of the lines sampled. *Yr17* was initially described as an ASR gene (Bariana et al. 1993). However, virulence to *Yr17* was identified in North America in 1990 and again in 2007. In 2010, the frequency of virulence to *Yr17* in isolates collected from North America was 82.5% in seedling tests (Wan et al., 2014). Yet, Milus et al. (2015) observed that winter wheat lines with *Yr17* appeared to have APR in the field when inoculated with *Yr17*-virulent isolates of stripe rust. Other studies have described seedling susceptibility and adult plant resistance on *Yr17* genotypes. When a Jagger × '2174' population was characterized in seedling and adult plant tests (Fang et al., 2011) with six *Yr17*-avirulent races, *Yr17* was identified only in the adult plant tests. These authors therefore characterized *Yr17* as an APR gene.

Several mapping studies have characterized genetic APR to stripe rust in hard red winter wheat populations adapted to the Great Plains of the United States. As discussed above, stripe rust resistance has been mapped in the Jagger × 2174 recombinant inbred population (Fang et al., 2011). This study identified a QTL for adult plant stripe resistance on the 2A chromosome, where Jagger had the resistance allele, and the QTL is presumed to be the effect of *Yr17*. In addition, a novel resistance QTL was found on chromosome 5A, where Jagger again contributed to the resistance. Stripe rust resistance also has been mapped in a 'TAM 112' × 'TAM 111' population (Yang et al., 2019). A total of eight QTLs (chromosomes 1A, 2A, 2B, 4A, 4B, 6B, and 7D) were identified, and two of them were novel. The most consistent QTL was located on the 2B chromosome (*QYr.tamu-2B*). This QTL had epistatic interactions with another QTL

(*QYr.tamu-2A1*) for both disease severity (SEV) and infection type (IT). High-temperature adult plant resistance to stripe rust also was mapped in 'Rio Blanco' × 'IDO444' (Chen et al., 2012). Eight QTLs were identified on six chromosomes, with QTLs on chromosomes 2B and 4A explaining the largest proportion of the phenotypic variation. A recent GWAS analysis of APR in North American winter wheat identified 20 significantly associated markers (Mu et al., 2020). Nearly all the APR-associated markers were present in the Great Plains HWW surveyed, some at frequencies > 50%.

To support the development of cultivars with durable resistance to stripe rust, the genetic architecture of adult plant resistance and the effect of the $2N^{v}S/2AS$ translocation, which confers *Yr17*, in the presence of other partial resistance genes, requires further characterization in the germplasm pool of regionally adapted hard winter wheat. The first objective of this study was to identify genomic regions associated with quantitative resistance to stripe rust in field trials using a mapping population derived from 'Overley' × 'Overland', varieties with contrasting stripe rust mean severity and infection type. Overley (PI 364974, pedigree U1275-1-4-2-2/ 'Heyne' sib// Jagger) is a hard red winter wheat variety released by Kansas State University in 2003. Overley carries the $2N^{v}S/2AS$ translocation with *Yr17* and perhaps other unidentified partial resistance alleles. Overland (PI 647959, pedigree 'Millennium' sib// 'Seward'/ 'Archer') was released by the University of Nebraska in 2007 (Baenziger et al., 2008). It was described at release as moderately resistant to stripe rust. The genetic basis of the partial resistance in Overland is unknown. Overland has a distinctive phenotypic reaction to stripe rust in the field, displaying a high degree of chlorosis and permitting only minimal sporulation of the pathogen. From 2013 to 2017, in the USDA-ARS screening nursery at Rossville, KS, the mean infection type (IT, 1 to 9 scale) for Overland was 5.4, an intermediate reaction. The mean severity (SEV) for Overland

was 52.8%. Overley, in comparison, had a lower mean IT (3.8) and lower mean SEV (7.4%). Both Overley and Overland have been successful commercial cultivars, and both have been used as parents in regional breeding programs. Overley was in peak production in 2007 (23.3 %) and 2009 (13.7 %) in Kansas (https://www.nass.usda.gov/Statistics_by_State/Kansas/Publications/Cooperative_Projects/Wheat_Varieties/; Accessed August 2, 2022). In Nebraska, Overland accounted for 4.7 % of the acreage in 2015 and 4.2 % in 2016 (https://www.nass.usda.gov/Statistics_by_State/Nebraska/Publications/Cooperative_Projects/index.php; Accessed August 2, 2022). This study aimed to provide marker technology to facilitate the retention of genomic regions associated with quantitative resistance to stripe rust during the development of new cultivars with additional stripe rust resistance alleles.

The second objective of this study was to compare the utility of two wheat genome references for SNP calling and genetic map construction. The IWGSC v2.1 reference sequence (Zhu et al., 2021; https://wheat-urgi.versailles.inra.fr/Seq-Repository/Annotations) is based on the reference genotype, 'Chinese Spring'. The 10+ genomes project (Wheat Genomes Project (http://www.10wheatgenomes.com/10-wheat-genomes-project-and-the-wheat-initiative/) has made available additional reference sequences, among which is a reference sequence for the hard winter wheat cultivar, Jagger. Jagger represents 50% of the parentage of Overley. Therefore, the genome of Jagger might be expected to improve reference-based SNP calling for map construction in the Overley × Overland population. Consequently, we report the results of reference-based SNP calling, map construction, and QTL detection using both the IWGSC v2.1 reference sequence and the Jagger reference sequence.

Materials and Methods

Population Construction and Phenotyping

The mapping population consisted of 204 recombinant inbred lines (RILs) developed through single seed descent, which proceeded to the F_9 generation for 178 families and the F_6 generation for 26 families. The population was developed by USDA Central Small Grain Genotyping Laboratory in Manhattan, KS. Individual F_6 or F_9 plants were grown in the greenhouse to produce $F_{6:7}$ and $F_{9:10}$ seeds. The RILs were then grown in single-row plots and hand-harvested in Yuma, AZ, to produce seeds for evaluation in field trials.

Field resistance to stripe rust was evaluated in seven trials: Rossville, KS (2018, 2019), Hays, KS (2019), Pullman, WA (2019, 2020), and Central Ferry, WA (2019, 2020). Abbreviations designating each environment are included in Table 1.1. The experimental design at Rossville, KS, was augmented design with highly replicated checks and two full replications of RILs. Here, entries were planted in single-row plots 1.4-m long and 30-cm apart with the parents as repeated checks. The field experiment at Hays was arranged in a partially replicated augmented design with one or two replications of each RIL. The parental checks (Overley and Overland) were represented in three blocks for each of the two replications at Hays, and RILs were distributed among blocks; not all RILs were present in each replication. Entries at Hays were planted in 6-row plots, 1.5-m wide and 3-m long. Entries at Pullman and Central Ferry were arranged in an augmented design with two replications and were planted in single-row plots, 1-m long and 50-cm apart, with the parents as repeated checks.

The trials at Rossville were inoculated using an inoculum consisting of equal parts of four isolates that were all virulent on *Yr9*. Two isolates were collected in Kansas in 2010 and had virulence to *Yr17* but not *QYr.tamu-2B*. The other two isolates were from Kansas in 2012 and

had virulence to *QYr.tamu-2B*, but not *Yr17*. Susceptible spreader rows ('KS89180B' carrying *Yr9*) were inoculated several times during the tillering stage in the evenings with an ultra-low volume sprayer using a suspension of 2 mL of fresh urediniospores in 1 L of Soltrol 170 (Chevron Phillips Chemical Company, The Woodlands, TX) isoparaffin oil. Trials at Pullman and Central Ferry were evaluated under natural inoculum supplemented by a mixture of isolates collected in the previous field season. The trial at Hays was assessed under natural infection.

Data collection at Rossville began once the susceptible check (KS89180B) had an infection severity coverage of ~10% and continued until senescence. In Rossville, disease ratings (infection type and severity) were collected on the 28th of May 2018 and 16, 22, and 28th of May 2019. In Pullman, disease ratings were collected on the 1st and 12th of July 2019. In Central Ferry, disease ratings were taken on the 12th and 18th of June 2019. The second ratings in Pullman and Central Ferry were recorded on June 26th and June 12th 2020, respectively. The second rating date was used for subsequent statistical analysis. Disease ratings in Hays were taken on June 1, 2019. Stripe rust evaluations were measured using two disease rating scales: IT (0-9; from no infection to highly susceptible) and SEV based on visual estimation of flag leaf area occluded by the pathogen (0-100%) and taken after heading.

Genotyping and Map Construction

Deoxyribonucleic acid was extracted from seedlings, and genotyping-by-sequencing (GBS) was conducted as described previously (Liu et al., 2020) on a subset of 189 lines (187 RILS and two parents), of which 23 were F_6-derived. Single nucleotide polymorphisms (SNPs) were identified in parallel using reference-based calling in the TASSEL (Trait Analysis by aSSociation, Evolution and Linkage pipeline) (Bradbury et al., 2007) using both the IWGSC v2.1 reference genome (Zhu et al., 2021) and the Jagger reference sequence (Wheat Genomes

Project; http://www.10wheatgenomes.com/10-wheat-genomes-project-and-the-wheat-initiative/). The TASSEL pipeline was executed using the default parameters. The resulting SNP datasets derived from each reference sequence were filtered in TASSEL by taxa (RILs) and sites (SNPs). The RILs were filtered to include those RILs for which at least 20% sites were present. The sites were filtered to include sites for which > 60% of RILs were called, minor allele frequency (MAF) > 0.25, and maximum heterozygous proportion < 0.25. The ABH plugin (parental allele assignment) in TASSEL was applied to this reduced dataset to identify parental genotypes.

A set of trait-specific competitive non-GBS KASP assay markers were added to the biparental SNP datasets prior to linkage mapping: Lr37-Yr17-Sr38, IWB29391, Ppd_D1_D2, KS0617_287045, KS617_288635, and Vrn_A1E4 (Table 3.12a). These KASP SNP assays were conducted for the RILs using the primer sequences and amplification conditions in Table 3.12b. The marker Lr37-Yr17-Sr38 was used to identify genotypes carrying the $2N^{v}S$ segment from Overley. The marker IWB29391 was associated with the *QYr.tamu-2B* QTL (Yang et al., 2019). The Ppd_D1_D2 and Vrn_A1E4 markers identified the genes for photoperiod and early release from vernalization in Overley. The two remaining KASP markers, KS0617_288536 and KS0617_287045, were developed from polymorphisms between Overley and Overland identified in the exome capture data, which delimited the 2DL genomic region for a YLD-related QTL.

The enriched biparental SNP datasets were further filtered through R/QTL and ASMap packages in R statistical computing software v.4.1.1 to produce a robust set of SNPs for genetic map construction (Broman et al., 2003; R Core Team, 2021). The ABH datasets of the reference maps were first filtered to remove RILs with missing genotype data using the number of genotyped markers per individual (*ntyped()* function) at cut-off threshold values of *ntyped* = 600

(IWGSC v2.1) and *ntyped* = 900 (Jagger). The *ntyped* values differed due to differences in the marker densities of the two reference maps. Information of the marker data sets of both genomes was plotted to measure the number of genotyped markers for each individual, *ntyped* values were selected to exclude outliers. These bi-parental SNP datasets for each reference genome were then filtered to drop duplicate markers and markers with >80% identical information; RILs with >80% matching genotypes among all individuals were also removed. Markers which were not segregating 1:1 were identified at a *p-value* < 0.05, and those with a *p-value* < 1e-10 were removed. Markers in these datasets also were checked for flipped allele calls using the *checkAlleles* function. From these filtered SNP datasets, linkage groups were produced using the *formLinkageGroups()* function at the parameters of maximum recombination frequency *(max.rf)* = 0.35 and a minimum LOD (*min.lod)*= 6.0. Linkage groups that contained < 3 markers were excluded. The remaining set of linkage groups was used for genetic map construction.

Linkage map construction was done using the MSTmap package, which is part of the ASMap package (Taylor et al., 2017). Genetic distances were obtained through the Kosambi function, and markers were clustered at a *p-value* = 1e-12. The markers remaining in the linkage map from this filter were processed through the *pull.cross* function using the following parameters: co-located, segregation distortion, and missing. The co-located parameter of the *pull.cross* function pulled co-located markers from the linkage map using the *findDupMarkers* infrastructure, a feature in the *qtl* package. These markers were set aside and stored in a *co-located* element. The *seg.thresh* parameter (*seg.thresh = 0.02)* within the *pull.cross* function removed any markers under the given threshold and stored those markers into a *seg.distortion* element. In the same *pull.cross* function the *miss.thresh* parameter (*miss.thresh = 0.04*) removed any markers with a proportional amount of missing allele data set aside into a *missing* element.

The updated makers in the linkage map were then re-clustered using MSTmap at *p-value* = 1e-10. The *push.cross* function was then used to push some of the markers pulled from the *pull.cross* into the linkage map with parameters set at *seg.threshold* =0.001 and *miss.thresh* = 0.5 to push pulled makers that followed these parameters back into the linkage map.

The genetic map was then constructed using the Kosambi function, and markers were added back into the linkage map from the *push.cross* function was clustered at a *p-value* = 2 to retain the linkage group structure. In addition, this map was scanned for genotype clones, using the function *genClones(),* looking for pairs of genotypes with a proportion of matching alleles >0.85 to be discarded. Marker profiles (*profileMark*) were evaluated for: segregation distortion, allele proportions, and the proportion of missing values of each marker using the Bonferroni method at a critical value of $\alpha = 0.05$. The marker profiles were also evaluated to remove RILs and markers with excessive recombination due to high numbers of crossover, double-crossover events, and missing data at the expected recombination rate of 100. The new subset data was processed through MSTmap at a *p-value* = 1e-10 to cluster the markers to linkage groups. Markers with a double crossover rate >2 were excluded, and the markers within linkage groups were ordered (*p-value* =2). This process was repeated four times with each reduced genetic map to produce reliable SNPs for QTL analysis.

Linkage groups within the reduced genetic map associated with the same chromosome were merged. The initial mapping parameters applied to order the combined linkage groups was the Kosambi mapping function (*p-value* = 2) using MSTmap. The secondary screening of the merged linkage groups of the genetic map was done at *p-value* = 1e-06, resulting in some of the linkage groups being split. This genetic linkage map was then processed through restoration analysis. The purpose of the restoration analysis was to ensure that all SNPs with significant trait

associations in single marker analysis were included in the final linkage map and subsequent QTL detection processes. All the markers present in the ABH dataset produced by TASSEL and excluded in the succeeding filtering in map construction were extracted. Single marker analysis was conducted in JMP Genomics 9.0 (SAS Institute, Inc., Cary, NC) to test the individual marker effects on IT and SEV from the multi-location BLUPs. Those SNPs (19 SNPs in IWGSC v2.1-based map: 41.85% avg. missing data rate, and 23 SNPs in Jagger-based map: 37.15% avg. data missing rate) that had significant associations (p-value < 0.001) with IT or SEV were pulled back into the genetic linkage map and mapped within the specific linkage groups to which they belonged. The linkage groups affected by this marker restoration included 2A, 2B.1, 2B.2, 2D.2, and 3A.2. The number of RILs, SNPs, and linkage groups at each stage of map construction is provided in Table 3.13. These refined linkage maps were used for QTL analysis.

QTL and Other Statistical Analyses

Phenotypic data were analyzed using the augmented design structure in JMP Genomics 9.0 (Segall et al., 2010; SAS Institute, Inc., Cary, NC). Check entries and environments were fit as fixed effects. Replications and RILs were fit as random effects. Inspection of the conditional residuals from model fit confirmed that IT and SEV could be analyzed as normally distributed, independent variables without transformation. The least-square means were estimated as intercept-adjusted best linear unbiased predictors (BLUPs) in each environment and across environments in JMP Genomics. Broad-sense heritability (H^2) was estimated on an entry-mean basis:

$$H^2 = \frac{\sigma_g^2}{\sigma_g^2 + \frac{\sigma_{ge}^2}{E} + \frac{\sigma_{error}^2}{E * r}}$$

where σ_g^2 is genotypic variance, σ_{ge}^2 is the genotype-by-environment variance, σ_{error}^2 is the residual error variance, *r* is the number of replications, and *E* is the number of environments.

Quantitative trait locus (QTL) analysis was performed using inclusive composite interval mapping in IciMapping v4.1 (Meng, Li, Zhang, & Wang, 2015). The QTL analysis for IT and SEV was conducted across all environments and in individual environments using BLUPs obtained from the analysis of the phenotypic data. The following parameters were used for QTL mapping: a 1 cM distance between QTL testing points; empirical LOD permutation testing with 1000 permutations and an experiment-wise alpha = 0.05; the control marker number = 10 and test window size = 7 cM; control marker selection via stepwise regression; significance level for entry into the model = significance level for staying in the model = 0.001 (Hussain et al., 2017). The Inclusive Composite Interval Mapping of digenic EPIstatic QTL (ICIM-EPI) module was used to identify QTLs with a significant epistatic interaction (Li et al., 2008). QTL × environment interactions (QEI) were evaluated using the ICIM-MET (Inclusive Composite Interval Mapping-Multiple Environmental Trials) module with empirical LOD thresholds.

Design and Analysis of QTL-associated Competitive SNP Assays

Overley and Overland are part of a large set of WheatCAP germplasm using the wheat exome capture data designed in collaboration with Nimblegen (Krasileva et al., 2017). The captured samples were prepared following the manufacturer's protocol. They were sequenced using an Illumina NextSeq 500 sequencer at Kansas State University Integrated Genomics Facility, producing 150 bp pair-end reads for all samples. Raw sequencing reads were checked for quality using NGSQC toolkit version 2.3.3 (Patel et al., 2012), and high-quality reads were exported for alignment to the IWGSC reference genome v.2.1 (Zhu et al., 2021) using HiSat2. Only uniquely mapped reads were retained for further analysis, and resulting alignments were

subsequently run through the GATK pipeline (McKenna et al., 2010) to generate variants segregating in the germplasm collection. SNPs between Overley and Overland within QTL regions (2BS: 50536339-58321611, 2BL: 770650575 – 771858040, 2DL: S2D_637621998 – S2D_639629011) were filtered using a custom Perl script. They were considered high quality if flanked by > 100bp of non-polymorphic sequence. High-quality SNPs and flanking sequences were subsequently processed through Polymarker software (Ramirez-Gonzalez et al., 2015) to design primers that discriminate the Overley and Overland genotypes in the polyploid genome. Candidate primer sets were selected from among the 88 designed primer sets based on their identification as chromosome-specific or chromosome-semi-specific (22 sets) and further filtered for those primer sets with three or fewer total BLAST hits (18 sets). This process produced seven primer sets for the 2BS (*QYr.hwwgIT–2B.1*$_a$ and *QYr.hwwgSEV–2B.1*$_a$) region and primer sets for the 2BL (*QYr.hwwgIT–2B.2*$_a$) region and eight primer sets for the 2DL (*QYr.hwwgIT–2D*$_a$ and *QYr.hwwgSEV–2D*$_a$) region. Primer sets were evaluated for functionality using parents and a synthetic heterozygote. Exome-capture data for the 2BL region, which contained SNPs and were processed through Polymarker, from which candidate primer sets were designed and evaluated using the parents and a synthetic heterozygote.

Predicted effects of QTL-associated SNPs were evaluated using single marker regression analysis and multiple regression analysis with model selection. Single marker analysis was conducted by fitting linear models for marker effect with the multi-location BLUPs as the response variable and marker scores expressed as Overland = 0, Overley = 2. Model selection and multiple regression analysis were conducted using PROC REG in SAS v9.4 (Segall et al., 2010; SAS Institute, Cary, NC) to administer stepwise forward/reverse model selection (Table

1.7). The criteria to enter the model set to $\alpha = 0.10$, and the requirements to remain in the model set to $\alpha = 0.10$.

Results

Phenotypic Data

Stripe rust IT varied with locations (*F*-value = 21.9***), with higher average IT (more susceptible, 6.3 to 6.9) observed in the PNW environments than those (4.5 to 4.8) observed in the Kansas environments (Table 1.1). The IT of the two parents (Overley = 5.7 ± 0.9, Overland = 5.9 ± 0.9) did not differ significantly, and the mean IT of the RILs (5.8 ± 0.1) was intermediate between the two parents. Disease severity also varied among environments (*F*-value = 76.5***). Site SEV means of the RIL population ranged from 7.7 ± 5.6% at Rossville, KS, in 2018 to 66.8 ± 5.6% at Central Ferry, WA, in 2020. The average SEV of the RILs (35.5% ± 1.2%) was intermediate between Overley (31.6% ± 10.5%) and Overland (38.4% ± 10.5%).

Table 1.1. Summary of field responses of IT and SEV.

Stripe rust infection type (IT) and severity (SEV) of the (A) recombinant inbred lines (RILs) were evaluated in seven environments. Data are least-squares means with standard errors in parentheses.

Environment	IT (1 to 9)	SEV (%)
Central Ferry, WA 2019 (CF19)	6.2 (0.77)	19.5 (8.5)
Central Ferry, WA 2020 (CF20)	6.8 (0.76)	66.8 (8.4)
Hays, KS 2019 (HZ19)	4.8 (0.83)	18.4 (9.1)
Pullman, WA 2019 (PL19)	6.9 (0.76)	58.9 (8.4)
Pullman, WA 2020 (PL20)	6.4 (0.76)	53.1 (8.4)
Rossville, KS 2018 (RS18)	4.5 (0.76)	7.7 (8.4)
Rossville, KS 2019 (RS19)	4.8 (0.76)	22.0 (8.5)

Genotypic variance and genotype × environment variance component estimates for IT and SEV were highly significant in Wald tests (Table 3.14). The broad-sense heritability estimates were high for IT (0.80) and SEV (0.82). The RIL population had a wide and continuous distribution for IT and SEV in each environment, with transgressive segregation in both directions (Figure 1.1). Median values for IT (Overley = 5.7, Overland = 5.9, RILs = 5.8) and SEV (Overley = 31.6, Overland = 38.4, RILs = 35.5) of the RILs were similar to both parents. Pairwise correlations of IT and SEV of RILs among the seven environments were also high (Table 1.2). The correlation of SEV among environments was generally greater than the correlation of IT.

Table 1.2. Pairwise correlation matrix of stripe rust infection type and severity responses.

Pairwise correlation of infection type (above the diagonal) and severity (below the diagonal) of best linear unbiased predictors of RILs evaluated in seven environments.

Environment	Pairwise correlation coefficient (*r*)*						
	CF19	CF20	HZ19	PL19	PL20	RS18	RS19
CF19	--	0.686	0.552	0.683	0.699	0.652	0.632
CF20	0.765	--	0.650	0.648	0.862	0.628	0.577
HZ19	0.761	0.718	--	0.647	0.643	0.680	0.705
PL19	0.814	0.817	0.734	--	0.638	0.715	0.703
PL20	0.791	0.843	0.709	0.774	--	0.637	0.571
RS18	0.860	0.749	0.783	0.781	0.730	--	0.760
RS19	0.738	0.709	0.726	0.710	0.668	0.809	--

***** All correlations are significant ($p < 0.001$).

Figure 1.1. Phenotypic data distributions of stripe rust field response of IT and SEV.

Distribution of best linear unbiased predictors (BLUPs) of stripe rust infection type (A) and severity (B) ratings across all environments in the Overley x Overland RIL population. Environments: CF19=Central Ferry, WA 2019; CF20=Central Ferry, WA 2020; HZ19 = Hays, KS 2019; PL19 = Pullman, WA 2019; PL20 = Pullman, WA 2020; RS18 = Rossville, KS 2018; RS19 = Rossville, KS 2019; MET = Multi-Environmental Trial.

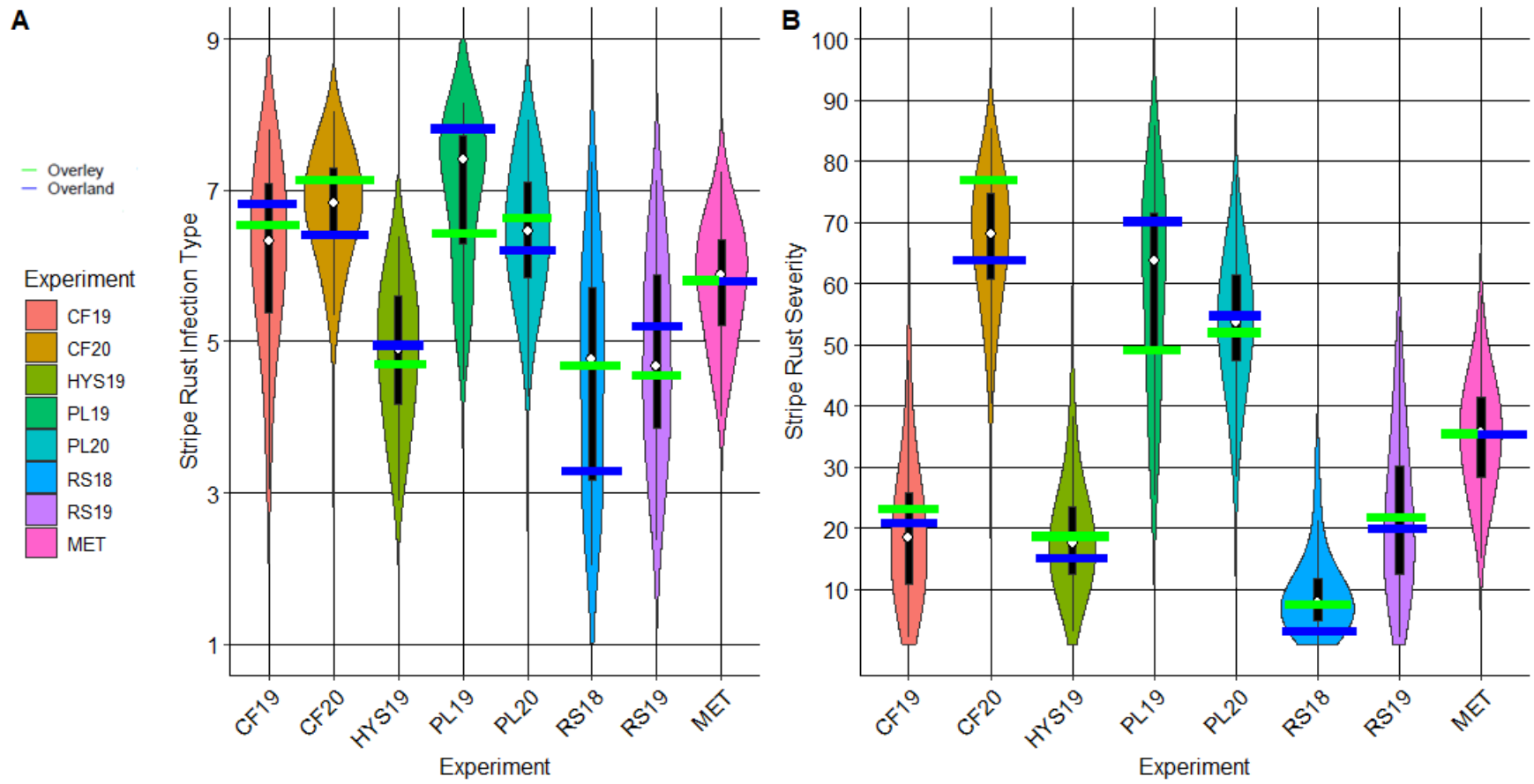
A
Overley
Overland
Experiment
CF19
CF20
HYS19
PL19
PL20
RS18
RS19
MET
Stripe Rust Infection Type
9
7
5
3
1
CF19
CF20
HYS19
PL19
PL20
RS18
RS19
MET
Experiment
B
Stripe Rust Severity
100
90
80
70
60
50
40
30
20
10
CF19
CF20
HYS19
PL19
PL20
RS18
RS19
MET
Experiment

SNP Calling and Genetic Map

The initial filtering process for missing data and minor allele frequency identified more SNP sites (30,286 SNP sites) using the Jagger reference sequence than those identified using the IWGSC v2.1 Chinese Spring reference sequence (29,832 sites, Table 1.3). The Jagger reference sequence called more SNP sites (2,716 sites, Table 1.3) than the Chinese Spring reference sequence (2,607 sites, Table 1.3). The reason why there are more SNPs detected in the Jagger reference sequence than in the IWGSCv2.1 reference sequence is due that Jagger is a parent of Overley. Therefore, there is a higher rate of alignment and SNP detection during GBS between the Jagger reference sequence and our population in comparison to the IWGSCv2.1 reference sequence. After the biparental SNP calling filter, the Jagger pipeline identified 41% more sites (1,664) than the IWGSC v2.1 pipeline (1,177 SNPs) (Table 1.3).

Further filtering for missing data, identical data (correlation > 0.8), and excess double-crossovers (>2) reduced the number of RILs used in map construction to 162 in the IWGSC v2.1 pipeline and 158 in the Jagger pipeline. After restoration analysis, the final numbers of RILs used for map construction were 162 for the IWGSCv2.1 pipeline and 158 for the Jagger pipeline. The final numbers of SNPs used in map construction were 1,156 for the Jagger pipeline and 802 for the IWGSC v2.1 pipeline (Table 1.3). These filters keep the markers and RILs that are the most informative. The SNPs identified through GBS for both reference genomes were both different. Studies have presented the importance of using curated, data to build genetic maps (Broman, 2012; Taylor et al., 2017). Using raw, unfiltered data can give rise to issues such as genotyping errors and segregation distortions that can deleteriously impact the genetic map. In addition, missing data can lead to problems in constructing the genetic map. Therefore, it is

preferred to use curated, parsimonious data to produce the most informative and robust genetic map for further analysis.

Table 1.3. Summary statistics of SNP calling and genetic map constructions of reference genomes.

Statistics for SNP calling and map construction pipelines using two alternative reference genomes, IWGSC v2.1 and Jagger.

	IWGSC v2.1 Reference Pipeline		Jagger Reference Pipeline	
Procedure	**RILs**	**SNPs**	**RILs**	**SNPs**
TASSEL SNP identification	184	29,832	184	30,286
TASSEL taxa & site filtering[1]	182	2,607	182	2,716
TASSEL ABH biparental plugin	182	1,177	182	1,664
R/QTL missing data filter[2]	180	1,177	179	1,604
Discard identical data[3]	162	877	162	1,246
Discard linkage groups < 3 SNPs	162	844	162	1,205
Filter RILs and SNPs for double crossovers[4]	162	783	158	1,133
Restoration	162	802	158	1,156

[1]Filter to remove RILs with < 20% data present. SNPs were filtered to contain a minimum count of 110 sites (60%) present, minor allele frequency (MAF) = 0.25, maximum allele frequency = 0.75, maximum heterozygous proportion = 0.25, and removal of minor SNP states (Tassel converts rare SNP states to missing data "N" to remove sequencing errors).
[2]Filter to remove RILs with < 50% data present. SNPs were filtered to contain a minimum count of 100 sites (56%).
[3]SNPs and RILs with a high proportion of matching information were removed at a threshold of ≥ 80%.
[4]SNPs and RILs with > 2 double-crossovers were removed.

The final linkage map was constructed using 802 SNPs called by the IWGSC v2.1 reference sequence distributed across 36 linkage groups representing all 21 chromosomes (Table 3.13, Table 3.15). Chromosomes 1A, 1B, 2B, 2D, 3A, 3B, 4A, 4B, 5A, 5B, 7B, and 7D were split into multiple linkage groups. The linkage map length constructed using the IWGSC v2.1 reference map was 3498.8 cM, with an average distance between markers of 4.60 cM. The A, B, and D genomes contained 350, 351, and 101 markers, respectively. The total map lengths of the sub-genomes were 1722.8 cM, 1419.1 cM, and 356.9 cM, respectively. Among the three genomes, the D genome had the lowest marker density (0.13 markers cM^{-1}), followed by the A genome (0.44 markers cM^{-1}) and B genome (0.44 markers cM^{-1}).

The linkage map constructed using SNPs called by the Jagger reference map contained 1,156 SNP markers distributed across 27 linkage groups representing all 21 chromosomes (Table 3.16). Chromosomes 1B, 1D, 2D, 3B, 5B, 7B, and 7D were split into multiple linkage groups. The total map length was 3981.9 cM, with an average distance of 3.50 cM between markers. The A, B, and D genomes contained 529, 488, and 139 markers with total lengths of 1943.8, 1534.1, and 504.2 cM, respectively. The D genome had the lowest marker density (0.12 markers cM^{-1}), followed by the B genome (0.42 markers cM^{-1}) and the A genome (0.46 markers cM^{-1}).

QTL Identification

Given the limited genotype × environment interaction (Table 3.14) and relatively high heritability (80%) of the traits, the BLUPs from the combined, multi-location analysis were used for QTL identification. Maps based on the SNPs called using the two reference genomes generally identified the same genomic regions with the most significant regions on chromosome group 2 (2AS, 2BS, 2BL, and 2DL) (Table 1.4 and Table 3.17). Results from both maps showed a difference for the 2BL QTLs, which were identified using the IWGSC v2.1 map but not the

Jagger map. Looking closely at QTL locations in the IWGSC v2.1 map, many genomic regions for IT and SEV overlap except for the 2BL QTL, whose genomic regions are adjacent (Table 1.4, Figure 1.2). The Jagger map also showed similar overlapping or identical genomic regions (Table 3.17, Figure 3.6). Therefore, the QTL regions on 2AS, 2BS, 2BL, and 2DL identified using both maps for both traits were consistently named *QYr.hwwg-2A, QYr.hwwg-2B.1, QYr.hwwg-2B.2, QYr.hwwg-2D,* with different QTL regions designated with a different letter (e.g., *QYr.hwwgIT–2A$_a$*).

The QTL analysis using the IWGSC v2.1-derived map indicated that Overley contributed the favorable alleles (resistance) for IT and SEV at *QYr.hwwg-2A (QYr.hwwgIT–2A$_a$, QYr.hwwgSEV–2A$_a$*) and *QYr.hwwg-2B.2* (*QYr.hwwgIT–2B.2$_a$, QYr.hwwgSEV–2B.2$_c$*) as indicated by negative values (favorable) of the additive effects of the Overley alleles (Table 1.4). The favorable alleles for IT and SEV at *QYr.hwwg-2B.1* (*QYr.hwwgIT–2B.1$_a$, QYr.hwwgSEV–2B.1$_a$*) and *QYr.hwwg-2D* (*QYr.hwwgIT–2D$_a$, QYr.hwwgSEV–2D$_a$*) were contributed by Overland, as indicated by positive values (unfavorable) of the additive effects of the Overley alleles. The QTL analysis using the Jagger map assigned alleles favorable for resistance at *QYr.hwwg-2A* (*QYr.hwwgIT–2A$_b$, QYr.hwwgSEV–2A$_b$*) and *QYr.hwwg-2B.2* (*QYr.hwwgSEV–2B.2$_b$*) to Overley and the favorable alleles at *QYr.hwwg-2B.1*(*QYr.hwwgIT–2B.1$_a$, QYr.hwwgSEV–2B.1$_a$*) and *QYr.hwwg-2D* (*QYr.hwwgIT–2D$_b$, QYr.hwwgSEV–2D$_b$*) to Overland (Table 1.4 and Table 3.17).

Table 1.4. QTLs identified from multi-location BLUPs using MET-QTL analysis for stripe rust IT and SEV response using the IWGSv2.1 reference map.

List of QTLs identified for stripe rust infection type (IT) and severity (SEV) using multi-location best linear unbiased predictors (ML-BLUP) for both reference genomes. The additive effect is expressed as the effect of the Overley allele. LOD = log odds ratio; PVE = percentage of variance explained. The LOD scores for the reference genomes are 3.29 (IWGSC v2.1; IT) and 3.40 (IWGSC v2.1; SEV).

QTL	Response	Chr.	Marker Interval	LOD	PVE (%)	A[1]	C.I.[2]	P.A.[3]
QYr.hwwgIT–2A$_a$	IT	2AS	S2A_13657961 – S2A_6171309	9.7	14.11	-0.32 score	11.5 – 19.5	OY
QYr.hwwgSEV–2A$_a$	SEV	2AS	S2A_13657961 – S2A_6171309	16.1	25.22	-4.81%	13.5 – 18.5	OY
QYr.hwwgIT–2B.1$_a$	IT	2BS	S2B_51126334 – S2B_72963487	8.8	14.81	0.33 score	37.5 – 47.5	OD
QYr.hwwgSEV–2B.1$_a$	SEV	2BS	S2B_51126334 – S2B_72963487	3.8	5.41	2.23%	35.5 – 47.5	OD
QYr.hwwgIT–2B.2$_a$	IT	2BL	S2B_776572012 – S2B_779238540	5.9	7.91	-0.24 score	173.5 – 179.5	OY
QYr.hwwgSEV–2B.2$_c$	SEV	2BL	S2B_781640346 – S2B_784820218	7.2	9.90	-3.01%	186.5 – 193.5	OY
QYr.hwwgIT–2D$_a$	IT	2DL	S2D_650602042 – S2D_650725039	9.3	13.38	0.31 score	47.5 – 52	OD
QYr.hwwgSEV–2D$_a$	SEV	2DL	S2D_650602042 – S2D_650725039	8.9	12.6	3.39%	47.5 – 52	OD

[1]Additive effect of the Overley allele
[2]Confidence interval (cM)
[3]Favorable parental allele contributing to resistance; OY = Overley OD = Overland.

All the QTL regions identified on 2AS (Table 1.4) containing the Lr37-Yr17-Sr38_GBG-KASP marker may be associated with the $2N^{v}S$ translocation conferring *Yr17*. The marker was mapped 4.05 cM away from the right interval marker (S2A_6171309) and 8.14 cM from the left interval marker (S2A_13657961) of the QTL using the IWGSCv2.1 map. In the Jagger map, the 2AS QTLs for IT and SEV were on the interval of S2A_20860853 – S2A_6690360. The Lr37-Yr17-Sr38_GBG-KASP marker is 3.94 cM from the right interval marker (S2A_6690360) and 2.04 cM from the left interval marker (S2A_20860853). The 2AS QTL is classified as *QYr.hwwg–2A;* they are designated by stripe rust disease type and continuous alphabetic terms such as *QYr.hwwgIT–2A$_a$* and *QYr.hwwgSEV–2A$_a$*. The *QYr.hwwg–2A* QTLs identified from the ML-BLUP data explained a similar proportion of PVE in both maps for IT (14.11% in the IWGSC v2.1 map and 14.88% in the Jagger map) and SEV (25.22% in IWGSC v2.1 map and 26.52% in the Jagger map) (Table 1.4; Table 3.17).

The 2BS QTL designated as *QYr.hwwg-2B.1* explained a greater proportion of the phenotypic variance for IT (14.81%) with the IWGSC v2.1 map than that from the Jagger map (11.04%). *QYr.hwwg-2B.1* explained similar phenotypic variation for SEV (5.41% from the IWGSC v2.1 map and 5.28% from the Jagger map). The 2BL QTL, *QYr.hwwg-2B.2*, explained 7.91% of the phenotypic variation for IT and was only identified in the IWGSC v2.1 map. However, *QYr.hwwg-2B.2* was identified for SEV in both maps, with PVE of 9.90% and 7.52% using the IWGSC v2.1 and Jagger maps, respectively. The 2DL QTL, *QYr.hwwg-2D,* was identified for both IT and SEV using both maps, with similar PVE identified for IT (13.38% - IWGSCV2.1 map; 18.6% Jagger map) using both maps and greater PVE for SEV (12.6% - IWGSCv2.1; 14.68% Jagger map) identified using the Jagger map (Table 1.4; Table 3.17).

Multi-environment analysis (MET) of QTLs evaluated the size of QTL x Environment (Q x E) interaction effects under seven environments (Table 1.5; Table 3.18). Major QTLs identified across seven environments using the IWGSC v2.1 map are presented in Table 1.5 and Figure 1.3. Similarly, QTLs mapped using the Jagger-derived map are presented in Table 3.18 and Figure 3.7. Major QTLs are claimed with LOD > 10. The MET analysis identified QTLs on 2A using both maps. Using the IWGSC v2.1-derived map, *QYr.hwwgIT–2A$_a$* explained 8.75% of the phenotypic variation and was not identified using the Jagger map (Table 1.5). *QYr.hwwgSEV–2A$_a$,* which explained a phenotypic variation of 27.40%, was not identified in the Jagger map. *QYr.hwwgIT–2A$_b$* explained a phenotypic variation of 14.48% and 15.97%, respectively, identified in the IWGSCv.2.1 and Jagger map. *QYr.hwwgSEV–2A$_b$* explained 5.31% phenotypic variation in the Jagger map. *QYr.hwwgIT–2A$_c$*, was identified only in the Jagger map with a phenotypic variation of 26.94%.

The MET analysis also identified QTLs on 2B using both reference maps. *QYr.hwwgIT–2B.1$_a$* explained 10.37% of the phenotypic variation for IT using the IWGSC v2.1 map ,and 13.65% of the phenotypic variation for IT using the Jagger map and 5.98% for SEV only in the IWGSC v2.1 map. *QYr.hwwgIT–2B.1$_b$* explained the 7.50% PVE in the IWGSCv2.1 map. *QYr.hwwgIT–2B.2$_a$*, which was only identified in the IWGSCv2.1 map, explained 7.49% of the phenotypic variation for IT. Similarly, *QYr.hwwgSEV–2B.2$_a$* explained 6.79% of the phenotypic variation using the Jagger map. *QYr.hwwg–2B.2$_b$* was only identified with the IWGSC v2.1 map with a similar PVE of 5.89% for IT and 7.54% for SEV. *QYr.hwwgIT–2D$_a$* explained 17.35% of the phenotypic variation for IT using the IWGSC v2.1 map. *QYr.hwwgIT–2D$_b$* and *QYr.hwwgSEV–2D$_b$* were identified using the Jagger map. They explained 21.54% and 19.11% of the phenotypic variation, respectively. These QTLs have different marker intervals (physical

positions) and confidence intervals. As shown in Table 1.5 and Table 3.18 *QYr.hwwgIT–2D$_a$* (S2D_650602042 -S2D_650725039; 50.5 – 52; IWGSCv2.1) and *QYr.hwwgIT–2D$_b$* (S2D_665681641 – S2D_666306598; 37.5 – 41.5; Jagger) are both located at the distal ends of 2DL. For SEV, *QYr.hwwgSEV–2D$_a$* explained 13.35% of the phenotypic variation using the IWGSC v2.1 map and 19.11% using the Jagger map (*QYr.hwwgSEV–2D$_b$)*.

Compared to ICIM ML-BLUP QTL analysis (Table 1.4), ICIM MET analysis (Table 1.5) identified more fragmented QTLs across both maps. For example, there were two adjacent QTLs for IT on 2A (*QYr.hwwgIT–2A$_a$*, *QYr.hwwgIT–2A$_b$*), 2BS (*QYr.hwwgIT–2B.1$_a$*), and 2BL (*QYr.hwwgIT–2B.2$_b$*). ICIM MET analysis also identified an adjacent QTL for SEV on the 2BL. Some minor QTLs (PVE ≥ 3%) were also identified in the MET analysis for IT on 1AL, 4AL, and 5AL that were not identified in Table 1.4. The MET-QTL analysis also identified minor QTLs for SEV on the 3AS, 4BL, 4DL, 5BL, 6BS, and 6AS using the IWGSC v2.1 map. The Jagger map also identified minor QTLs for IT on the 2BL, 5AS, 6AS, 2BS, 4AL, and 1BS, and for SEV on the 2AS, 2BL, 2BS, 6AL, 5AS, 4AL, and 4BL.

Table 1.5. QTLs identified from MET-QTL analysis for stripe rust IT and SEV across multiple locations in the IWGSCv2.1 reference map.

List of QTLs identified using the multi-environment trial (MET)-QTL analysis based on permutation LOD: IT (6.64) and SEV (6.48) for best linear unbiased predictors for stripe rust infection type (IT) and severity (SEV) in each of seven trials using the IWGSCv2.1 reference-derived map LOD = log odds ratio; PVE = percentage of variance explained. A = additive (main) effect of genotype, A × E = additive effect × environment interaction.

QTL Name	Resp.*	Chr.	Marker Interval	LOD	PVE (%)	PVE[1]	PVE[2]	A[3]	C.I.[4]	P.A.[5]
QYr.hwwgIT–2A$_a$	IT	2AS	S2A_13657985 – S2A_13657961	24.5	8.75	5.01	3.74	-0.19 score	13.5 – 17.5	OY
QYr.hwwgIT–2A$_b$	IT	2AS	S2A_18817759 – S2A_21578103	26.2	14.48	5.20	9.27	-0.19 score	23.5 – 27.5	OY
QYr.hwwgSEV–2A$_a$	SEV	2AS	S2A_13657961 – S2A_6171309	81.70	27.40	23.87	3.53	-4.97%	15.5 – 17.5	OY
QYr.hwwgIT–2B.1$_a$	IT	2BS	S2B_51126334 – S2B_72963487	24.6	10.37	7.30	3.06	0.23 score	41.5 – 47.5	OD
QYr.hwwgIT–2B.1$_b$	IT	2BS	S2B_80274906 – S2B_89895913	17.6	7.50	2.14	5.36	0.12 score	53.5 – 59.5	OD
QYr.hwwgSEV–2B.1$_a$	SEV	2BS	S2B_72963470 – S2B_80117186	18.6	5.98	3.76	2.23	1.97%	47.5 – 50.5	OD
QYr.hwwgIT–2B.2$_a$	IT	2BL	S2B_776572012 – S2B_779238540	19.2	7.49	4.36	3.14	-0.18 score	176.5 – 178.5	OY
QYr.hwwgIT–2B.2$_b$	IT	2BL	S2B_778217149 – S2B_784550723	16.2	5.89	2.82	3.07	-0.14 score	181.5– 183.5	OY
QYr.hwwgSEV–2B.2$_b$	SEV	2BL	S2B_778217149 – S2B_784550723	23.9	7.54	4.32	3.23	-2.11%	182.5 – 183.5	OY

QYr.hwwgIT–2D$_a$	IT	2DL	S2D_650602042 – S2D_650725039	46.9	17.35	17.11	0.25	0.35 score	50.5 – 52	OD
QYr.hwwgSEV–2D$_a$	SEV	2DL	S2D_650602042 – S2D_650725039	42.4	13.35	12.05	1.30	3.53%	49.5 – 52	OD

[1]PVE due to additive effect (A)
[2]PVE due to A x E interaction
[3]Additive effect of the Overley allele.
[4]Confidence interval (cM)
[5]Favorable parental allele contributing to resistance; OY = Overley OD = Overland.
[*]Response stripe rust disease trait: IT = Infection Type, SEV = Severity

Table 1.6. Additive effects and AX E effects at each of the seven environments for stripe rust using the IWGSCv2.1 reference map.

The A x E effects for IT and SEV resistance across locations associated with QTLs on the IWGSCv2.1 reference map from MET analysis, from Table 1.5 and Table 3.18. C.I. =Confidence interval (cM).

				A x E							
QTL Name	**Chr.**	**Unit**	**A**	**CF19**	**CF20**	**HZ19**	**PL19**	**PL20**	**RS18**	**RS19**	**P.A.[1]**
QYr.hwwgIT–2A$_a$	2AS	score	-0.19	-0.14	0.12	-0.07	-0.31	0.11	0.15	0.13	OY
QYr.hwwgSEV–2A$_a$	2AS	percent	-4.97	0.29	1.24	0.68	-4.32	1.69	1.17	-0.76	OY
QYr.hwwgIT–2A$_b$	2AS	score	-0.19	0.15	0.16	0.19	0.14	0.17	-0.38	-0.43	OY
QYr.hwwgIT–2B.1$_a$	2BS	score	0.23	0.21	-0.05	0.07	0.02	-0.02	0.30	-0.11	OD
QYr.hwwgSEV–2B.1$_a$	2BS	percent	1.97	-0.78	0.17	-0.39	0.52	-0.83	-1.95	3.26	OD
QYr.hwwgIT–2B.2$_a$	2BL	score	-0.18	0.14	0.15	-0.04	-0.06	-0.17	-0.21	0.18	OY
QYr.hwwgIT–2B.2$_b$	2BL	score	-0.14	-0.19	-0.10	0.14	0.13	0.12	0.10	-0.21	OY
QYr.hwwgSEV–2B.2$_b$	2BL	percent	-2.11	-1.26	1.83	0.22	-1.53	-3.00	1.90	1.85	OY
QYr.hwwgIT–2D$_a$	2DL	score	0.35	-0.04	-0.05	-0.04	0.006	0.05	0.05	0.03	OD
QYr.hwwgSEV–2D$_a$	2DL	percent	3.53	0.06	0.50	-0.84	2.35	0.23	-1.46	-0.85	OD

[1]Favorable parental allele contributing to resistance; OY = Overley OD = Overland

*Additive effect of the Overley allele

Additive x environment (AxE) interactions of the major QTL(s) across locations were identified using the IWGSVv2.1 map (Table 1.6) and Jagger map (Table 3.19). Using the IWGSCv2.1 map, the additive effects of the Overley allele for the IT QTLs (*QYr.hwwgIT–2A$_a$*, *QYr.hwwgIT–2A$_b$*, and *QYr.hwwgIT–2B.2$_a$*) was negative, indicating more resistance to stripe rust. The Overley allele of *QYr.hwwgIT–2A$_a$* was most favorable for resistance at PL19, relative to all other locations. The Overley allele of *QYr.hwwgIT–2A$_b$* was most favorable for resistance at RS18 and RS19, relative to all other locations (Table 1.6). The Overley allele of *QYr.hwwgIT–2B.2$_a$* was most favorable for resistance at RS18, relative to all other locations. The Overley allele of *QYr.hwwgIT–2B.2$_b$* was most favorable for resistance at RS19 as well, relative to all other locations (Table 1.6). The additive effects of the Overland parental allele for the IT QTLs (*QYr.hwwgIT–2B.1$_a$* and *QYr.hwwgIT–2D$_a$*) were positive, indicating more resistance to stripe rust. The Overland allele of *QYr.hwwgIT–2B.1$_a$* was most favorable at CF19 and RS18 relative to all other locations. The Overland allele of *QYr.hwwgIT–2D$_a$* was most favorable at PL20 and RS18 relative to all other locations (Table 1.6). The QTL x E interaction effect did not predominate the additive effect for the list QTLs.

Using the IWGSCv2.1 map, the additive effects of the Overley allele for the SEV QTLs (*QYr.hwwgSEV–2A$_a$* and *QYr.hwwgSEV–2B.2$_b$*) were negative, indicating more resistance to stripe rust (Table 1.6). The Overley allele of *QYr.hwwgSEV–2A$_a$* was most favorable for resistance at PL19, relative to all other locations. The Overley allele of *QYr.hwwgSEV–2B.2$_b$* was most favorable at PL20 relative to all other locations (Table 1.6). The Overland allele for the SEV QTLs (*QYr.hwwgSEV–2B.1$_a$* and *QYr.hwwgSEV–2D$_a$* was positive, indicating more resistance to stripe rust. The Overland allele of *QYr.hwwgSEV–2B.1$_a$* was most favorable at RS19 relative to all other locations (Table 1.6). The Overland allele of *QYr.hwwgSEV–2D$_a$* was most favorable at PL19, relative to all other locations.

Figure 1.2. Linkage maps of IWGSCv2.1 map using ML-BLUPs for stripe rust infection type and severity.
Linkage maps of chromosome group 2 (2A, 2B, and 2D) using the IWGSCv2.1 map showing QTL peaks for A) IT and B) SEV using multi-location BLUPs (ML-BLUP).

A.) Stripe rust infection type

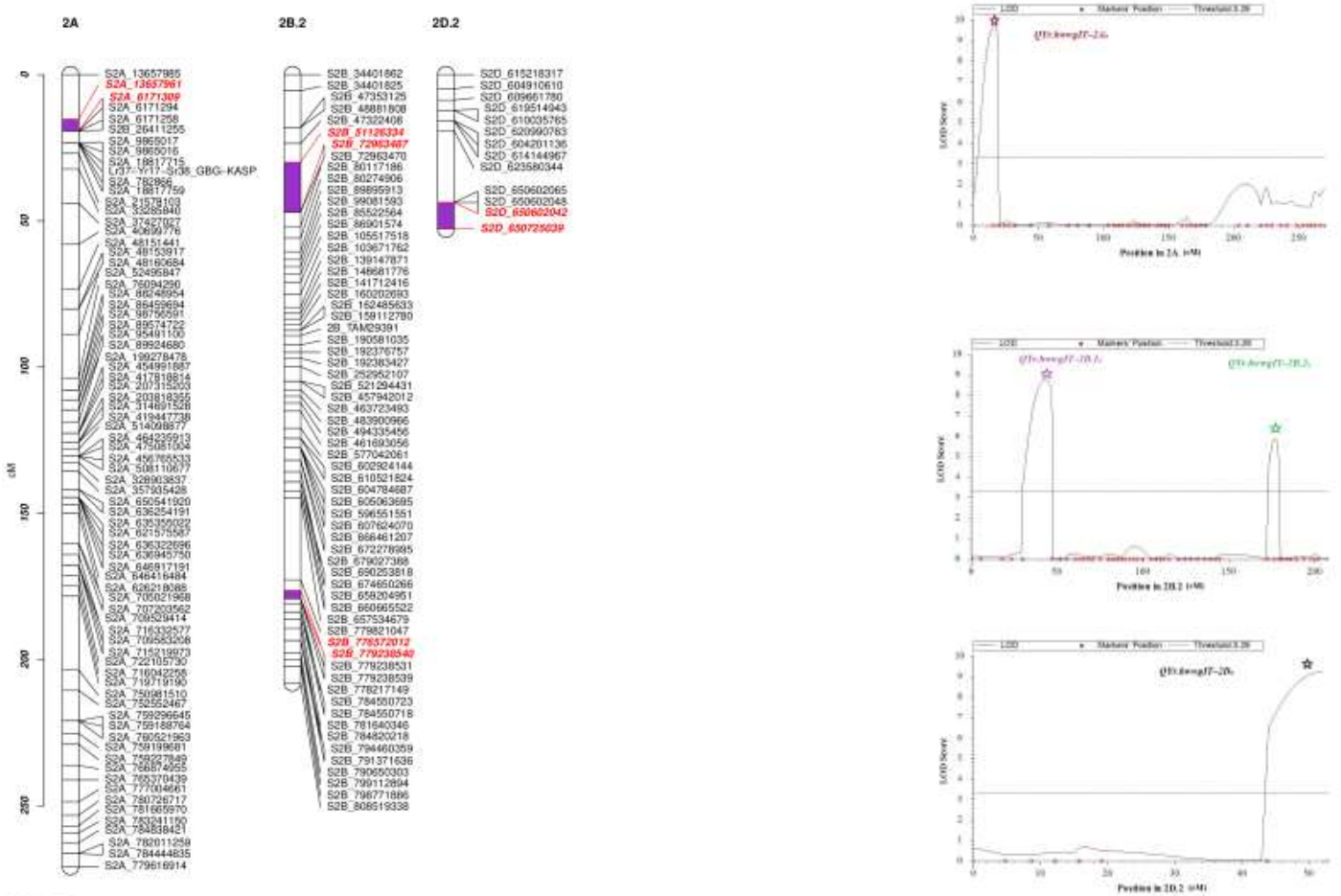

B.) Stripe rust severity

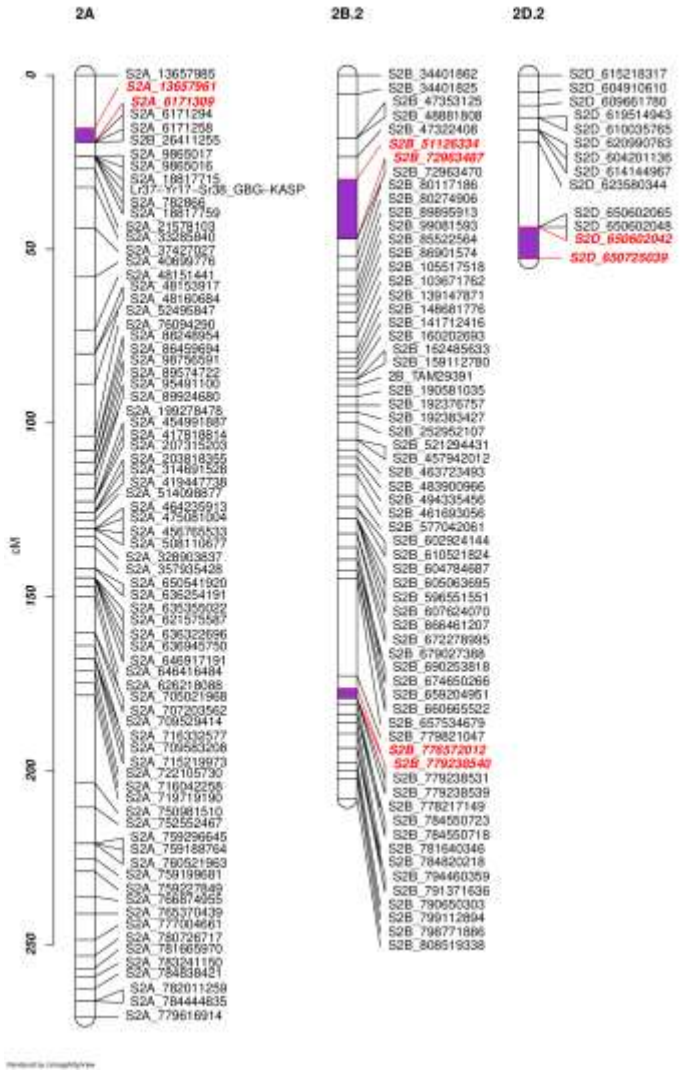

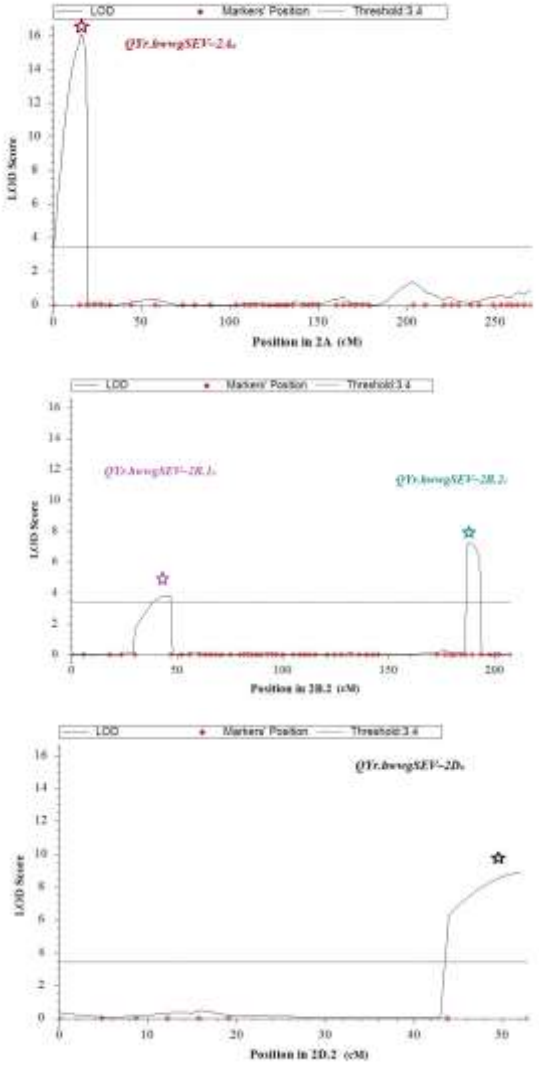

Figure 1.3. Genetic linkage maps of significant QTLs using MET- analysis for stripe rust IT and SEV using the IWGSCv2.1 reference map.

Major QTLs using a linkage map developed from SNPs identified for stripe rust infection type (IT) (A) and severity (SEV) (B) across seven trials (MET-analysis; Table 1.5) using the IWGSCv2.1 reference-derived map.

A.) Stripe rust infection type

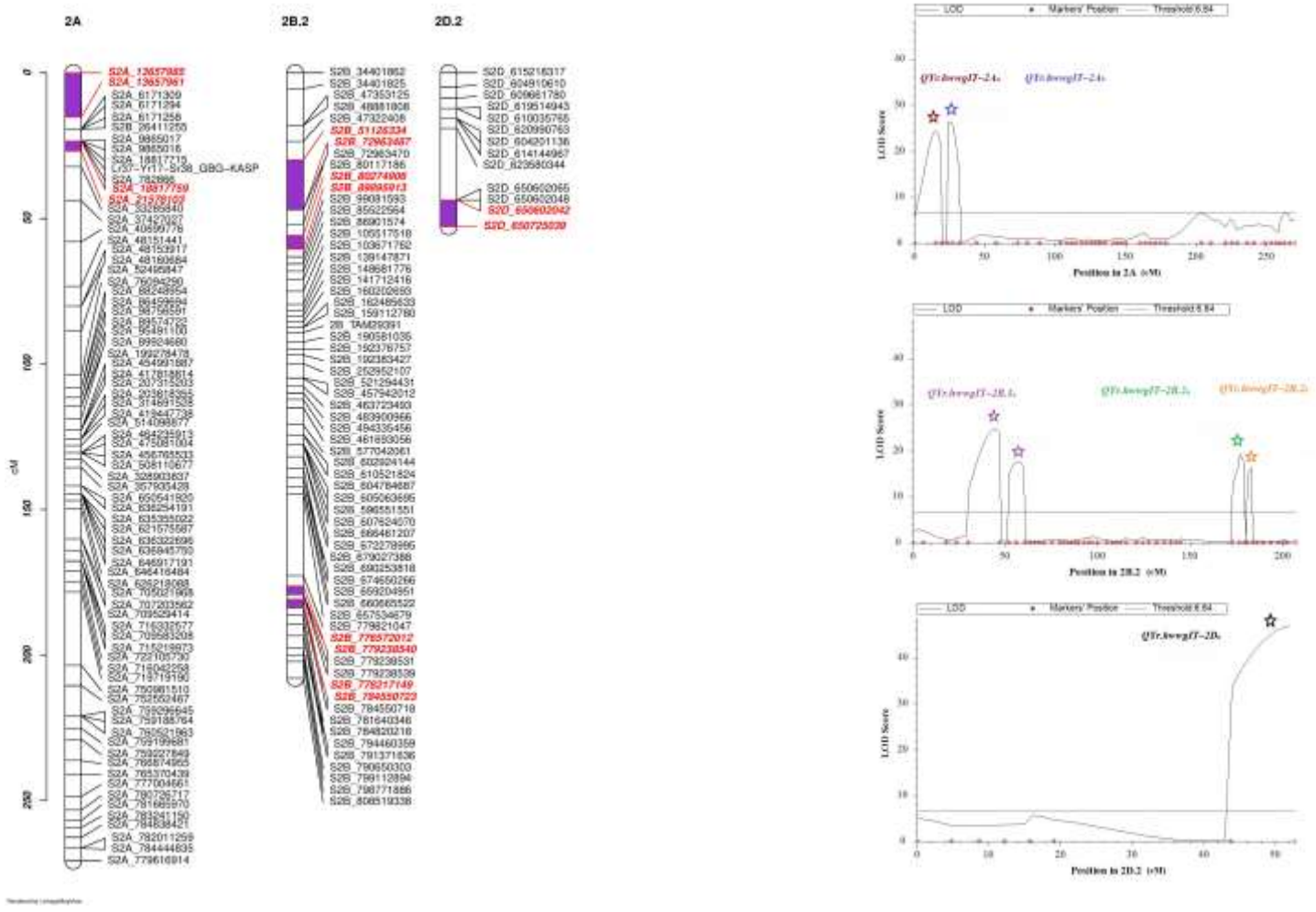

B.) Stripe rust severity

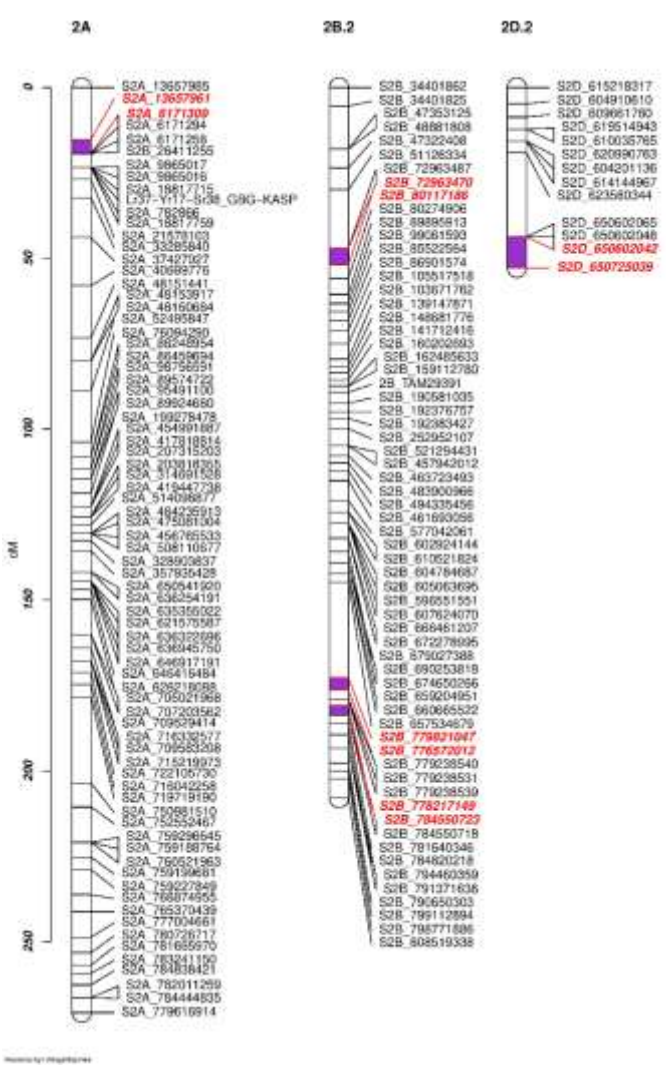

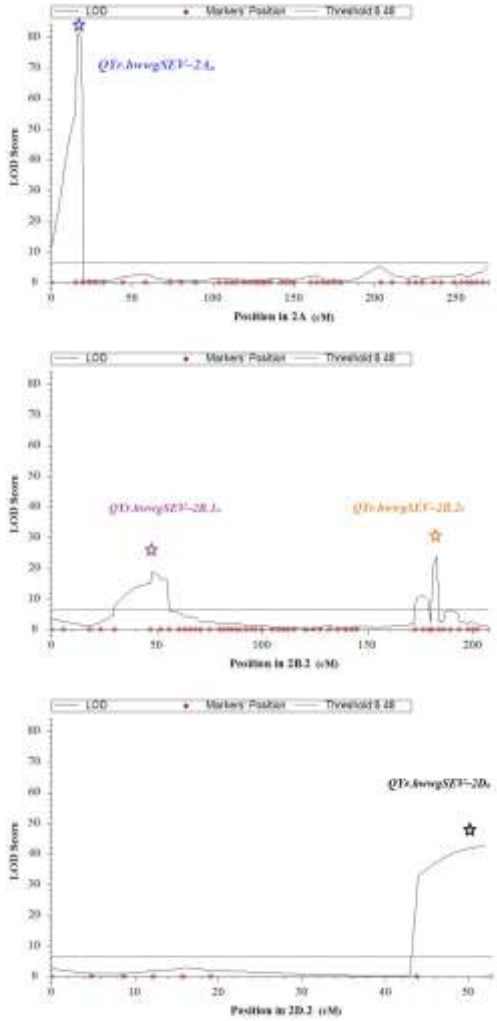

QTL-associated SNP Assays

Kompetitive allele-specific PCR (KASP) marker assays were developed by using the exome capture marker data (https://wheat-arsks.triticeaetoolbox.org). The 2B KASP assays (2BS:53467101 and 2BS:57674889) were most reliable for *QYr.hwwgIT–2B.1*$_a$ and *QYr.hwwgSEV–2B.1*$_a$. In addition, one useful KASP assay was identified for *QYr.hwwgIT–2B.2*$_a$ (2BL:770650575) that detects adjacent SNPs at 779821067 in the IWGSC v2.1 reference. The 2D KASP assays 2D:638369560 and 2D:639534738 were most reliable for *QYr.hwwgIT–2D*$_a$ and *QYr.hwwgSEV–2D*$_a$. Single marker analysis for the effect of these specific SNPs and the marker for the 2N^{v}S translocation are shown in Table 1.7. The multiple regression model incorporated SNPs for the four primary QTLs on chromosomes 2A, 2B, and 2D, which explained 55% of the phenotypic variation for IT and SEV (Table 1.7). All SNP assays are listed in Table 3.12.

Table 1.7. Marker regression analysis for stripe rust IT and SEV.
Marker regression analyses to predict multilocation best linear unbiased predictors of stripe rust infection type and severity expressed as the effect of the Overley allele. Coefficients for multiple regression models were developed using forward-reverse regression analysis. Standard errors are shown in parentheses.

	Single marker regression					
	Infection type (Score)		Severity (%)		Multiple regression coefficients	
Marker assay	R^2	Effect	R^2	Effect	Infection type (Score)	Severity (%)
Lr37-Yr17-Sr38_GBG-KASP	0.09	-0.25 (0.06)	0.20	-4.10 (0.61)	-0.29 (0.04)	-4.61 (0.49)
2B:53467101	0.08	0.24 (0.06)	0.01	1.21 (0.67)		
2B:57674889	0.09	0.33 (0.06)	0.02	1.52 (0.69)	0.31 (0.04)	2.17 (0.50)
2B:770650575	0.04	-0.18 (0.06)	0.08	-2.77 (0.68)	-0.26 (0.04)	-3.23 (0.52)
2D:638369560	0.13	0.33 (0.06)	0.08	2.99 (0.76)		
2D:639534738	0.20	0.36 (0.06)	0.13	3.31 (0.65)	0.43 (0.04)	4.25 (0.49)
Intercept					5.57 (0.09)	38.38 (1.03)
Model R^2					0.55	0.55

Discussion

Our study evaluated genomic regions associated with the IWGSC v2.1 and Jagger reference-derived maps. We identified four genomic regions (2AS, 2BS, 2BL, and 2DL) associated with field resistance to stripe rust. The QTL analysis using both stripe rust IT and SEV generally identified the same genomic regions with a relatively high correlation (r = 0.88) between the two traits. Our results showed that Overley contributed the resistance alleles at 2AS (*QYr.hwwgIT–2A$_a$*, *QYr.hwwgSEV–2A$_a$*) and 2BL (*QYr.hwwgIT–2B.2$_a$*, *QYr.hwwgSEV–2B.2$_c$*) QTL, whereas Overland contributed the resistance alleles at 2BS (*QYr.hwwgIT–2B.1$_a$*, *QYr.hwwgSEV–2B.1$_a$*) and 2DL (*QYr.hwwgIT–2D$_a$*, *QYr.hwwgSEV–2D$_a$*) QTLs. There were no meaningful differences in interpreting the data from both maps, beyond the Jagger linkage map being longer due to fragmentation within the map. Analysis using the multi-location (average across environments) BLUPs presented a more concise interpretation of the genomic regions associated with rust resistance than multi-environmental trial analysis. The multi-environment QTL analysis presented more fragmented QTL analysis results, which may be indicative of the reactive nature of each environment in response to stripe rust field resistance.

The 2N^{v}S translocation segment from *Aegilops ventricosa* has been utilized in wheat disease-resistant breeding programs since the 1990s (Gao et al., 2020). This segment has been known to provide resistance to different diseases such as stem rust, leaf rust, stripe rust, and root knot nematode (*Meloidogyne* spp). The 2AS QTL is associated with the 2N^{v}S translocation conferring *Yr17*. This translocation has been characterized in a recent study using *de novo* assembly in 'CDC Stanley' and Jagger that delimited the translocation to a 33 Mb region. Gao et al. (2020) outlined the 2N^{v}S translocation to a genomic segment size of 32.53 Mb in Jagger and 24.64 Mb in Chinese Spring. All SNPs associated with the QTL on 2AS identified in our map

were in the distal region of the 2AS, which fits into the 2N^{v}S translocation region. Recombination was not observed within the < 24.64 Mb region where the Lr37-Yr17-Sr38_GBG-KASP marker was mapped in the IWGSC v2.1 map. The Jagger map included 36 SNPs together with the Lr37-Yr17-Sr38_GBG-KASP marker within the 33 Mb translocation region. Gao et al. (2020) determined that the 2N^{v}S translocation does not recombine with the wheat chromosome, so any recombination events discovered in our study can be due to alignment or sequencing errors when implementing the TASSEL-SNP calling pipeline. The 2AS QTLs identified in our study are within the 2N^{v}S translocation region, where the favorable allele for resistance is from Overley. Therefore, all 2AS QTLs identified in this 2AS region are the QTLs of 2N^{v}S translocation (*QYr.hwwg-2A*: *QYr.hwwgIT–2A$_a$, QYr.hwwgSEV–2A$_a$, QYr.hwwgIT–2A$_b$, QYr.hwwgSEV–2A$_b$, QYr.hwwgSEV–2A$_c$*)

The 2AS QTLs associated with the 2N^{v}S translocation was important for IT and SEV in the Overley × Overland population, although virulence to *Yr17* occurred in the pathogen population. A similar trend of this QTL was observed in the Jagger × 2174 population (*Qyr.osu-2A*) but explained a much larger proportion of the phenotypic variation (80 - 93%) in four U.S. environments tested between 2008 and 2010 (Fang et al., 2011). In 2010, a predominant race of stripe rust broke the long-effective *Yr17* resistance in the U.S. Great Plains. However, a few cultivars remained resistant to the *Yr17*-virulent race (Basnet et al., 2014). The reduced effectiveness of the 2AS QTL in our study relative to the earlier study in Jagger × 2174 likely is likely due to differences in virulence to *Yr17*. The findings in our study indicated that resistance of the 2AS QTLs is from the 2N^{v}S translocation and could be associated with the *Yr17* gene continuing to provide effective resistance. The *Yr17* gene has not been cloned, and the 2N^{v}S fragment has no recombination with wheat. So, the *Yr* gene may consist of several genes, some

lacking resistance but others still resistant. The recent *de novo* assembly of the 2N^{v}S segment in Jagger and 'CDC Stanley' (Gao et al., 2020) identified 535 high-confidence genes in this 33 Mb segment, among which 58 genes were annotated as containing > 10% nucleotide-binding domain leucine-rich repeats (NLRs), and several genes were annotated as ABC transporters which may serve as candidates for disease resistance against multiple fungal pathogens. In addition, evaluation of NLR genes found that the number of NLR gene(s) in 2N^{v}S (n = 58) was greater than that in Chinese Spring (n = 35). Further investigation may determine the specific gene(s) within the 2N^{v}S segment that confers the partial APR to *Yr17*-virulent pathogen populations.

The 2B chromosome provides a rich source of genes for resistance to the stripe rust pathogen. The Catalog of Gene Symbols of Wheat (https://shigen.nig.ac.jp/wheat/komugi/genes/symbolClassList.jsp, accessed October 26, 2020) lists *Yr5* and *Yr7*, which appear to be allelic (Zhang et al., 2009), *Yr27*, *Yr31*, *Yr41*, *Yr43*, *Yr44*, *Yr53*, and *Yr72*. A meta-analysis of adult plant resistance QTLs (Rosewarne et al., 2013) grouped the numerous QTL into four meta-QTL regions, *QRYr2B.1* to *QRYr2B.4*. The *QRYr2B.1* region is located at the telomere of 2BS, which is not consistent with the location of *QYr.hwwg-2B.1*. The genomic positions of flanking markers of *QYr.hwwg-2B.1* (51.3 – 89.89 Mb, IWGSC v2.1map) are consistent with the QTL region *QRYr2B.2*, which is flanked by *Xwmc154* (41.2 Mb, IWGSC v2.1 map), and includes *wPt0079* (195.6 Mb, IWGSC v2.1 map). The genomic positions of flanking markers of *QYr.hwwg-2B.2* (776.6 – 784.8 Mb, IWGSC v2.1 map) are consistent with the QTL region *QRYr2B.4*, which includes *WMS526* (*Yr7*) (782.3 Mb, IWGSC v2.1 map). The major QTL in the hard winter wheat TAM 111, *QYr.tamu-2BL* (Basnet et al., 2014b), was mapped to the interval 154.3 – 159.7 Mb (Yang et al., 2019). No QTLs were identified in this region in the Overley × Overland population. A GWAS on North American

winter wheat (Mu et al., 2020) identified APR-associated SNPs at 9 and 47 Mb. *QYr.hwwg-2B.1* may be related to *QYrwww.wgp.2B-2* at 47 Mb. The GWAS analysis did not identify any APR-associated SNPs in the region of *QYr.hwwg-2B.2* identified in our study.

The named stripe rust resistance genes on 2D include *Yr8, Yr16, Yr37, Yr54,* and *Yr55.* The SNPs flanking *QYr.hwwg–2D* was at 650.6 and 650.7 Mb (IWGSC v2.1 map) near the distal end of 2DL. This position is consistent with the adult plant resistance gene *Yr54* from the spring wheat 'Quaiu' (Basnet et al., 2014a). The DArT markers *wPt-667054* (654.3 Mb, IWGSC v2.1 map) and *wPt-667485* (652.0 Mb, IWGSC v2.1 map) were associated with the QTL *QYr.tam-2D* as well as microsatellite marker *Xgwm301* (648.9 Mb, IWGSC v2.1 map) (Somers et al., 2004), which was designated *Yr54* and explained 49-54% of phenotypic variation. *Xgwm301* is located at 649Mb, relatively close to the QTLs associated with *QYr.hwwg–2D*. In our initial map construction, the telomeric region of 2DL was eliminated based on filtering parameters, as described in the genotyping and map construction section. Still, using the ASMap package, the 2DL telomeric region was recovered through restoration analysis. This QTL was not identified in the GWAS of North American Winter Wheat (Mu et al., 2020).

The combination of KASP marker assays for the QTLs identified in this study explained a substantial proportion of the phenotypic variation (55%) across seven environments. In our study, the 2AS and 2DL QTLs generally explained a larger proportion of variance for both disease traits using both the Jagger and IWGCS v2.1 reference maps than the QTLs identified on 2B. The KASP-SNPs associated with *QYr.hwwg-2B.1, QYr.hwwg-2B.2,* and *QYr.hwwg-2D* in combination with the KASP assay for the $2N^{v}S$ translocation explained 55% of the phenotypic variation for IT and 55% of the variation for severity. The markers designed in this study can be used by breeders working with germplasm derived from the Overley and Overland pedigrees.

Further efforts to refine the QTL intervals would be challenging for *QYr.hwwg-2B.1* and *QYr.hwwg-2B.2,* which have relatively modest and environmentally responsive effects in regions with abundant resistance genes. Further efforts to refine the QTL interval for *QYr.hwwg-2D* might be more advantageous due to better environmental stability of this resistance and larger effect.

Our QTL x environment results from MET analysis were significant for both IWGSCv2.1 and Jagger reference maps. We identified the same chromosomal arms in both maps from this analysis (2AS, 2BS, 2BL, and 2DL). But the key observation from the MET analysis was that the QTLs were significantly stronger (LOD > 12; PVE > 10 %) and more fragmented than the results from ML-BLUP data. Our results effectively identified environments that contributed to the responses of major QTLs for both maps. In addition, this analysis could identify which QTL and which environment contributed to the QTLs identified for IT or SEV resistance. The $2N^{v}S$ segment (2AS) for IT and SEV resistance identified strong QTLs using the IWGSCv2.1 map in 2019 (CF: IT, RS: IT, PL: SEV). Using the Jagger map, the $2N^{v}S$ segment identified strong QTLs for stripe rust resistance in 2019 (CF: IT) and 2020 (PL: SEV) which had more resistance to stripe rust at the respective locations. The 2BS QTLs for IT and SEV were strong in 2019 (RS: IT and SEV) using the IWGSCv2.1 map, indicating more stripe rust resistance. Using the Jagger map for IT, there was strong stripe rust resistance in 2020 (CF and PL) on 2BS. There were no stripe rust SEV QTL identified on 2BS. The 2BL QTLs for IT were stronger, indicating more stripe rust resistance in 2018 and 2019 using the IWGSCv2.1 map (2018: RS; 2019: RS and CF). For SEV resistance, the QTLs were stronger in 2020 (PL) than in 2019. Using the Jagger map QTLs for resistance to stripe rust severity were found on 2BL in 2018 (RS). The 2DL QTLs using the IWGSCv2.1 map were strong for IT resistance in 2018

(RS) and 2020 (PL). The 2DL QTLs for SEV resistance were stronger in CF and PL relative to all other environments in 2019 than in 2020. Using the Jagger map for IT, the 2DL QTLs were stronger in 2018 (RS) than in the other years, and for SEV, the QTLs were stronger in 2020 (CF and PL) for stripe rust resistance than in 2018 (RS).

Conclusion

We learned two lessons in conducting this analysis. First, the construction of genetic maps using the two alternative reference sequences produced similar resulting final maps. Although one of the parents of the population, Overley, has Jagger as a direct parent, the map developed on the Jagger reference sequence did not appear to have obvious advantages for this population. The second lesson is that it is vital to exercise caution in filtering SNPs before map construction. While it is desirable to ensure that SNPs used in map construction are high quality and that a parsimonious set of SNPs are used, there is a real risk of losing valuable information in filtering. A review of discarded SNPs can be instrumental in retaining valuable information.

The take-home messages for breeders using the Great Plains germplasm pool are that: 1) the $2N^{v}S$ translocation conferring *Lr37-Yr17-Sr38* continues to have additive value for adult plant resistance to stripe rust; QTL regions on 2BS and 2BL contribute additive resistance to stripe rust; the region defined by *QYr.hwwg-2D,* also contributes allele(s) for adult plant resistance to stripe rust; and 2) The four major QTL regions identified in this study would be valuable to retain in combination with new, major gene resistance alleles as part of a long-term strategy for durable resistance to stripe rust.

References

Alaux, M., Rogers, J., Letellier, T., Flores, R., Alfama, F., Pommier, C., … Quesneville, H. (2018). Linking the International Wheat Genome Sequencing Consortium bread wheat reference genome sequence to wheat genetic and phenomic data. *Genome Biology*. https://doi.org/10.1186/s13059-018-1491-4

Baenziger, P. S., Beecher, B., Graybosch, R. A., Ibrahim, A. M. H., Baltensperger, D. D., Nelson, L. A., … Bai, G. (2008). Registration of 'NE01643' Wheat. *Journal of Plant Registrations*. https://doi.org/10.3198/jpr2007.06.0327crc

Bariana, H. S., & McIntosh, R. A. (1993). Cytogentic studies in wheat. XV. Location of rust resistance genes in VPM1 and their genetic linkage with other disease resistance genes in chromosome 2A. *Genome*. https://doi.org/10.1139/g93-065

Basnet, B. R., Singh, R. P., Ibrahim, A. M. H., Herrera-Foessel, S. A., Huerta-Espino, J., Lan, C., & Rudd, J. C. (2014). Characterization of Yr54 and other genes associated with adult plant resistance to yellow rust and leaf rust in common wheat Quaiu 3. *Molecular Breeding*, *33*(2), 385–399. https://doi.org/10.1007/s11032-013-9957-2

Basnet, Bhoja R., Ibrahim, A. M. H., Chen, X., Singh, R. P., Mason, E. R., Bowden, R. L., … Rudd, J. C. (2014a). Molecular mapping of stripe rust resistance in hard red winter wheat TAM 111 adapted to the U.S. High Plains. *Crop Science*. https://doi.org/10.2135/cropsci2013.09.0625

Basnet, Bhoja R., Ibrahim, A. M. H., Chen, X., Singh, R. P., Mason, E. R., Bowden, R. L., … Rudd, J. C. (2014b). Molecular mapping of stripe rust resistance in hard red winter wheat TAM 111 adapted to the U.S. High Plains. *Crop Science*, *54*(4), 1361–1373. https://doi.org/10.2135/cropsci2013.09.0625

Bayles, R. A., Flath, K., Hovmoller, M. S., & De Vallavieille-Pope, C. (2000). Breakdown of the Yr17 resistance to yellow rust of wheat in northern Europe. *Agronomie*. https://doi.org/10.1051/agro:2000176

Bradbury, P. J., Zhang, Z., Kroon, D. E., Casstevens, T. M., Ramdoss, Y., & Buckler, E. S. (2007). TASSEL: Software for association mapping of complex traits in diverse samples. *Bioinformatics*. https://doi.org/10.1093/bioinformatics/btm308

Broman, K. W., Wu, H., Sen, Ś., & Churchill, G. A. (2003). R/qtl: QTL mapping in experimental crosses. *Bioinformatics*, *19*(7), 889–890. https://doi.org/10.1093/bioinformatics/btg112

Carter, A. H., Allan, R. E., Shelton, G. B., Burke, A. B., Balow, K. A., Hagemeyer, K. E., … Klarquist, E. F. (2020). How 'Madsen' has shaped Pacific Northwest wheat and beyond. *Journal of Plant Registrations*. https://doi.org/10.1002/plr2.20049

Chen, J., Chu, C., Souza, E. J., Guttieri, M. J., Chen, X., Xu, S., … Zemetra, R. (2012). Genome-wide identification of QTL conferring high-temperature adult-plant (HTAP) resistance to stripe rust (Puccinia striiformis f. sp. tritici) in wheat. *Molecular Breeding*. https://doi.org/10.1007/s11032-011-9590-x

Chen, X. (2013). Review Article: High-Temperature Adult-Plant Resistance, Key for Sustainable Control of Stripe Rust. *American Journal of Plant Sciences*. https://doi.org/10.4236/ajps.2013.43080

Chen, X. M. (2005a). Epidemiology and control of stripe rust [Puccinia striiformis f. sp. tritici] on wheat. *Canadian Journal of Plant Pathology*. https://doi.org/10.1080/07060660509507230

Chen, X. M. (2005b). Epidemiology and control of stripe rust [Puccinia striiformis f. sp. tritici] on wheat. *Canadian Journal of Plant Pathology*, *27*(3), 314–337. https://doi.org/10.1080/07060660509507230

Cruppe, G., DeWolf, E., Jaenisch, B. R., Andersen Onofre, K., Valent, B., Fritz, A. K., & Lollato, R. P. (2021). Experimental and producer-reported data quantify the value of foliar fungicide to winter wheat and its dependency on genotype and environment in the U.S. central Great Plains. *Field Crops Research*, *273*(September), 108300. https://doi.org/10.1016/j.fcr.2021.108300

Fang, T., Campbell, K. G., Liu, Z. Y., Chen, X., Wan, A., Li, S., … Yan, L. (2011). Stripe rust resistance in the wheat cultivar Jagger is due to Yr17 and a novel resistance gene. *Crop Science*, *51*(6), 2455–2465. https://doi.org/10.2135/cropsci2011.03.0161

Gao, L., Koo, D. H., Juliana, P., Rife, T., Singh, D., Lemes da Silva, C., … Poland, J. (2020). The Aegilops ventricosa 2NvS segment in bread wheat: cytology, genomics and breeding. *Theoretical and Applied Genetics*. https://doi.org/10.1007/s00122-020-03712-y

Hussain, W., Stephen Baenziger, P., Belamkar, V., Guttieri, M. J., Venegas, J. P., Easterly, A., … Poland, J. (2017). Genotyping-by-Sequencing Derived High-Density Linkage Map and its Application to QTL Mapping of Flag Leaf Traits in Bread Wheat. *Scientific Reports*. https://doi.org/10.1038/s41598-017-16006-z

Jaenisch, B. R., de Oliveira Silva, A., DeWolf, E., Ruiz-Diaz, D. A., & Lollato, R. P. (2019). Plant population and fungicide economically reduced winter wheat yield gap in kansas. *Agronomy Journal*, *111*(2), 650–665. https://doi.org/10.2134/agronj2018.03.0223

Krasileva, K. V., Vasquez-Gross, H. A., Howell, T., Bailey, P., Paraiso, F., Clissold, L., … Dubcovsky, J. (2017). Uncovering hidden variation in polyploid wheat. *Proceedings of the National Academy of Sciences*, *114*(6), E913–E921. https://doi.org/10.1073/PNAS.1619268114

Krattinger, S. G., Lagudah, E. S., Spielmeyer, W., Singh, R. P., Huerta-Espino, J., McFadden, H., … Keller, B. (2009). A Putative ABC Transporter Confers Durable Resistance to Multiple Fungal Pathogens in Wheat. *Science*, *323*(5919), 1360 LP – 1363.

https://doi.org/10.1126/science.1166453

Kumar, D., Kumar, A., Chhokar, V., Gangwar, O. P., Bhardwaj, S. C., Sivasamy, M., … Tiwari, R. (2020). Genome-Wide Association Studies in Diverse Spring Wheat Panel for Stripe, Stem, and Leaf Rust Resistance. *Frontiers in Plant Science*. https://doi.org/10.3389/fpls.2020.00748

Li, H., Ribaut, J. M., Li, Z., & Wang, J. (2008). Inclusive composite interval mapping (ICIM) for digenic epistasis of quantitative traits in biparental populations. *Theoretical and Applied Genetics*. https://doi.org/10.1007/s00122-007-0663-5

Liu, G., Liu, X., Xu, Y., Bernardo, A., Chen, M., Li, Y., … Bai, G. (2020). Reassigning Hessian fly resistance genes H7 and H8 to chromosomes 6A and 2B of the wheat cultivar 'Seneca' using genotyping-by-sequencing. *Crop Science*, *60*(3). https://doi.org/10.1002/csc2.20148

Maccaferri, M., Zhang, J., Bulli, P., Abate, Z., Chao, S., Cantu, D., … Dubcovsky, J. (2015). A genome-wide association study of resistance to stripe rust (Puccinia striiformis f. sp. tritici) in a worldwide collection of hexaploid spring wheat (Triticum aestivum L). *G3: Genes, Genomes, Genetics*, *5*(3), 449–465. https://doi.org/10.1534/g3.114.014563

McKenna, A., Hanna, M., Banks, E., Sivachenko, A., Cibulskis, K., Kernytsky, A., … DePristo, M. A. (2010). The genome analysis toolkit: A MapReduce framework for analyzing next-generation DNA sequencing data. *Genome Research*, *20*(9), 1297–1303. https://doi.org/10.1101/gr.107524.110

Meng, L., Li, H., Zhang, L., & Wang, J. (2015). QTL IciMapping: Integrated software for genetic linkage map construction and quantitative trait locus mapping in biparental populations. *Crop Journal*. https://doi.org/10.1016/j.cj.2015.01.001

Milus, E. A., Lee, K. D., & Brown-Guedira, G. (2015). Characterization of stripe rust resistance in wheat lines with resistance gene Yr17 and implications for evaluating resistance and virulence. *Phytopathology*. https://doi.org/10.1094/PHYTO-11-14-0304-R

Mu, J., Liu, L., Liu, Y., Wang, M., See, D. R., Han, D., & Chen, X. (2020). Genome-Wide Association Study and Gene Specific Markers Identified 51 Genes or QTL for Resistance to Stripe Rust in U.S. Winter Wheat Cultivars and Breeding Lines. *Frontiers in Plant Science*, *11*(July). https://doi.org/10.3389/fpls.2020.00998

Patel, R. K., & Jain, M. (2012). NGS QC toolkit: A toolkit for quality control of next generation sequencing data. *PLoS ONE*, *7*(2). https://doi.org/10.1371/journal.pone.0030619

Ramirez-Gonzalez, R. H., Uauy, C., & Caccamo, M. (2015). PolyMarker: A fast polyploid primer design pipeline. *Bioinformatics*, *31*(12), 2038–2039. https://doi.org/10.1093/bioinformatics/btv069

Rathore, A., & Icrisat, B. U. (2012). *Genetic map construction with R / qtl*. 1–41. Retrieved from http://www.rqtl.org

Rosewarne, G. M., Herrera-Foessel, S. A., Singh, R. P., Huerta-Espino, J., Lan, C. X., & He, Z. H. (2013). Quantitative trait loci of stripe rust resistance in wheat. *TAG. Theoretical and Applied Genetics. Theoretische Und Angewandte Genetik*, *126*(10), 2427–2449. https://doi.org/10.1007/s00122-013-2159-9

Sears, R. G., Moffatt, J. M., Martin, T. J., Cox, T. S., Bequette, R. K., Curran, S. P., … Witt, M. D. (1997). Registration of 'Jagger' Wheat. *Crop Science*. https://doi.org/10.2135/cropsci1997.0011183x003700030062x

Segall, R. S., Zhang, Q., & Pierce, R. M. (2010). Data mining supercomputing with SAS JMP® genomics. *WMSCI 2010 - The 14th World Multi-Conference on Systemics, Cybernetics and Informatics, Proceedings*.

Singh, R. P., Huerta-Espino, J., Bhavani, S., Herrera-Foessel, S. A., Singh, D., Singh, P. K., … Crossa, J. (2011). Race non-specific resistance to rust diseases in CIMMYT spring wheats. *Euphytica*, *179*(1), 175–186. https://doi.org/10.1007/s10681-010-0322-9

Singh, R. P., Huerta-Espino, J., & Rajaram, S. (2000). Achieving Near-immunity to Leaf and Stripe Rusts in Wheat by Combining Slow Rusting Resistance Genes. *Acta Phytopathologica et Entomologica Hungarica*.

Singh, R. P., Mujeeb-Kazi, A., & Huerta-Espino, J. (1998). Lr46: A gene conferring slow-rusting resistance to leaf rust in wheat. *Phytopathology*, *88*(9), 890–894. https://doi.org/10.1094/PHYTO.1998.88.9.890

Singh, R. P., & Rajaram, S. (1992). Genetics of adult-plant resistance of leaf rust in "Frontana" and three CIMMYT wheats. *Genome*, *35*(1), 24–31. https://doi.org/10.1139/g92-004

Singh, Ravi Prakash, Huerta-Espino, J., & William, H. M. (2005). Genetics and breeding for durable resistance to leaf and stripe rusts in wheat. *Turkish Journal of Agriculture and Forestry*, *29*(2), 121–127. https://doi.org/10.3906/tar-0402-2

Somers, D. J., Isaac, P., & Edwards, K. (2004). A high-density microsatellite consensus map for bread wheat (Triticum aestivum L). *Theoretical and Applied Genetics*, *109*(6), 1105–1114. https://doi.org/10.1007/s00122-004-1740-7

Taylor, A. J., Butler, D., & Taylor, M. J. (2018). *Package ' ASMap .'*

Taylor, J., & Butler, D. (2017). R package ASMap: Efficient genetic linkage map construction and diagnosis. *Journal of Statistical Software*, *79*(Stam 1993). https://doi.org/10.18637/jss.v079.i06

Wan, A., & Chen, X. (2014). Virulence characterization of puccinia striiformis f. Sp. tritici using a new set of yr single-gene line differentials in the united states in 2010. *Plant Disease*, *98*(11), 1534–1542. https://doi.org/10.1094/PDIS-01-14-0071-RE

William, M., Singh, R. P., Huerta-Espino, J., Ortiz Islas, S., & Hoisington, D. (2003). Molecular marker mapping of leaf rust resistance gene Lr46 and its association with stripe rust

resistance gene Yr29 in wheat. *Phytopathology*. https://doi.org/10.1094/PHYTO.2003.93.2.153

Yang, Y., Basnet, B. R., Ibrahim, A. M. H., Rudd, J. C., Chen, X., Bowden, R. L., … Liu, S. (2019). Developing KASP markers on a major stripe rust resistance QTL in a popular wheat TAM 111 using 90K array and genotyping-by-sequencing SNPs. *Crop Science*, *59*(1), 165–175. https://doi.org/10.2135/cropsci2018.05.0349

Zhang, P., McIntosh, R. A., Hoxha, S., & Dong, C. (2009). Wheat stripe rust resistance genes Yr5 and Yr7 are allelic. *Theoretical and Applied Genetics*, *120*(1), 25–29. https://doi.org/10.1007/s00122-009-1156-5

Zhu, T., Wang, L., Rimbert, H., Rodriguez, J. C., Deal, K. R., De Oliveira, R., … Luo, M. C. (2021). Optical maps refine the bread wheat Triticum aestivum cv. Chinese Spring genome assembly. *Plant Journal*, *107*(1), 303–314. https://doi.org/10.1111/tpj.15289

Chapter 2 - Review of Genetic Architecture of Wheat Yield Components

Introduction

Bread wheat (*Triticum aestivum* L) is an allohexaploid species derived from two hybridization events and has evolved through ancient human migration across the world (Balfourier et al., 2019). The dispersion of wheat across Europe and Asia led to domesticated wheat populations adapting to local environments, producing landraces. In the past two centuries, breeding programs were developed in Europe and Asia to improve these landraces. (Balfourier et al., 2019). Wheat is a major staple food crop that provides 20% of energy and protein in the human diet globally. But, there will be a tremendous increase in food demand by 2050 due to population growth, socio-economic needs, and dietary changes (Crespo-Herrera et al., 2018).

In wheat, grain yield (GY) is the product of plant density, tiller number, number of spikes per plant, spikelet number per spike (SNS), grain number per spike (GNS), and grain weight (GWT) per unit of land area (https://smallgrains.ucanr.edu/Growth_-_Development/Yield_Components/ ; Slafer et al., 2022). These components of GY can be associated with pleiotropic factors such as plant height (PHT), flowering time (FT), and physiological maturity (PMAT) (Chen, 2005b; Slafer et al., 1990; Trachsel et al., 2017). The genetic architecture of these traits affects the individual components of GY. Individual components of GY can be defined as spikes per area, GNS, and average GWT, which all have relatively high heritability (Zhang et al., 2018). Therefore, understanding the underlying genetic mechanisms these yield (YLD) components is essential to increasing GY and satisfying food demands (Fischer, 2008; Serrago et al., 2013; Slafer et al., 2014). Characterizing the phenotypic expression of these traits in different genetic backgrounds can make it possible to identify better performing cultivars. In addition, this characterization can determine how each YLD-related trait

contributes to the genetic improvement of YLD. Many QTL studies have identified genomic regions that contribute to the phenotypic expression of YLD-related traits (Cao et al., 2020; Dubcovsky et al., 2006; Li et al., 2019; Maccaferri et al., 2008; Muhammad et al., 2020; Naruoka et al., 2011; Tyagi et al., 2015). In this review, we will discuss the findings of these studies to explain the genetic architecture of YLD components.

Table 2.1. Equations to Characterize Yield and Yield Components.

Equations modified from Acquaah, G. (2009). Principles of plant genetics and breeding. John Wiley & Sons.

Equation No.	Equation	Details
[1.0]	$\frac{G * W}{A} = \frac{G_n}{A} \times \frac{W}{G_i}$	*G*W* = grain weight; *A* = unit area; G_n = number of grains; G_i = individual grain; *W* = Weight. Yield in this equation is measured by grain weight per unit area focusing on the number of grains per unit area as the object of measurement.
[1.1]	$\frac{G_n}{A} = \frac{Sp}{A} \times \frac{G_n}{Sp}$	G_n = number of grains; *A* = unit area; *Sp* = number of spikes. Yield is measured by the number of grains per unit area. Yield in this equation uses the wheat spike density and prolificacy to measure the number of grains per unit area.
[1.2]	$\frac{G_n}{Sp} = \frac{Spl}{Sp} \times \frac{G_n}{Spl}$	G_n = number of grains; *Sp* = number of spikes; *Spl* = number of spikelets. Yield in this equation is using the wheat spike and spikelet structures to measure the number of grains per spike.
[1.3]	$\frac{G * W}{A} = \frac{P}{A} \times \frac{Sp}{P} \times \frac{Spl}{Sp} \times \frac{G_n}{Spl} \times \frac{W}{G_i}$	*G*W* = grain weight; *A*= unit area; *P* = number of plants; *Sp* = number of spikes; *Spl* = number of spikelets; G_i = number of grains; *W* = weight. Yield in this equation combines all previous variables described in equations [1.0] - [1.2] to measure the grain weight per unit area.

Genetic Architecture of Grain, Spikelet, and Yield Components

Grain development in wheat begins with fertilizing the ovary, a maternal structure containing the ovule, and ends with the mature grain. The ripe grain is comprised of three primary tissues, the embryo, endosperm, and maternal outer layers (Brinton et al., 2019). These tissues contain large amounts of starch, proteins, and other nutrients accumulated during grain development (Brinton et al., 2019). Nutrient uptake efficiency also plays a role in grain development and improvement in GY. Nutrient uptake efficiency depends on the crop root traits and nutrient mobility in the soil (Thorup-Kristensen, 2001). Two complementary characteristics in the root system regulate the efficiency of nutrient distribution within a crop—first, the capacity of the root to explore the soil profile (rate of root-soil penetration). The second is the roots' ability to capture nitrogen (e.g., nitrogen uptake per unit root length) (Rasmussen et al., 2015). Winter wheat roots reach a depth of 2.2 m due to an extended growth period (Thorup-Kristensen et al., 2009; Rasmussen et al., 2015). Breeding to improve nutrient uptake efficiency by targeting thinner roots would have more capacity to extract nutrients and enhance the grain development traits such as GWT (Aziz et al., 2017). The importance of acquiring nutrients by using the wheat roots system is defined by three main mechanisms: (i) mass flow, which is mainly dependent on water flow and soil solution concentration, and (ii) diffusion, which is dependent on soil characteristics such as soil buffer capacity, porosity tortuosity, water content and the concentration gradient from soil particles to root surface, and (iii) the rhizosphere effect, which is particularly vital for the interaction between crop roots, soil, and microorganisms (Slafer et al., 2020). Nutrient accumulation in wheat tissues is divided into two groups based on biomass accumulation. Group I: N, P, K, S, Ca, and Fe accumulate in advance to biomass, and group II: Mg, Zn, Cu, Mn, and B are delayed in early developmental stages based on the

availability of the element in the soil (Slafer et al., 2020). At anthesis, 70%, 80%, and 90% of the total N, P, and K uptake has occurred (Clarke et al., 1990; Malhi et al., 2007).

Flowering time, measured at 10.5.1-10.5.3 on the Feekes scale, typically occurs after the head has fully emerged and lasts 3-5 days. Grain development, which is characterized by the grain filling (Feekes 10.5.4 – 11.3) and grain ripening stages (Feekes 11.4), continues during the days post-anthesis (DPA) (White et al., 2008). In early DPA, the grain increases in size relative to the ovary. At this early stage, cytokinin levels are highest, which initiates a phase of rapid cell division (Hess et al., 2002). Trehalose-6-Phosphate (T6P), a sugar metabolite that regulates growth and development in response to assimilate availability, is also at very high levels in the grain tissue during the pre-grain filling and early grain development stages (Martínez-Barajas et al., 2011; O'Hara et al., 2013).

After the basic structure of the grain has been established, the grain filling period begins. The grain-filling period can be divided into four phases that evaluate the dynamics of grain growth post-pollination (Loss et al., 1989; Malloch et al., 1986; Slafer et al., 2020). The first phase in grain development is either the "lag phase" (a delay in starting growth), "grain set phase" (pollinated fertile florets may abort immediately after anthesis), or "watery ripe" (grain water uptake drives a rapid increase in volume (> 70%)) phase (Slafer et al., 2020). In this phase, cell division and endosperm development occur first, with the embryo's development later (Slafer et al., 2020). First, the endosperm creates the sink strength for each grain by producing the endosperm cells where dry matter is accumulated during grain filling. Then, grain weight potential (GWP) is established by the size of the ovary, which is determined by the number of endosperm cells and the volume of each grain (Slafer et al., 2020).

The second phase of grain development ("milky ripe") shows a strong liner relationship with GWT increasing dramatically. The water content of the grains has stabilized, and > 70% of the grain is starch, which is the driving force for grain growth (Slafer et al., 2020). Protein in the grain structure is only essential for grain quality, and complex carbohydrates are a source of dietary fibers developed in this phase (Slafer et al., 2020). The third phase of grain development ("dough grain") is the final stage, where the accumulation of dry matter and water content begins to decrease. This phase reaches completion when PMAT is reached, which is the state when the dry matter has peaked and the grain enters a quiescent state (Malloch et al., 1986).

The simplified calculation of GY is the product of grain number (GN) per unit area and grain size (GS), which has a positive correlation to grain weight (GWT) (Fischer, 2008; Li et al., 2017; Sinclair et al., 2006). Therefore, YLD improvement depends on the relationship between GWT and GN in all cereal crops. Grain weight is the simplest component to measure for GY, as explained by equation [1.0] (Table 2.1). It can be further defined by its sub-components, including carpel size, grain morphological parameters (length, width, height), and the dynamics of grain development that influence grain filling rate (Brinton et al., 2019; Slafer, 2007; Xie et al., 2015). Typically, a wheat spike consists of 15-20 spikelets, each containing two glumes and a variable number of florets. Each floret consists of a lemma and palea, encompassing the carpel and stamens, fertilizing to produce grain (Brinton et al., 2019; Slafer et al., 2020). Grains can vary in the developmental stage, weight, number, and fruiting efficiency when comparing different spikelets and even within individual spikelets of the same spike (Philipp et al., 2018). Variation in GWT can be due to the developmental rate of the spike and spikelet structures and competition for resource availability – although wheat is rarely sink-limited (Borrás et al., 2004). Not all spike and spikelet structures initiate or develop simultaneously. The time frame for

developing these structures can vary by day(s) or week(s), varying among cultivars. But, the general rule is that spike growth takes place approximately three weeks before anthesis (Kirby et al., 1987; González et al., 2003a). During this short period of spike development, florets have completed their development, presenting a strong correlation between the number of fertile florets and spike dry matter during anthesis (Slafer et al., 2020). After anthesis, grains become the major sink as reserves have accumulated to fill the grains (Slafer et al., 2020). Spike and spikelet development usually progresses bi-directionally, initiating from the center of the spike. Grains in the central spikelets are higher in GWT than in the remaining structure (Brinton et al., 2019). Floret development in a single spikelet can also present GWT variation. The floret structure develops sequentially and uni-directionally from the bottom up with alternating sides on the spikelet meristem (Brinton et al., 2019). In this structure, florets produced later develop smaller grains than the bottom basal floret that carries the larger grains. Previous studies have identified a strong association between carpel size and GWT (Brinton et al., 2019).

Different genes and molecular functions characterize GS and GWT by regulating cell numbers, which can affect cell size. For example, the *GW2* gene controls GS by hindering rice and wheat cell division. The cell size reduction occurs due to the interaction with *DA1*, a downstream target of the Arabidopsis *GW2* ortholog that negatively regulates cell number, and the two genes work together to influence GS (Dong et al., 2017; Song et al., 2007; Xia et al., 2013). Cell size can be modified directly or indirectly with different proteins or genes. For example, *XTH* is a gene that results in cellular expansion, and expansins are proteins that loosen the plant cell wall. They affect grain length in some cereal crops by disrupting the structural framework in cells. Simmonds et al. (2016) performed a study evaluating the *gw2-A1* mutant allele that shifted GS in tetraploid and hexaploid wheat across 13 experiments. A fundamental

discovery in this study is that *TaGW2* increases the carpel size by 10% in the A-genome mutant lines compared to the wild-type lines, increasing final GWT. Plant cell death (PCD) is also a factor involved in grain development in various tissues and stages of growth. For example, PCD plays a crucial role in enlarging the pericarp to supplement endosperm growth (Radchuk et al., 2018; Radchuk et al., 2011). In wheat, the size of the maternal outer layer tissues determines the final GS and allows for a greater capacity for grain filling (e.g., increased sink strength) (Adamski et al., 2009; Brinton et al., 2017; Calderini et al., 1999; Hasan et al., 2011; Xie et al., 2015).

Grain number (GN) is defined as the number of grains m^{-2} and is one of the most critical determinants of YLD in wheat (Abbate et al., 1995). Grain number can be increased genetically by modifying day length phases, influencing GN determination, and increasing YLD in various environmental conditions (Ochagavía et al., 2021). Grain number tends to be correlated with growth conditions that favor growth in the 20-d period preceding flowering plus the subsequent 10-d period post-flowering (Fischer, 1985; Miralles et al., 2000; Slafer et al., 2001). Furthermore, GN can reflect the availability and accumulation of resources such as carbon and water, affecting the development of different plant structures. Complex G × E × M interaction driving greater availability of plant-development resources can result in greater tillering ability, resulting in more fertile tillers, spike number, and GN (Jaenisch et al., 2022). The positive trend of these traits can all increase GY (equation [1.3], Table 2.1). The same factors may control GN and YLD as both positively correlate. Furthermore, based on equation [1.3] (Table 2.1), GY is expected to increase as GWT and GN increase under ideal conditions. But, studies have shown that intra-plant competition, genetic variability among cultivars, and nutrient and water availability can affect the balance among these GY-related variables, many times resulting in a

trade-off where increased GN reduces GWT (Fischer, 2008; Sinclair et al., 2006; Sinclair et al., 2004).

Only florets that develop fully functioning floral organs (pollen and ovules) at the time of spike emergence can potentially develop grains (Langer et al., 1973; Sibony et al., 1988). Nitrogen use has shown to influence GN and GNS as it has a major role in reproductive development. Fischer (1993) showed a high correlation (r^2 = 0.94) between nitrogen accumulation at 50% anthesis and GN. High nitrogen levels can expedite the rate of spikelet development, floret initiation, and GNS. Sibony (1988) showed that nitrogen fertilizer treatments increased florets and GNS. Demotes-Mainard et al. (1999, 2004) also presented similar findings between GNS and spike nitrogen which had high correlations.

There have been reports on QTL studies involved with GN. Lin et al. (2021) performed a QTL mapping study for GNS using a high-density genetic map using a RIL population of 'H461' x 'Chinese Spring' where H461 had high GNS, and Chinese Spring had low GNS. The mapping population was genotyped using a 55K SNP array that produced a genetic map containing 21,197 SNPs with markers spanning the wheat genome with a total linkage of 3792.7 cM. Three QTL were identified for GNS, one on 2B (*QGns.sicau-2B*) and two on 2D (*QGns.sicau-2D-1* and *QGns.sicau-2D-2*), where the alleles for increasing GNS came from H461. The phenotypic variation of these three QTLs ranged from 3.07 % - 26.57 %, out of all the QTLs *QGns.sicau-2D-2* (222.96 cM – 229.64 cM) presented the highest phenotypic variation of 19.59% – 26.57%. Other previously reported grain number genes have been on 2A (*GNI-A1*), 2B (*GNI-B1*: 573,974,813 bp – 573,975,706 bp), and 2D (*GNI-D1*: 490,117,188 bp – 490,117,827 bp). The different locations of the QTLs indicate that they are novel loci. Zhai et al. (2018) performed a fine-mapping study identifying a novel allele of *TaGW2-A1,* which had pleiotropic effects on

TGW, GNS, and other grain parameters. The gene produced an inverse relationship between GWT (increases) and GN (decreases). In this study, 191 RILs were evaluated, and genomic regions were identified on chromosomes 1B, 3A, 3B, 5B, 6A, and 7A. The QTL of interest was on the 6A (*QTgw/Gns.cau-6A)*, which was mapped at an interval < 0.538 cM using NILs. The NILs showed that TGW increased by 8.3%, and GNS decreased by 3.1% due to the 6A QTL, *QTgw/Gns.cau-6A. Grain Weight 2* (*TaGW2-A1*) is a gene that negatively regulates TGW, and grain width was near *QTgw/Gns.cau-6A*. As TGW increases, the promoter activity of *TaGW2-A1* decreases, and the trade-off between TGW and GNS can help develop cultivars with higher/lower TGW or GNS (Zhai et al., 2018).

Average GWT is an essential element of YLD, and agronomic characteristics such as seedling vigor can affect grain and embryo size (Richards et al., 2002; Slafer et al., 2020). Average GWT is linked to grain weight potential (GWP), is defined as the intrinsic capacity of grains to accumulate dry matter (Bremner et al., 1978). In wheat, the grain growing period is between anthesis and PMAT (Slafer et al., 2020). The simplest way to evaluate GWP is through the characterization of the rate and duration of dry matter accumulation in grain in the absence of growth restrictions (pests, disease, and other stresses) (Slafer et al., 2020). Variation in GWP is due to the variation in the rate of grain filling during the duration from anthesis to PMAT (Asanar & Williams, 1965; Calderini & Reynolds, 2000; Loss et al., 1989; Millet & Pinthus, 1984; Miralles et al., 1996; Wardlaw et al., 1994). Other components that influence GWP are tissue structures of grain development in wheat (Brinton et al., 2019). Studies have shown that final GWT is associated with endosperm cell number (Brocklehurst, 1977), which supports the concept of the capacity of the grain to accumulate carbohydrates into the inner tissues, which regulates GWP (Slafer et al., 2020). In addition, there is also an association between GWT and

the volume of the floret cavity, which indicates that the development of maternal tissues could affect the growth of the endosperm (Millet, 1986). The relationships between final GWT, ovary size, and endosperm cell number as components of GWP are not mutually exclusive due to endosperm cell division which starts at the pericarp (Slafer et al., 2020). This relationship indicates that the number of endosperm cells is linked to the size of the pericarp and the internal volume delimited by the pericarp, which impacts GWT and GY (Brinton et al., 2019; Hasan et al., 2011; Kino et al., 2020).

Yield, the product of the number of grains per m^2 and average GWT, has a unique relationship with the YLD components (Slafer et al., 2020). Due to trade-offs between the YLD components, the components are not independent. Improving one YTC will not neccesarily increase net GY. The elements contributing to the feedback mechanism are the overlapping GN, potential GWT, grain set, and storage of water-soluble carbohydrates that fill the grains (Slafer et al., 2020). The lack of feedback is due to competition, which can arise due to a short supply of assimilates to meet the demands of growing grains. Through this process, the final GWT reflects the availability of resources pre-grain set and the rate of grain growth during the grain filling stage will be reflected based on the avaliabilityof assimilates(Acreche & Slafer, 2006; Miralles et al., 1995). Any increase in grain (increasing grain number per m^2) would result in smaller grain if at a distal position within spikelets or a lower-rank spike (Slafer et al., 2020). The strength of the sink and sources during grain filling impact the positive relationship between GY and GN. Wheat may have evolved to a conservative strategy to handle high source:sink ratio (Borrill et al., 2015; Reynolds et al., 2005; Serrago et al., 2013; Borrill et al., 2015) that would guarantee grain fill and viable GS in majority circumstances (Sadras, 2007; Sadras & Slafer, 2012). Yield

can therefore increase if the number of grains is improved without any hindrances to the size of the grains and vice versa if GS improves without any restrictions to GN (Slafer et al., 2020).

Several studies have evaluated grain traits, such as GWT and GS, which are important when characterizing GY. Gaining a deeper understanding of the genetic architecture of different grain traits can aid the development of robust breeding programs for crop yield improvement. Tyagi et al. (2015) performed MQTL (Meta Quantitative Trait Loci) analysis using 16 published QTL studies that evaluated grain traits in > 30 different mapping populations, identifying 322 QTLs across all wheat chromosomes. The distribution of these QTLs across the sub-genomes was reported as follows A and B (~40%) genomes than the D (20%) genomes. In addition to the MQTL analysis, an ICIM analysis evaluated GWT and other grain traits using a 'Rye Selection 111' x Chinese Spring RIL population (n = 92). The ICIM (Interval Composite Interval Mapping) analysis identified 45 QTLs across 19 wheat chromosomes; 19 QTLs for grain traits were identified on 2A,3B, 6B, 6D, 7A, and 7D. For the MQTL analysis, 80 individual QTLs that were previously identified mostly on the 1B, 2A, 2D, 3B, 4A, 5A, 6A, and 6B chromosomes across these studies were used. The QTLs for all the traits were on the following chromosomes: grain length (1B, 2A, 2B, 3A, 3B, 5A, 6B, 7A, 7B), grain width (1D, 2A, 3B,6B,6D,7D), grain surface area (2A, 2B, 3B, 4B,5A, 5B, 6D, 7A), grain volume (2A, 4B, 6A, 7D), grain vertical perimeter (2B, 3B, 5D, 7D). The PVE for the traits measured in this study ranged from 6.97 % (grain length) to 29.87 % (grain surface area). From these 80 QTLs, those with sufficient information were integrated to produce 23 MQTLs. Out of 23 MQTLs that were identified in this study, only 17 MQTLs were useful, 2A (4), 5A (3), 1B (2), 2D (2), 4A (2), 6A (2), 3B (1), 6B (1). Six MQTLs identified were associated with resistance to *Yr, Lr, FHB,* tan spot, GWT, and PHT (Tyagi et al., 2015; Zhang et al., 2010). MQTL4 (2A: GWT; Huang et al., 2003; Wang et

al., 2009), MQTL8 (2D: *Lr22a*; Zhang et al., 2010), MQTL 20 (6A: GWT, size, TGW; 3.51cM away from *Tagw2-6A*; Mir et al., 2012; Su et al., 2011; Yang et al., 2007).

Zhang et al. (2018) evaluated YLD and YLD-related traits in the GWAS (Genome-Wide Association Study) study, including GY, SNS, GNS, and GWT (Refer to List of Abbreviations). A total of 14 QTLs were validated for GY, 15 for SNS, one for GNS, and 11 for GWT. Grain yield QTLs were identified on the 1A, 1B, 1D, 3A, 3B, 4A, 4B, 5A, and 6B across two environments, full irrigation and terminal drought conditions (H^2_{irr} = 0.68; H^2_{dry} = 0.47). Grain weight QTLs were identified on 2A, 2B, 4A, 5A, 5B, 6A, 6D, 7D (H^2_{irr} = 0.86; H^2_{dry} = 0.83). Spikelet number per spike QTLs were identified on 1A, 1B, 2B, 3D, 4B, 5A, 5B, 6A, and 7A (H^2_{irr} = 0.84; H^2_{dry} = 0.59). Grain number per spike QTLs were identified only on 6A (H^2_{irr} = 0.64; H^2_{dry} = 0.40).

Genetic studies on cereal crops have reported many QTLs and genetic regulatory pathways responsible for GS. More than 40 genes have been identified, and these genes have primarily been associated with three genetic pathways: proteasomal degradation, G-protein signaling, and phytohormone signaling (Li et al., 2015; Orozco-Arroyo et al., 2015; Zuo et al., 2014). In addition to these pathways, new genes have been identified for grain traits such as GS, GWT, and grain length (GL). Genes identified for these traits include *GS2* (Hu et al., 2015), *GS5* (Li et al., 2011), *GLW7* (Si et al., 2016), *GW5* (Duan et al., 2017; Weng et al., 2008), *GW7* (Wang et al., 2015), *GW8* (Wang et al., 2012) in rice. At the cellular level, genes that could result in increased GS due to an increase in cell number within the grain structure of rice are *GS5* (Li et al., 2011), *FER* (Yu et al., 2014), and *GLW7* (Si et al.2016), and *GS2* (Hu et al. 2015). Grain size in wheat has shown variation across different cultivars and morphological subspecies through domestication due to significant genes and QTLs (Gegas et al., 2010). Recent studies

have identified wheat homologs of rice GS through QTL and association mapping studies that increase GWT and GS. These homologs are *GW2, TaGW2-6A,* and *TaGW2-6B* (Jaiswal et al., 2015; Qin et al., 2014; Su et al., 2011) and *TaGW2* RNAi transgenic wheat (Hong et al., 2014), which increase GS and GW.

Increases in YLD tend to be associated with modifying the number and arrangement of spikelets on a plant (Boden et al., 2015; Brinton & Uauy, 2019; Gustavo A. Slafer et al., 2020; Zhou et al., 2021). Multiple genes that control spikelet development have been identified in other cereal crops such as maize, rice, and barley (Ashikari et al., 2005; Boden et al., 2015; Miura et al., 2010; Ramsay et al., 2011; Vollbrecht et al., 2005). The physical architecture of the wheat spike is characterized as unbranched with single spikelets at opposite ends of the central rachis in alternating phyllotaxy, with a terminal spikelet at the distal end of the spike. The spikelet is indeterminate and typically has three to four fertile florets (Boden et al., 2015). The acquisition and distribution of photoassimilates determine GY assimilates in sink organs. Sink size is influenced by the signaling networks regulating sink strength and source resources. Sink size is typically characterized by SNS, GNS, and GWT. The variation in GY due to these components is described by equations [1.1] and [1.2] (Table 2.1). Spikelet number per spike is determined by the number of lateral spikelet meristems generated by the spike meristem before it proceeds to terminal spikelet formation (Ma et al., 2019). Environmentally, SNS can be affected by levels of nitrogen nutrition, day length, temperature, light intensity, duration of spike development, and plant spacing (Ma et al., 2019). Day length and temperature also influence spike length and spikelet number. The genetic influence of these environmental factors is regulated by *Ppd*, *Vrn*, and *Eps* genes which secure the reproductive success of wheat. Typically, a long spike combined with proper climate conditions promotes the initiation of more spikelets. Studies have already

discovered genes (e.g., *Ppd-1*, *TEOSINTE BRANCHED* 1, and *FRIZZY PANICLE*) that influence the spike or spikelet architecture (Boden et al., 2015; Dobrovolskaya et al., 2015; Dixon et al., 2018). Spikelet number per spike can be influenced by the *TtBH-A1,* which controls the spike-branching phenotype that can support SNS and potentially increase GNS and GY. But this depends on spikelet fertility, the development of reproductive organs, and environmental conditions. Grain number per spike is affected more by the abortion of florets and grains in the latter part of the growing season. The strength of these traits is driven by high heritability associated with them, average SNS (H^2 = 0.84), and GNS (H^2 = 0.64) (Kuzay et al., 2019; Zhang et al., 2018). More spikelets will produce more grains for a single spikelet with fertile florets. But, the increase in SNS may potentially reduce GWT due to two distinct reasons: (i) due to physiological conditions where a single grain assimilates fewer nutrients, as increased SNS compliments increased GNS due to competition with nutrients under nutrient-limited conditions (Pinthus et al., 1978), or (ii) due to a greater number of grains developed in distal positions of the spike and spikelets, which are naturally smaller, concomitantly reducing GWT due to a greater proportion of smaller grains.

Boden's (2015) study on structural features involved in spikelet development indicated that regulatory pathways might contribute to the spikelet structure. Comprehensive QTL analyses with a four-way, multi- paired advanced intercross generation MAGIC (Multiparent advanced generation intercross) population and a 90K SNP array identified 104 QTLs (> 80%). These QTLs were refined to evaluate only 18 QTLs with co-located markers associated with paired spikelets. Robust QTLs were designated with a high LOD score and appeared across multiple locations. These QTLs were identified on 1B, 2D, 3A, 5B, with 2D being the strongest (LOD = 11.32). The QTL on the 2D was associated with the *Ppd-D1* gene.

Kuzay et al. (2019) identified three significant QTLs for SNS on 2BS, 7AS, and 7AL from the 'Berkut' x 'RAC875' population. All QTLs had LOD > 2.0 and had significant (*p-value* < 0.05) interactions among the QTLs were not significant. The 7AL QTL contains a candidate gene (87 kb) flanked by *Treas1400-I4V* and *IWA5913* markers. The QTL is responsible for SNS, whose genetic contribution is explained by the *WAPO-1* gene, identified as a wheat ortholog of rice gene *APO-1*. Other GWAS studies have identified associations between GNS and SNS. Reports on QTLs associated with SNS were found on 1A, 1D, 2A, 2B, 3A, 5B, 6A, and 7A in wheat (Boeven et al., 2016; Ward et al., 2019; Voss-Fels et al., 2019). The 7AL chromosomal region has also been identified in other wheat crosses as a source of spikelet architecture. These crosses include Chinese Spring x 'SQ1' (Quarrie et al., 2006) and 'Q1028' x 'Zhengmai 9023' (Luo et al., 2016). The candidate gene region identified in this study contained four genes, *TraesCS7A02G481600*, *TraesCS7A02G481500*, *TraesCS7A02G481700,* and *TraesCS7A02G481800* responsible for the SNS QTL. *TraesCS7A02G481500* and *TraesCS7A02G481800* are excluded from the SNS QTL because the promoter region of these genes is outside the candidate gene region. *TraesCS7A02G481700* is within the candidate gene (CG) region. Still, the SNPs within this CG were not conserved in the promoter region or the transcription factor (TF) binding site. This led to the CG being excluded from any genetic regulation pathways for spike architecture. The *WAPO-1* gene *(TraesCS7A02G481600)* affects the number of spikelets per panicle in rice (Ikeda-Kawakatsu et al., 2009) and has a similar function in wheat. There are two alleles in the *WAPO-1* gene (*WAPO-1a* and *WAPO-1b*) involved in the functionality of the gene. The different amino acid compositions in these alleles and the expression levels of the *WAPO-1* gene influence the fluctuations in SNS; therefore, the *WAPO-1* gene is heavily involved in spikelet architecture.

Cui et al. (2014) identified a QTL for GNS, *QKnps-4A.1*, Cao et al. (2020) identified the same QTL, *QKNS.caas-4AL*. A further fine-mapping study by Cui et al. (2017) for a QTL for GNS, *QKnps-4A*, which was 40Mb from *QKnps-4A.1* and *QKNS.caas-4AL*. Another QTL *QGns.cau.-4A.4* was near *QKnps-4A* (Guan et al., 2018). This finding confirmed that at least one major QTL controls GNS in a target region on 4A and that *QKnps-4A* and *QGns.cau.-4A.4* are potentially controlled by the same gene. Final findings on the genetic architecture of these traits indicate that different allelic combinations and QTLs/MQTLs influence the phenotypic expression of yield-trait components (YTCs).

Several comprehensive studies have evaluated YLD and YLD-related traits, which gives a scope on the current progress of characterizing the genetic architecture of YLD. For example, Zhang et al. (2010) performed a comprehensive meta-QTL analysis study on YTCs. A total of 541 QTLs were identified for YLD (178), GNS (68), grain weight per spike (GWS) (47), SNS (47), TGW (116), and plant height (PHT) (85). These QTLs were distributed across the whole wheat genome. Grain yield had the greatest coverage (33 %), followed by TGW (21%) and PHT (16%). The frequency distribution of the QTLs across the ABD genome is as follows, A (40%), B (~30%), and D (~30%). Regarding individual traits, chromosome 2 had the most QTLs associated with TGW, SNS, GWS, and GNS.

The meta-QTL analysis for YLD and YLD-related traits revealed a total of 257 QTLs, which produced a total of 55 MQTLs identified among which 12 were significant and located on chromsomes1B (2 MQTLs), 2A (2 MQTLs), 2D (2 MQTLs), 3B (2 MQTLs), 4A (1 MQTL), and 5A (3 MQTLs). Previous QTLs have been identified on 1BL associated with YLD (Huang et al., 2003; Maccaferri et al., 2008), GWS and GNS (Verma et al., 2005), YLD, SNS, and GNS (Peng et al., 2003), and TGW (Wang et al., 2009a; Wang et al., 2009b). In addition, initial QTLs

that were repeatedly identified in several different studies and associated with several traits clustered into MQTLs were considered significant. These MQTLs were MQTL4 (1B), MQTL5 (1B), MQTL8 (2A), MQTL9 (2A), MQTL14 (2D), MQTL16 (2D), MQTL24 (3B), MQTL26 (3B), MQTL32 (4A), MQTL39 (5A), MQTL40 (5A), and MQTL42 (5A) which were all associated with different YLD and YLD-related traits. In addition, there have been 8 QTLs identified on 2AS linked to YLD and YLD-related characteristics (Huang et al., 2003; Huang et al., 2004; McCartney et al., 2005; Kunert et al., 2007; Li et al., 2007; Sun et al., 2009; Yao et al., 2009), MQTLs identified in this study for 2AS (MQTL8:19.11 cM; MQTL9: 53.6cM) were associated with GNS. In addition, the 2D MQTLs (MQTL14:17.55 cM; MQTL16: 30.2 cM) identified were associated with *Rht8*.

Several QTLs on chromosome 3B have been linked to the YTCs discussed in previous reports (Börner et al., 2002; Cuthbert et al., 2008; Elouafi et al., 2004; Groos et al., 2003; Huang et al., 2004; Li et al., 2007; Marza et al., 2006; Wang et al., 2009a). In this comprehensive study (Zhang et al., 2010), an MQTL spanned the centromeric region of 3B and was associated with TGW. Meta-QTLs identified on 4AL (MQTL 30-4A: 57.23cM) were also linked to TGW. The MQTLs on 5AL (MQTL41: 68.02 cM) were near *Vrn-A1*, and previous studies have presumed that QTLs in this region contribute to the expression of traits such as tiller number, spike length, and heading date (Chu et al., 2008; Cuthbert et al., 2008; Groos et al., 2003; Huang et al., 2006; Kato et al., 1999, 2000; Kumar et al., 2007; Ma et al., 2007; Mathews et al., 2008). The information gathered in this study could improve the genetic characterization of wheat YLD traits in the future.

A recent comprehensive review by Cao et al. (2020) dissected the genetic architecture of YTC in wheat from the past decade (2009 – 2019). There have been 253 QTLs reported, which

spanned all 21 chromosomes with different distribution patterns. Chromosomes containing > 20 QTLs were 4B, 5A, and 7A, whereas < 3 QTLs were identified on 1D, 6B, and 6D. No QTLs for YTCs were identified on 3DS, 5BS, 5DS, 6BS, and 6DL. The distribution of QTLs associated with YTCs are TGW (139), GNS (67), and spike number per square meter (SN) (34). Different types of association analyses using different molecular markers used to identify YTCs. Association mapping studies using SNPs, DarT, and SSR marker systems have identified 142 YTC-associated loci (Breseghello et al., 2007; Garcia et al., 2019; Griffiths et al., 2012; Guo et al., 2015; Li et al., 2019; Liu et al., 2017; Lozada et al., 2018; Shi et al., 2017; Sukumaran et al., 2015; Sukumaran et al., 2018; Sun et al., 2017; Wang et al., 2017; Wang et al., 2012; Wang et al., 2017; Yao et al., 2009; Zhang et al., 2012; Zhang et al., 2012). Further dissection of the 142 YTC-associated loci from the association mapping studies showed that the most QTLs were identified for TGW (88), GNS (18), and SN (5). A closer evaluation of the association loci distribution showed that > 10 loci were on 2A, 5A, 5B, 6A, and 7A. Chromosome 5B carried 26 loci associated with YTC (Ma et al., 2018). Although association mapping studies identified one YTC-related loci on 4B, linkage mapping studies identified 28 YTC-QTLs, with most associated loci linked to TGW, GNS, and SN.

Cao et al. (2020) identified 58 QTL-rich clusters (QRC), regions with two or more QTLs for the same trait from different studies. There were 27 QRCs exclusive to TGW; two QRCs were exclusive to GNS and SN. Yield trait component combinations identified 24 QRCs for TGW and GNS; 13 QRCs were associated with all three traits. Chromosomal distributions of QRCs showed that 30 QRCs were identified on sub-genome A and 14 on sub-genomes B and D. These findings indicate that sub-genome A possesses the most genetic variation compared to B and D sub-genomes for YTCs. Smaller clusters were identified on 2A, 5A,6A, and 7A.

Different genes involved in the physiological mechanisms contribute to the variation in the phenotypic of GY and GY-related traits. For example, *Ppd-D1* is a regulator gene that controls the photoperiod-dependent floral induction responses. It is a member of the pseudo-response regulator (PRR) gene family that contains components related to the circadian clock that directly monitors the expression of the core genes and transcription factors (Li et al., 2011; Nakamichi et al., 2005). The allelic variations of the *Ppd-1* gene influences day length photoperiod sensitivity, both long-day (LD) and short-day (SD). The loss of function of the alleles results in a delayed flowering response when transitioning from SD to LD. Conversely, the insensitive alleles will encourage LD response to all photoperiods (Beales et al., 2007; Díaz et al., 2012; Shaw et al., 2013; Shaw et al., 2012; Turner et al., 2005). In addition, variation in day length can affect the YLD output. Boden et al. (2015) performed a study comparing the inflorescences phenotypes of NILs, which were photoperiod insensitive (flower early regardless of photoperiod) or strongly photoperiod sensitive (flower earlier in LD than SD photoperiods). The sensitive lines carried a single copy of *Ppd-B1* and sensitive *Ppd-D1* allele. The insensitive lines carried a single copy of the *Ppd-D1a* allele and three copies of the *Ppd-B1* gene. Under SD conditions (12 hr. light/ 12 hr. dark), the sensitive lines flowered later, produced more spikelets, and 20% more rachis nodes. Under LD conditions (16 hr. light/ 8 hr. dark), the sensitive lines had fewer spikelets, and both lines (sensitive/insensitive) flowered earlier. These results indicated that LD photoperiods and *Ppd-1* alleles suppress spikelet development, and there was no significant difference in transcript expression levels for *Ppd-D1*, *Ppd-B1*, *Ppd-A1*.

FLOWERING LOCUS T (FT) is a crucial component in the flowering pathway that can interact with photoperiod pathways and fluctuate transcript expression levels. Spikelet architecture development is associated with reduced expression of *FT* in the early stages of spike

development. Weak floral signals result in a delayed conversion of axillary meristems to spikelet meristems. These spikes produce a spike with lateral and terminal spikelets instead of a single spikelet with a short branch. The genetic basis of this behavior may be due to the *Ppd-D1a* sequence, which may include mutations that enhance the expression of meristem identity genes as in maize and rice (Endo-Higashi et al., 2011; McSteen et al., 2000). Modifying the expression of these flowering genes can allow a more robust arrangement and increased number of grain-producing spikelets (Boden et al., 2015). Different transcription factors (TF) regulate spikelet development. *TEOSINTE BRANCHED 1* (*TB1*) is a TF that regulates spikelet inflorescence (Dixon et al., 2018). *Grain Number Increase 1* (*GN1*) is a TF responsible for increased floret fertility in wheat (Sakuma et al., 2019). *FRIZZY PANICLE* (*FZP*) encodes the APETALA2 TF that produces supernumerary spikelets in wheat (Dobrovolskaya et al., 2015). Genes identified as spike regulators are, *TaAGLG1-5A, TaTFL1-2D,* and *TaHOX2-2B* (Wang et al., 2017a, b).

Genetic Architecture of Anthesis and Physiological Maturity

Wheat breeding programs focus on developing cultivars that thrive under different environmental conditions ensuring maximum crop production and GY stability. Developing robust cultivars depends on germplasm selection and understanding genetic factors that control the cultivars' adaptability. Flowering time plays a vital role in cultivar adaptability, which is characterized by vernalization (*Vrn*), photoperiod (*Ppd*), and earliness per se (*Eps*) genetic systems (Kamran et al., 2014). The three respective gene systems account for different percentages (*Vrn* = 75%, *Ppd* = 25%, *Eps* = 5%) of genetic variability in heading time in wheat (Stelmakh, 1998). Photoperiod and vernalization response genes can accelerate or stall the FT in response to environmental conditions (Law et al., 1997).

Vernalization is defined as the acceleration of flowering ability due to chilling temperatures (Chouard, 1960). The rate of vernalization depends on the intensity of cold temperatures and the duration of exposure to temperatures below a given threshold (Rawson et al., 1998; Wang et al., 1995). Differences in vernalization are due to genetic and allelic variability expressed as, *Vrn-1*, *Vrn-2*, *Vrn-3*, and *Vrn-4* loci (Distelfeld et al., 2009; Flood et al., 1986). Winter wheat contains the dominant allele of *Vrn-2* and recessive forms of the other vernalization genes, which results in the demand for cold exposure before the onset of flowering. The *Vrn-2* is a floral repressor, which can delay flowering until vernalization. Trevaskis et al. (2007) performed a study in barley, which determined that the *Vrn-2* gene transcribed a protein with a zinc-finger motif, which represses the long-day flowering gene. Vernalization (*Vrn-1)* genes are generally orthologous genes (*Vrn-A1*, *Vrn-B1*, and *Vrn-D1*) which are located on the 5A, 5B, and 5D chromosomes (Dubcovsky et al., 1998; Fu et al., 2005; Law et al.,1976; Pugsley, 1971). Vernalization genes can each have a different effect on a plant's growth and development.

The *Vrn-A1* gene has the most potent effect of inhibiting vernalization, and *Vrn-B1* is the weakest (Goncharov, 2004). The expression of these genes occurs at different stages of development. The different alleles within these *Vrn* genes (*Vrn-A1*, *Vrn-B1*, and *Vrn-D1*) can regulate the response in FT, PHT, and YLD components among wheat cultivars. Specifically, allelic combinations can influence floral initiation, the number of leaves, tiller number, and timing of growth stages until flag leaf emergence (Levy et al., 1972). Other studies have reported that *Vrn* genes (*Vrn-A1* and *Vrn-D1)* can increase the number of spikelets and spikelet initiation rate (González et al., 2002; Whitechurch et al., 2003). It has also been reported that spikelet fertility at anthesis increases with an extended period of stem growth (González et al., 2003a). Dominant *Vrn* genes expedite vegetative growth from emergence to floral initiation and reduce

final leaf number (Whitechurch et al., 2003; Hay et al., 1991; Slafer et al., 1944; Wang et al., 1995). The recessive *Vrn* alleles extend the vegetative phase with an increase in the number of leaves due to a constant growth rate of leaf primordia. These recessive *Vrn* alleles delay flag leaf appearance (Amir et al., 1991; Kirby, 1990; Miglietta, 1989). The *Vrn* genes have a more noticeable effect during the vegetative phase (e.g., floral initiation), after which there is no developmental response (Wang et al., 2003; Whitechurch et al., 2003).

Photoperiod is the second component of the genetic system that relates to FT. Flowering time is determined by sensitivity or insensitivity to photoperiod. A photoperiod-insensitive cultivar can switch to reproductive growth when temperature increases. A photoperiod-sensitive cultivar remains in the vegetative state until an increase in day length meets the photoperiod requirements. Different photoperiod genes define the architecture and underlying genetic mechanisms influencing plant development (Kamran et al., 2014). Photoperiod response is genetically influenced by *Ppd* genes located on homoeologous group 2 chromosomes of wheat (Worland et al., 2001). The genes are *Ppd-A1*, *Ppd-B1*, and *Ppd-D1*, located on the 2A, 2B, and 2D chromosomes (Law et al., 1978; Scarth et al., 1983). The *Ppd-D1* is the most insensitive to photoperiod (*Ppd-D1a),* followed by *Ppd-B1*, then *Ppd-A1* (Worland, 1996). González et al. (2003) found that both fertile spikelets and spike dry weight increased at anthesis during late reproductive phases due to greater portioning of assimilates to the spike than the stem. In addition, close associations have been found between spikelet fertility and stem elongation, which increases GY potential by improving the GNS (Slafer et al., 1996).

Kato et al. (2001) defined earliness per se (*Eps*) as "the difference in flowering time of varieties whose requirements of vernalization and photoperiod have been fulfilled." Photoperiod and vernalization genes (*Vrn*) control FT in response to specific day lengths and temperature

conditions. In contrast, earliness per se genes affect flowering time independent of the stimuli from the environment (Worland et al., 1996). Therefore, earliness can be determined by a minimum vegetative growth that can instigate floral primordia independent of external stimuli. Earliness per se is a quantitatively inherited trait controlled by mostly minor genes whose effect can only be determined without the confounding effects of *Ppd* and *Vrn* genes (Kato et al., 1999). The heritability of *Eps* is generally high (H^2 = 0.90-0.99). Therefore, it can be used in breeding programs to reduce the life cycle of wheat independent of environmental factors that modify FT (Kato et al., 1999a, 1999b, 1999c). The first *Eps* gene was reported on 2BL affecting ear emergence time in recombinant inbred lines of Chinese Spring (Scarth et al., 1983).

Many QTL studies have identified chromosomal regions associated with FT and other related traits across the wheat genome. For example, Kamran et al. (2014) reported that QTLs for earliness per se were located on 1A (Bennett et al., 2012; Bullrich et al., 2002; Shindo et al., 2003),3A (Miura et al., 1994), 4A, 4B (Bennett et al., 2012; Hanocq et al., 2007), 5A (Bennett et al., 2012; Kato et al., 1999a,1999b) 1B, 5B (Bennett et al., 2012; Hanocq et al., 2004; Hanocq et al., 2007; Kamran et al., 2013; Tóth et al., 2003), 2B, 2D (Hanocq et al., 2007; Hanocq et al., 2004), 7A (Bennett et al., 2012; Hanocq et al., 2007), 7B (Bennett et al., 2012) and 7D (Carter et al., 2011). The *Eps* genes/QTL have been reported to be most frequent on 5A (Kato et al., 1999a,1999b; Griffiths et al., 2009; Bennett et al., 2012), 2B (Scarth et al., 1983; Sourdille et al., 2003; Shindo et al., 2003; Maccaferri et al., 2008), 3A (Hoogendoorn, 1985; Miura et al.,1994) , 5B, 7B, and 4D (Hoogendoorn 1985; Kulwal et al. 2003; Lin et al. 2008).

For heading, QTLs were found on 1A (Shindo et al., 2003), 1B (Griffiths et al., 2009; Zhang et al., 2009), 1D (Griffiths et al., 2009), 2A (Griffiths et al., 2009; Maccaferri et al., 2008), 2B (Maccaferri et al., 2008), 2D (Kulwal et al., 2003), 3A, 3B, 4B (Griffiths et al., 2009), 4D

(Griffiths et al., 2009; Sourdille et al., 2003; Zhang et al., 2009), 5A, 5B, 6A, 6B (Griffiths et al., 2009),6D (Shindo et al., 2009), 7A (Griffiths et al., 2009), 7B (Griffiths et al., 2009; Maccaferri et al.; 2008; Sourdille et al., 2003), and 7D (Griffiths et al., 2009; Shindo et al., 2003; Sourdille et al., 2003). Vernalization QTLs were identified on the 2A, 3A, 4D (Shindo et al; 2003), 5A, 2B, 5B, 6D (Hanocq et al; 2004). Photoperiod QTLs were identified on 5A, 7A, 2B, 5B, 7B, (Shindo et al., 2003), 4B (Shindo et al., 2003; Sourdille et al., 2003), 2D,7D (Hanocq et al.,2004). Flowering time QTLs were found across all the chromosomes in wheat (Kamran et al., 2014); the frequency (%) of the QTLs across the sub-genomes were as follows, B genome (41%), A genome (30%), and D genome (28.5%). Chromosomes 2 and 5 contained the most QTLs pertaining to vernalization and photoperiod genes, which leads to the conclusion that these chromosomes influence FT-related genes the most.

When a crop reaches maximum GY potential at physiological maturity, grains cease growing. Physiological maturity has complex underlying genetic mechanisms. Three QTLs associated with FT genes were discovered on 2D, 5A, and 7D in the Jagger x '2174' RIL population, which contributed to the variation in the final developmental stages of wheat (Chen et al., 2010). Flowering time genes identified were *VRN-A1* (5A), *PPD-D1* (2D), and *VRN-D3* (7D). All of the flowering genes evaluated in this study expressed different degrees of variation. *VRN-A1* explained 21.5 % of phenotypic variation for stem elongation and 17.4 % of phenotypic variation for PMAT. *PPD-1* explained 6.7% of phenotypic variation for stem elongation, 29.7 % of phenotypic variation was explained for FT, and 20.1 % of phenotypic variation was explained for PMAT. *VRN-D3* had a more significant effect on FT (14.6 % of PVE) and PMAT (20.5 % of PVE) rather than stem elongation. Ultimately, these three genes have the most critical influence on PMAT, heading, and stem elongation. The source behind the variability of these traits

ultimately then depends on different allele combinations of these genes that regulate the gene expression of these traits.

In addition to the QTLs reported by Chen et al. (2010), other QTLs were also discovered on 1B (Wang et al., 2009), 1D (Kulwal et al., 2003), 2A, 2B, 3D, 4B (Wang et al., 2009), 5D (Haung et al., 2006), 6D (Wang et al., 2009), 7B (Kulwal et al., 2003). These QTLs always appear in conjunction with other FT genes and traits. Tahmasebi et al. (2016) performed a QTL study evaluating a RIL population, 'SeriM82' x 'Babax,' under drought and heat stress conditions. Physiological maturity QTLs were identified on the 1D, 3A, 5A,6D, and 7D chromosomes. The PVE of these QTLs spanned from 0.5-5.7 %. In addition, the MQTLs on 1D, 6D, and 7D have significant epistatic interactions. In conclusion, FT and PMAT have a complex underlying genetic architecture. Underlying factors such as polygenic, epistatic, and allelic combinations influence the phenotypic expression of these traits.

Genetic Architecture of Plant Height

Plant height has pleiotropic effects on crop development which can influence GY response. Tall plants are at a greater risk of lodging, so PHT reduction is a target trait in breeding programs (Berry et al., 2003). There have been 25 *Rht* genes identified from previous studies *Rht1-Rht25* (Chen et al., 2015; Li et al., 2015; McIntosh et al., 2013; Mo et al., 2018; Tian et al., 2017; Würschum et al., 2017; Zhao et al., 2018) which are distributed across the wheat genome. Chromosomal locations of known *Rht* genes include: *Rht1* (4B), *Rht2* (4D), *Rht3* (4B), *Rht4* (2B), *Rht5* (3B), *Rht7* (2A), *Rht8* (2D), *Rht9* (7B), *Rht12* (5A) *Rht13* (7B), *Rht14* (6A), *Rht16* (6A), *Rht17* (6A), *Rht18* (6A), *Rht22*(7A), *Rht23* (5D), *Rht24* (6A), *Rht25* (6A) (McIntosh et al., 2013). During the Green Revolution, semi-dwarfing genes, *Rht-B1b* and *Rht-D1b* led to dramatic increases in GY. Dwarfism is caused by the partial inability of internode cells to elongate in

response to internal gibberellic acid. Grain yield is a secondary consequence of reduced stem growth rates during ear development, leading to heavier ears and more fertile florets. Additionally, shorter plants can fertilize with greater N rates, and reduced lodging risk, which drove about 75% of the wheat YLD gain during the Green Revolution (Fischer et al., 2022).

The reduction in height is caused by the limited response to phytochrome gibberellic acid (GA), leading to better resistance to stem lodging and YLD through increased GN. These genes encode the DELLA proteins, which repress the growth mechanisms related to GA (Pearce et al., 2011). As a result, these genes improve harvest index, biomass, and spikelet fertility. These YLD advantages from the *Rht* genes are due to the increased portioning of assimilates to the spike (Maeoka et al., 2020) and reducing the need for stem elongation. This mechanism reduces pre-anthesis abortion of distal florets in each spikelet and increases the total number of viable florets at anthesis (Youssefian et al., 1992a, 1992b). Reductions in assimilate demand for stem growth are due to potent combinations of *Rht* alleles that increase spikelet fertility. Previous studies have noted that maximum GYs are gathered from plants of medium height that experience varied *Rht* effects based on their genetic background (Allan, 1989; Fischer et al., 1990; Richards, 1992). Law et al. (1978) proposed the "tall dwarf" model, which argues that GY can be maximized by combining gibberellin-insensitive *Rht* alleles with other genes which increase both PHT and GY.

Interactions between genotype and temperature also influence the effects of *Rht* on PHT, leaf size, spike weight, and grain set. Stress during spike initiation reduces the number of functional florets, while heat stress hinders grain-filling after anthesis. These conditions vary based on the genetic background in which the *Rht* alleles are evaluated. The best plants are defined by their genotypic, environmental, and agronomic variables. These variables produce phenotypic variation in PHT (Bush et al., 1988; Flintham et al., 1997). In addition to these

factors, both pleiotropic and epistatic effects play a meaningful role in producing the phenotypic variation of *Rht* genotypes. Pleiotropic association between GA-insensitivity and dwarfism comes from the strong correlations between the degree of dwarfism and the inhibition of the elongation growth response to GA in lines possessing different *Rht* alleles (Appleford et al., 1991; Lenton et al., 1987; Pinthus et al., 1989). The effects of different allelic combinations influence plant stature, biomass, and other YTC components, thus correlating with their impact on cell length and number. Evidence suggests that *Rht* genes reach these effects by expediting the loss of cell wall pliability, thus lowering the time available for cell elongation growth (Tonkinson et al., 1995).

Flintham et al. (1997) evaluated four sets of near-isogenic lines (NIL) with different allelic combinations of *Rht-B1b, Rht-D1b, and Rht-B1c* for GA-insensitive dwarfism. Yield advantages of shorter plants relative to tall controls were evident. *Rht* genotypes were the key source of variation in PHT, with differences between varieties being consistent and associated with significant *Rht* x variety interactions. Reduction in PHT were due to different *Rht* allelic combinations, *Rht-B1b* (14%), *Rht-D1b* (17%), *Rht-B1c* (50%), *Rht-B1b+ Rht-D1b* (42%), *Rht-B1c+ Rht-D1b* (59%). The *Rht-B1b* and *Rht-D1b* genotypes showed increased GY by increasing harvest index while maintaining total biomass. In this study, the highest yielding variety was the shortest, and the highest overall yields occurred in semi-dwarf cultivars – which are similar to the results presented by Maeoka et al. (2020). The average yields of *Rht-B1b, Rht-D1b, Rht-B1b + Rht-D1b, and Rht-B1c* NILs were similar, but the tall controls had lower yields in all trials. Across six trials, there was variation in tiller number, GN, and GWT. In most cases, the *Rht* alleles increased GN over the tall controls, except for *Rht-Bc + Rht-Db* genotype, but GWT was varied.

Spikelet number is not affected by *Rht* dwarfism, as the increase in GN is due to an increase in the fertility of distal florets within spikelets (Greco et al., 2012; Sakuma et al., 2019). Increased post-antithetic assimilate increases sink size due to increased grain numbers and is essential to the physiological component of *Rht* YLD advantages (Ferrante et al., 2013; Gambín et al., 2008; Nazir et al., 2021; Rotundoet al., 2009; Spiertz, 1977; Tao et al., 2021). Since average GS is reduced as GN increases, successful grain filling from the proper supply of assimilates is required to sustain the YLD potential (Flintham et al., 1997). Therefore, the best strategy for maximizing GY is to use *Rht* alleles that reduce PHT at an optimum level, reducing potential GY penalties linked to reduced biomass and GS in substandard environments (Flintham et al., 1997). Still, identifying more genes that can reduce plant height without reducing GY potential is necessary to create more robust breeding programs.

Griffiths et al. (2012) identified multiple QTL regions responsible for the variation in crop height among four elite European cultivar populations in an MQTL analysis study. There were 104 individual QTLs identified among the four populations. There were 16 MQTLs identified on chromosomes 1A-1D, 2A-2D, 3A, 3B, 4B, 4D, 5A, 5B, 6A-6D, and 7D. Results showed a high correlation for the variability of PHT among all populations and environments (r^2 > 0.69). The *Rht* genes (*Rht-D1b* and *Rht-B1b*) had varying degrees of segregation among the four double haploid populations evaluated (‘Charger’ x ‘Badger’ (C x B); ‘Spark’ x ‘Rialto’ (S x R); ‘Savannah’ x ‘Rialto’ (Sv x R), and ‘Avalon’ x ‘Cadenza’ (A x C)). *Rht-D1* was segregating for the A x C and S x R populations. Their additive effects were 4.4 cm – 7.2 cm (S x R) and 2.5 cm – 4.8cm (A x C) across environments. The 2DS QTL had an additive effect of 6.4 cm in the A x C population, which coincides with the Xgwm261 marker, linked to the GA-sensitive semi-dwarfing gene *Rht8*. In the same population, the 2AS QTL is located in *Xgwm359,* distal to *Ppd-*

A1 (Griffiths et al., 2012; Mcintosh et al., 2013). Stronger evidence of PHT segregation was present in QTLs identified on the 3AS (all populations), 3BS (3 populations), and 6A (3 populations) in the centromeric regions; allelic variations of genes controlling PHT may be in common for these loci. Zhang et al. (2010) identified 85 QTLs in an MQTL analysis study associated with PHT. Although PHT QTLs were identified across all 21 chromosomes, chromosome 4B contained the most QTLs. MQTLs mapped on group 4 (MQTL34-4B: 59.23 cM) may have contained the *Rht* gene (*Rht-B1*).

Zanke et al. (2014) did a GWAS study on PHT in wheat and found similar overlapping QTL regions as presented in Griffith et al. (2012) through marker-trait associations (MTA) with SSR markers. The overlapping QTL regions were identified on chromosomes, 1A, 1D, 2A- 2D, 3A, 4B, 4D, 5A, 5B, 6A, 6D, and 7D. This study also identified the same 2DS QTL associated with *Rht8* and *Ppd-D1* identified by the *GWM4815* and *GWM1481* markers. Additional *Rht* genes identified in this study were *Rht4* (2BL), *Rht5* (3BS), *Rht9* (5AL), *Rht12 (*5AL), and *Rht13* (7B). The genomic regions that showed the greatest reduction in PHT were on chromosomes 2A-2D, 5A-5D, and 7B. Furthermore, candidate gene (CG) analysis in this study identified cytochrome P450 as the functional gene responsible for PHT. In recent years, the correlation between crop PHT and GY (Law et al., 1978) has been dissected into single QTL effects (Maccaferri et al., 2008; Zhang et al., 2004), showing that crop-height-increasing effects also increase GY in some cases. The optimal combinations of these alleles are most likely necessary for GY potential in any target environment.

Conclusion

Yield is generally characterized by low heritability, large G x E interactions, and epistatic interactions among multiple QTLs or genes. Due to this complexity, there are challenges in

pinpointing the causal genes responsible for YTC traits. This review supplied genetic studies on the YLD and YTC of spikelet, FT, PMAT, PHT, and grain traits. Information provided includes QTLs, MQTLs, genes, and candidate genes responsible for each trait's morphological and underlying genetic properties. Findings reported in this review may help validate future findings in breeding programs related to YTC and implement the development of versatile high-yielding wheat cultivars.

References

Abbate, P. E., Andrade, F. H., & Culot, J. P. (1995). The effects of radiation and nitrogen on number of grains in wheat. *The Journal of Agricultural Science*, *124*(3). https://doi.org/10.1017/S0021859600073317

Acreche, M. M., & Slafer, G. A. (2006). Grain weight response to increases in number of grains in wheat in a Mediterranean area. *Field Crops Research*, *98*(1), 52–59. https://doi.org/10.1016/j.fcr.2005.12.005

Adamski, N. M., Anastasiou, E., Eriksson, S., O'Neill, C. M., & Lenhard, M. (2009). Local maternal control of seed size by KLUH/CYP78A5-dependent growth signaling. *Proceedings of the National Academy of Sciences of the United States of America*, *106*(47). https://doi.org/10.1073/pnas.0907024106

Allan, R. E. (1989). Agronomic Comparisons Between *Rht 1* and *Rht 2* Semidwarf Genes in Winter Wheat . *Crop Science*, *29*(5). https://doi.org/10.2135/cropsci1989.0011183x002900050001x

Amir, J., & Sinclair, T. R. (1991). A model of the temperature and solar-radiation effects on spring wheat growth and yield. *Field Crops Research*, *28*(1–2). https://doi.org/10.1016/0378-4290(91)90073-5

Appleford, N. E. J., & Lenton, J. R. (1991). Gibberellins and leaf expansion in near-isogenic wheat lines containing *Rht1* and *Rht3* dwarfing alleles. *Planta*, *183*(2). https://doi.org/10.1007/BF00197793

Asanar, R. D., & Williams, F. (1965). The effect of temperature stress on grain development in wheat. *Australian Journal of Agricultural Research*, *16*(1). https://doi.org/10.1071/AR9650001

Ashikari, M., Sakakibara, H., Lin, S., Yamamoto, T., Takashi, T., Nishimura, A., … Matsuoka, M. (2005). Plant science: Cytokinin oxidase regulates rice grain production. *Science*, *309*(5735), 741–745. https://doi.org/10.1126/science.1113373

Austin, R. B. (1999). Feeding the Ten Billion: Plants and Population Growth , by L. T. Evans . xiv+247 pp. Cambridge: Cambridge University Press (1998). *The Journal of Agricultural Science*, *133*(4). https://doi.org/10.1017/s0021859699217078

Aziz, M. M., Palta, J. A., Siddique, K. H. M., & Sadras, V. O. (2017). Five decades of selection for yield reduced root length density and increased nitrogen uptake per unit root length in Australian wheat varieties. *Plant and Soil*, *413*(1–2). https://doi.org/10.1007/s11104-016-3059-y

Balfourier, F., Bouchet, S., Robert, S., DeOliveira, R., Rimbert, H., Kitt, J., … Paux, E. (2019). Worldwide phylogeography and history of wheat genetic diversity. *Science Advances*, *5*(5). https://doi.org/10.1126/sciadv.aav0536

Beales, J., Turner, A., Griffiths, S., Snape, J. W., & Laurie, D. A. (2007). A Pseudo-Response Regulator is misexpressed in the photoperiod insensitive *Ppd-D1a* mutant of wheat (*Triticum aestivum* L). *Theoretical and Applied Genetics*, *115*(5), 721–733. https://doi.org/10.1007/s00122-007-0603-4

Bennett, D., Izanloo, A., Edwards, J., Kuchel, H., Chalmers, K., Tester, M., … Langridge, P. (2012). Identification of novel quantitative trait loci for days to ear emergence and flag leaf glaucousness in a bread wheat (*Triticum aestivum* L) population adapted to southern Australian conditions. *Theoretical and Applied Genetics*, *124*(4). https://doi.org/10.1007/s00122-011-1740-3

Berry, P. M., Sterling, M., Baker, C. J., Spink, J., & Sparkes, D. L. (2003). A calibrated model of wheat lodging compared with field measurements. *Agricultural and Forest Meteorology*, *119*(3–4), 167–180. https://doi.org/10.1016/S0168-1923(03)00139-4

Boden, S. A., Cavanagh, C., Cullis, B. R., Ramm, K., Greenwood, J., Jean Finnegan, E., … Swain, S. M. (2015). *Ppd-1* is a key regulator of inflorescence architecture and paired spikelet development in wheat. *Nature Plants*, *1*(January), 2–7. https://doi.org/10.1038/nplants.2014.16

Börner, A., Schumann, E., Fürste, A., Cöster, H., Leithold, B., Röder, M. S., & Weber, W. E. (2002). Mapping of quantitative trait loci determining agronomic important characters in hexaploid wheat (*Triticum aestivum* L). *Theoretical and Applied Genetics*, *105*(6–7), 921–936. https://doi.org/10.1007/s00122-002-0994-1

Borrás, L., Slafer, G. A., & Otegui, M. E. (2004). Seed dry weight response to source-sink manipulations in wheat, maize and soybean: A quantitative reappraisal. *Field Crops Research*, *86*(2–3), 131–146. https://doi.org/10.1016/j.fcr.2003.08.002

Borrill, P., Fahy, B., Smith, A. M., & Uauy, C. (2015). Wheat grain filling is limited by grain filling capacity rather than the duration of flag leaf photosynthesis: A case study using NAM RNAi plants. *PLoS ONE*, *10*(8). https://doi.org/10.1371/journal.pone.0134947

Bremner, P., & Rawson, H. (1978). The Weights of Individual Grains of the Wheat Ear in Relation to Their Growth Potential, the Supply of Assimilate and Interaction Between Grains. *Functional Plant Biology*, *5*(1). https://doi.org/10.1071/pp9780061

Breseghello, F., & Sorrells, M. E. (2007). QTL analysis of kernel size and shape in two hexaploid wheat mapping populations. *Field Crops Research*, *101*(2). https://doi.org/10.1016/j.fcr.2006.11.008

Brinton, J., Simmonds, J., Minter, F., Leverington-Waite, M., Snape, J., & Uauy, C. (2017). Increased pericarp cell length underlies a major quantitative trait locus for grain weight in hexaploid wheat. *New Phytologist*, *215*(3). https://doi.org/10.1111/nph.14624

Brinton, J., & Uauy, C. (2019). A reductionist approach to dissecting grain weight and yield in wheat. *Journal of Integrative Plant Biology*, *61*(3), 337–358. https://doi.org/10.1111/jipb.12741

Brocklehurst, P. A. (1977). Factors controlling grain weight in wheat [14]. *Nature*, Vol. 266. https://doi.org/10.1038/266348a0

Bullrich, L., Appendino, M. L., Tranquilli, G., Lewis, S., & Dubcovsky, J. (2002). Mapping of a thermo-sensitive earliness per se gene on Triticum monococcum chromosome 1Am. *Theoretical and Applied Genetics*, *105*(4). https://doi.org/10.1007/s00122-002-0982-5

Bush, M. G., & Evans, L. T. (1988). Growth and development in tall and dwarf isogenic lines of spring wheat. *Field Crops Research*, *18*(4). https://doi.org/10.1016/0378-4290(88)90018-4

Calderini, D. F., Abeledo, L. G., Savin, R., & Slafer, G. A. (1999). Effect of temperature and carpel size during pre-anthesis on potential grain weight in wheat. *Journal of Agricultural Science*, *132*(4). https://doi.org/10.1017/S0021859699006504

Calderini, Daniel F., & Reynolds, M. P. (2000). Changes in grain weight as a consequence of de-graining treatments at pre- and post-anthesis in synthetic hexaploid lines of wheat (*Triticum durum* x *T. tauschii*). *Australian Journal of Plant Physiology*, *27*(3). https://doi.org/10.1071/pp99066

Cao, S., Xu, D., Hanif, M., Xia, X., & He, Z. (2020). Genetic architecture underpinning yield component traits in wheat. *Theoretical and Applied Genetics*, *133*(6), 1811–1823. https://doi.org/10.1007/s00122-020-03562-8

Carter, A. H., Garland-Campbell, K., & Kidwell, K. K. (2011). Genetic mapping of quantitative trait loci associated with important agronomic traits in the spring wheat (*Triticum aestivum* L) Cross "Louise" × "Penawawa." *Crop Science*, *51*(1), 84–95. https://doi.org/10.2135/cropsci2010.03.0185

Chen, S., Gao, R., Wang, H., Wen, M., Xiao, J., Bian, N., … Wang, X. (2015). Characterization of a novel reduced height gene (*Rht23*) regulating panicle morphology and plant architecture in bread wheat. *Euphytica*, *203*(3). https://doi.org/10.1007/s10681-014-1275-1

Chen, X. M. (2005). Epidemiology and control of stripe rust [Puccinia striiformis f. sp. tritici] on wheat. *Canadian Journal of Plant Pathology*, *27*(3), 314–337. https://doi.org/10.1080/07060660509507230

Chen, Y., Carver, B. F., Wang, S., Cao, S., & Yan, L. (2010). Genetic regulation of developmental phases in winter wheat. *Molecular Breeding*, *26*(4), 573–582. https://doi.org/10.1007/s11032-010-9392-6

Chouard, P. (1960). Vernalization and its Relations to Dormancy. *Annual Review of Plant Physiology*, *11*(1). https://doi.org/10.1146/annurev.pp.11.060160.001203

Chu, C. G., Xu, S. S., Friesen, T. L., & Faris, J. D. (2008). Whole genome mapping in a wheat doubled haploid population using SSRs and TRAPs and the identification of QTL for agronomic traits. *Molecular Breeding*, *22*(2). https://doi.org/10.1007/s11032-008-9171-9

Clarke, J. M., Campbell, C. A., Cutforth, H. W., DePauw, R. M., & Winkleman, G. E. (1990). Nitrogen and Phosphorus Uptake, Translocation, and Utilization Efficiency of Wheat in Relation To Environment and Cultivar Yield and Protein Levels. *Canadian Journal of Plant Science*, *70*(4), 965–977. https://doi.org/10.4141/cjps90-119

Crespo-Herrera, L. A., Crossa, J., Huerta-Espino, J., Vargas, M., Mondal, S., Velu, G., … Singh, R. P. (2018). Genetic gains for grain yield in cimmyt's semi-arid wheat yield trials grown in suboptimal environments. *Crop Science*, *58*(5), 1890–1898. https://doi.org/10.2135/cropsci2018.01.0017

Cui, F., Zhao, C., Ding, A., Li, J., Wang, L., Li, X., … Wang, H. (2014). Construction of an integrative linkage map and QTL mapping of grain yield-related traits using three related wheat RIL populations. *TAG. Theoretical and Applied Genetics. Theoretische Und Angewandte Genetik*, *127*(3). https://doi.org/10.1007/s00122-013-2249-8

Cui, Fa, Zhang, N., Fan, X. L., Zhang, W., Zhao, C. H., Yang, L. J., … Li, J. M. (2017). Utilization of a Wheat660K SNP array-derived high-density genetic map for high-resolution mapping of a major QTL for kernel number. *Scientific Reports*, *7*(1). https://doi.org/10.1038/s41598-017-04028-6

Cuthbert, J. L., Somers, D. J., Brûlé-Babel, A. L., Brown, P. D., & Crow, G. H. (2008). Molecular mapping of quantitative trait loci for yield and yield components in spring wheat (*Triticum aestivum* L). *Theoretical and Applied Genetics*, *117*(4), 595–608. https://doi.org/10.1007/s00122-008-0804-5

Demotes-Mainard, S., Jeuffroy, M. H., & Robin, S. (1999). Spike dry matter and nitrogen accumulation before anthesis in wheat as affected by nitrogen fertilizer: Relationship to kernels per spike. *Field Crops Research*, *64*(3). https://doi.org/10.1016/S0378-4290(99)00046-5

Díaz, A., Zikhali, M., Turner, A. S., Isaac, P., & Laurie, D. A. (2012). Copy number variation affecting the photoperiod-B1 and vernalization-A1 genes is associated with altered flowering time in wheat (Triticum aestivum). *PLoS ONE*, *7*(3). https://doi.org/10.1371/journal.pone.0033234

Distelfeld, A., Li, C., & Dubcovsky, J. (2009). Regulation of flowering in temperate cereals. *Current Opinion in Plant Biology*, Vol. 12. https://doi.org/10.1016/j.pbi.2008.12.010

Dixon, L. E., Greenwood, J. R., Bencivenga, S., Zhang, P., Cockram, J., Mellers, G., … Boden, S. A. (2018). TEOSINTE BRANCHED1 regulates inflorescence architecture and development in bread wheat (*Triticum aestivum*). *Plant Cell*, *30*(3), 563–581. https://doi.org/10.1105/tpc.17.00961

Dobrovolskaya, O., Pont, C., Sibout, R., Martinek, P., Badaeva, E., Murat, F., … Salse, J. (2015). Frizzy panicle drives supernumerary spikelets in bread wheat. *Plant Physiology*, *167*(1). https://doi.org/10.1104/pp.114.250043

Dong, H., Dumenil, J., Lu, F. H., Na, L., Vanhaeren, H., Naumann, C., … Bevan, M. W. (2017). Ubiquitylation activates a peptidase that promotes cleavage and destabilization of its activating E3 ligases and diverse growth regulatory proteins to limit cell proliferation in Arabidopsis. *Genes and Development*, *31*(2). https://doi.org/10.1101/gad.292235.116

Duan, P., Xu, J., Zeng, D., Zhang, B., Geng, M., Zhang, G., … Li, Y. (2017). Natural Variation in the Promoter of GSE5 Contributes to Grain Size Diversity in Rice. *Molecular Plant*, *10*(5), 685–694. https://doi.org/10.1016/j.molp.2017.03.009

Dubcovsky, J., Lijavetzky, D., Appendino, L., & Tranquilli, G. (1998). Comparative RFLP mapping of Triticum monococcum genes controlling vernalization requirement. *Theoretical and Applied Genetics*, *97*(5–6). https://doi.org/10.1007/s001220050978

Dubcovsky, Jorge, Loukoianov, A., Fu, D., Valarik, M., Sanchez, A., & Yan, L. (2006). Effect of photoperiod on the regulation of wheat vernalization genes *VRN1* and *VRN2*. *Plant Molecular Biology*, *60*(4), 469–480. https://doi.org/10.1007/s11103-005-4814-2

Elouafi, I., & Nachit, M. M. (2004). A genetic linkage map of the Durum x Triticum dicoccoides backcross population based on SSRs and AFLP markers, and QTL analysis for milling traits. *Theoretical and Applied Genetics*, *108*(3). https://doi.org/10.1007/s00122-003-1440-8

Endo-Higashi, N., & Izawa, T. (2011). Flowering time genes heading date 1 and early heading date 1 together control panicle development in rice. *Plant and Cell Physiology*, *52*(6), 1083–1094. https://doi.org/10.1093/pcp/pcr059

Fischer, R. A. (1985). Number of kernels in wheat crops and the influence of solar radiation and temperature. *The Journal of Agricultural Science*, *105*(2). https://doi.org/10.1017/S0021859600056495

Fischer, R. A. (1993). Irrigated spring wheat and timing and amount of nitrogen fertilizer. II. Physiology of grain yield response. *Field Crops Research*, *33*(1–2). https://doi.org/10.1016/0378-4290(93)90094-4

Fischer, R. A. (2008). The importance of grain or kernel number in wheat: A reply to Sinclair and Jamieson. *Field Crops Research*, *105*(1–2), 15–21. https://doi.org/10.1016/j.fcr.2007.04.002

Fischer, R. A., & Quail, K. J. (1990). The effect of major dwarfing genes on yield potential in spring wheats. *Euphytica*, *46*(1). https://doi.org/10.1007/BF00057618

Fischer, T., Ammar, K., Monasterio, I. O., Monjardino, M., Singh, R., & Verhulst, N. (2022). Sixty years of irrigated wheat yield increase in the Yaqui Valley of Mexico: Past drivers, prospects and sustainability. *Field Crops Research*, *283*(December 2021), 108528. https://doi.org/10.1016/j.fcr.2022.108528

Flintham, J. E., Börner, A., Worland, A. J., & Gale, M. D. (1997). Optimizing wheat grain yield: Effects of *Rht* (gibberellin-insensitive) dwarfing genes. *Journal of Agricultural Science*, *128*(1), 11–25. https://doi.org/10.1017/S0021859696003942

Flood, R. G., & Halloran, G. M. (1986). Genetics and Physiology of Vernalization Response in Wheat. *Advances in Agronomy*, *39*(C). https://doi.org/10.1016/S0065-2113(08)60466-6

Fu, D., Szűcs, P., Yan, L., Helguera, M., Skinner, J. S., Von Zitzewitz, J., … Dubcovsky, J. (2005). Large deletions within the first intron in *VRN*-1 are associated with spring growth habit in barley and wheat. *Molecular Genetics and Genomics*, *273*(1). https://doi.org/10.1007/s00438-004-1095-4

Gambín, B. L., Borrás, L., & Otegui, M. E. (2008). Kernel weight dependence upon plant growth at different grain-filling stages in maize and sorghum. *Australian Journal of Agricultural Research*, *59*(3). https://doi.org/10.1071/AR07275

Garcia, M., Eckermann, P., Haefele, S., Satija, S., Sznajder, B., Timmins, A., … Fleury, D. (2019). Genome-wide association mapping of grain yield in a diverse collection of spring wheat (*Triticum aestivum* L) evaluated in southern Australia. *PLoS ONE*, *14*(2), 1–19. https://doi.org/10.1371/journal.pone.0211730

Gegas, V. C., Nazari, A., Griffiths, S., Simmonds, J., Fish, L., Orford, S., … Snape, J. W. (2010). A genetic framework for grain size and shape variation in wheat. *Plant Cell*, *22*(4), 1046–1056. https://doi.org/10.1105/tpc.110.074153

Goncharov, N. P. (2004). Response to vernalization in wheat: Its quantitative or qualitative nature. *Cereal Research Communications*, Vol. 32. https://doi.org/10.1007/bf03543317

González, F. G., Slafer, G. A., & Miralles, D. J. (2002). Vernalization and photoperiod responses in wheat pre-flowering reproductive phases. *Field Crops Research*, *74*(2–3). https://doi.org/10.1016/S0378-4290(01)00210-6

González, F. G., Slafer, G. A., & Miralles, D. J. (2003a). Floret development and spike growth as affected by photoperiod during stem elongation in wheat. *Field Crops Research*, *81*(1). https://doi.org/10.1016/S0378-4290(02)00196-X

González, F. G., Slafer, G. A., & Miralles, D. J. (2003b). Grain and floret number in response to photoperiod during stem elongation in fully and slightly vernalized wheats. *Field Crops Research*, *81*(1), 17–27. https://doi.org/10.1016/S0378-4290(02)00195-8

González, F. G., Slafer, G. A., & Miralles, D. J. (2003c). Grain and floret number in response to photoperiod during stem elongation in fully and slightly vernalized wheats. *Field Crops Research*, *81*(1), 17–27. https://doi.org/10.1016/S0378-4290(02)00195-8

Greco, M., Chiappetta, A., Bruno, L., & Bitonti, M. B. (2012). In Posidonia oceanica cadmium induces changes in DNA methylation and chromatin patterning. *Journal of Experimental Botany*, *63*(2), 695–709. https://doi.org/10.1093/jxb/err313

Griffiths, S., Simmonds, J., Leverington, M., Wang, Y., Fish, L., Sayers, L., … Snape, J. (2009). Meta-QTL analysis of the genetic control of ear emergence in elite European winter wheat germplasm. *Theoretical and Applied Genetics*, *119*(3). https://doi.org/10.1007/s00122-009-1046-x

Griffiths, S., Simmonds, J., Leverington, M., Wang, Y., Fish, L., Sayers, L., … Snape, J. (2012). Meta-QTL analysis of the genetic control of crop height in elite European winter wheat germplasm. *Molecular Breeding*, *29*(1), 159–171. https://doi.org/10.1007/s11032-010-9534-x

Groos, C., Robert, N., Bervas, E., & Charmet, G. (2003). Genetic analysis of grain protein-content, grain yield and thousand-kernel weight in bread wheat. *Theoretical and Applied Genetics*, *106*(6), 1032–1040. https://doi.org/10.1007/s00122-002-1111-1

Guan, P., Lu, L., Jia, L., Kabir, M. R., Zhang, J., Lan, T., … Peng, H. (2018). Global QTL analysis identifies genomic regions on chromosomes 4A and 4B harboring stable loci for yield-related traits across different environments in wheat (*Triticum aestivum* L). *Frontiers in Plant Science*, *9*. https://doi.org/10.3389/fpls.2018.00529

Guo, J., Hao, C., Zhang, Y., Zhang, B., Cheng, X., Qin, L., … Cheng, S. (2015). Association and validation of yield-favored alleles in Chinese cultivars of common wheat (*Triticum aestivum* L). *PLoS ONE*, *10*(6), 1–18. https://doi.org/10.1371/journal.pone.0130029

Hanocq, E., Laperche, A., Jaminon, O., Lainé, A. L., & Le Gouis, J. (2007). Most significant genome regions involved in the control of earliness traits in bread wheat, as revealed by QTL meta-analysis. *Theoretical and Applied Genetics*, *114*(3). https://doi.org/10.1007/s00122-006-0459-z

Hanocq, E., Niarquin, M., Heumez, E., Rousset, M., & Le Gouis, J. (2004). Detection and mapping of QTL for earliness components in a bread wheat recombinant inbred lines population. *Theoretical and Applied Genetics*, *110*(1). https://doi.org/10.1007/s00122-004-1799-1

Hasan, A. K., Herrera, J., Lizana, C., & Calderini, D. F. (2011). Carpel weight, grain length and stabilized grain water content are physiological drivers of grain weight determination of wheat. *Field Crops Research*, *123*(3). https://doi.org/10.1016/j.fcr.2011.05.019

Hess, J. R., Carman, J. G., & Banowetz, G. M. (2002). Hormones in wheat kernels during embryony. *Journal of Plant Physiology*, *159*(4). https://doi.org/10.1078/0176-1617-00718

Hong, Y., Chen, L., Du, L. P., Su, Z., Wang, J., Ye, X., … Zhang, Z. (2014). Transcript suppression of *TaGW2* increased grain width and weight in bread wheat. *Functional and Integrative Genomics*, *14*(2), 341–349. https://doi.org/10.1007/s10142-014-0380-5

Hoogendoorn, J. (1985). A reciprocal F1 monosomic analysis of the genetic control of time of ear emergence, number of leaves and number of spikelets in wheat (*Triticum aestivum* L). *Euphytica*, *34*(2). https://doi.org/10.1007/BF00022954

Hu, J., Wang, Y., Fang, Y., Zeng, L., Xu, J., Yu, H., … Qian, Q. (2015). A rare allele of *GS2* enhances grain size and grain yield in rice. *Molecular Plant*, *8*(10), 1455–1465. https://doi.org/10.1016/j.molp.2015.07.002

Huang, X. Q., Cloutier, S., Lycar, L., Radovanovic, N., Humphreys, D. G., Noll, J. S., … Brown, P. D. (2006). Molecular detection of QTLs for agronomic and quality traits in a doubled haploid population derived from two Canadian wheats (*Triticum aestivum* L). *Theoretical and Applied Genetics*, *113*(4). https://doi.org/10.1007/s00122-006-0346-7

Huang, X. Q., Cöster, H., Ganal, M. W., & Röder, M. S. (2003). Advanced backcross QTL analysis for the identification of quantitative trait loci alleles from wild relatives of wheat (*Triticum aestivum* L). *Theoretical and Applied Genetics*, *106*(8), 1379–1389. https://doi.org/10.1007/s00122-002-1179-7

Huang, X. Q., Kempf, H., Canal, M. W., & Röder, M. S. (2004). Advanced backcross QTL analysis in progenies derived from a cross between a German elite winter wheat variety and a synthetic wheat (*Triticum aestivum* L). *Theoretical and Applied Genetics*, *109*(5). https://doi.org/10.1007/s00122-004-1708-7

Ikeda-Kawakatsu, K., Yasuno, N., Oikawa, T., Iida, S., Nagato, Y., Maekawa, M., & Kyozuka, J. (2009). Expression level of ABERRANT PANICLE ORGANIZATION1 determines rice inflorescence form through control of cell proliferation in the meristem. *Plant Physiology*, *150*(2), 736–747. https://doi.org/10.1104/pp.109.136739

Jaenisch, B. R., Munaro, L. B., Jagadish, S. V. K., & Lollato, R. P. (2022). Modulation of Wheat Yield Components in Response to Management Intensification to Reduce Yield Gaps. *Frontiers in Plant Science*, *13*(May), 1–18. https://doi.org/10.3389/fpls.2022.772232

Jaiswal, V., Gahlaut, V., Mathur, S., Agarwal, P., Khandelwal, M. K., Khurana, J. P., … Gupta, P. K. (2015). Identification of novel SNP in promoter sequence of *TaGW2*-6A associated with grain weight and other agronomic traits in wheat (*Triticum aestivum* L). *PLoS ONE*, *10*(6), 1–15. https://doi.org/10.1371/journal.pone.0129400

Kamran, A., Iqbal, M., Navabi, A., Randhawa, H., Pozniak, C., & Spaner, D. (2013). Earliness per se QTLs and their interaction with the photoperiod insensitive allele *Ppd-D1a* in the Cutler × AC Barrie spring wheat population. *Theoretical and Applied Genetics*, *126*(8). https://doi.org/10.1007/s00122-013-2110-0

Kamran, Atif, Iqbal, M., & Spaner, D. (2014). Flowering time in wheat (*Triticum aestivum* L): A key factor for global adaptability. *Euphytica*, *197*(1), 1–26. https://doi.org/10.1007/s10681-014-1075-7

Kato, K., Miura, H., & Sawada, S. (1999a). Detection of an earliness per se quantitative trait locus in the proximal region of wheat chromosome 5AL. *Plant Breeding*, *118*(5). https://doi.org/10.1046/j.1439-0523.1999.00395.x

Kato, K., Miura, H., & Sawada, S. (1999b). QTL mapping of genes controlling ear emergence time and plant height on chromosome 5A of wheat. *Theoretical and Applied Genetics*, *98*(3–4). https://doi.org/10.1007/s001220051094

Kato, K., Miura, H., & Sawada, S. (2000). Mapping QTLs controlling grain yield and its components on chromosome 5A of wheat. *Theoretical and Applied Genetics*, *101*(7). https://doi.org/10.1007/s001220051587

Kato, Taketa, Ban, Iriki, & Murai. (2001). The influence of a spring habit gene, *Vrn-D1*, on heading time in wheat. *Plant Breeding*, *120*(2). https://doi.org/10.1046/j.1439-0523.2001.00586.x

Kino, R. I., Pellny, T. K., Mitchell, R. A. C., Gonzalez-Uriarte, A., & Tosi, P. (2020). High post-anthesis temperature effects on bread wheat (*Triticum aestivum* L) grain transcriptome during early grain-filling. *BMC Plant Biology*, *20*(1). https://doi.org/10.1186/s12870-020-02375-7

Kirby, E. J. M. (1990). Co-ordination of leaf emergence and leaf and spikelet primordium initiation in wheat. *Field Crops Research*, *25*(3–4), 253–264. https://doi.org/10.1016/0378-4290(90)90008-Y

Kulwal, P. L., Roy, J. K., Balyan, H. S., & Gupta, P. K. (2003). QTL mapping for growth and leaf characters in bread wheat. *Plant Science*, *164*(2). https://doi.org/10.1016/S0168-9452(02)00409-0

Kumar, N., Kulwal, P. L., Balyan, H. S., & Gupta, P. K. (2007). QTL mapping for yield and yield contributing traits in two mapping populations of bread wheat. *Molecular Breeding*, *19*(2), 163–177. https://doi.org/10.1007/s11032-006-9056-8

Kunert, A., Naz, A. A., Dedeck, O., Pillen, K., & Léon, J. (2007). AB-QTL analysis in winter wheat: I. Synthetic hexaploid wheat (T. turgidum ssp. dicoccoides × T. tauschii) as a source of favourable alleles for milling and baking quality traits. *Theoretical and Applied Genetics*, *115*(5). https://doi.org/10.1007/s00122-007-0600-7

Kuzay, S., Xu, Y., Zhang, J., Katz, A., Pearce, S., Su, Z., … Dubcovsky, J. (2019). Identification of a candidate gene for a QTL for spikelet number per spike on wheat chromosome arm 7AL by high-resolution genetic mapping. *Theoretical and Applied Genetics*. https://doi.org/10.1007/s00122-019-03382-5

Langer, R. H. M., & Hanif, M. (1973). A study of floret development in wheat (*Triticum aestivum* L). *Annals of Botany*, *37*(4). https://doi.org/10.1093/oxfordjournals.aob.a084743

Law, C. N., Sutka, J., & Worland, A. J. (1978). A genetic study of day-length response in wheat. *Heredity*, *41*(2). https://doi.org/10.1038/hdy.1978.87

Law, C. N., & Worland, A. J. (1997). Genetic analysis of some flowering time and adaptive traits in wheat. *New Phytologist*, *137*(1), 19–28. https://doi.org/10.1046/j.1469-8137.1997.00814.x

Law, C. N., Worland, A. J., & Giorgi, B. (1976). The genetic control of ear-emergence time by chromosomes 5A and 5D of wheat. *Heredity*, *36*(1). https://doi.org/10.1038/hdy.1976.5

Lenton, J. R., Hedden, P., & Gale, M. D. (1987). Gibberellin insensitivity and depletion in wheat - consequences for development. In *Hormone Action in Plant Development–Acritical Appraisal*. https://doi.org/10.1016/b978-0-408-00796-2.50015-3

Levy, J., & Peterson, M. L. (1972). Responses of Spring Wheats to Vernalization and Photoperiod 1 . *Crop Science*, *12*(4). https://doi.org/10.2135/cropsci1972.0011183x001200040029x

Li, C., Distelfeld, A., Comis, A., & Dubcovsky, J. (2011). Wheat flowering repressor *VRN2* and promoter CO_2 compete for interactions with NUCLEAR FACTOR-Y complexes. *Plant Journal*, *67*(5), 763–773. https://doi.org/10.1111/j.1365-313X.2011.04630.x

Li, F., Wen, W., Liu, J., Zhang, Y., Cao, S., He, Z., … Xia, X. (2019). Genetic architecture of grain yield in bread wheat based on genome-wide association studies. *BMC Plant Biology*, *19*(1), 1–19. https://doi.org/10.1186/s12870-019-1781-3

Li, H., Ye, G., & Wang, J. (2007). A modified algorithm for the improvement of composite interval mapping. *Genetics*. https://doi.org/10.1534/genetics.106.066811

Li, N., & Li, Y. (2015). Maternal control of seed size in plants. *Journal of Experimental Botany*, *66*(4), 1087–1097. https://doi.org/10.1093/jxb/eru549

Li, S., Jia, J., Wei, X., Zhang, X., Li, L., Chen, H., … Li, L. (2007). A intervarietal genetic map and QTL analysis for yield traits in wheat. *Molecular Breeding*, *20*(2). https://doi.org/10.1007/s11032-007-9080-3

Li, W., & Yang, B. (2017). Translational genomics of grain size regulation in wheat. *Theoretical and Applied Genetics*, *130*(9), 1765–1771. https://doi.org/10.1007/s00122-017-2953-x

Li, X., Xia, X., Xiao, Y., He, Z., Wang, D., Trethowan, R., … Chen, X. (2015). QTL mapping for plant height and yield components in common wheat under water-limited and full irrigation environments. *Crop and Pasture Science*, *66*(7). https://doi.org/10.1071/CP14236

Li, Y., Fan, C., Xing, Y., Jiang, Y., Luo, L., Sun, L., … Zhang, Q. (2011). Natural variation in *GS5* plays an important role in regulating grain size and yield in rice. *Nature Genetics*, *43*(12), 1266–1269. https://doi.org/10.1038/ng.977

Lin, Y., Jiang, X., Hu, H., Zhou, K., Wang, Q., Yu, S., … Liu, Y. (2021). QTL mapping for grain number per spikelet in wheat using a high-density genetic map. *Crop Journal*, *9*(5), 1108–1114. https://doi.org/10.1016/j.cj.2020.12.006

Liu, Y., Lin, Y., Gao, S., Li, Z., Ma, J., Deng, M., … Zheng, Y. (2017). A genome-wide association study of 23 agronomic traits in Chinese wheat landraces. *Plant Journal*, *91*(5). https://doi.org/10.1111/tpj.13614

Loss, S. P., Kirby, E. J. M., Siddique, K. H. M., & Perry, M. W. (1989). Grain growth and development of old and modern Australian wheats. *Field Crops Research*, *21*(2). https://doi.org/10.1016/0378-4290(89)90049-X

Lozada, D. N., Mason, R. E., Babar, M. A., Carver, B. F., Guedira, G. B., Merrill, K., … Dreisigacker, S. (2017). Association mapping reveals loci associated with multiple traits that affect grain yield and adaptation in soft winter wheat. *Euphytica*. https://doi.org/10.1007/s10681-017-2005-2

Lozada, D. N., Mason, R. E., Sukumaran, S., & Dreisigacker, S. (2018). Validation of grain yield QTLs from soft winter wheat using a CIMMYT spring wheat panel. *Crop Science*, *58*(5). https://doi.org/10.2135/cropsci2018.04.0232

Luo, W., Ma, J., Zhou, X. H., Sun, M., Kong, X. C., Wei, Y. M., … Lan, X. J. (2016). Identification of quantitative trait loci controlling agronomic traits indicates breeding potential of tibetan semiwild wheat (*Triticum aestivum* ssp. *tibetanum*). *Crop Science*, *56*(5), 2410–2420. https://doi.org/10.2135/cropsci2015.11.0700

Ma, F., Xu, Y., Ma, Z., Li, L., & An, D. (2018). Genome-wide association and validation of key loci for yield-related traits in wheat founder parent Xiaoyan 6. *Molecular Breeding*, *38*(7). https://doi.org/10.1007/s11032-018-0837-7

Ma, J., Ding, P., Liu, J., Li, T., Zou, Y., Habib, A., … Lan, X. (2019). Identification and validation of a major and stably expressed QTL for spikelet number per spike in bread wheat. *Theoretical and Applied Genetics*, *132*(11), 3155–3167. https://doi.org/10.1007/s00122-019-03415-z

Ma, Y., Shabala, S., Li, C., Liu, C., Zhang, W., & Zhou, M. (2015). Quantitative trait loci for salinity tolerance identified under drained and waterlogged conditions and their association with flowering time in barley (*Hordeum vulgare*. L). *PLoS ONE*, *10*(8), 1–15. https://doi.org/10.1371/journal.pone.0134822

Ma, Z., Zhao, D., Zhang, C., Zhang, Z., Xue, S., Lin, F., … Luo, Q. (2007). Molecular genetic analysis of five spike-related traits in wheat using RIL and immortalized F2 populations. *Molecular Genetics and Genomics*, *277*(1), 31–42. https://doi.org/10.1007/s00438-006-0166-0

Maccaferri, M., Sanguineti, M. C., Corneti, S., Ortega, J. L. A., Salem, M. Ben, Bort, J., … Tuberosa, R. (2008). Quantitative trait loci for grain yield and adaptation of durum wheat (*Triticum durum* Desf) across a wide range of water availability. *Genetics*, *178*(1), 489–511. https://doi.org/10.1534/genetics.107.077297

Maeoka, R. E., Sadras, V. O., Ciampitti, I. A., Diaz, D. R., Fritz, A. K., & Lollato, R. P. (2020). Changes in the Phenotype of Winter Wheat Varieties Released Between 1920 and 2016 in Response to In-Furrow Fertilizer: Biomass Allocation, Yield, and Grain Protein Concentration. *Frontiers in Plant Science*, *10*(January). https://doi.org/10.3389/fpls.2019.01786

Malhi, S. S., Johnston, A. M., Schoenau, J. J., Wang, Z. H., & Vera, C. L. (2007). Seasonal biomass accumulation and nutrient uptake of pea and lentil on a black chernozem soil in Saskatchewan. *Journal of Plant Nutrition*, *30*(5), 721–737. https://doi.org/10.1080/01904160701289578

Malloch, A. J. C., Bewley, J. D., & Black, M. (1986). Seeds: Physiology of Development and Germination. *The Journal of Ecology*, *74*(3). https://doi.org/10.2307/2260407

Martínez-Barajas, E., Delatte, T., Schluepmann, H., de Jong, G. J., Somsen, G. W., Nunes, C., … Paul, M. J. (2011). Wheat grain development is characterized by remarkable trehalose 6-phosphate accumulation pregrain filling: Tissue distribution and relationship to SNF1-related protein kinase1 activity. *Plant Physiology*, *156*(1). https://doi.org/10.1104/pp.111.174524

Marza, F., Bai, G. H., Carver, B. F., & Zhou, W. C. (2006). Quantitative trait loci for yield and related traits in the wheat population Ning7840 x Clark. *Theoretical and Applied Genetics*, *112*(4), 688–698. https://doi.org/10.1007/s00122-005-0172-3

Mathews, K. L., Malosetti, M., Chapman, S., McIntyre, L., Reynolds, M., Shorter, R., & Van Eeuwijk, F. (2008). Multi-environment QTL mixed models for drought stress adaptation in wheat. *Theoretical and Applied Genetics*, *117*(7). https://doi.org/10.1007/s00122-008-0846-8

McCartney, C. A., Somers, D. J., Humphreys, D. G., Lukow, O., Ames, N., Noll, J., … McCallum, B. D. (2005). Mapping quantitative trait loci controlling agronomic traits in the spring wheat cross RL4452 x "AC Domain." *Genome*, *48*(5). https://doi.org/10.1139/G05-055

Mcintosh, R. a, Dubcovsky, J., Rogers, W. J., Morris, C. F., Appels, R., Xia, X. C., … Hayden, M. (2013). Catalogue of Gene Symbols for Wheat: 2013-2014 Supplement. *12th International Wheat Genetics Symposium*.

McIntosh, R., & Yamazaki, Y. (2008). Catalogue of gene symbols for wheat. *International Wheat Genetics Symposium*, *4*(September), 1–197. Retrieved from http://www.cabdirect.org/abstracts/20083014739.html%5Cnhttp://scabusatest1.com/ggpages/wgc/2003/Catalogue.pdf

McSteen, P., Laudencia-Chingcuanco, D., & Colasanti, J. (2000). A floret by any other name: Control of meristem identity in maize. *Trends in Plant Science*, *5*(2), 61–66. https://doi.org/10.1016/S1360-1385(99)01541-1

Miglietta, F. (1989). Effect of photoperiod and temperature on leaf initiation rates in wheat (*Triticum* spp). *Field Crops Research*, *21*(2). https://doi.org/10.1016/0378-4290(89)90048-8

Millet, E., & Pinthus, M. J. (1984). The association between grain volume and grain weight in wheat. *Journal of Cereal Science*, *2*(1). https://doi.org/10.1016/S0733-5210(84)80005-3

Millet, Eitan. (1986). Relationships between grain weight and the size of floret cavity in the wheat spike. *Annals of Botany*, *58*(3). https://doi.org/10.1093/oxfordjournals.aob.a087220

Mir, R. R., Kumar, N., Jaiswal, V., Girdharwal, N., Prasad, M., Balyan, H. S., & Gupta, P. K.

(2012). Genetic dissection of grain weight in bread wheat through quantitative trait locus interval and association mapping. *Molecular Breeding*, *29*(4), 963–972. https://doi.org/10.1007/s11032-011-9693-4

Miralles, D. J., Dominguez, C. F., & Slafer, G. A. (1996). Relationship between grain growth and postanthesis leaf area duration in dwarf, semidwarf and tall isogenic lines of wheat. *Journal of Agronomy and Crop Science*, *177*(2). https://doi.org/10.1111/j.1439-037x.1996.tb00600.x

Miralles, D. J., Richards, R. A., & Slafer, G. A. (2000). Duration of the stem elongation period influences the number of fertile florets in wheat and barley. *Australian Journal of Plant Physiology*, *27*(10). https://doi.org/10.1071/pp00021

Miralles, Daniel J., & Slafer, G. A. (1995). Individual grain weight responses to genetic reduction in culm length in wheat as affected by source-sink manipulations. *Field Crops Research*, *43*(2–3). https://doi.org/10.1016/0378-4290(95)00041-N

Miura, K., Ikeda, M., Matsubara, A., Song, X. J., Ito, M., Asano, K., … Ashikari, M. (2010). *OsSPL14* promotes panicle branching and higher grain productivity in rice. *Nature Genetics*, *42*(6), 545–549. https://doi.org/10.1038/ng.592

Mo, Y., Vanzetti, L. S., Hale, I., Spagnolo, E. J., Guidobaldi, F., Al-Oboudi, J., … Dubcovsky, J. (2018). Identification and characterization of *Rht25*, a locus on chromosome arm 6AS affecting wheat plant height, heading time, and spike development. *Theoretical and Applied Genetics*, *131*(10). https://doi.org/10.1007/s00122-018-3130-6

Muhammad, A., Hu, W., Li, Z., Li, J., Xie, G., Wang, J., & Wang, L. (2020). Appraising the genetic architecture of kernel traits in hexaploid wheat using GWAS. *International Journal of Molecular Sciences*, *21*(16), 1–21. https://doi.org/10.3390/ijms21165649

Nakamichi, N., Kita, M., Ito, S., Yamashino, T., & Mizuno, T. (2005). Pseudo-response regulators, PRR9, PRR7 and PRR5, together play essential roles close to the circadian clock of Arabidopsis thaliana. *Plant and Cell Physiology*, *46*(5), 686–698. https://doi.org/10.1093/pcp/pci086

Naruoka, Y., Talbert, L. E., Lanning, S. P., Blake, N. K., Martin, J. M., & Sherman, J. D. (2011). Identification of quantitative trait loci for productive tiller number and its relationship to agronomic traits in spring wheat. *Theoretical and Applied Genetics*. https://doi.org/10.1007/s00122-011-1646-0

Nazir, M. F., Sarfraz, Z., Mangi, N., Shah, M. K. N., Mahmood, T., Mahmood, T., … Sabagh, A. E. L. (2021). Post-anthesis mobilization of stem assimilates in wheat under induced stress. *Sustainability (Switzerland)*, *13*(11). https://doi.org/10.3390/su13115940

O'Hara, L. E., Paul, M. J., & Wingler, A. (2013). How do sugars regulate plant growth and development? New insight into the role of trehalose-6-phosphate. *Molecular Plant*, Vol. 6. https://doi.org/10.1093/mp/sss120

Ochagavía, H., Prieto, P., Savin, R., & Slafer, G. A. (2021). Developmental patterns and rates of organogenesis across modern and well-adapted wheat cultivars. *European Journal of Agronomy*, *126*(April), 126280. https://doi.org/10.1016/j.eja.2021.126280

Orozco-Arroyo, G., Paolo, D., Ezquer, I., & Colombo, L. (2015). Networks controlling seed size in Arabidopsis. *Plant Reproduction*, *28*(1), 17–32. https://doi.org/10.1007/s00497-015-0255-5

Pearce, S., Saville, R., Vaughan, S. P., Chandler, P. M., Wilhelm, E. P., Sparks, C. A., … Thomas, S. G. (2011). Molecular characterization of *Rht-1* dwarfing genes in hexaploid wheat. *Plant Physiology*, *157*(4), 1820–1831. https://doi.org/10.1104/pp.111.183657

Peng, J., Ronin, Y., Fahima, T., Röder, M. S., Li, Y., Nevo, E., & Korol, A. (2003). Domestication quantitative trait loci in Triticum dicoccoides, the progenitor of wheat. *Proceedings of the National Academy of Sciences of the United States of America*, *100*(5). https://doi.org/10.1073/pnas.252763199

Philipp, N., Weichert, H., Bohra, U., Weschke, W., Schulthess, A. W., & Weber, H. (2018). Grain number and grain yield distribution along the spike remain stable despite breeding for high yield in winter wheat. *PLoS ONE*, *13*(10). https://doi.org/10.1371/journal.pone.0205452

Pinthus, M. J., & Millet, E. (1978). Interactions among number of spikelets, number of grains and grain weight in the spikes of wheat (*Triticum aestivum* L). *Annals of Botany*, *42*(4). https://doi.org/10.1093/oxfordjournals.aob.a085523

Pinthus, Moshe J., Gale, M. D., Appleford, N. E. J., & Lenton, J. R. (1989). Effect of temperature on gibberellin (GA) responsiveness and on endogenous GA1 content of tall and dwarf wheat genotypes. *Plant Physiology*, *90*(3). https://doi.org/10.1104/pp.90.3.854

Pugsley, A. T. (1971). A genetic analysis of the spring-winter habit of growth in wheat. *Australian Journal of Agricultural Research*, *22*(1). https://doi.org/10.1071/AR9710021

Qin, L., Hao, C., Hou, J., Wang, Y., Li, T., Wang, L., … Zhang, X. (2014). Homologous haplotypes, expression, genetic effects and geographic distribution of the wheat yield gene *TaGW2*. *BMC Plant Biology*, *14*(1). https://doi.org/10.1186/1471-2229-14-107

Quarrie, S. A., Pekic Quarrie, S., Radosevic, R., Rancic, D., Kaminska, A., Barnes, J. D., … Dodig, D. (2006). Dissecting a wheat QTL for yield present in a range of environments: From the QTL to candidate genes. *Journal of Experimental Botany*, *57*(11), 2627–2637. https://doi.org/10.1093/jxb/erl026

Radchuk, V., Tran, V., Radchuk, R., Diaz-Mendoza, M., Weier, D., Fuchs, J., … Borisjuk, L. (2018). Vacuolar processing enzyme 4 contributes to maternal control of grain size in barley by executing programmed cell death in the pericarp. *New Phytologist*, *218*(3). https://doi.org/10.1111/nph.14729

Radchuk, V., Weier, D., Radchuk, R., Weschke, W., & Weber, H. (2011). Development of maternal seed tissue in barley is mediated by regulated cell expansion and cell disintegration and coordinated with endosperm growth. *Journal of Experimental Botany*, *62*(3). https://doi.org/10.1093/jxb/erq348

Ramsay, L., Comadran, J., Druka, A., Marshall, D. F., Thomas, W. T. B., MacAulay, M., … Waugh, R. (2011). INTERMEDIUM-C, a modifier of lateral spikelet fertility in barley, is an ortholog of the maize domestication gene TEOSINTE BRANCHED 1. *Nature Genetics*, *43*(2), 169–172. https://doi.org/10.1038/ng.745

Rasmussen, I. S., Dresbøll, D. B., & Thorup-Kristensen, K. (2015). Winter wheat cultivars and nitrogen (N) fertilization-Effects on root growth, N uptake efficiency and N use efficiency. *European Journal of Agronomy*, *68*. https://doi.org/10.1016/j.eja.2015.04.003

Rawson, H. M., Zajac, M., & Penrose, L. D. J. (1998). Effect of seedling temperature and its duration on development of wheat cultivars differing in vernalization response. *Field Crops Research*, *57*(3). https://doi.org/10.1016/S0378-4290(98)00073-2

Reynolds, M. P., Pellegrineschi, A., & Skovmand, B. (2005). Sink-limitation to yield and biomass: A summary of some investigations in spring wheat. *Annals of Applied Biology*, *146*(1), 39–49. https://doi.org/10.1111/j.1744-7348.2005.03100.x

Richards, R. A. (1992). The effect of dwarfing genes in spring wheat in dry environments. I. Agronomic characteristics. *Australian Journal of Agricultural Research*, *43*(3). https://doi.org/10.1071/AR9920517

Richards, R. A., & Lukacs, Z. (2002). Seedling vigour in wheat - Sources of variation for genetic and agronomic improvement. *Australian Journal of Agricultural Research*, *53*(1). https://doi.org/10.1071/AR00147

Rotundo, J. L., Borrás, L., Westgate, M. E., & Orf, J. H. (2009). Relationship between assimilate supply per seed during seed filling and soybean seed composition. *Field Crops Research*, *112*(1). https://doi.org/10.1016/j.fcr.2009.02.004

Sadras, V. O. (2007). Evolutionary aspects of the trade-off between seed size and number in crops. *Field Crops Research*, Vol. 100. https://doi.org/10.1016/j.fcr.2006.07.004

Sadras, V. O., & Slafer, G. A. (2012). Environmental modulation of yield components in cereals: Heritabilities reveal a hierarchy of phenotypic plasticities. *Field Crops Research*, *127*. https://doi.org/10.1016/j.fcr.2011.11.014

Sakuma, S., Golan, G., Guo, Z., Ogawa, T., Tagiri, A., Sugimoto, K., … Komatsuda, T. (2019). Unleashing floret fertility in wheat through the mutation of a homeobox gene. *Proceedings of the National Academy of Sciences of the United States of America*, *116*(11), 5182–5187. https://doi.org/10.1073/pnas.1815465116

Scarth, R., & Law, C. N. (1983). The location of the photoperiod gene, *Ppd2* and an additional genetic factor for ear-emergence time on chromosome 2B of wheat. *Heredity*, *51*(3), 607–619. https://doi.org/10.1038/hdy.1983.73

Serrago, R. A., Alzueta, I., Savin, R., & Slafer, G. A. (2013). Understanding grain yield responses to source-sink ratios during grain filling in wheat and barley under contrasting environments. *Field Crops Research*, *150*, 42–51. https://doi.org/10.1016/j.fcr.2013.05.016

Shaw, L. M., Turner, A. S., Herry, L., Griffiths, S., & Laurie, D. A. (2013). Mutant alleles of Photoperiod-1 in Wheat (*Triticum aestivum* L) that confer a late flowering phenotype in long days. *PLoS ONE*, *8*(11). https://doi.org/10.1371/journal.pone.0079459

Shaw, L. M., Turner, A. S., & Laurie, D. A. (2012). The impact of photoperiod insensitive *Ppd-1a* mutations on the photoperiod pathway across the three genomes of hexaploid wheat (*Triticum aestivum*). *Plant Journal*, *71*(1), 71–84. https://doi.org/10.1111/j.1365-313X.2012.04971.x

Shi, W., Hao, C., Zhang, Y., Cheng, J., Zhang, Z., Liu, J., … Guo, J. (2017). A combined association mapping and linkage analysis of kernel number per spike in common wheat (*Triticum aestivum* L). *Frontiers in Plant Science*, *8*. https://doi.org/10.3389/fpls.2017.01412

Shindo, C., Tsujimoto, H., & Sasakuma, T. (2003). Segregation analysis of heading traits in hexaploid wheat utilizing recombinant inbred lines. *Heredity*, *90*(1). https://doi.org/10.1038/sj.hdy.6800178

Si, L., Chen, J., Huang, X., Gong, H., Luo, J., Hou, Q., … Han, B. (2016). *OsSPL13* controls grain size in cultivated rice. *Nature Genetics*, *48*(4), 447–456. https://doi.org/10.1038/ng.3518

Sibony, M., & Pinthus, M. J. (1988). Floret initiation and development in spring wheat (*Triticum aestivum* L). *Annals of Botany*, *61*(4). https://doi.org/10.1093/oxfordjournals.aob.a087578

Simmonds, J., Scott, P., Brinton, J., Mestre, T. C., Bush, M., del Blanco, A., … Uauy, C. (2016). A splice acceptor site mutation in *TaGW2-A1* increases thousand grain weight in tetraploid and hexaploid wheat through wider and longer grains. *Theoretical and Applied Genetics*, *129*(6), 1099–1112. https://doi.org/10.1007/s00122-016-2686-2

Sinclair, T. R., & Jamieson, P. D. (2006). Grain number, wheat yield, and bottling beer: An analysis. *Field Crops Research*, *98*(1), 60–67. https://doi.org/10.1016/j.fcr.2005.12.006

Sinclair, Thomas R., Purcell, L. C., & Sneller, C. H. (2004). Crop transformation and the challenge to increase yield potential. *Trends in Plant Science*, *9*(2), 70–75. https://doi.org/10.1016/j.tplants.2003.12.008

Slafer, G. A. (2007). Physiology of Determination of Major Wheat Yield Components. In *Wheat Production in Stressed Environments*. https://doi.org/10.1007/1-4020-5497-1_68

Slafer, G. A., Abeledo, L. G., Miralles, D. J., Gonzalez, F. G., & Whitechurch, E. M. (2001). Photoperiod sensitivity during stem elongation as an avenue to raise potential yield in wheat. *Euphytica*, *119*(1–2). https://doi.org/10.1023/A:1017535632171

Slafer, Gustavo A., Andrade, F. H., & Satorre, E. H. (1990). Genetic-improvement effects on pre-anthesis physiological attributes related to wheat grain-yield. *Field Crops Research*, *23*(3–4). https://doi.org/10.1016/0378-4290(90)90058-J

Slafer, Gustavo A., Calderini, D. F., & Miralles, D. J. (1996). Yield Components and Compensation in Wheat: Opportunities for Further Increasing Yield Potential. *Increasing Yield Potential in Wheat: Breaking the Barriers*.

Slafer, Gustavo A., García, G. A., Serrago, R. A., & Miralles, D. J. (2022). Physiological drivers of responses of grains per m2 to environmental and genetic factors in wheat. *Field Crops Research*, *285*(May), 108593. https://doi.org/10.1016/j.fcr.2022.108593

Slafer, Gustavo A., Savin, R., Pinochet, D., & Calderini, D. F. (2020). Wheat. In *Crop Physiology Case Histories for Major Crops*. https://doi.org/10.1016/B978-0-12-819194-1.00003-7

Slafer, Gustavo A., Savin, R., & Sadras, V. O. (2014). Coarse and fine regulation of wheat yield components in response to genotype and environment. *Field Crops Research*, *157*, 71–83. https://doi.org/10.1016/j.fcr.2013.12.004

Song, X. J., Huang, W., Shi, M., Zhu, M. Z., & Lin, H. X. (2007). A QTL for rice grain width and weight encodes a previously unknown RING-type E3 ubiquitin ligase. *Nature Genetics*, *39*(5). https://doi.org/10.1038/ng2014

Sourdille, P., Cadalen, T., Guyomarc'h, H., Snape, J. W., Perretant, M. R., Charmet, G., … Bernard, M. (2003). An update of the Courtot x Chinese Spring intervarietal molecular marker linkage map for the QTL detection of agronomic traits in wheat. *Theoretical and Applied Genetics*, *106*(3). https://doi.org/10.1007/s00122-002-1044-8

Spiertz, J. H. J. (1977). Grain production and assimilate utilization of wheat in relation to cultivar characteristics, climatic factors and nitrogen supply. *Centre for Agricultural Publishing and Documentation*, *25*.

Stelmakh, A. F. (1998). Genetic systems regulating flowering response in wheat. *Euphytica*, *100*(1–3), 359–369. https://doi.org/10.1023/a:1018374116006

Su, Z., Hao, C., Wang, L., Dong, Y., & Zhang, X. (2011). Identification and development of a functional marker of *TaGW2* associated with grain weight in bread wheat (*Triticum aestivum* L). *Theoretical and Applied Genetics*, *122*(1), 211–223. https://doi.org/10.1007/s00122-010-1437-z

Sukumaran, S., Dreisigacker, S., Lopes, M., Chavez, P., & Reynolds, M. P. (2015). Genome-wide association study for grain yield and related traits in an elite spring wheat population grown in temperate irrigated environments. *Theoretical and Applied Genetics*, *128*(2). https://doi.org/10.1007/s00122-014-2435-3

Sun, C., Zhang, F., Yan, X., Zhang, X., Dong, Z., Cui, D., & Chen, F. (2017). Genome-wide association study for 13 agronomic traits reveals distribution of superior alleles in bread wheat from the Yellow and Huai Valley of China. *Plant Biotechnology Journal*, *15*(8). https://doi.org/10.1111/pbi.12690

Sun, X. Y., Wu, K., Zhao, Y., Kong, F. M., Han, G. Z., Jiang, H. M., … Li, S. S. (2009). QTL analysis of kernel shape and weight using recombinant inbred lines in wheat. *Euphytica*, *165*(3), 615–624. https://doi.org/10.1007/s10681-008-9794-2

Tahmasebi, S., Heidari, B., Pakniyat, H., McIntyre, C. L., & Lukens, L. (2016). Mapping QTLs associated with agronomic and physiological traits under terminal drought and heat stress conditions in wheat (*Triticum aestivum* L). *Genome*, *60*(1), 26–45. https://doi.org/10.1139/gen-2016-0017

Tao, Y., Trusov, Y., Zhao, X., Wang, X., Cruickshank, A. W., Hunt, C., … Jordan, D. R. (2021). Manipulating assimilate availability provides insight into the genes controlling grain size in sorghum. *Plant Journal*, *108*(1). https://doi.org/10.1111/tpj.15437

Thorup-Kristensen, K. (2001). Are differences in root growth of nitrogen catch crops important for their ability to reduce soil nitrate-N content, and how can this be measured? *Plant and Soil*, *230*(2), 185–195. https://doi.org/10.1023/A:1010306425468

Thorup-Kristensen, K., Cortasa, M. S., & Loges, R. (2009). Winter wheat roots grow twice as deep as spring wheat roots, is this important for N uptake and N leaching losses? *Plant and Soil*, *322*(1). https://doi.org/10.1007/s11104-009-9898-z

Tian, X., Wen, W., Xie, L., Fu, L., Xu, D., Fu, C., … Cao, S. (2017). Molecular mapping of reduced plant height gene *Rht24* in bread wheat. *Frontiers in Plant Science*, *8*. https://doi.org/10.3389/fpls.2017.01379

Tonkinson, C. L., Lyndon, R. F., Arnold, G. M., & Lenton, J. R. (1995). Effect of the *Rht3* dwarfing gene on dynamics of cell extension in wheat leaves, and its modification by gibberellic acid and paclobutrazol. *Journal of Experimental Botany*, *46*(9). https://doi.org/10.1093/jxb/46.9.1085

Tóth, B., Galiba, G., Fehér, E., Sutka, J., & Snape, J. W. (2003). Mapping genes affecting flowering time and frost resistance on chromosome 5B of wheat. *Theoretical and Applied Genetics*, *107*(3). https://doi.org/10.1007/s00122-003-1275-3

Trachsel, S., Burgueno, J., Suarez, E. A., San Vicente, F. M., Rodriguez, C. S., & Dhliwayo, T. (2017). Interrelations among early vigor, flowering time, physiological maturity, and grain yield in tropical maize (*Zea mays* L) under multiple abiotic stresses. *Crop Science*, *57*(1). https://doi.org/10.2135/cropsci2016.06.0562

Trevaskis, B., Hemming, M. N., Dennis, E. S., & Peacock, W. J. (2007). The molecular basis of vernalization-induced flowering in cereals. *Trends in Plant Science*, Vol. 12. https://doi.org/10.1016/j.tplants.2007.06.010

Turner, A., Beales, J., Faure, S., Dunford, R. P., & Laurie, D. A. (2005). Botany: The pseudo-response regulator Ppd-H1 provides adaptation to photoperiod in barley. *Science*, *310*(5750), 1031–1034. https://doi.org/10.1126/science.1117619

Tyagi, S., Mir, R. R., Balyan, H. S., & Gupta, P. K. (2015). Interval mapping and meta-QTL analysis of grain traits in common wheat (*Triticum aestivum* L). *Euphytica*, *201*(3), 367–380. https://doi.org/10.1007/s10681-014-1217-y

Verma, V., Worland, A. J., Sayers, E. J., Fish, L., Caligari, P. D. S., & Snape, J. W. (2005). Identification and characterization of quantitative trait loci related to lodging resistance and associated traits in bread wheat. *Plant Breeding*, *124*(3). https://doi.org/10.1111/j.1439-0523.2005.01070.x

Vollbrecht, E., Springer, P. S., Goh, L., Buckler IV, E. S., & Martienssen, R. (2005). Architecture of floral branch systems in maize and related grasses. *Nature*, *436*(7054), 1119–1126. https://doi.org/10.1038/nature03892

Wang, K., Liu, H., Du, L., & Ye, X. (2017). Generation of marker-free transgenic hexaploid wheat via an Agrobacterium-mediated co-transformation strategy in commercial Chinese wheat varieties. *Plant Biotechnology Journal*, *15*(5). https://doi.org/10.1111/pbi.12660

Wang, L., Ge, H., Hao, C., Dong, Y., & Zhang, X. (2012). Identifying loci influencing 1,000-kernel weight in wheat by microsatellite screening for evidence of selection during breeding. *PLoS ONE*, *7*(2). https://doi.org/10.1371/journal.pone.0029432

Wang, R.X. (2009). QTL Mapping for Grain Filling Rate and Thousand-Grain Weight in Different Ecological Environments in Wheat. *ACTA AGRONOMICA SINICA*, *34*(10). https://doi.org/10.3724/sp.j.1006.2008.01750

Wang, R. X., Hai, L., Zhang, X. Y., You, G. X., Yan, C. S., & Xiao, S. H. (2009). QTL mapping for grain filling rate and yield-related traits in RILs of the Chinese winter wheat population Heshangmai x Yu8679. *Theoretical and Applied Genetics*, *118*(2), 313–325. https://doi.org/10.1007/s00122-008-0901-5

Wang, S., Li, S., Liu, Q., Wu, K., Zhang, J., Wang, S., … Fu, X. (2015). The OsSPL16-GW7 regulatory module determines grain shape and simultaneously improves rice yield and grain quality. *Nature Genetics*, *47*(8), 949–954. https://doi.org/10.1038/ng.3352

Wang, S., Wu, K., Yuan, Q., Liu, X., Liu, Z., Lin, X., … Fu, X. (2012). Control of grain size, shape and quality by *OsSPL16* in rice. *Nature Genetics*, *44*(8), 950–954. https://doi.org/10.1038/ng.2327

Wang, S. X., Zhu, Y. L., Zhang, D. X., Shao, H., Liu, P., Hu, J. B., … Ma, C. X. (2017). Genome-wide association study for grain yield and related traits in elite wheat varieties and advanced lines using SNP markers. *PLoS ONE*, *12*(11). https://doi.org/10.1371/journal.pone.0188662

Wang, S. Y., Ward, R. W., Ritchie, J. T., Fischer, R. A., & Schulthess, U. (1995). Vernalization in wheat I. A model based on the interchangeability of plant age and vernalization duration. *Field Crops Research*, *41*(2). https://doi.org/10.1016/0378-4290(95)00006-C

Ward, B. P., Brown-Guedira, G., Kolb, F. L., Van Sanford, D. A., Tyagi, P., Sneller, C. H., & Griffey, C. A. (2019). Genome-wide association studies for yield-related traits in soft red winter wheat grown in Virginia. *PLoS ONE*, *14*(2), 1–28. https://doi.org/10.1371/journal.pone.0208217

Wardlaw, I. (1994). The Effect of High Temperature on Kernel Development in Wheat: Variability Related to Pre-Heading and Post-Anthesis Conditions. *Functional Plant Biology*, *21*(6). https://doi.org/10.1071/pp9940731

Weng, J., Gu, S., Wan, X., Gao, H., Guo, T., Su, N., … Wan, J. (2008). Isolation and initial characterization of *GW5*, a major QTL associated with rice grain width and weight. *Cell Research*, *18*(12), 1199–1209. https://doi.org/10.1038/cr.2008.307

White, J., & Edwards, J. H. (2008). *Wheat Growth and Development (Procrop)*. (May), 9. Retrieved from http://www.dpi.nsw.gov.au/__data/assets/pdf_file/0008/516185/Procrop-wheat-growth-and-development.pdf

Whitechurch, E. M., & Snape, J. W. (2003). Developmental responses to vernalization in wheat deletion lines for chromosomes 5A and 5D. *Plant Breeding*, *122*(1). https://doi.org/10.1046/j.1439-0523.2003.00749.x

Worland, A. J. (1996). The influence of flowering time genes on environmental adaptability in European wheats. *Euphytica*, *89*(1). https://doi.org/10.1007/BF00015718

Würschum, T., Langer, S. M., Longin, C. F. H., Tucker, M. R., & Leiser, W. L. (2017). A modern Green Revolution gene for reduced height in wheat. *Plant Journal*, *92*(5). https://doi.org/10.1111/tpj.13726

Xia, T., Li, N., Dumenil, J., Li, J., Kamenski, A., Bevan, M. W., … Li, Y. (2013). The ubiquitin receptor DA1 interacts with the E3 ubiquitin ligase DA2 to regulate seed and organ size in Arabidopsis. *Plant Cell*, *25*(9). https://doi.org/10.1105/tpc.113.115063

Xie, Q., Mayes, S., & Sparkes, D. L. (2015). Carpel size, grain filling, and morphology determine individual grain weight in wheat. *Journal of Experimental Botany*, *66*(21). https://doi.org/10.1093/jxb/erv378

Yang, D. L., Jing, R. L., Chang, X. P., & Li, W. (2007). Identification of quantitative trait loci and environmental interactions for accumulation and remobilization of water-soluble carbohydrates in wheat (*Triticum aestivum* L) stems. *Genetics*, *176*(1), 571–584. https://doi.org/10.1534/genetics.106.068361

Yao, J., Wang, L., Liu, L., Zhao, C., & Zheng, Y. (2009). Association mapping of agronomic traits on chromosome 2A of wheat. *Genetica*, *137*(1), 67–75. https://doi.org/10.1007/s10709-009-9351-5

Youssefian, S., Kirby, E. J. M., & Gale, M. D. (1992a). Pleiotropic effects of the GA-insensitive *Rht* dwarfing genes in wheat. 1. Effects on development of the ear, stem and leaves. *Field Crops Research*, *28*(3). https://doi.org/10.1016/0378-4290(92)90039-C

Youssefian, S., Kirby, E. J. M., & Gale, M. D. (1992b). Pleiotropic effects of the GA-insensitive *Rht* dwarfing genes in wheat. 2. Effects on leaf, stem, ear and floret growth. *Field Crops Research*, *28*(3). https://doi.org/10.1016/0378-4290(92)90040-G

Yu, F., Li, J., Huang, Y., Liu, L., Li, D., Chen, L., & Luan, S. (2014). FERONIA receptor kinase controls seed size in Arabidopsis thaliana. *Molecular Plant*, *7*(5), 920–922. https://doi.org/10.1093/mp/ssu010

Zanke, C., Ling, J., Plieske, J., Kollers, S., Ebmeyer, E., Korzun, V., … Röder, M. S. (2014). Genetic architecture of main effect QTL for heading date in European winter wheat. *Frontiers in Plant Science*, *5*(MAY), 1–12. https://doi.org/10.3389/fpls.2014.00217

Zhai, H., Feng, Z., Du, X., Song, Y., Liu, X., Qi, Z., … Ni, Z. (2018). A novel allele of *TaGW2-A1* is located in a finely mapped QTL that increases grain weight but decreases grain number in wheat (Triticum aestivum L). *Theoretical and Applied Genetics*, *131*(3), 539–553. https://doi.org/10.1007/s00122-017-3017-y

Zhang, J., Gizaw, S. A., Bossolini, E., Hegarty, J., Howell, T., Carter, A. H., … Dubcovsky, J. (2018). Identification and validation of QTL for grain yield and plant water status under contrasting water treatments in fall-sown spring wheats. *Theoretical and Applied Genetics*, *131*(8), 1741–1759. https://doi.org/10.1007/s00122-018-3111-9

Zhang, K., Tian, J., Zhao, L., Liu, B., & Chen, G. (2009). Detection of quantitative trait loci for heading date based on the doubled haploid progeny of two elite Chinese wheat cultivars. *Genetica*, *135*(3). https://doi.org/10.1007/s10709-008-9274-6

Zhang, L. Y., Liu, D. C., Guo, X. L., Yang, W. L., Sun, J. Z., Wang, D. W., & Zhang, A. (2010). Genomic distribution of quantitative trait loci for yield and yield-related traits in common wheat. *Journal of Integrative Plant Biology*, *52*(11), 996–1007. https://doi.org/10.1111/j.1744-7909.2010.00967.x

Zhao, K., Xiao, J., Liu, Y., Chen, S., Yuan, C., Cao, A., … Wang, X. (2018). *Rht23* (5Dq′) likely encodes a *Q* homeologue with pleiotropic effects on plant height and spike compactness. *Theoretical and Applied Genetics*, *131*(9). https://doi.org/10.1007/s00122-018-3115-5

Zuo, J., & Li, J. (2014). Molecular genetic dissection of quantitative trait loci regulating rice grain size. *Annual Review of Genetics, 48.* https://doi.org/10.1146/annurev-genet-120213-092138

Chapter 3 - QTL Analysis of Yield and Yield-related Components in 'Overley' x 'Overland' Population

Introduction

In 2021, the U.S. planted 1.9 x 10^7 ha, harvested 1.5 x 10^7 ha, and produced 4.49 x 10^7 metric tons of wheat. Kansas has produced 9.91 x 10^7 metric tons of wheat (https://www.nass.usda.gov March 11, 2022). Grain yield (GY) of cereal crops is a complex trait, reflecting the cumulative nature of different developmental stages and their interactions with the environment. Despite its complexity, yield is still the trait of most importance to breeders. Therefore, identifying stably expressed genes that lead to higher GY is crucial for wheat breeding. Increasing GY can be done by increasing either the total biomass produced by the crop or the proportion of the total biomass accumulated in grains (de Oliveira et al., 2020; Maeoka et al., 2020). Grain yield represents the product of grain number and mean weight per grain (Quarrie et al., 2006). Generally, components determining grain number per area are plants per area, spike number per plant, and grain number per spike (GNS); the latter two are determined by the number of spikelets per spike (SNS) and GNS (Quarrie et al., 2006). Slafer (2003) compartmentalized the determinants of yield components into different phases of the plant's life cycle, with some overlap between phases. Typically, SNS is determined before GNS both overlapping with the determination of spikes per plant (Quarrie et al., 2006). By studying how different yield components vary within a particular genetic background, one can understand the potential function of one or more genes that influence yield.

There have been many QTL studies which have looked into different yield components such as thousand grain weight (TGW), GNS, and SNS (Avni et al., 2018; Cao et al., 2020; Liu et

al., 2020; Saini et al., 2022; Swamy et al., 2011; Tyagi et al., 2015; Zhang et al., 2010). These studies have identified numerous QTLs for any given yield trait component (YTC). These QTLs are spread across different wheat chromosomes, reflecting the polygenic nature of the yield (YLD) and YLD-related components. Zhang et al. (2010) identified over 500 QTLs related to YTCs, yield (YLD: 178), grain number per spike (GNS: 68), grain weight (GWT: 47), spikelet number per spike (SNS: 47), thousand grain weight (TGW: 116), and plant height (PHT: 85). The QTLs for these traits were identified on 2A, 2B, 2D, 3B, and 4A. In addition to the YTCs, studies have also been performed on other factors that influence YLD with pleiotropic effects, including flowering time (FT) and physiological maturity (PMAT) (refer to chapter 2). Further characterization of genes in the germplasm pool of regionally adapted hard winter wheat is imperative for breeding programs to support the development of high-yielding cultivars. Therefore, this study aimed to identify genomic regions associated with the variation in yield and its components in field trials with a recombinant inbred population derived from Overley x Overland.

Materials & Methods

Population Construction and Phenotyping

Overley is a bronze-chaffed semi-dwarf hard winter wheat variety with medium height, good straw strength, and good yield potential. It is an early maturing cultivar with good winter hardness and a large seed (Fritz et al., 2004). Overland is a bright-chaffed semi-dwarf cultivar with medium maturity and plant height. It has good straw strength, winter hardness, and yield potential (Wolf, 1994). Both Overley and Overland have been successful commercial cultivars, and both have been used as parents in regional breeding programs. Population construction is described in Chapter 1, where the population was developed by USDA Central Small Grain

Genotyping Laboratory in Manhattan, KS. The population consisted of 204 RILs through SSD (single seed descent) to the F_6 and F_9 generations. The experiment was conducted in two crop years, 2018 and 2019, at two locations, Ashland Bottoms, KS, and Hays, KS. The RILs were arranged in a partially replicated augmented design. The partially replicated augmented design consisted of blocks which contained 50 plots, 5 of which were check cultivars (Overley, Overland, Tatanka, TAM114, and WB-Grainfield). The plot dimensions for 2018 and 2019 were 15 rows by 20 ranges with a plot size of 4.6 m^2. Information on the experimental design is presented in Table 3.1.

Table 3.1. Field design of yield trials.

	2018 Ashland Bottoms	2019 Ashland Bottoms	2018 Hays	2019 Hays
Trials	AS18	AS19	HZ18	HZ19
Number of Entries	144	209	182	208
Number of Plots	300	300	300	300
Replications	2	2	2	2
Date Planted	10/28/2017	10/24/2018	10/30/2017	9/28/2018
Date Harvested	7/6/2018	7/7/2019	7/2/2018	7/1/2019

Data Collection

From these trials, sub-samples of spikes were collected from Hays (6 spikes) and Ashland (10 spikes) for the 2018 and 2019 trials. Each spike was manually counted for SNS measurements, then threshed using a Wintersteiger LD180 Laboratory Thresher (Wintersteiger AG, 2018; https://www.agriexpo.online/prod/wintersteiger-ag/product-175745-20776.html). Seed samples were counted on the Seed Counter R-25 Plus (https://data-technologies.com/product/seed-counter-r25plus/). These seed samples were then weighed, and data was compiled for statistical analysis. In addition, a sub-sample of 50g was collected from each plot from the Ashland trials in 2018 and 2019 for SKCS (Single Grain Characterization

System 4100; Perten Instruments, Springfield, IL). The SKCS analyzed 300 grains per sample, providing an output of average GWT (mg), grain diameter (GDM) (mm), moisture content, and hardness index. The samples from Hays 2018 and 2019 were not analyzed by SKCS because subsamples were not collected at harvest.

From the four locations, field data on other agronomic traits were measured. Field data on PHT was recorded at all locations as the height of plants at maturity, excluding awns. Flowering time data was recorded when 50% of the anthers emerged from the spike at all location-years. Physiological maturity data was recorded at Ashland Bottoms in both years when the peduncle was yellow, the glumes and flag leaf had lost their green color. Grain yield in 2018 (Ashland Bottoms, KS) was harvested using the Hege combine, and the grain was weighed to obtain GY data. In all other years GY was measured using the HarvestMaster weighing system (Zürn 150 combine), which provided GY data for each plot.

Genotyping and Map Construction

Refer to Chapter 1 for more information on constructing GBS libraries, obtaining SNP data, and building genetic maps using RefSeq of IWGSCv2.1 and Jagger.

QTL and Other Statistical Analyses

Refer to Chapter 1 for more information on QTL software and respective parameters implemented for QTL analysis; major QTLs were selected based on the threshold of LOD $\geq$ 4.5 and PVE $\geq$ 10%. Statistical analysis such as correlations and mixed model analysis for obtaining BLUPs were processed in JMP (SAS Institute, Inc., Cary, NC). Further, information on the statistical model and analysis are provided in Chapter 1.

Results

Phenotypic Data

The YLD traits and other factors responded differently in the different locations evaluated in this study. There were differences for YLD, GWT, GDM, and PHT among our environments (Table 3.2). Yield showed differences across all locations, with HZ19 being the highest yielding environment (4318.5 ± 111.7 kg/ha) and AS18 the lowest yielding environment (1833 ± 112.5 kg/ha). The G x E interactions for YLD were predominate ($\sigma_{G\ x\ E}$= 148473.3***; Table 3.4), and yield had low heritability (H^2 = 0.19; Table 3.4). There were differences in GWT among the two years at Ashland, in 2018 (20.8 ± 0.7 mg), and in 2019 (29.3 ± 0.7 mg), with high heritability (H^2 = 0.76; Table 3.4). Grain diameter also was measured in two locations, AS18 and AS19. Grain diameter was higher in AS19 (2.8 ± 0.02 mm) than AS18 (2.3 ± 0.02 mm). Among the locations, plants were taller in HZ19 (85.6 ± 1.4 cm) than in the other locations, AS19 (69.6 ± 1.4 cm), AS18 (68.2 ± 1.4 cm), HZ18 (68.2 ± 1.4 cm). Flowering time, measured in Julian Days (J.D), was similar across both locations (133 ± 0.6 J.D). Spikelet per spike, which was measured across four year-locations (AS18, AS19, HZ18, HZ19), was higher in AS19 than the other locations AS18 and HZ18. Spike samples collected in all location-years were used to measure data on TGW and GNS. Thousand grain weight was higher in AS19 (33.1 ± 0.9 g) compared to the other locations AS18 (21.4 ± 0.9 g), HZ18 (29.2 ± 0.9 g), and HZ19 (30.2 ± 0.9 g). Number of grains per spike presented small differences across locations. Physiological maturity differed between AS18 (162.8 ± 0.4 J.D) and AS19 (169.7 ± 0.4 J.D) The means of the RILs were typically intermediate between the parents (Table 3.3).

Genotype and genotype × environment (G x E) variance component estimates for FT, GNS, GWT, and TGW were highly significant ($p < 0.001$) (Table 3.4). Strong G x E

significance was seen for YLD, PMAT, and GDM. The genotypic variance was highly significant for SNS and PHT. The broad-sense heritability estimates (Table 3.4) were generally high for most traits ranging from (H^2: 0.50 – 0.88); but lower broad-sense heritability was observed for YLD (0.19), PMAT (0.13), and GDM (0.18).

Table 3.2. Summary of yield and yield components performance across field trials.

The mean performance in each trial for each trait. Data are least-squares means with standard errors in parentheses.

	Environment			
Trait	**AS18**	**AS19**	**HZ18**	**HZ19**
Yield (kg/h)	1833.0 (112.5)	3193.8 (111.6)	2251.2 (111.9)	4318.5 (111.7)
Plant Height (cm)	68.2 (1.4)	69.6 (1.4)	68.2 (1.4)	85.6 (1.4)
Flowering Time*	133.4 (0.6)	133.5 (0.6)	133.4 (0.6)	133.4 (0.6)
Physiological Maturity	162.8 (0.4)	169.7 (0.4)	-	-
Grain Weight (mg)	20.8 (0.7)	29.3 (0.7)	-	-
Grain Diameter (mm)	2.3 (0.02)	2.8 (0.02)		
Spikelet per Spike	14.0 (0.3)	14.3 (0.3)	13.8 (0.3)	14.3 (0.3)
Thousand Grain Weight (g)	21.4 (0.9)	33.1 (0.9)	29.2 (0.9)	30.2 (0.9)
Grains per Spike	33.3 (1.3)	32.7 (1.3)	34.7 (1.3)	34.1 (1.3)

Table 3.3. Summary of yield and yield components of parents and RIL population across field trials.
The mean performance of the parents and the population of RILs averaged across all environments.

Trait	Overley	Overland	RILs
Yield (kg/ha^{-1})	2758 (250)	2965 (251)	2889 (150)
Plant Height (cm)	71.3 (2.8)	76.6 (2.8)	72.95 (2.06)
Flowering Time*	133.3 (1.6)	137.3 (1.6)	135.0 (0.89)
Physiological Maturity*	166 (0.9)	167.6 (0.9)	166.2 (0.47)
Grain Weight (mg)	27.3 (1.8)	25.5 (1.8)	25.0 (1.2)
Grain Diameter (mm)	2.7 (0.06)	2.6 (0.06)	2.6 (0.03)
Spikelet per Spike	13.3 (0.7)	13.9 (0.7)	14.1 (0.5)
Thousand Grain Weight (g)	31.5 (2.3)	27.8 (2.3)	28.5 (1.5)
Grains per Spike	34.6 (3.0)	30.1 (3.0)	33.7 (2.0)

*Measured in Julian Days (J.D)

Table 3.4. Estimated variances and broad-sense heritabilities of yield and other related components.

Traits	Estimated Variance				Heritability (H^2)
	Block (Environment)	Genotype	Genotype x Environment	Residual	
Yield (kg/ha^{-1})	15823.4 ns	15614.7 ns	148473.3***	223242.1	0.19
Grain Weight (mg)	0.332 ns	2.7***	0.778 ***	1.8	0.76
Spikelet Number per Spike	0.1 ns	0.431***	0.139*	1.1	0.65
Plant Height (cm)	5.0ns	4.9 ***	5.7***	28.4	0.50
Physiological Maturity	0.146 ns	0.119 ns	1.081***	1.0	0.13
Flowering Time	0.09 ns	2.4***	0.829***	1.0	0.88
Grains per Spike	1.4 ns	7.9 ***	2.7 ***	14.4	0.76
Thousand Grain Weight (g)	0.482	4.5***	2.1***	7.5	0.75
Grain Diameter (mm)	0.0001 ns	0.0007 ns	0.005***	0.003	0.18

*, *** indicate significance of variance of estimates using Wald tests at $p < 0.05$, 0.001, respectively; ns, non-significant.

Figure 3.1. Distributions of best linear unbiased predictors (BLUPs) for GNS and SNS in the Overley x Overland RIL population at Ashland Bottoms and Hays in 2018 and 2019.

Distribution of best linear unbiased predictors (BLUPs) of A) GNS and B) SNS. Environments: AS18 = Ashland Bottoms, KS, 2018; AS19 = Ashland Bottoms, KS, 2019; HZ=Hays, KS 2019; MET=Multi-environment BLUPs. The white dot is the median, the black box is the interquartile range, and the lines extending from the black box represents the rest of the distribution measured as interquartile range * 1.5. Parent least-square means are indicated by green (Overley) and blue (Overland) lines.

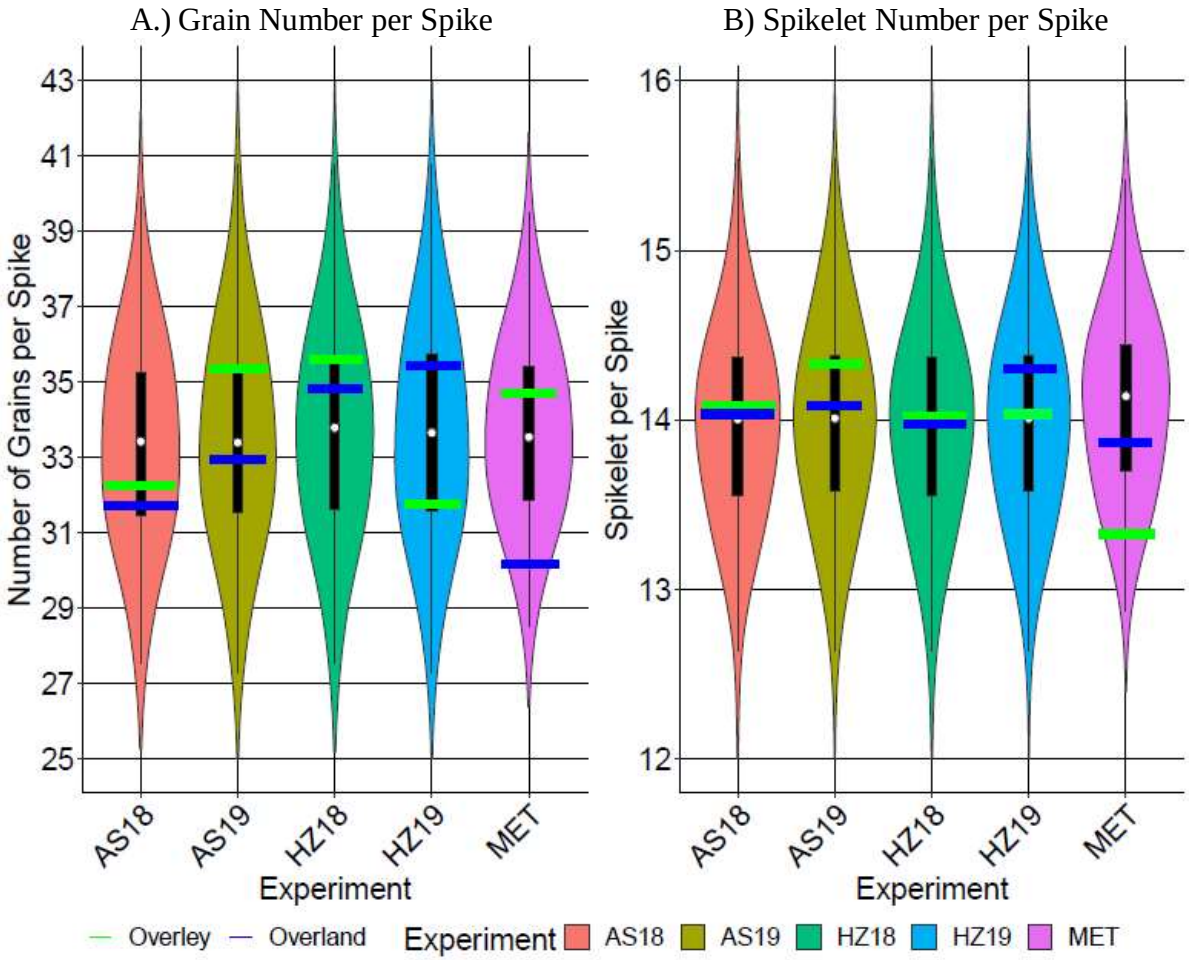

Figure 3.2. Distributions of best linear unbiased predictors (BLUPs) for yield in the Overley x Overland RIL population at Ashland Bottoms and Hays in 2018 and 2019.

Distribution of best linear unbiased predictors (BLUPs) of yield. Environments: AS18 = Ashland Bottoms, KS, 2018; AS19 = Ashland Bottoms, KS, 2019; HZ=Hays, KS 2019; MET=Multi-environment BLUPs. The white dot is the median, the black box is the interquartile range, and the lines extending from the black box represents the rest of the distribution measured as interquartile range * 1.5. Parent least-square means are indicated by green (Overley) and blue (Overland) lines.

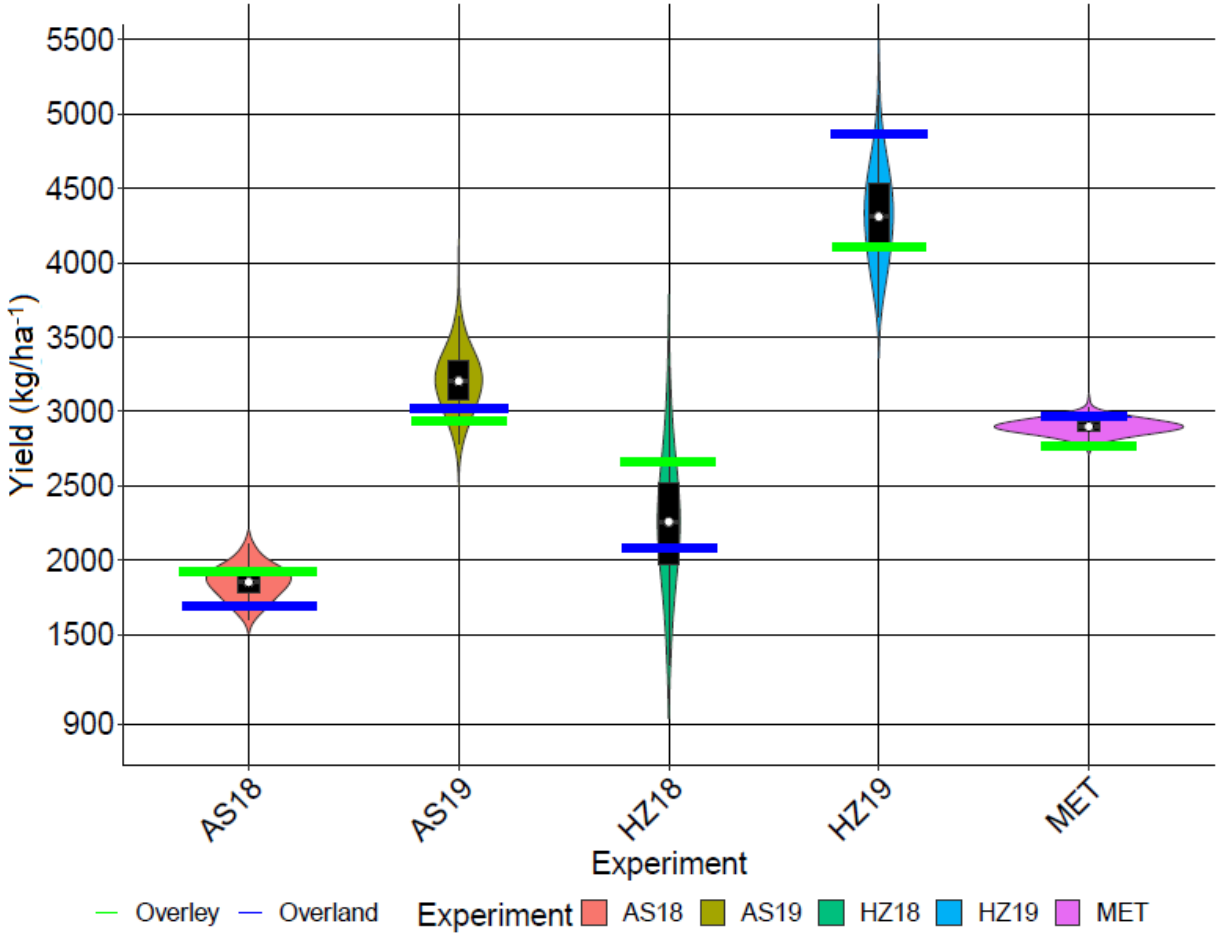

Figure 3.3. Distributions of best linear unbiased predictors (BLUPs) for GDM and GWT in the Overley x Overland RIL population at Ashland Bottoms and Hays in 2018 and 2019.

Distribution of best linear unbiased predictors (BLUPs) of A) GDM and B) GWT. Environments: AS18 = Ashland Bottoms, KS, 2018; AS19 = Ashland Bottoms, KS; MET=Multi-environment BLUPs. The white dot is the median, the black box is the interquartile range, and the lines extending from the black box represents the rest of the distribution measured as interquartile range * 1.5. Parent least-square means are indicated by green (Overley) and blue (Overland) lines.

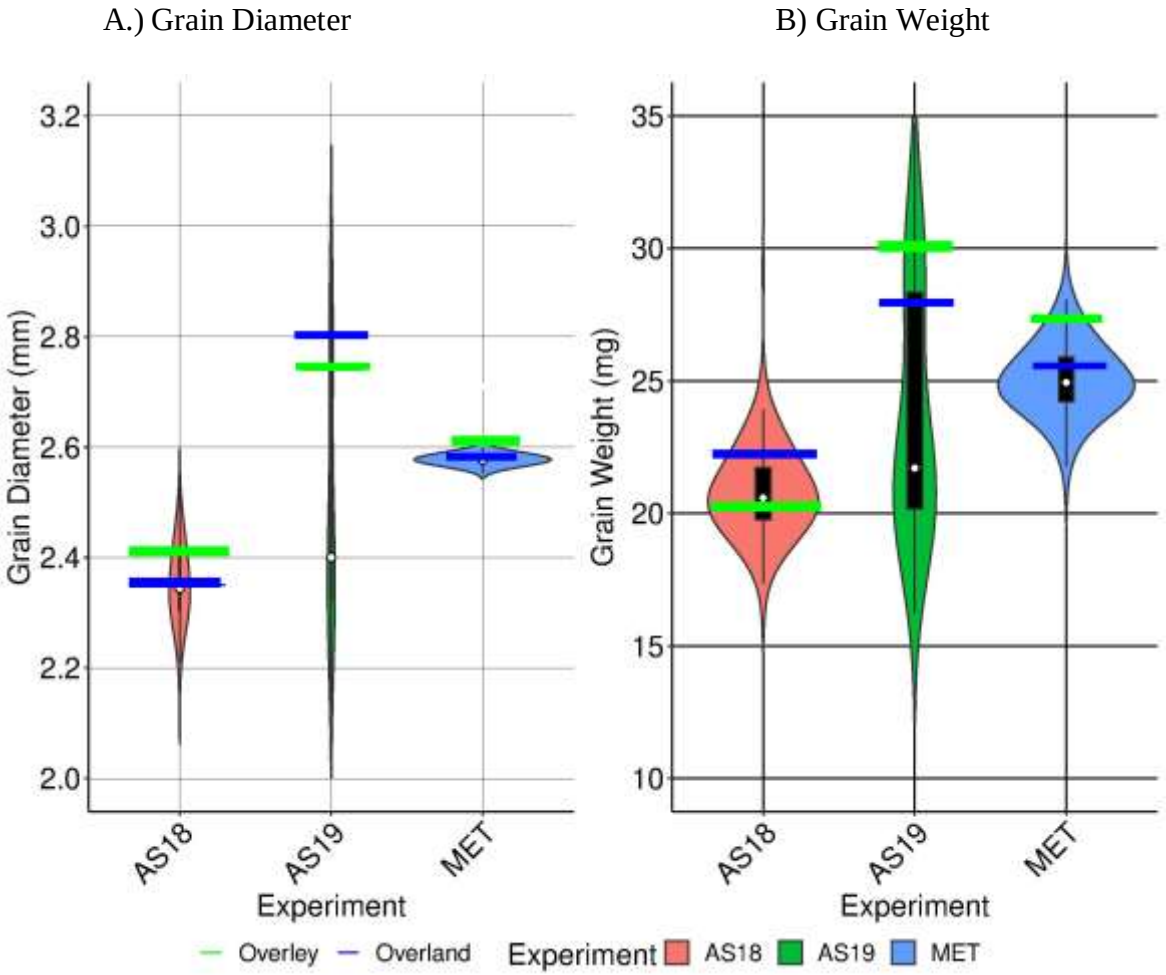

The RIL population had a wide and continuous distribution for all traits evaluated in each environment, and the parents' relative performance varied with environments (Table 3.2 and Table 3.3; Figure 3.1 - Figure 3.3 and Figure 3.8). Pairwise genotypic correlations of the traits for RILs are presented in Table 3.5. Correlations of YLD were low ($r < 0.2$) with all yield component traits. Correlation of GWT with TGW was high ($r = 0.71$) as would be expected, SNS ($r_{SNS:GNS} = 0.65$, $r_{SNS:FT} = 0.47$), and PMAT ($r_{PMAT:FT} = 0.67$) were strong and positive. Grain weight and TGW also were correlated with GDM. We observed an inverse relationship between GWT and SNS ($r = -0.23$; $p = 0.001$), and GNS ($r = -0.44$; $p < 0.0001$). The correlation indicates that RILs that set more seed produced seeds with lower GWT. In addition to these grain traits, there was a relationship between $r_{GWT:FT} = -0.41$,and $r_{GWT:PMAT} = -0.25$. The correlations indicate that early flowering and early maturing RILs produced seed with greater diameter and weight.

Table 3.5. Genotypic correlation of yield and yield components.

Pairwise correlations among yield traits evaluated. Significant ($p < 0.001$) positive correlations are in blue, significant negative correlations are in red, and non-significant correlations are in gray.

	Pearson Correlation Coefficient (*r*)								
GNS	0.10	0.15	-0.44	0.28	0.45	0.65	-0.22	-0.45	--

QTL identification: Multi-location BLUPs

Given the presence of genotype x environment interaction for all traits (Table 3.4), and high heritability for yield trait components and relatively high heritability of the traits (e.g. H^2_{GWT} = 76%, H^2_{GNS} = 76%, and H^2_{SNS} = 65%), the BLUPs from the combined, multi-location analysis (ML-BLUPs) across multiple environments were used for QTL identification. The QTLs identified from ML-BLUP analysis are presented in Table 3.6 (IWGSCv2.1 map; 15 QTLs) and Table 3.7 (Jagger map; 19 QTLs). Multi-environmental analysis (MET) of QTLs evaluated the size of QTL x Environment (Q x E) interaction effects under four environments (Table 3.8, Table 3.9). The QTLs identified from multiple environments (MET analysis) are presented in Table 3.8 (IWGSCv2.1 map; 15 QTLs) and Table 3.9 (Jagger map; 21 QTLs). Strong QTLs were defined as having a LOD > 4.5 and PVE > 10% in all cases. Maps based on the SNPs using the two reference genomes generally identified the same genomic regions with overlap among both reference maps for some of the traits evaluated in this study. Comparing the list of QTLs identified in the multiple environment trial analysis (Table 3.8 and Table 3.9), the Jagger map identified more QTLs (21 QTLs) for the traits evaluated in comparison to the IWGSCv2.1 map (15 QTLs).

Major QTLs were identified using the ML-BLUPs with both reference maps (Table 3.6 and Table 3.7). Using the IWGSCv2.1 map, major QTLs were identified for GNS (*Qyld.hwwgGNS -4A.2$_a$*: LOD = 9.10, PVE = 18.35%) and GWT (*Qyld.hwwgGWT -4A.2$_b$*: LOD = 9.34, PVE = 14.93%) using ML-BLUPs (Table 3.6). Using the Jagger map, major QTLs identified using ML-BLUPs were TGW (*Qyld.hwwgTGW-2B.1$_a$*: LOD = 6.09, PVE = 12.07%) and GNS (*Qyld. hwwgGNS-4A.2$_b$*: LOD = 18.32, PVE = 25.54%; Table 3.7). Major QTLs also were identified in the MET analysis across multiple environments using both reference maps

(Table 3.8 and Table 3.9). Using the IWGSCv2.1 map (Table 3.8) major QTLs were identified for GNS (*Qyld.hwwgGNS -4A.2$_a$*: LOD = 30.95, PVE = 18.31%) and GWT (*Qyld.hwwgGWT-4A.2$_a$*: LOD = 13.77, PVE = 16.28%). Using the Jagger map (Table 3.9), major QTLs identified were YLD (*Qyld.hwwgYLD-3B.2$_c$*: LOD = 9.04, PVE = 15.77%) and GNS (*Qyld. hwwgGNS-4A.2$_b$*: LOD = 56.68, PVE = 27.56%). The reference-based maps of both genomes also provide overlapping results for combinations of traits. For example, a QTL for GNS (*Qyld.hwwgGNS -4A.2$_a$*) overlapped with a QTL for GWT (*Qyld.hwwgGWT-4A.2$_b$*) in the IWGSCv2.1 reference map (Table 3.6). Using the Jagger map, GNS (*Qyld.hwwgGNS-4A.2$_b$*) overlapped with GWT (*Qyld.hwwgGWT-4A.2$_c$*) among other traits (Table 3.7). These identified QTLs may indicate that similar genomic regions may influence or interact with similar traits that characterize yield due to underlying pleiotropic effects.

The QTL results using ML-BLUPs are presented in Table 3.6, Table 3.7, Figure 3.4 and Figure 3.5. The YLD QTLs were designated as *Qyld.hwwgYLD-3B.2$_b$* (IWGSCv2.1 map) and *Qyld.hwwgYLD-3B.2$_d$* (Jagger map), respectively. The PVE rates of QTLs were similar to each other 9.36 % (IWGSCv2.1 map) and 10.69% (Jagger map). For YLD the Overley parental alleles had the less favorable response of lower yield unfavorable yield response of lower yield for both reference maps. The desirable response for GWT is the higher GWT, which would increase GY. Using the IWGSCv2.1 map (Table 3.6) three GWT QTLs were identified, *Qyld.hwwgGWT-2A.2$_a$*, *Qyld.hwwgGWT-4A.2$_b$*, and *Qyld.hwwgGWT-6B.2$_a$*. The PVE of these QTLs were 5.59%, 14.93%, and 8.71%. Out of the three GWT QTLs, *Qyld.hwwgGWT-6B.2$_a$* was the only QTL where the Overley parental allele had a favorable response of higher GWT. The Jagger map (Table 3.7) also identified two GWT QTLs designated as, *Qyld.hwwgGWT-1A.2$_b$* and *Qyld.hwwgGWT-4A.2$_c$* with the unfavorable response (lower GWT) for these QTLs was due to

the Overley allele. The phenotypic variation explained by these QTLs was 9.25% and 11.56%. Two GDM QTLs were identified, one on each reference map, respectively. Using the IWGSCv2.1 map (Table 3.6) the GDM QTL was designated as *Qyld.hwwgGDM-5A.2*$_a$ and using the Jagger map (Table 3.7) as *Qyld.hwwgGDM-5A.2*$_b$. The QTLs in both maps had similar PVE responses of 10.78% and 13.07% with the favorable response (higher GDM) due to the parental allele of Overley.

Two TGW QTLs were identified using the IWGSCv2.1 map and three QTLs using the Jagger map. Using the IWGSCv2.1 map the QTLs identified were *Qyld.hwwgTGW-2B.2*$_a$ and *Qyld.hwwgTGW-4A.2*$_a$ with PVE of 8.04% and 12.04% (Table 3.6). Out of the two QTLs *Qyld.hwwgTGW-2B.2*$_a$ indicated the favorable response of higher TGW due the Overley parental allele, the other QTL had a favorable response due to the Overland parental allele. The QTLs identified using the Jagger map (Table 3.7) were designated as *Qyld.hwwgTGW-2A.2*$_a$, *Qyld.hwwgTGW-2B.1*$_a$, and *Qyld.hwwgTGW-4A.2*$_b$. The PVE of these QTLs using the Jagger map were 9.29%,12.07%, and 9.16%, respectively. Out of these three QTLs, *Qyld.hwwgTGW-2B.2*$_a$ demonstrated the favorable response of higher TGW with respect to the Overley parental allele, the others were attributed to the Overland allele (Table 3.7).

There were a total of six GNS QTLs identified in the maps. Using the IWGSCv2.1 map, the two GNS QTLs were *Qyld.hwwgGNS-2A.2*$_a$ and *Qyld.hwwgGNS-4A.2*$_a$ (Table 3.6). The PVE of these QTLs were 8.34% and 18.35%, respectively with the favorable response of higher GNS due to the Overley parental allele. Using the Jagger map (Table 3.7) there were four GNS QTLs designated as *Qyld.hwwgGNS-2A.2*$_c$, *Qyld.hwwgGNS-2B.1*$_b$, *Qyld.hwwgGNS-4A.2*$_b$, and *Qyld.hwwgGNS-5A.2*$_a$. The respective phenotypic variation explained by theses QTLs are as follows, 9.2%, 6.06%, 25.54%, and 5.48%, respectively. From the QTLs listed using the Jagger

map, *Qyld.hwwgGNS-2A.2$_c$* and *Qyld.hwwgGNS-5A.2$_a$* demonstrated the favorable response (higher GNS) due to the Overley parental allele, the favorable responses of the other QTLs were attributed to the Overland allele.

Other traits evaluated were FT, SNS, PMAT, and PHT. For FT, the favorable response was later flowering. Using the IWGSCv2.1 map (Table 3.6), there was only one FT QTL designated as *Qyld.hwwgFT-5A.2$_a$*, with a PVE of 8.34% with the Overley parental allele demonstrating the unfavorable response (early flowering time). Using the Jagger map (Table 3.7), there were three FT QTLs designated as *Qyld.hwwgFT-2B.1$_c$*, *Qyld.hwwgFT-3B.2$_a$*, and *Qyld.hwwgFT-5A.2$_b$*. The PVE of the QTLs identified in the Jagger map were 38.27%, 7.40%, and 4.53%, respectively with all QTLs demonstrating a favorable response (later flowering) to the Overley allele except *Qyld.hwwgFT-2B.1$_c$*. Three QTLs in total were associated with PMAT in both maps. One PMAT QTL designated as *Qyld.hwwgPMAT-2B.1$_b$* was identified using the IWGSCv2.1 map (Table 3.6) with a PVE of 11.49% and the favorable parental allele contribution from Overley. Using the Jagger map (Table 3.7), two QTLs were associated with PMAT which were designated as, *Qyld.hwwgPMAT-2B.1$_a$* and *Qyld.hwwgPMAT-5A.2$_a$*, *Qyld.hwwgPMAT-2B.1$_a$* was the only QTL of the two that demonstrated the favorable response (late maturity) from the Overley parental allele. The respective PVE of the QTLs were 4.68% and 16.44%, respectively. There was only overlap with *Qyld.hwwgPMAT-2B.1$_a$* (Jagger map) and *Qyld.hwwgFT-2B.1$_a$* (Jagger map).

Spikelet numbers per spike associated QTLs were identified in both reference maps. They were designated as *Qyld.hwwgSNS-4A.2$_a$* (PVE = 8.43%) using the IWGSCv2.1 map (Table 3.6) and *Qyld.hwwgSNS-2B.1$_b$* (PVE = 4.86%) using the Jagger map (Table 3.7). *Qyld.hwwgSNS-4A.2$_a$* demonstrated the favorable response from the Overley parental allele.

Both maps also identified PHT QTLs that were designated as *Qyld.hwwgPHT-6A.1*$_a$ (IWGSCv2.1 map) and *Qyld.hwwgPHT-6A.1*$_c$ (Jagger map), whose favorable parental allele was Overley (shorter height), with PVE responses similar to each other at 17.31% and 17.9%, respectively.

Among the QTLs identified in Table 3.6 and Table 3.7 (ML-BLUPs), both maps identified overlapping QTLs associated with grain characteristics. Using the IWGSCv2.1 map the overlapping QTLs were *Qyld.hwwgGNS-4A.2*$_a$, and *Qyld.hwwgTGW-4A.2*$_a$ whose marker intervals were S4A_682313475 – S4A_671836181 and S4A_626473103 – S4A_682313475, respectively (Table 3.6). In addition, *Qyld.hwwgGWT-4A.2*$_b$ (S4A_682313475 – S4A_67183618) overlapped with QTLs mentioned earlier. Using the Jagger map the overlapping QTLs were *Qyld.hwwgGNS-2B.1*$_b$, *Qyld.hwwgPMAT-2B.1*$_a$, and *Qyld.hwwgSNS-2B.1*$_b$, and *Qyld.hwwgFT-3B.2*$_c$ whose marker intervals were S2B_48673126 – SUN_24253245, SUN_24253245 – S2B_70479277, and SUN_24253245 –S2B_7047927, respectively (Table 3.7). *Qyld.hwwgGNS-4A.2*$_b$ overlapped with *Qyld.hwwgGWT-4A.2*$_c$ with marker intervals of S4A_633516822 – S4A_647775911 and S4A_633516822 – S4A_647775911, respectively. *Qyld.hwwgFT-5A.2*$_b$ and *Qyld.hwwgGDM-5A.2*$_b$ overlapped with marker intervals of S5A_598382451 –Vrn-A1-E4-vern-KASP and Vrn-A1-E4-vern-KASP – S5A_618710758, respectively. There were no overlapping QTLs in the IWGSCv2.1 map for these traits.

There were also major QTLs (LOD ≥ 4.5, PVE ≥ 10%) identified in both maps. Using the IWGSCv2.1 map (Table 3.6) the major QTLs were *Qyld.hwwgPMAT-2B.1*$_b$, *Qyld.hwwgGNS-4A.2*$_a$, *Qyld.hwwgGWT-4A.2*$_b$, and *Qyld.hwwgPHT-6A.1*$_a$. There were also map- and analysis-specific QTLs observed with both reference maps using ML-BLUPs (Table 3.6 and Table 3.7). These QTLs were present in only one reference map. Using the IWGSCv2.1 map the QTLs were

GWT (6BL, 2AL), SNS (4AL, 7AS), and TGW (2BL). For the Jagger reference map, there were QTLs for GWT (1AL), TGW (2AL, 2BS), FT (2BS, 3BL), PMAT (5AL), and GNS (2BS, 5AL).

Table 3.6. QTLs identified from multi-location BLUPs for yield and yield components with the IWGSv2.1 reference map. List of QTLs identified for yield traits and other traits using multi-location best linear unbiased predictors (ML-BLUP) with the IWGSCv2.1 reference-derived map. The LOD threshold was set by permutation tests repeated 1,000 times at $\alpha = 0.05$ LOD = log odds ratio; PVE = percentage of variance explained.

QTL	Resp.	Chr.	Marker Interval	LOD Threshold	LOD	PVE (%)	A[1]	C.I.[2]
Qyld.hwwgGWT-2A.2$_a$	GWT	2AL	S2A_207315203 – S2A_203818355	3.28	3.87	5.59	-0.32 mg	122.5 – 125.5
Qyld.hwwgGNS-2A.2$_a$	GNS	2AL	S2A_646416484 – S2A_626218088	3.35	4.94	8.34	0.68 grains spike^{-1}	63.5 – 73.5
Qyld.hwwgSNS-2B.1$_a$	SNS	2BS	S2B_51126334 – S2B_72963487	3.37	4.18	10.41	-0.16 spikelet spike^{-1}	24.5 – 41.5
Qyld.hwwgPMAT-2B.1$_b$	PMAT	2BS	S2B_34401825 – S2B_47353125	3.36	4.65	11.49	0.15 Days	59.5 – 72.5
Qyld.hwwgTGW-2B.2$_a$	TGW	2BL	S2B_463723493 – S2B_483900966	3.31	3.77	8.04	0.49 g	59.5 – 72.5
Qyld.hwwgYLD-3B.2$_b$	YLD	3BL	S3B_756599263 – S3B_754456717	3.37	3.52	9.36	-14.57 kg ha^{-1}	105.5 – 109.5
Qyld.hwwgGNS-4A.2$_a$	GNS	4AL	S4A_682313475 – S4A_671836181	3.35	9.10	18.35	1.00 grains spike^{-1}	125.5 – 129.5
Qyld.hwwgTGW-4A.2$_a$	TGW	4AL	S4A_626473103 – S4A_682313475	3.31	4.32	12.04	-0.59 g	59.5 – 72.5
Qyld.hwwgSNS-4A.2$_a$	SNS	4AL	S4A_619213122 – S4A_624993521	3.37	3.72	8.43	0.15 spikelet spike^{-1}	41.5 – 55.5
Qyld.hwwgGWT-4A.2$_b$	GWT	4AL	S4A_682313475 – S4A_671836181	3.28	9.34	14.93	-0.52 mg	63.5 – 73.5
Qyld.hwwgFT-5A.2$_a$	FT	5AL	S5A_481667813 – S5A_482347862	3.24	3.02	8.34	-0.42 Days	139.5 – 151.5
Qyld.hwwgGDM-5A.2$_a$	GDM	5AL	S5A_615280034 – S5A_618936457	3.18	3.22	10.78	0.003 mm	59.5 – 72.5

Qyld.hwwgPHT-6A.1$_a$	PHT	6AS	S6A_80483834 – S6A_65650958	3.30	8.26	17.31	-0.65 cm	100.5 – 107.5
Qyld.hwwgGWT-6B.2$_a$	GWT	6BL	S6B_479824020 – S6B_458739122	3.28	5.83	8.71	0.40 mg	113.5 – 119.5
Qyld.hwwgSNS-7A.1$_a$	SNS	7AS	S7A_89224345 – S7A_95661462	3.37	3.84	8.43	-0.15 spikelet spike^{-1}	126.5 – 134.5

[1]Additive Effect of the Overley allele
[2]Confidence interval (cM)
[3] Favorable parental allele for yield and other traits; OY = Overley OD = Overland

Figure 3.4. Major QTLs identified for yield and yield components using the IWGSCv2.1 map with multi-location best linear unbiased predictors.

Linkage maps of major QTLs from table 3.5 (ML-BLUP; LOD ≥4.5 and PVE ≥10%) using the IWGSCv2.1 map for yield and other traits. Permutations were used to obtain LOD thresholds listed for ML-BLUPs.

A.) Plant height

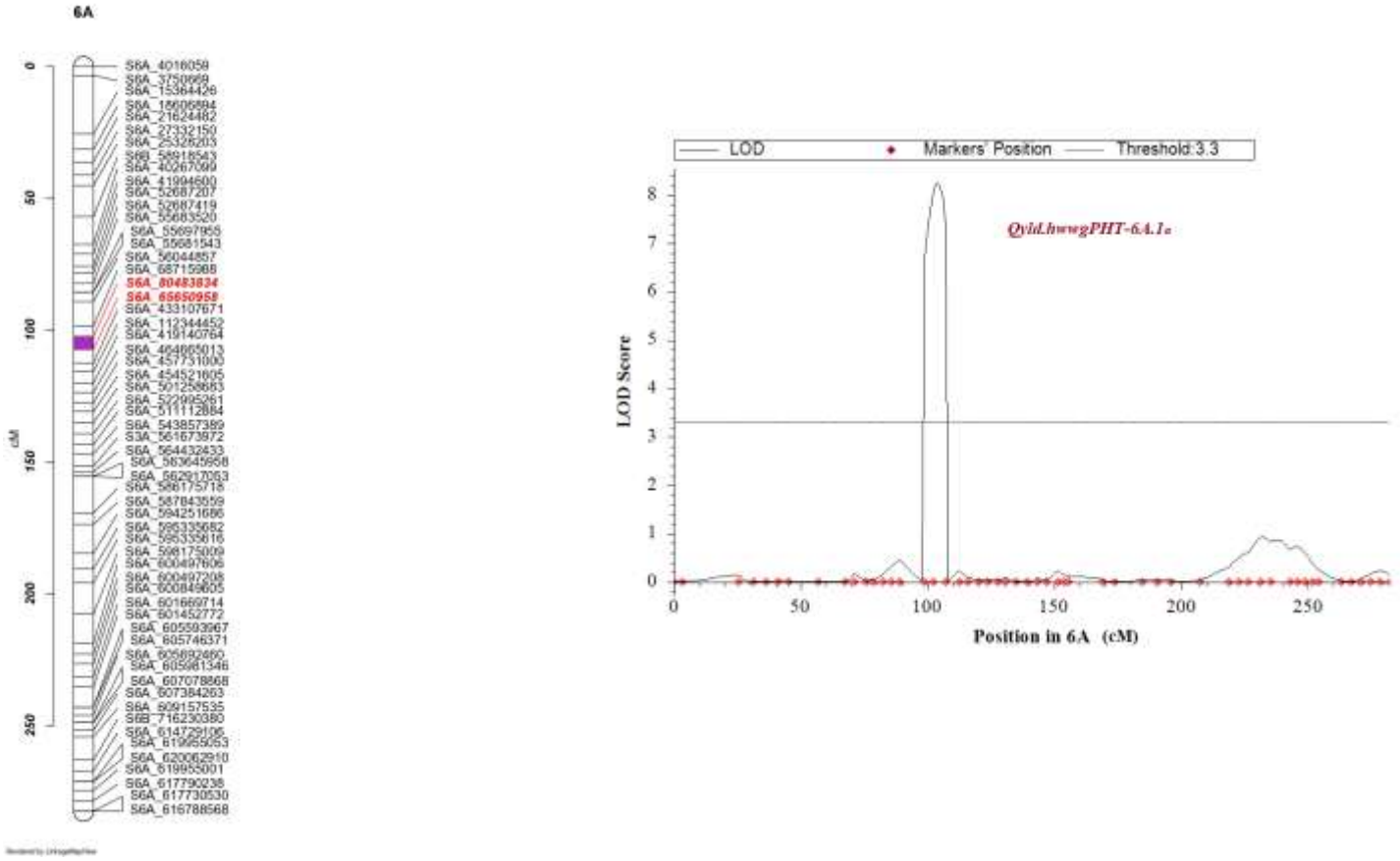

B.) Grain weight

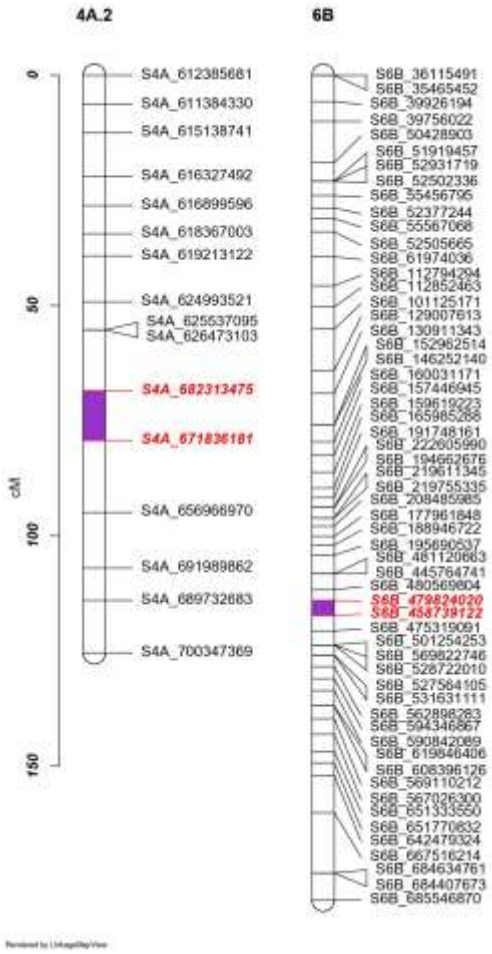

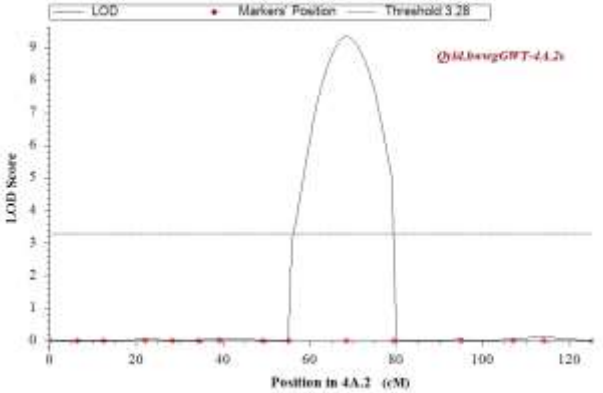

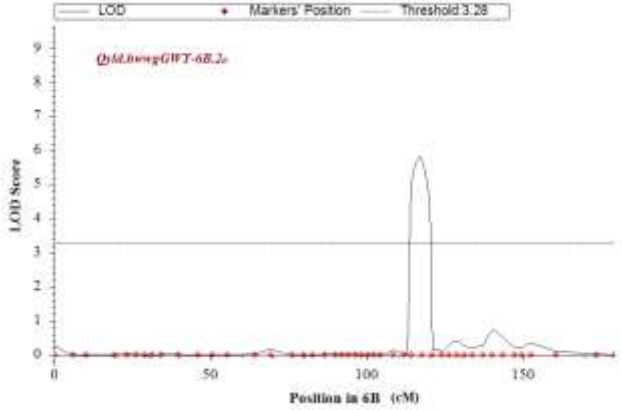

C.) Grain number per spike

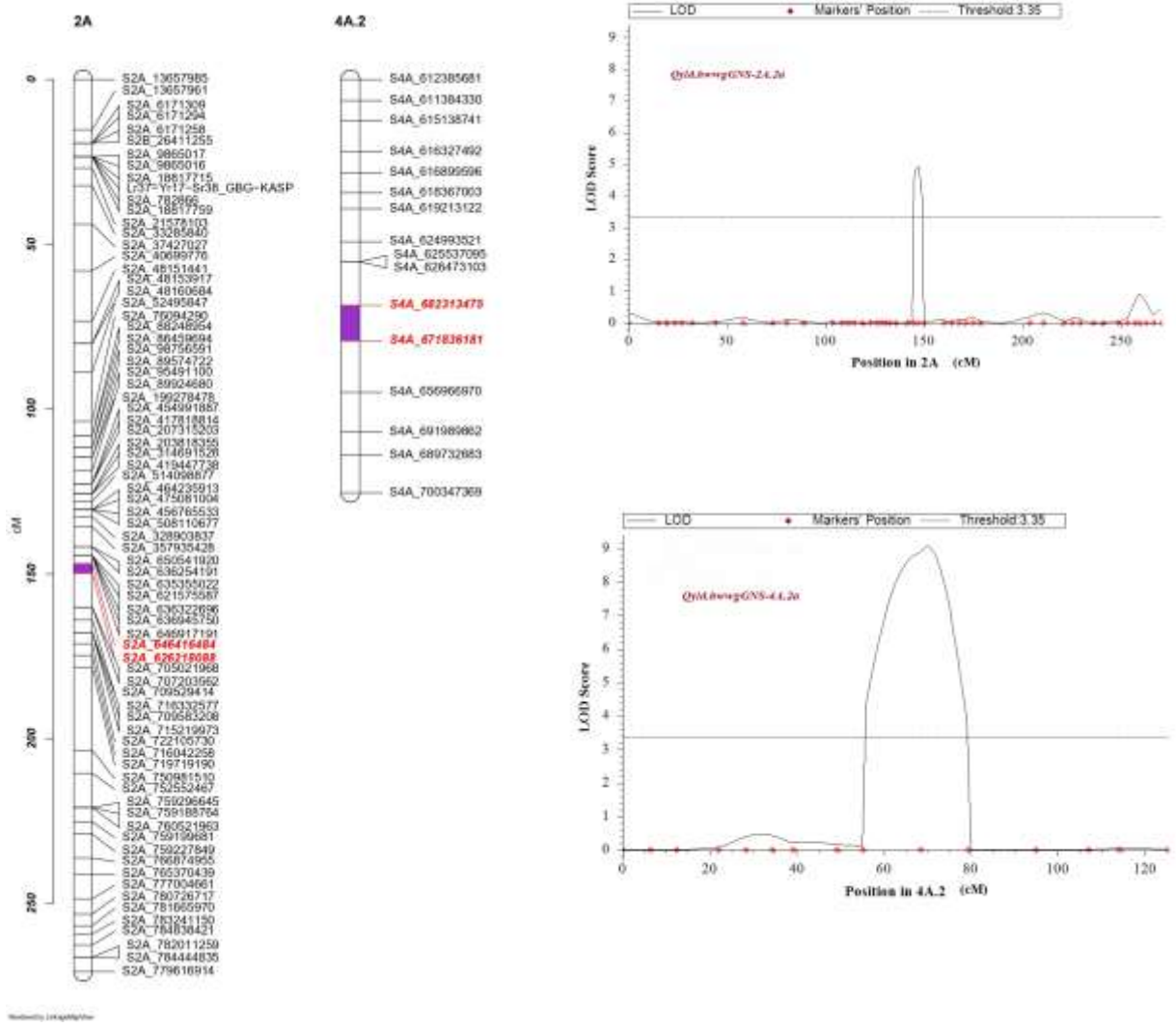

D.) Physiological maturity

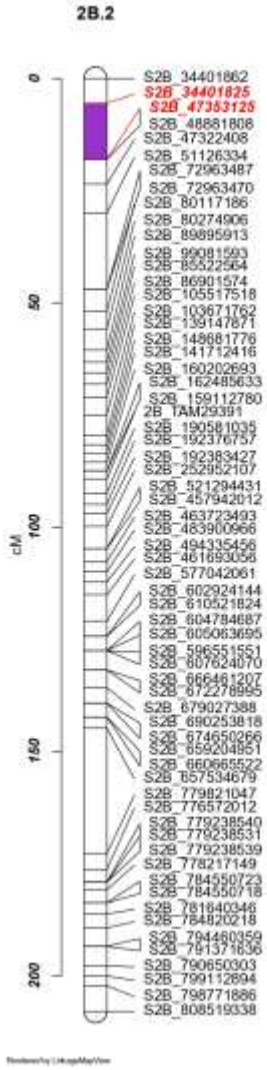

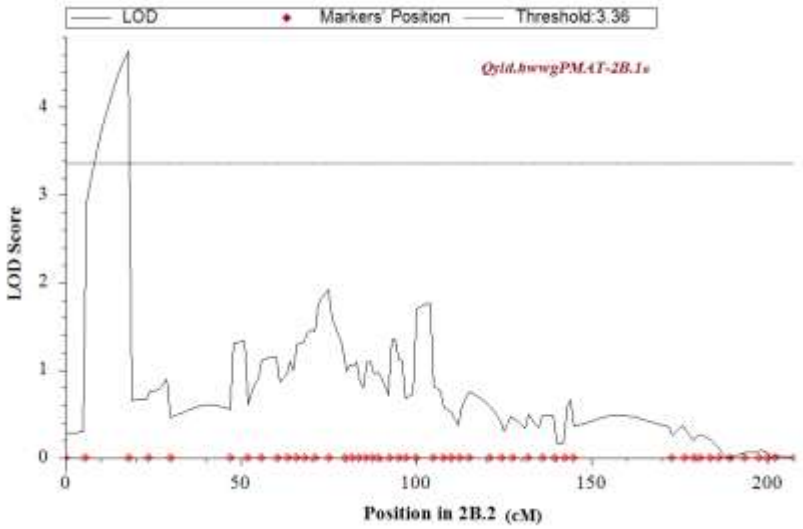

Table 3.7. QTLs identified from multi-location BLUPs for yield and yield components using the Jagger map.
List of QTLs identified for yield traits and other traits using multi-location best linear unbiased predictors (ML-BLUP) with the Jagger reference-derived map. The LOD threshold was set by permutation tests repeated 1,000 times at $\alpha = 0.05$ LOD = log odds ratio; PVE = percentage of variance explained.

QTL Name	Resp.	Chr.	Marker Interval	LOD Threshold	LOD	PVE (%)	A[1]	C.I.[2]
Qyld.hwwgGWT-1A.2$_b$	GWT	1AL	S1A_566818453 – S1A_576782223	3.97	5.23	9.25	-0.38 mg	210.5 – 215.5
Qyld.hwwgGWT-1A.2$_c$	GWT	1AL	S1A_375153723 – S1A_463488574	3.97	4.66	6.32	0.31 mg	102.5 – 107.5
Qyld.hwwgTGW-2A.2 $_a$	TGW	2AL	S2A_638220735 – S2A_648997997	3.23	4.79	9.29	-0.5 g	123.5 – 129.5
Qyld.hwwgGNS-2A.2$_c$	GNS	2AL	S2A_215641731 – S2A_659513001	3.54	7.87	9.2	0.77 grains spike^{-1}	121.5 – 123.5
Qyld.hwwgTGW-2B.1 $_a$	TGW	2BS	S2B_70476108 – S2B_77745640	3.23	6.09	12.07	0.57 g	116.5 – 124.5
Qyld.hwwgGNS-2B.1$_b$	GNS	2BS	S2B_48673126 – SUN_24253245	3.54	4.55	6.06	-0.62 grains spike^{-1}	95.5 – 108.5
Qyld.hwwgPMAT-2B.1$_a$	PMAT	2BS	SUN_24253245 – S2B_70479277	3.32	6.56	4.68	0.17 days	111.5 – 116.5
Qyld.hwwgSNS-2B.1$_b$	SNS	2BS	S2B_48673126 – SUN_24253245	3.24	4.86	13.19	-0.18 spikelet spike^{-1}	97.5 – 108.5
Qyld.hwwgFT-2B.1$_c$	FT	2BS	SUN_24253245 – S2B_70479277	3.28	25.60	38.27	-0.95 days	110.5 –115.5
Qyld.hwwgFT-3B.2$_a$	FT	3BL	SUN_112692714 – S3B_793708361	3.28	2.60	7.4	0.39 days	184.5 – 193.5
Qyld.hwwgYLD-3B.2$_d$	YLD	3BL	S3B_771823448 – S3B_771959309	5.11	3.24	10.69	-14.01 kg ha^{-1}	159.5 – 162.5
Qyld.hwwgGNS-4A.2$_b$	GNS	4AL	S4A_633516822 – S4A_647775911	3.54	18.32	25.54	1.28 grains spike^{-1}	117.5 – 122.5

Qyld.hwwgTGW-4A.2$_b$	TGW	4AL	S4A_740652590 – S4A_741021326	3.23	4.47	9.16	-0.49 g	235.5 – 242.5
Qyld.hwwgGWT-4A.2$_c$	GWT	4AL	S4A_633516822 – S4A_647775911	3.97	6.02	11.56	-0.42 mg	115.5 – 119.5
Qyld.hwwgFT-5A.2$_b$	FT	5AL	S5A_598382451 –Vrn-A1-E4-vern-KASP	3.28	4.53	4.53	0.34 Days.	273.5 –281.5
Qyld.hwwgGNS-5A.2$_a$	GNS	5AL	S5A_588428650 – S5A_592083734	3.54	5.04	5.48	0.59 grains spike^{-1}	265.5 – 269.5
Qyld.hwwgGDM-5A.2$_b$	GDM	5AL	Vrn-A1-E4-vern-KASP – S5A_618710758	3.39	3.44	13.07	0.003 mm	284.5 – 289.5
Qyld.hwwgPMAT-5A.2$_a$	PMAT	5AL	S5A_668553847 – S5A_671845643	3.32	18.3	16.44	-0.31 days	328.5 – 332.5
Qyld.hwwgPHT-6A.1$_c$	PHT	6AS	S6A_429204568 – S6A_453486127	3.35	8.11	17.9	-0.64 cm	115.5 – 120.5

[1]Additive Effect of Overley allele
[2]Confidence interval (cM)
[3] Favorable parental allele contributing to the desired response for yield and other traits; OY = Overley OD = Overland

Figure 3.5. Major QTLs identified for yield and yield components using with the Jagger map with multi-location best linear unbiased predictors.
Linkage maps of major QTLs from table 3.5 (ML-BLUP; LOD ≥4.5 and PVE ≥10%) using the Jagger map for yield and other traits. Permutations were used to obtain LOD thresholds listed for ML-BLUPs.

A.) Plant height

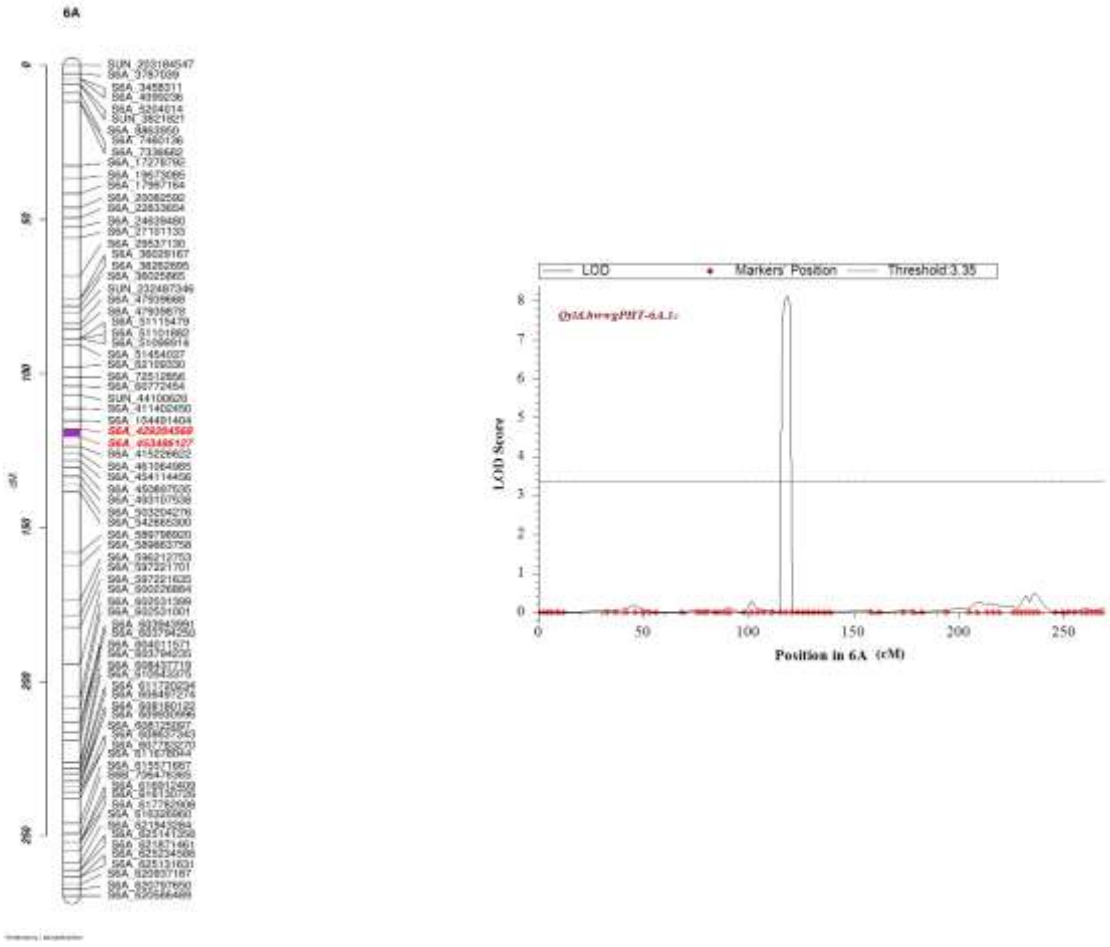

B.) Yield

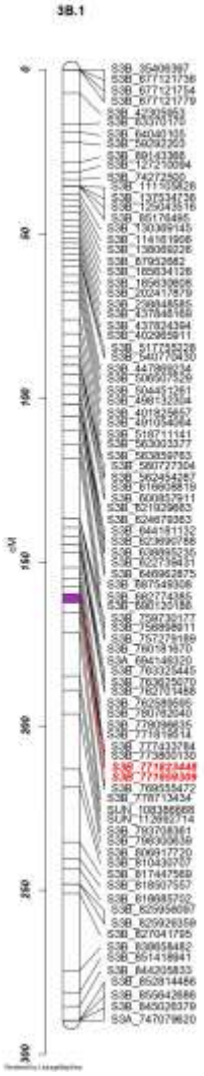
3B.1
0
50
100
150
200
250
300
350
cM

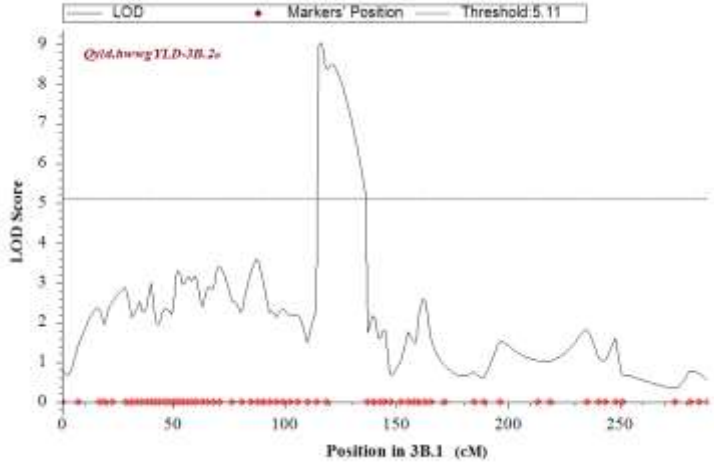
LOD
Markers' Position
Threshold:5.11
QtdAnwegYLD-3B.2a
LOD Score
0
1
2
3
4
5
6
7
8
9
0
50
100
150
200
250
Position in 3B.1 (cM)

C.) Grain weight

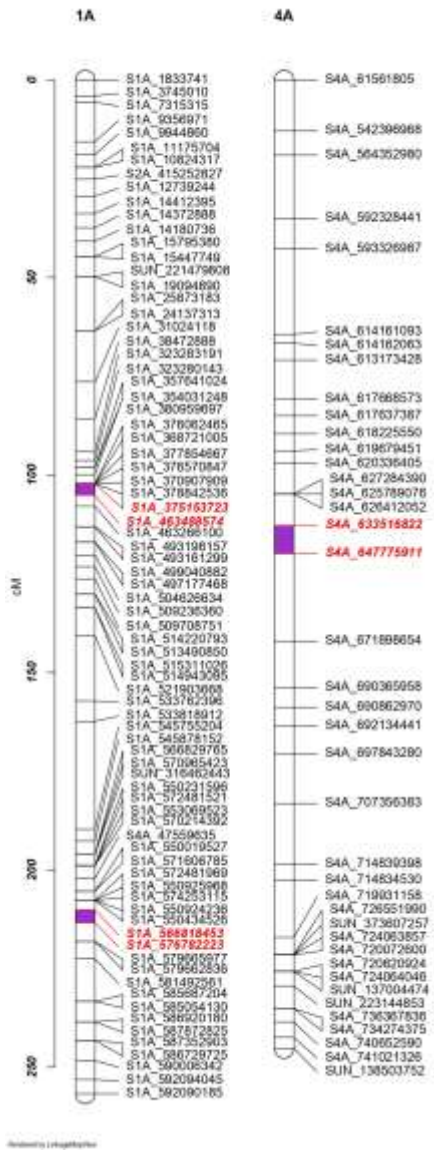

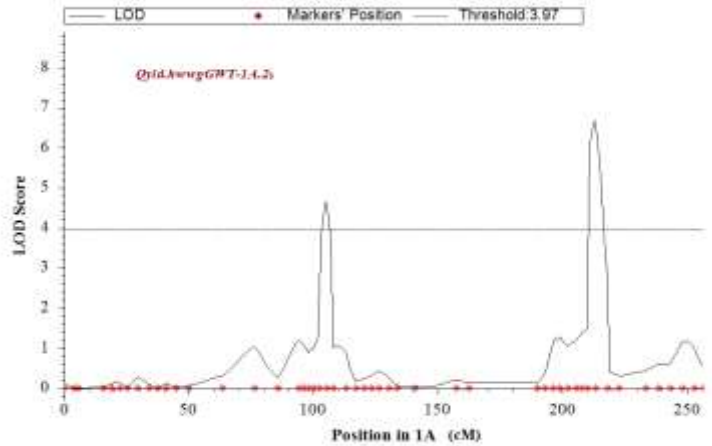

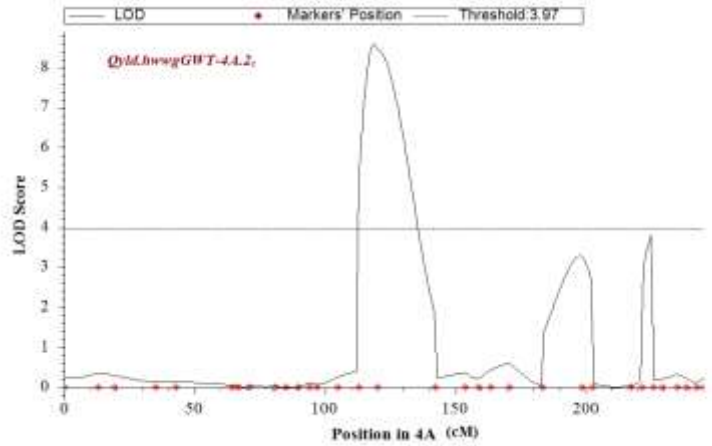

D.) Spikelet per spike

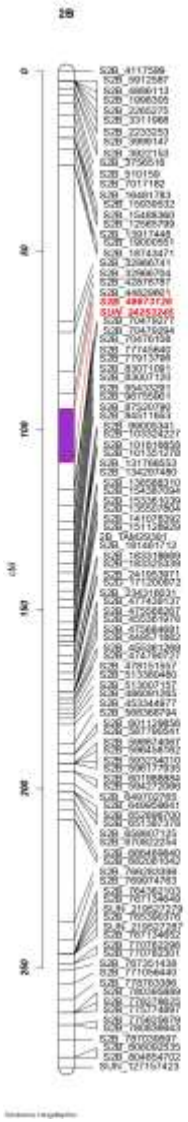

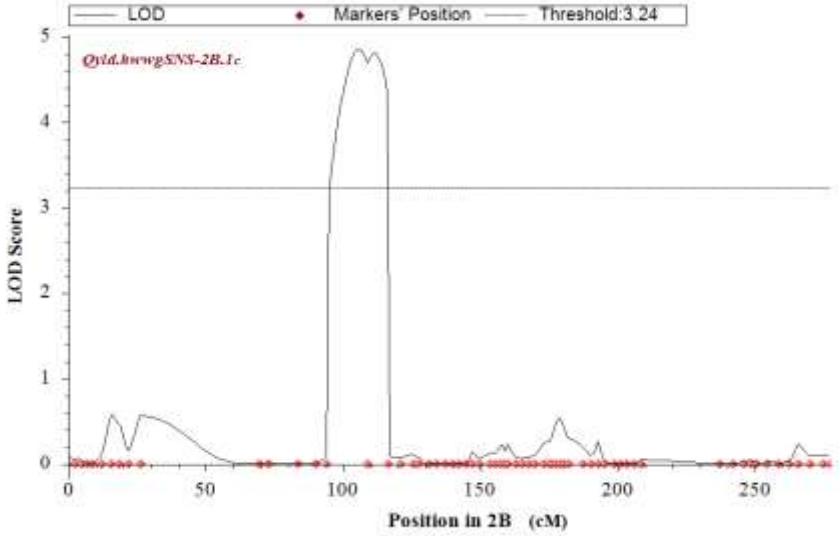

E.) Physiological maturity

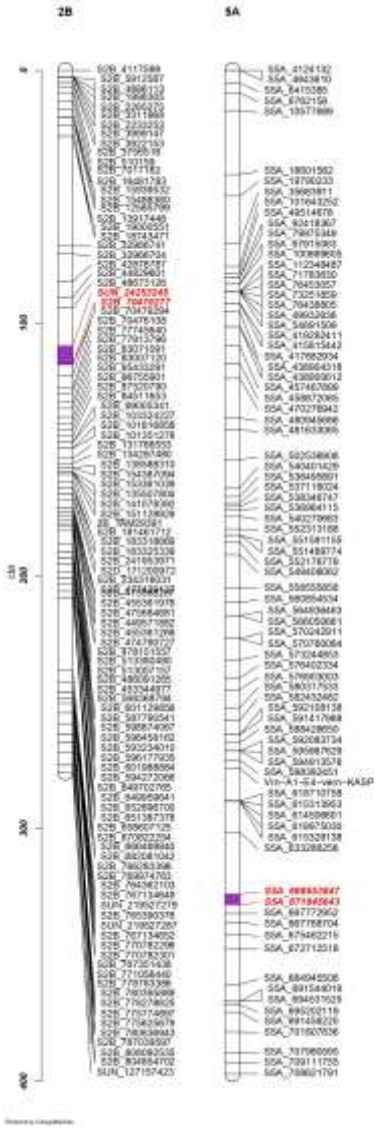

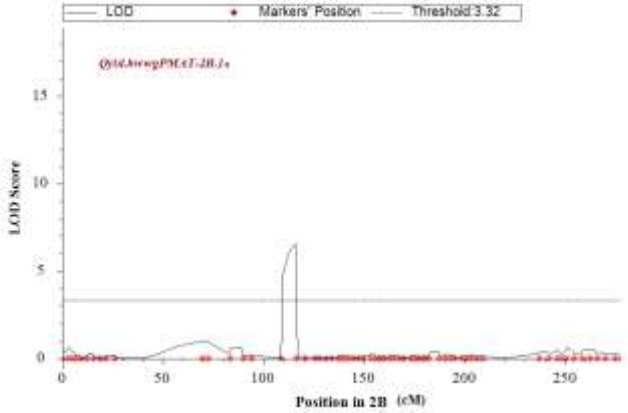

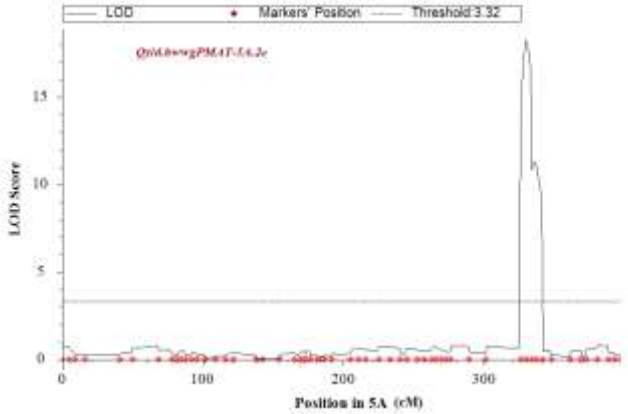

F) Grain number per spike

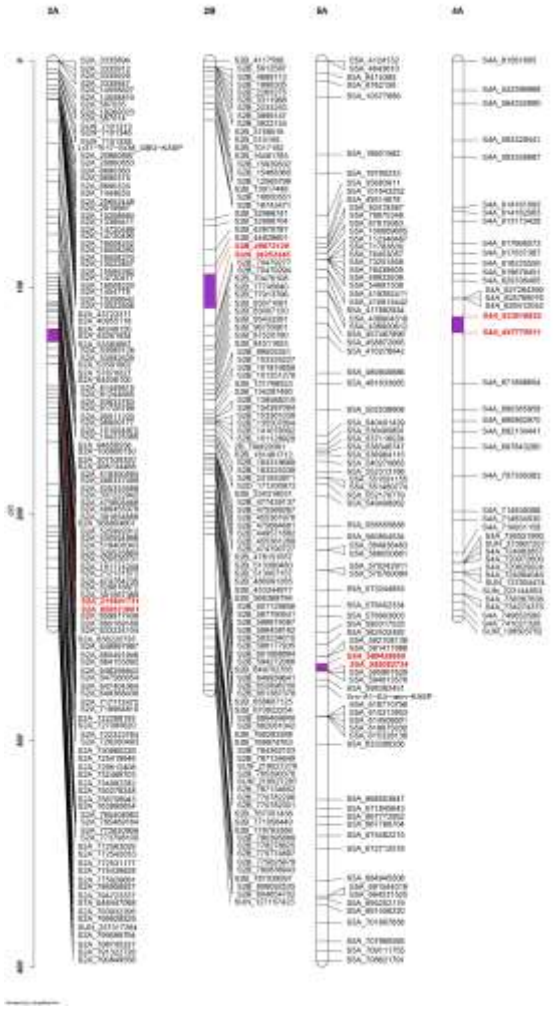

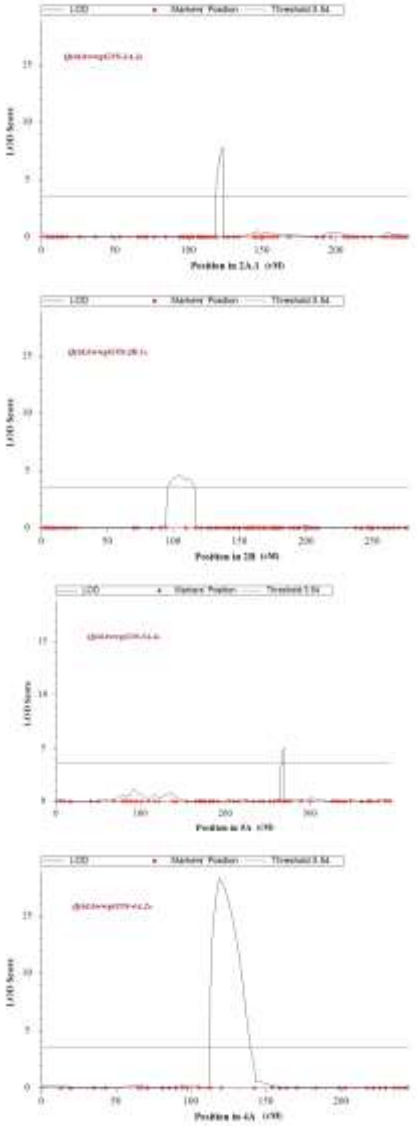

G) Thousand grain weight

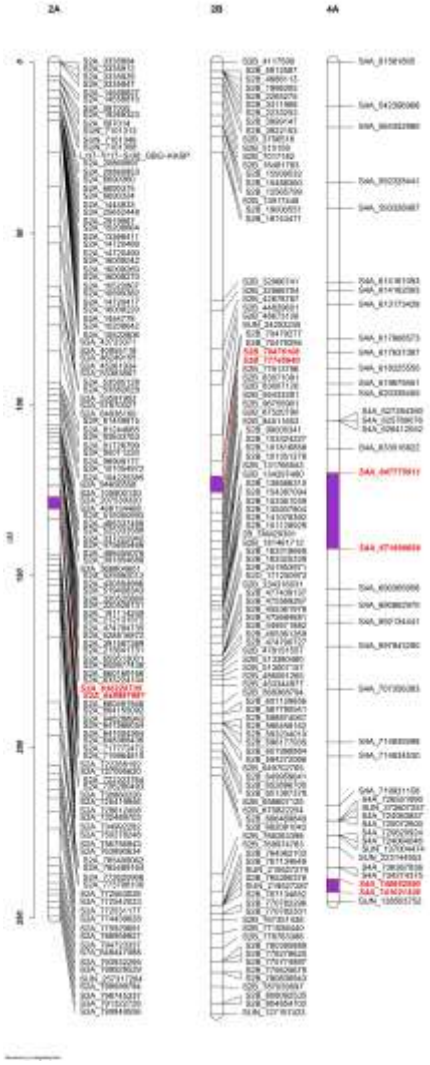

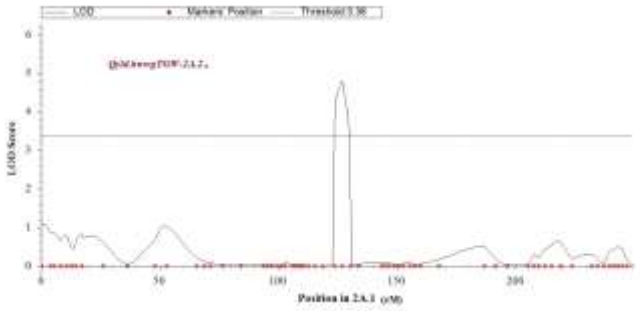

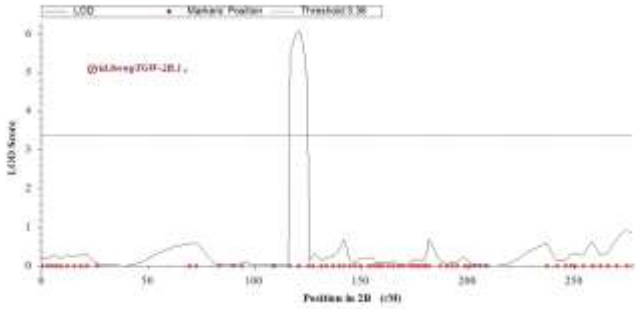

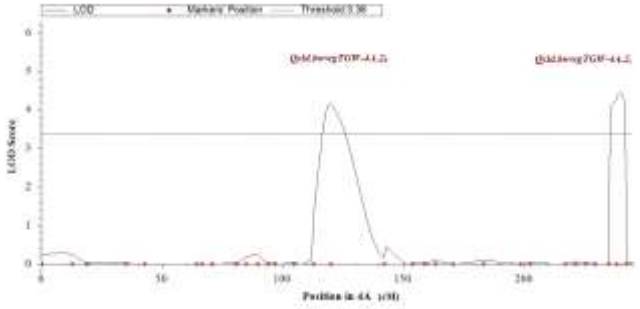

H) Flowering time

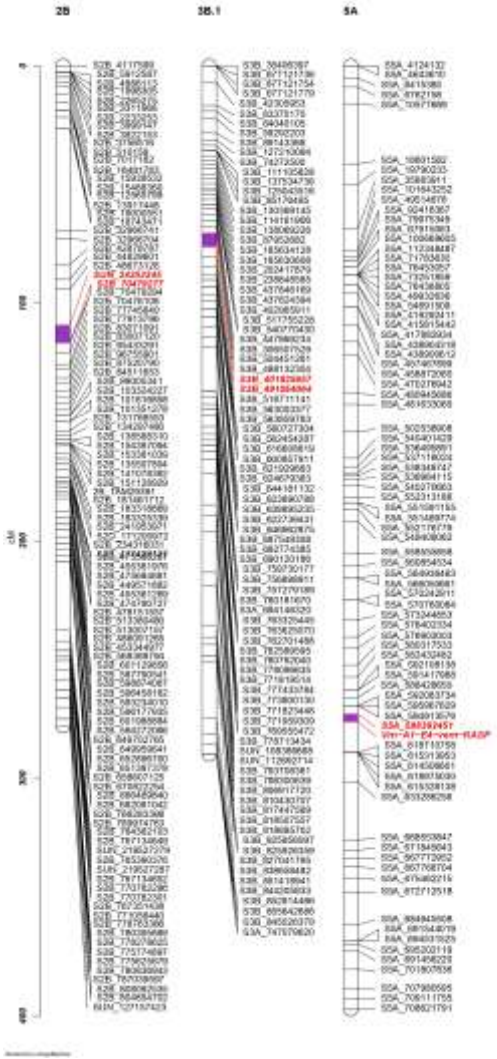

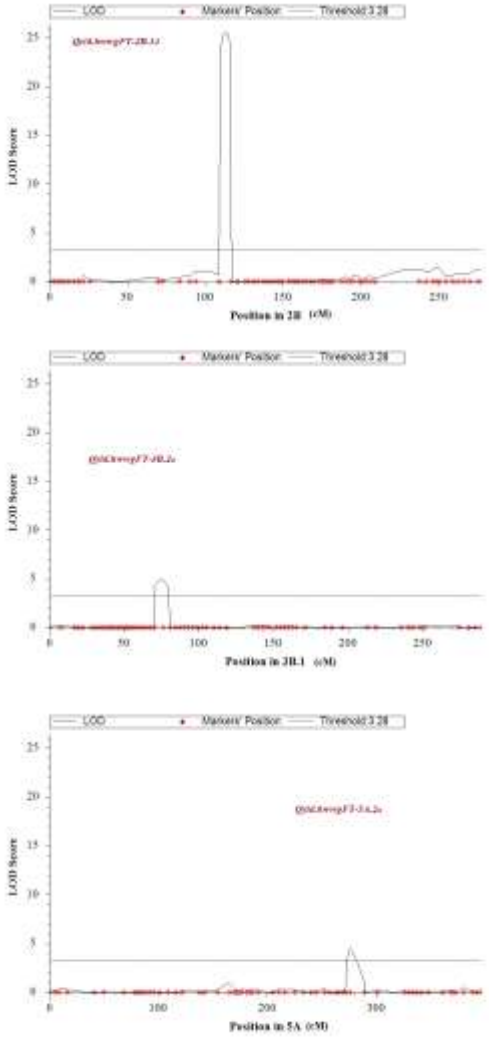

QTL identification: Multi Environment Trials Analysis

Results from ICIM MET analysis are presented in Table 3.8 (IWGSCv2.1 map) and Table 3.9 (Jagger map). Using the IWGSCv2.1 map there was a total of 15 QTLs and using the Jagger map there were a total of 21 QTLs. In total there were two YLD QTLs for both reference maps that were designated as, *Qyld.hwwgYLD-3B.2*$_a$ (IWGSCv2.1 map) and *Qyld.hwwgYLD-3B.2*$_c$ (Jagger map), respectively. The PVE of these QTLs were 20.29% and 15.77%, respectively with the unfavorable response (lower yield) due to the Overley parental allele. There were four GWT QTLs identified in total for both maps. Using the IWGSCv2.1 map the QTLs were *Qyld.hwwgGWT-1A.2*$_a$ and *Qyld.hwwgGWT-4A.2*$_a$ (Table 3.8). The PVE of these QTLs were 6.61% and 16.28%, respectively, and with the Overley parental allele being the unfavorable (lower GWT) parental allele. Using the Jagger map, the GWT QTLs were designated as *Qyld.hwwgGWT-1A.2*$_b$ and *Qyld.hwwgGWT-4A.2*$_c$ (Table 3.9). The PVE of these QTLs was 9.37% and 12.74%, respectively, and Overley was the unfavorable parental allele. There were in total three QTLs for GDM. Using the IWGSCv2.1 map the GDM QTLs were designated as *Qyld.hwwgGDM-1A.2*$_a$ and *Qyld.hwwgGDM-2B.1*$_a$ (Table 3.8). The PVE of these QTLs were 26.59% and 24.26%, respectively with only *Qyld.hwwgGDM-2B.1*$_a$ demonstrating the favorable response (higher GDM) due to the Overley parental allele. Using the Jagger map the GDM QTL was *Qyld.hwwgGDM-2B.1*$_b$ with a PVE of 33%, and the favorable parental allele being Overley (Table 3.9).

For GNS, three QTLs were identified using the IWGSCv2.1 map and four using the Jagger map (Table 3.8 and Table 3.9). Using the IWGSCv2.1 map, the QTLs were designated as *Qyld.hwwgGNS-2A.2*$_a$, *Qyld.hwwgGNS-2D.1*$_a$, and *Qyld.hwwgGNS-4A.2*$_a$. The PVE of these QTLs were 4.93%, 5.88%, and 18.31% respectively. Using the Jagger map, the QTLs were

designated as *Qyld.hwwgGNS-2A.2$_b$*, *Qyld.hwwgGNS-2B.1$_a$*, *Qyld.hwwgGNS-4A.2$_b$*, and *Qyld.hwwgGNS-5A.2$_a$* (Table 3.8). All of the QTLs in both maps had favorable parental contributions from Overley except *Qyld.hwwgGNS-2B.1$_a$*. The PVE of these QTLs were 6.31%, 7.20%, 27.56%, and 5.07%, respectively. Overall, QTLs identified using the Jagger reference map were stronger (PVE ≥10 % and LOD ≥ 4.5) for GNS. There were four TGW QTLs identified using the Jagger map (Table 3.9) none using the IWGSCv2.1 map. The QTLs were *Qyld.hwwgTGW-2D.1$_a$*, *Qyld.hwwgTGW-2D.1$_b$*, *Qyld.hwwgTGW-3B.2$_a$*, and *Qyld.hwwgTGW-4B.2$_a$*, respectively (Table 3.9). The PVE of these QTLs were 17.87%, 17.09%, 23.80%, and 23.63%, respectively. There was no overlapping associated with TGW and other traits.

There was a total of three FT QTLs for both reference maps. Using the IWGSCv2.1 map, the FT QTL was designated as *Qyld.hwwgFT-2B.1$_a$*, and Overley was the unfavorable parental allele with a PVE of 20.34% (Table 3.8). Using the Jagger map the FT QTLs were designated as *Qyld.hwwgFT-2B.1$_b$*, and *Qyld.hwwgFT-2B.1$_c$*, respectively. Overley was the unfavorable parental allele (early flowering), with similar PVE of 10.79% and 10.60% (Table 3.9). For PMAT there were a total of two QTLs in both reference maps. These QTLs were designated as, *Qyld.hwwgPMAT-2B.1$_a$* and *Qyld.hwwgPMAT-4A.2$_b$*. The favorable parental allele for both QTLs were Overley and the PVE for both QTLs were 4.07% and 10.09%. Using the IWGSCv2.1 map there were three SNS QTLs designated as *Qyld.hwwgSNS-2B.1$_a$*, *Qyld.hwwgSNS-4A.2$_a$*, and *Qyld.hwwgSNS-3D.2$_a$* with Overley being the favorable parental allele for all QTLs except *Qyld.hwwgSNS-2B.1$_a$*. The PVE of these QTLs were 12.09%, 6.31% and 5.85%, respectively (Table 3.8). Using the Jagger map, there were three SNS QTLs designated as *Qyld.hwwgSNS-1A.2$_a$*, *Qyld.hwwgSNS-2B.1$_b$*, and *Qyld.hwwgSNS-4A.2$_b$*, respectively. The PVE of these QTLs

were 5%,11.98%, and 3.86%, with Overley being the favorable parental allele for all QTLs listed except *Qyld.hwwgSNS-2B.1$_b$* (Table 3.9).

Two PHT QTLs were identified using the IWGSCv2.1 map (Table 3.8) designated as *Qyld.hwwgPHT-4D.1$_a$* and *Qyld.hwwgPHT-6A.1$_a$* with the favorable parental allele being Overley (shorter height). The PVE of these QTLs were 6.16% and 12.92%. Using the Jagger map three QTLs were identified, *Qyld.hwwgPHT-4B.1$_a$*, *Qyld.hwwgPHT-6A.1$_c$*, and *Qyld.hwwgPHT-6A.2$_a$* with Overley as the favorable parental allele. The phenotypic variation explained by the QTLs were 6.91%, 9.65%, and 13.86%, which were generally similar to the PVE of the IWGSCv2.1 map (Table 3.8 and Table 3.9).

There was also overlapping present with the QTLs listed in Table 3.8 and 3.9 for both reference maps. Using the IWGSCv2.1 map overlapping QTLs were *Qyld.hwwgGWT-1A.2$_a$*, and *Qyld.hwwgGDM-1A.2$_a$*, with marker intervals of S1A_567393593 – S1A_553417513 and S1A_567393593 – S1A_553417513, respectively (Table 3.8). *Qyld.hwwgFT-2B.1$_a$*, *Qyld.hwwgPMAT-2B.1$_a$*, and *Qyld.hwwgSNS-2B.1$_a$* overlapped with each other. The maker intervals of these QTLs were S2B_51126334 – S2B_72963487, S2B_47322408 – S2B_51126334, and S2B_51126334 – S2B_72963487, respectively. Overlapping was also present for *Qyld.hwwgGWT-4A.2$_a$* and *Qyld.hwwgGNS-4A.2$_a$* (S4A_682313475 – S4A_671836181) (Table 3.8). Using the Jagger map, *Qyld.hwwgGNS-2B.1$_b$* and *Qyld.hwwgSNS-2B.1$_b$* presented overlap at the marker intervals of S2B_48673126 – SUN_24253245 and SUN_24253245 – S2B_70479277, respectively (Table 3.9). *Qyld.hwwgFT-2B.1$_c$* overlapped on the same interval as *Qyld.hwwgSNS-2B.1$_b$*. *Qyld.hwwgGNS-4A.2$_b$* overlapped with *Qyld.hwwgGWT-4A.2$_c$* (S4A_633516822 – S4A_647775911). There were also map- and analysis-specific QTLs observed in both reference maps using MET ICIM BLUPs (Table 3.8 and

Table 3.9). These QTLs were present in only one reference map. In the IWGSCv2.1 map the QTLs were GNS (2DS), SNS (3DL), PMAT (2BS), and GDM (1AL). For the Jagger reference map, there were QTLs for GNS (2BS, 5AL), SNS (1AL), PMAT (4AL), and PHT (6AL).

Table 3.8. QTLs identified from multi-environmental QTL analysis (MET-QTL) of yield and yield components using the IWGSCv2.1 reference map.

List of QTLs identified for yield and other plant developmental traits using the multi-environment trial (MET)-QTL analysis based on permutation LOD for best linear unbiased predictors for yield and related traits across multiple environments using the IWGSCv2.1 reference-derived map. The LOD threshold was set by permutation tests repeated 1,000 times at $\alpha = 0.05$. LOD = log odds ratio; PVE = percentage of variance explained. A = additive (main) effect of genotype, Resp. = Response.

QTL	Resp.	Chr.	Marker Interval	LOD Threshold	LOD	PVE (%)	P[1]	P[2]	A[3]	C.I.[4] (cM)
Qyld.hwwgGWT-1A.2$_a$	GWT	1AL	S1A_567393593 – S1A_553417513	3.88	5.65	6.61	5.68	0.93	-0.33 mg	16.5 – 19.5
Qyld.hwwgGDM-1A.2$_a$	GDM	1AL	S1A_567393593 – S1A_553417513	3.90	4.32	26.59	5.94	20.64	-0.0063 mm	16.5 – 19.5
Qyld.hwwgGNS-2A.2$_a$	GNS	2AL	S2A_646416484 – S2A_626218088	5.02	9.15	4.93	4.32	0.61	0.50 grains spike^{-1}	145.5 – 148.5
Qyld.hwwgFT-2B.1$_a$	FT	2BS	S2B_51126334 – S2B_72963487	5.0	41.84	20.34	20.33	0.003	-1.22 days	32.5 – 38.5
Qyld.hwwgPMAT-2B.1$_a$	PMAT	2BS	S2B_47322408 – S2B_51126334	3.62	3.62	4.07	4.07	0.0003	-0.70 days	23.5 – 36.5
Qyld.hwwgSNS-2B.1$_a$	SNS	2BS	S2B_51126334 – S2B_72963487	5.11	16.21	12.09	12.06	0.03	-0.16 spikelet spike^{-1}	28.5 – 37.5
Qyld.hwwgGDM-2B.1$_a$	GDM	2BS	S2B_80117186 – S2B_80274906	3.90	4.07	24.26	4.98	19.27	0.0058 mm	51.5 – 58.5
Qyld.hwwgGNS-2D.1$_a$	GNS	2DS	S2D_59007363 – S2D_61243683	5.02	10.77	5.88	5.41	0.46	-0.56 grains spike^{-1}	61.5 – 65.5
Qyld.hwwgYLD-3B.2$_a$	YLD	3BL	S3B_680171380 – S3B_687519082	5.14	9.39	20.29	9.64	10.66	-46.86 kg ha^{-1}	92.5 – 97.5

Qyld.hwwgSNS-3D.2$_a$	SNS	3DL	S3D_611534849 – S3D_614193584	5.11	8.51	5.85	5.64	0.20	0.11 spikelet spike^{-1}	0 – 2.5
Qyld.hwwgGWT-4A.2$_a$	GWT	4AL	S4A_682313475 – S4A_671836181	3.88	13.77	16.28	1563	0.65	-0.55 mg	65.5 – 72.5
Qyld.hwwgSNS-4A.2$_a$	SNS	4AL	S4A_619213122 – S4A_624993521	5.11	8.43	6.31	5.34	0.97	0.11 spikelet spike^{-1}	44.5 – 52.5
Qyld.hwwgGNS-4A.2 $_a$	GNS	4AL	S4A_682313475 – S4A_671836181	5.02	30.95	18.31	18.2	0.10	1.03 grains spike^{-1}	65.5 – 71.5
Qyld.hwwgPHT-4D.1$_a$	PHT	4DL	S4D_351747244 – S4D_426497943	5.18	5.73	6.16	3.79	2.37	-0.28 cm	0 – 5.5
Qyld.hwwgPHT-6A.1$_a$	PHT	6AS	S6A_80483834 – S6A_65650958	5.18	14.47	12.92	10.54	2.38	-0.48 cm	101.5 – 107.5

[1] PVE of Additive Effect
[2] PVE of A x E interaction
[3]Additive effect of the Overley allele
[4]Confidence interval (cM)

Table 3.9. QTLs identified from multi-environmental QTL analysis (MET-QTL) of yield and yield components using the for Jagger map.

List of QTLs identified for yield and other plant developmental traits using the multi-environment trial (MET)-QTL analysis based on permutation LOD for best linear unbiased predictors for yield and related traits across multiple environments using the Jagger reference-derived map. The LOD threshold was set by permutation tests repeated 1,000 times at $\alpha = 0.05$. LOD = log odds ratio; PVE = percentage of variance explained. A = additive (main) effect of genotype, Resp. = Response.

QTL	Resp.	Chr.	Marker Interval	LOD Threshold	LOD	PVE (%)	P[1]	P[2]	A[3]	C.I.[4] (cM)
Qyld.hwwgSNS-1A.2$_a$	SNS	1AL	S1A_380959697 – S1A_376062465	3.24	8.24	5.0	5.0	1.19	0.11 spikelet spike^{-1}	98.5 – 101.5
Qyld.hwwgGWT-1A.2$_b$	GWT	1AL	S1A_566818453 – S1A_576782223	3.27	6.68	9.37	8.69	0.67	-0.36 mg	210.5 – 214.5
Qyld.hwwgGNS-2A.2$_b$	GNS	2AL	S2A_215641731 – S2A_659513001	5.26	17.39	7.20	5.16	2.04	0.54 grains spike^{-1}	122.5 – 123.5
Qyld.hwwgGNS-2B.1$_a$	GNS	2BS	S2B_48673126 – SUN_24253245	5.26	15.15	6.31	5.89	0.42	-0.58 grains spike^{-1}	99.5 – 110.5
Qyld.hwwgGDM-2B.1$_b$	GDM	2BS	S2B_70479294 – S2B_70476108	3.94	6.32	33.0	7.43	25.57	0.008 mm	116.5 – 125.5
Qyld.hwwgSNS-2B.1$_b$	SNS	2BS	SUN_24253245 – S2B_70479277	3.24	15.82	11.98	11.41	0.57	-0.16 spikelet spike^{-1}	109.5 – 115.5
Qyld.hwwgFT-2B.1$_b$	FT	2BS	S2B_44829601 – S2B_48673126	5.02	19.26	10.79	10.79	0.002	-0.70 days	92.5 – 97.5
Qyld.hwwgFT-2B.1$_c$	FT	2BS	SUN_24253245 – S2B_70479277	5.02	18.63	10.60	10.60	0.002	-0.70 days	114.5 – 116.5
Qyld.hwwgTGW-2D.1$_a$	TGW	2DS	S2D_48633474 – S2D_53051094	5.15	3.69	17.87	2.16	15.71	0.22 g	134.5 – 141.5
Qyld.hwwgTGW-2D.1$_b$	TGW	2DS	S2D_63887119 – S2D_102129747	5.15	3.85	17.09	0.48	16.60	0.10 g	174.5 – 188.5
Qyld.hwwgTGW-3B.2$_a$	TGW	3BL	S3B_401825657 – S3B_491054064	5.15	3.43	23.80	5.28	18.52	0.34 g	70.5 – 78.5

Qyld.hwwgYLD-3B.2$_c$	YLD	3BL	S3B_682774385 – S3B_690120186	3.21	9.04	15.77	7.59	8.18	-46.6 kg ha^{-1}	114.5 – 118.5
Qyld.hwwgGNS-4A.2$_b$	GNS	4AL	S4A_633516822 – S4A_647775911	5.26	56.68	27.56	26.95	0.61	1.2 grains spike^{-1}	117.5 – 120.5
Qyld.hwwgSNS-4A.2$_b$	SNS	4AL	S4A_619679451 – S4A_620336405	3.24	8.20	3.86	3.86	2.09	0.09 spikelet spike^{-1}	91.5 – 96.5
Qyld.hwwgGWT-4A.2$_c$	GWT	4AL	S4A_633516822 – S4A_647775911	3.27	8.60	12.74	11.16	1.59	-0.41 mg	115.5 – 125.5
Qyld.hwwgPMAT-4A.2$_b$	PMAT	4AL	S4A_564352980 – S4A_592328441	4.04	6.26	10.09	10.09	0.003	1.1 days	23.5 – 33.5
Qyld.hwwgPHT-4B.1$_a$	PHT	4BS	S4B_12718161 – S4B_18668627	3.35	8.71	6.91	6.65	0.26	-0.39 cm	42.5 – 50.5
Qyld.hwwgTGW-4B.2$_a$	TGW	4BL	S4B_601835018 – S4B_618081673	5.15	4.13	23.63	2.41	21.21	0.23 g	86.5 – 101.5
Qyld.hwwgGNS-5A.2$_a$	GNS	5AL	S5A_588428650 – S5A_592083734	5.26	12.67	5.07	4.33	0.74	0.50 grains spike^{-1}	265.5 – 269.5
Qyld.hwwgPHT-6A.1$_c$	PHT	6AS	S6A_62109330 – S6A_72512856	3.35	12.83	9.65	6.42	3.23	-0.39 cm	100.5 – 103.5
Qyld.hwwgPHT-6A.2$_a$	PHT	6AL	S6A_429204568 – S6A_453486127	3.35	12.29	13.86	7.53	6.33	-0.42 cm	116.5 – 120.5

[1] PVE of Additive Effect
[2] PVE of A x E interaction
[3]Additive effect of the Overley allele
[4]Confidence interval (cM)

The A x E interactions of the major QTL(s) across locations were identified using the IWGSVv2.1 map and Jagger map (Table 3.10 and Table 3.11). Using the IWGSCv2.1 map the additive effects of the Overley alleles at the GWT QTLs (*Qyld.hwwgGWT-1A.2$_a$*, *Qyld.hwwgGWT-4A.2$_a$*) was negative, indicating lower GWT (Table 3.10). The Overley allele of *Qyld.hwwgGWT-1A.2$_a$* was less unfavorable at AS18, relative to AS19. The Overley allele of *Qyld.hwwgGWT-4A.2$_a$* was also less unfavorable at AS18, relative to AS19. The additive effects predominated over the QTL x E interaction which is evidenced by the PVE values in Table 3.8 and Table 3.9.

The additive effects of the Overley allele at the GDM QTL, *Qyld.hwwgGDM-1A.2$_a$* and *Qyld.hwwgGDM-2B.1 $_a$* were negligible for both parental alleles, respectively (Table 3.10). The Overley allele of GNS QTL (*Qyld.hwwgGNS-2D.1$_a$*) was negative, indicating the less favorable response of lower GNS. The Overley allele of *Qyld.hwwgGNS-2D.1$_a$* was less unfavorable at AS18 and HZ18, relative to the other locations. The Overley allele of the GNS QTL (*Qyld.hwwgGNS-2A.2$_a$* and *Qyld.hwwgGNS-4A.2$_a$*) was positive, indicating the favorable response of higher GNS. The Overley allele of *Qyld.hwwgGNS-2A.2$_a$* was most favorable at HZ19, relative to the other locations. The Overley allele of *Qyld.hwwgGNS-4A.2$_a$* was most favorable at HZ19, relative to the other locations (Table 3.10).

The Overley allele at the YLD QTL (*Qyld.hwwgYLD-3B.2$_a$*) was negative indicating the less favorable response of decrease in yield (Table 3.10). The Overley allele of *Qyld.hwwgYLD-3B.2$_a$* was less unfavorable at AS18 and HZ18, relative to the other locations. The Overley allele of the FT QTL (*Qyld.hwwgFT-2B.1$_a$*) was negative, indicating the less favorable response of earlier flowering time. The Overley allele of *Qyld.hwwgFT-2B.1$_a$* was less unfavorable at AS18, HZ18, and HZ19, relative to AS19. The Overley allele of the PMAT QTL (*Qyld.hwwgPMAT-*

2B.1$_a$) was negative indicating the less favorable response of earlier maturity. The Overley allele of *Qyld.hwwgPMAT-2B.1$_a$* was less unfavorable at AS18, relative to AS19 (Table 3.10). The Overley allele of the SNS QTL (*Qyld.hwwgSNS-2B.1$_a$*) was negative, indicating the less favorable response of lower SNS. The Overley allele of *Qyld.hwwgSNS-2B.1$_a$* was less unfavorable at AS18 and AS19, relative to the other locations. The Overley allele of the SNS QTL (*Qyld.hwwgSNS-3D.2$_a$* and *Qyld.hwwgSNS-4A.2$_a$*) was positive, indicating an increase in SNS. The Overland allele of *Qyld.hwwgSNS-3D.2$_a$* was most favorable at AS19 and HZ19, relative to the other locations. The Overland allele of *Qyld.hwwgSNS-4A.2$_a$* was most favorable at HZ18 and HZ19, relative to the other locations. The Overley allele of the PHT QTLs (*Qyld.hwwgPHT-4D.1$_a$* and *Qyld.hwwgPHT-6A.1$_a$*) was negative, indicating favorable response of lower PHT. The Overley allele of *Qyld.hwwgPHT-4D.1$_a$* was most favorable at HZ19, relative to the other locations. The Overley allele of *Qyld.hwwgPHT-6A.1$_a$* was most favorable at AS18 and HZ18, relative to the other locations (Table 3.10). The QTL x E interaction effect did not show a predominate difference with the additive effect for the majority of the traits except for yield where the QTL x E interaction effect predominated additive.

Table 3.10. Additive and A X E effects at each of the four environments for yield and yield-related traits using the IWGSCv2.1 map.

The additive and A x E effects for yield and other traits across locations associated with significant QTLs (LOD ≥4.5 and PVE ≥10%) on the IWGSVv2.1 reference map, associated with the data presented in Table 3.8 (MET analysis). Abbreviations are E = Environment, C.I. =Confidence interval (cM), A x E = Additive by environment interaction.

			A x E Effect			
QTL Name	**Unit**	**A**	**AS18**	**AS19**	**HZ18**	**HZ18**
Qyld.hwwgGWT-1A.2$_a$	mg	-0.33	0.13	-0.13		
Qyld.hwwgGDM-1A.2 $_a$	mm	-0.006	-0.01	0.01		
Qyld.hwwgGNS-2A.2$_a$	grains spike^{-1}	0.50	-0.01	0.10	-0.30	0.21
Qyld.hwwgFT-2B.1$_a$	days	-1.22	0.01	-0.02	0.004	0.006
Qyld.hwwgPMAT-2B.1$_a$	days	-0.70	0.006	-0.006		
Qyld.hwwgSNS-2B.1$_a$	spikelet spike^{-1}	-0.16	0.002	0.01	-0.003	-0.010
Qyld.hwwgGDM-2B.1 $_a$	mm	0.006	0.01	-0.01		
Qyld.hwwgGNS-2D.1$_a$	grains spike^{-1}	-0.56	0.03	-0.13	0.03	-0.15
Qyld.hwwgYLD-3B.2$_a$	kg ha^{-1}	-46.86	29.25	-17.07	59.07	-71.25
Qyld.hwwgSNS-3D.2$_a$	spikelet spike^{-1}	0.11	-0.04	0.01	0.001	0.01
Qyld.hwwgGWT-4A.2$_a$	mg	-0.55	0.11	-0.11		
Qyld.hwwgSNS-4A.2$_a$	spikelet spike^{-1}	0.11	-0.03	-0.05	0.02	0.07

Qyld.hwwgGNS-4A.2 $_a$	grains spike^{-1}	1.03	-0.06	-0.08	-0.12	0.02
Qyld.hwwgPHT-4D.1 $_a$	cm	-0.28	0.20	-0.07	0.20	-0.33
Qyld.hwwgPHT-6A.1 $_a$	cm	-0.48	-0.14	0.39	-0.14	-0.10

*Additive effect of the Overley allele.

Table 3.11 Additive and A X E effects at each of the four environments for yield and yield-related traits using the Jagger map. The A x E effects for yield and other traits across locations associated with significant QTLs (LOD ≥4.5 and PVE ≥10%) on the Jagger reference map, associated with the data presented in Table 3.9. Abbreviations are E = Environment, C.I. =Confidence interval (cM), A x E = Additive by environment interaction.

			A x E Effect			
QTL Name	**Unit**	**A**	**AS18**	**AS19**	**HZ18**	**HZ19**
Qyld.hwwgSNS-1A.2 $_a$	spikelet spike^{-1}	0.11	-0.09	0.04	0.01	0.04
Qyld.hwwgGWT-1A.2 $_b$	mg	-0.36	0.10	-0.10		
Qyld.hwwgGNS-2A.2 $_b$	grains spike^{-1}	0.54	-0.05	-0.53	0.22	0.36
Qyld.hwwgGNS-2B.1 $_a$	grains spike^{-1}	-0.58	0.20	-0.15	0.11	-0.15
Qyld.hwwgGDM-2B.1 $_b$	mm	0.008	0.008	0.015		
Qyld.hwwgSNS-2B.1 $_b$	spikelet spike^{-1}	-0.16	0.02	-0.03	0.05	-0.04
Qyld.hwwgFT-2B.1 $_b$	days	-0.70	0.009	-0.02	0.003	0.004
Qyld.hwwgFT-2B.1 $_c$	days	-0.70	0.01	-0.02	0.003	0.004
Qyld.hwwgTGW-2D.1 $_a$	grams	0.22	-0.89	0.74	0.05	0.10

Qyld.hwwgTGW-2D.1$_b$	grams	0.10	-0.78	0.71	-0.36	0.42
Qyld.hwwgTGW-3B.2$_a$	grams	0.34	-0.06	-0.32	-0.65	1.03
Qyld.hwwgYLD-3B.2$_c$	kg ha^{-1}	-46.6	30.2	-10.8	54.2	-73.5
Qyld.hwwgGNS-4A.2$_b$	grains spike^{-1}	1.2	-0.20	-0.14	0.27	0.07
Qyld.hwwgSNS-4A.2$_b$	spikelet spike^{-1}	0.09	0.04	-0.05	0.04	-0.08
Qyld.hwwgGWT-4A.2$_c$	mg	-0.41	0.15	-0.15		
Qyld.hwwgPMAT-4A.2$_b$	days	1.1	-0.02	0.02		
Qyld.hwwgPHT-4B.1$_a$	cm	-0.39	-0.07	0.11	-0.07	0.04
Qyld.hwwgTGW-4B.2$_a$	grams	0.23	-0.55	0.70	0.65	-0.79
Qyld.hwwgGNS-5A.2$_a$	grains spike^{-1}	0.50	-0.15	-0.25	0.24	0.16
Qyld.hwwgPHT-6A.1$_c$	cm	-0.39	-0.27	0.24	-0.27	0.30
Qyld.hwwgPHT-6A.2$_a$	cm	-0.42	-0.07	0.11	-0.07	0.04

*Additive effect of the Overley allele.

Discussion

Phenotypic Data

Many components define the underlying genetics of YLD. So, maximizing YLD improvement depends on improving the production of these components, such as GWT, SNS, and GNS. The desirable phenotypic expressions of these traits are influenced by genotype and G x E. Our study evaluated YLD and its components across two seasons at two locations in an Overley x Overland hard winter wheat RIL population. All traits were considered in both years and locations except GWT and GDM, which were only measured for samples from Ashland. Our phenotypic data showed that our RIL population phenotypic responses of YLD and YLD-related traits were intermediate among the parents. The high heritabilities of yield component traits suggests that a YLD improvement target should focus on the components rather than YLD alone.

QTL Analysis: Plant Height

We identified a PHT QTL on 6AS using the IWGSCv2.1 map (*Qyld.hwwgPHT-6A.1$_a$*) and on 6AL using the Jagger map (*Qyld.hwwgPHT-6A.2$_a$*) using the ML-BLUPs both having similar PVE (17%) and LOD (8). There have been reports on QTLs identified on 6AS for PHT (Mcintosh et al., 2013; Tian et al., 2017) associated with *Rht14, Rht16*, or *Rht18* which have not yet been cloned. Further investigation will need to be done to determine which *Rht* gene(s) from the list above is closely associated with our 6AS QTL. The 6AL QTL using the Jagger map *Qyld.hwwgPHT-6A.2$_a$* may be associated with the *Rht24* gene (Tian et al., 2017). The *Rht24* is flanked between *TaAP2* (434.8 Mb) and *TaFAR* (405.5 Mb) with a genetic distance of 1.85 cM (Tian et al., 2017). Our 6AL QTL discovered in the Jagger map, *Qyld.hwwgPHT-6A.2$_a$*, overlaps with the *Rht24* marker interval (429.0 Mb – 453.5 Mb). In the MET analysis, additional PHT QTLs were identified on 4DL (*Qyld.hwwgPHT-4D.1$_a$*) with the IWGSCv2.1 map, and on 4BS

(*Qyld.hwwgPHT-4B.1*$_a$), and 6AS (*Qyld.hwwgPHT-6A.1*$_a$) using the Jagger map. No QTLs have been reported on the 4DL for PHT, which indicates that this may be a novel QTL region. There have been several PHT QTLs reported on the 4BS, *Rht-B1*$_b$ (Peng et al., 1999), *Rht-B1*$_c$ (Pearce et al., 2011), *QHt.fra-4B* (Jinrong Peng et al., 1999), *Pht.Sparc-4B* (Bokore et al., 2022). The *Rht-B1* gene is cloned and its position is known, and both parents are *Rht1* wheats. Our 4BS QTLs may be closely associated with the QTLs reported, but further investigation is needed. Other meta-QTL analysis studies have also reported QTLs associated with PHT spanning the entire wheat genome (Griffiths et al., 2009; Mcintosh et al., 2013; Zanke et al., 2014; Zhang et al., 2010).

QTL Analysis: Flowering Time

Using the ML-BLUP data we identified a 5AL QTL (*Qyld.hwwgFT-5A.2*$_a$) using the IWGSCv2.1 map (Table 3.6) and 3BL (*Qyld.hwwgFT-3B.2*$_a$), 5AL (*Qyld.hwwgFT-5A.2*$_b$), and 2BS (*Qyld.hwwgFT-2B.1*$_c$) QTLs using the Jagger map (Table 3.7). With MET-QTL analysis we identified associations on the 2BS chromosome (IWGSCv2.1: *Qyld.hwwgFT-2B.1*$_a$; Jagger: *Qyld.hwwgFT-2B.1*$_b$; Jagger: *Qyld.hwwgFT-2B.1*$_c$). Using the IWGSCv2.1 map, the 5AL QTL, did include the Vrn-A1-E4-vern-KASP marker (~145 cM) region, but it may be related to other FT QTLs reported on 5A in other MQTL studies (refer to Ch. 2). We identified multiple QTLs on 2BS; there was no overlap between QTLs identified with the different maps for the 2BS chromosome. Using the IWGSCv2.1 map (Table 3.6), there was only one FT QTL designated as *Qyld.hwwgFT-5A.2*$_a$, with a PVE of 8.34%. The QTLs identified with the Jagger map had adjacent markers and were fragmented with tight confidence intervals. These 2BS QTLs may be associated with *Ppd-B1* (61.2 Mb, Jagger map)(Díaz et al., 2012; Mcintosh et al., 2013). Diaz et al. (2012) investigated genetic variants in commercial varieties of wheat that regulate FT by

altering photoperiod response, *Ppd -B1* alleles, or *Vrn-A1* alleles. It was determined that increased copy numbers of the gene alters gene expression, and FT decreases. In cases where there was an increase of copy number for *Ppd-B1* resulted in an early flowering phenotype (photoperiod insensitive-varieties flower quickly in both short or long days) response. A similar response was observed for *Vrn-A1;* as there is an increase in *Vrn-A1,* an increase in vernalization requirement (longer exposure time to the cold) will increase the potency of the FT response. Information gathered from our QTLs will further enhance our understanding of underlying genetic mechanisms involved with FT.

QTL Analysis: Physiological Maturity

Physiological maturity is defined as the stage of grain development when grains stop growing and maximum GY potential is achieved. Physiological maturity is influenced by the same genes /allelic variants involved in FT (mentioned in the previous section). Our study identified PMAT QTLs using ML-BLUPs on *Qyld.hwwgPMAT-2B.1*$_b$ (IWGSCv2.1), *Qyld.hwwgPMAT-2B.1*$_a$ (Jagger), and *Qyld.hwwgPMAT-5A.2*$_a$ (Jagger). The marker interval of *Qyld.hwwgPMAT-5A.2*$_a$ was near Vrn-A1-E4-vern-KASP (S5A_668553847: 50cM and S5A_671845643: 54cM) in comparison to *Qyld.hwwgFT-5A.2*$_b$. The remaining two QTLs are located on the 2BS. They may be associated with *Ppd-B1*; this may not be unusual as studies have shown that FT and PMAT responses are correlated (Kamran et al., 2014).

Using MET-QTL analysis, we identified two PMAT QTLs *Qyld.hwwgPMAT-2B.1*$_a$ (IWGSCv2.1) and *Qyld.hwwgPMAT-4A.2*$_b$ (Jagger). There are no reports of PMAT QTLs on these chromosomes, but they may still be associated with yield-related traits. Our data suggest that there is a relationship between PMAT, SNS, and FT which may hold based on our correlations with SNS (r = 0.36) and FT (r = 0.67), which can positively influence YLD. The

relationship with PMAT and grain traits were negatively correlated (inversely proportional) indicating that late maturing varieties produced grains of lower weight and diameter (Table 3.5). Studies have reported that the length of PMAT can influence GWT and other dynamics through the regulation of sink-source pathways and underlying genetic mechanisms (Brooking, 1990; Parvej et al., 2020; Sala et al., 2007). Furthermore, just as FT QTLs are found across the entire genome, the same goes for PMAT (Chen et al., 2010; Kulwal et al., 2003; Wang et al., 2009).

QTL Analysis: Grain Weight Characteristics

Various grain morphological parameters and dynamics influence grain-filling rate from source-sink relations to spike development. Identifying major QTLs and functional genes is urgently required for molecular improvements in wheat GY. In our study, we identified the most QTLs for GWT-related traits. Using the IWGSCv2.1 map with the ML-BLUP data we identified the following QTLs on 2AL (GWT), 2BL (TGW), 4AL (TGW, GWT), 5AL (GDM), 6BL (GWT). In the Jagger map using the ML-BLUP data, we identified QTLs on 1AL (GWT), 2AL (TGW, GNS), 2BS (TGW, GNS, PMAT, SNS), 3BL (FT, YLD), 4AL (GNS, TGW, GWT), 5AL (FT, GNS, GDM, PMAT), and 6AS (PHT). Additional QTLs identified using MET-QTL analysis in both maps.

There have been reports of GWT QTLs (Mcintosh et al., 2013) being found on 4AL (*QGwe.ipk-4A)*, 4AS (*QGwe.ocs-4A.1*), and 2DS (*QGwe.ipk-2D*). Other meta-QTL analysis studies (Goffinet et al., 2000) have reported GWT QTLs located on the 1B, 2A, 2D, 3B, 4A, 5A, 6A, 6B,7A, and 7D (Tyagi et al., 2015; J. Zhang et al., 2018). Most of our GWT QTLs may be associated with similar chromosome groups mentioned in the MQTL studies. However, further investigation will be needed to evaluate their proximity to currently reported GWT QTLs. There may also be novel QTLs from our study not yet identified (e.g., *Qyld.hwwgGWT-1A.2*$_b$).

Thousand grain weight can be a significant determinant of GY potential in wheat, influenced by genetic, management, and environmental factors (Avni et al., 2018; Cruppe et al., 2021; Duan et al., 2017; Wang et al., 2012). In comparison to other YLD components, previous research showed that TGW might have more stable PVE and higher heritability (Cheng et al., 2015; Duan et al., 2020; Gao et al., 2021; Krishnappa et al., 2017; Miao et al., 2022; Qu et al., 2021; Xin et al., 2020; Xu et al., 2017; Yang et al., 2020). This was also the case for our study, (H^2 = 0.75; $r_{GWT:GDM}$ =0.46; $r_{GWT:TGW}$ =0.71) where we presented high heritabilities and significant correlations ($p < 0.001$). Most of our YLD components showed genotype and G x E as the strong variance components contributing to their response ($\sigma^2_{g\,TGW} = 4.5^{***}$, $\sigma^2_{ge\,TGW} = 2.1^{***}$). These results validate that TGW is mainly controlled by genetic factors that express QTLs under various environmental conditions. The TGW QTLs were only identified using the ML-BLUP data for both reference maps from our study. The most significant QTLs for both reference maps were located on the 2BS chromosome. A recent MQTL study (Miao et al., 2022) identified 45 MQTLs spanning the entire wheat genome explaining 1.8-12.9% PVE. Their 2BS MQTL, *Qtgw.acs-2B*, flanked by *Xgwm257* (IWGSCv2.1 map: 51.0 Mb; Jagger map: 48.5 Mb) and *Xgwm429* (IWGSv2.1 map:81.2 Mb; Jagger map: 78.8 Mb), is also located on the short arm. Further investigation will need to further validate the proximity of our QTL to these studies. This study also supports our other QTLs for TGW chromosomal groups.

In ML-BLUP data, the GDM QTLs were *Qyld.hwwgGDM-5A.2*$_a$ (IWGSCv2.1) *Qyld.hwwgGDM-5A.2*$_b$ (Jagger). With our MET-QTL analysis data, we identified *Qyld.hwwgGDM-1A.2*$_a$, *Qyld.hwwgGDM-2B.1*$_a$ (IWGSCv2.1) and *Qyld.hwwgGDM-2B.1*$_b$ (Jagger). As stated earlier, a factor that characterizes GWT is GDM, and homologous forms of *TaGW2* may influence the magnitude of GDM, which can influence YLD. For the IWGSCv2.1

map with the ML-BLUP dataset, only the QTL on the 5AL was identified (*Qyld.hwwgGDM-5A.2$_a$*). There was also only one QTL identified for GDM, *Qyld.hwwgGDM-5A.2$_b$*, using the Jagger map. Both GDM QTLs identified using both reference maps had a positive additive effect (A = 0.003). There was a strong correlation between GDM and GWT ($r_{GDM:GWT}$ = 0.46). In the second data set (MET analysis), there were more fragmented and overlapping results among different traits. Using the IWGSCv2.1 map GDM QTLs were on 1AL (*Qyld.hwwgGDM-1A.2$_a$*) and 2BS (*Qyld.hwwgGDM-2B.1$_a$*). Both had relatively small additive effects (-0.006 ,0.006). In addition, QTLs for GWT and GDM on 1AL overlapped. This QTL was found in both maps using MET analysis and the Jagger map using the ML-BLUP data. The 2BS QTL was not identified using the Jagger map.

Yang et al. (2020) measured grain characteristics and performed QTL analysis in using a RIL population consisting of 266 lines. Four genetic regions (1AL, 2BS, 3AL, and 5B) affected TGW-like traits. The 1AL QTL associated with grain width (*Qgw.caas-1AL*) had a PVE of 5-20% with a physical interval of 307.8 - 356.7 Mb. Our QTL, however, is distal (553.4 – 567.3 Mb; with a PVE of 27%). There were QTLs also identified on 2BS. The QTL linked to grain width, *Qgw.caas-2BS*, had a PVE of 4.2 – 8.1% and a physical position of 41.4 – 44.3 Mb. The 5AL QTL we identified using the ML-BLUP data may be a novel QTL as current studies report that grain-dimension-related QTLs are mainly located on 5AS (Kumari et al., 2018; Li et al., 2022).

QTL Analysis: Spikelet Number per Spike and Grains per Spike

Spikelet number per spike (sink strength) is an important trait that characterizes YLD as we expect that SNS and GNS will increase and YLD will increase if there sufficient photosynthate is available to fill the grain. We observed strong correlations between GNS and

SNS ($r_{GNS:SNS}$ = 0.65), but no correlation with YLD. For our study, it seems that SNS is not significantly influenced by the environment, but is affected by genotype (σ_G = 0.43***), which is similar to recent findings (Jaenisch et al., 2022; Slafer et al., 2022). The major QTLs in both maps for SNS were on 2BS, *Qyld.hwwgSNS-2B.1$_b$* (Jagger map) and *Qyld.hwwgSNS-2B.1$_a$* (IWGSCv2.1 map).

Our study identified multiple QTLs for SNS and GNS in both datasets (ML-BLUP, MET analysis). In the first dataset (ML-BLUPs) using the IWGSCv2.1 map, 5 QTLS (3 SNS and 2 GNS) are designated *Qyld.hwwgSNS-2B.1$_a$* ,*Qyld.hwwgSNS-7A.1$_a$* , *Qyld.hwwgSNS-4A.2$_a$*, *Qyld.hwwgGNS-2A.2$_a$* ,and *Qyld.hwwgGNS-4A.2$_a$*. The only overlap observed was with TGW (*Qyld.hwwgTGW-4A.2$_a$* ; A = -0.59 g) and GNS (*Qyld.hwwgGNS-4A.2$_a$* ; OY ; A = 1.0 grains spike^{-1}) which may be expected as these traits may interrelated as grain characteristics. The increase in TGW is linked to the Overland allele, and an increase in GNS has been linked to the Overley allele. The correlation between these two traits was inversely proportional ($r^2_{GNS:\ TGW}$ = -0.45). This relationship between increased GNS and low TGW can be due to environmental conditions and lack of assimilates.

Using the Jagger map, we identified seven QTLs, three for SNS and four for GNS. Our correlations ($r^2_{GNS:\ SNS}$ = 0.65) show that there is a positive proportional relationship with these traits. There was also an overlap was on the 4AL QTLs of GWT (*Qyld.hwwgGWT-4A.2$_c$* ; A = -0.42 mg) and GNS (*Qyld.hwwgGNS-4A.2$_b$* ; A =1.28 grains spike^{-1}). These QTLs have the same type of relationship that we discussed earlier with TGW and SNS. In MET analysis, using the IWGSv2.1 map we found six QTLs (3 SNS, 3 GNS) designated as *Qyld.hwwgSNS-2B.1$_a$* ,*Qyld.hwwgSNS-4A.2$_a$* ,*Qyld.hwwgSNS-3D.2$_a$* , *Qyld.hwwgGNS-4A.2$_a$*,*Qyld.hwwgGNS-2D.1$_a$*, and *Qyld.hwwgGNS-2A.2$_a$* . There was overlap in QTLs found on the 2BS and 4AL

chromosomes. The 2BS overlapping QTLs were *Qyld.hwwgSNS-2B.1*$_a$ (A = -0.16 spikelet spike^{-1}) and *Qyld.hwwgFT-2B.1*$_a$ (A = -1.2 days). These QTLs present a directly proportional relationship with the traits; later FT plants have larger SNS. The 4AL overlapping QTLs were *Qyld.hwwgGNS-4A.2*$_a$ (A = 1.0 grains spike^{-1}) and *Qyld.hwwgGWT-4A.2*$_a$ (A = -0.55 mg); these QTLs have the similar relationship described above between TGW and SNS. Using the Jagger map, we found seven QTLs, three for SNS and four for GNS. There were overlapping QTLs on 2BS (*Qyld.hwwgGNS-2B.1*$_a$: A = 0.58 grains spike^{-1}, *Qyld.hwwgSNS-2B.1*$_b$: A = -0.16 spikelet spike^{-1}; *Qyld.hwwgFT-2B.1*$_c$: A = -0.7 days) and 4AL (*Qyld.hwwgGNS-4A.2*$_b$:A = 1.2 grains spike^{-1}, *Qyld.hwwgGWT-4A.2*$_c$:A = - 0.4 mg).

Spikelet number per spike and GNS can significantly contribute to GY (Slafer et al., 2020). Many environmental and genetic factors influence these traits. Reports of QTLs have identified and validated these traits across different genomic regions. Reported regions for SNS had been identified on the 7AL (Kuzay et al., 2022, 2019; Muqaddasi et al., 2019; Zhai et al., 2016), 2DS (Ma et al., 2019), and other regions identified in MQTL studies. Li et al. (2021) performed a QTL study using a DH population, 'Kechengmai1' x 'Chuanmai42'. There were 27 QTLs identified for spike architecture traits such as total spikelet number per spike (TSN), and fertile spikelet number per spike (FSN) identified on chromosomes 1B, 1D, 2B, 2D, 3D, 4A, 4D, 5A, 5B, 5D, 6A, 6B, and 7D in multiple environments. The 2BS QTL, *QTsn.cib-2B.1* (1.26 – 1.86 cM), flanked by was only identified for TSN and a PVE of 4.1 %. There were two on the 4A (*QFsn.cib-4A.1*: 97.3 – 98.0 cM; *QFsn.cib-4A.2*: 108.3 – 113.4 cM) associated with FSN, with their respective PVE percentages being 18.3 % and 9.7 %. The 3D QTL on the long arm, *QFsn.cib-3D*/*QTsn.cib-3D* (103.64 –108.09 cM), was identified across all environments tested, and their phenotypic variation ranged from 6 – 23 %. Our QTLs are in the general vicinity of

some of these QTLs (e.g., *QFsn.cib-3D*/*QTsn.cib-3D*: 549.5 Mb – 555.2 Mb; *Qyld.hwwgSNS-3D.2*$_a$: 611.5 Mb – 614.2 Mb). This still provides some supporting insight that there is evidence of QTLs being identified in similar regions to our study.

In this trial (Chen et al., 2020), GNS was not used for QTL analysis, but it was a trait measured in this study that indicated a strong association with spike-related traits. The 3DL QTL presented a positive effect with TSN (5.56%***; $p < 0.001$), FSN (5.31%***; $p < 0.001$), and GNS (7.61%***; $p < 0.001$) it presented a similar trend with other spike morphology traits. Furthermore, correlations among GNS, TSN, and FSN were strong ($r^2_{TSN} = 0.57^{***}$, $r^2_{FSN} = 0.63^{***}$), and a similar trend of strong correlations among spikelet-related traits was also observed in another study (Chen et al., 2020) for spike-related traits ($r^2_{TSN:\ FSN} = 0.93^{***}$). These findings indicate that increasing SNS produced more grains (GNS) in fertile florets and effectively GY.

Saini et al. (2022) evaluated 230 studies (1990 – 2022) discovering 2,852 strong QTLs out of 8,998 QTLs used for meta-QTL analysis that identified 141 MQTLs for YLD and YLD-related traits. Of the 141 MQTLs, 58 contributed to GNS and other YLD-related traits (e.g., GWT). The GNS MQTLs spanned all 21 chromosomes with varying QTL stats (e.g., LOD, PVE, interval size). There were no direct overlaps between our GNS QTLs and the MQTLs from the study, *MQTL4A.3* (709.9 Mb – 713.5 Mb) and *Qyld.hwwgGNS-4A.2*$_a$ (671.8 Mb – 682.3 Mb) *Qyld.hwwgGNS-4A.2*$_b$ (633.5 Mb – 647.8 Mb) were loosely in the general area of the MQTLs the other QTLs from our study were not near any MQTLs discovered in this study. Other reported QTLs have been *QGnu.ipk-4A, QKps.u* (Li et al., 2022) *nl-3A.1,Qkps.unl-3A.2* (Mcintosh et al., 2013), *QGns.cau-1B.1, QGns.cau-3A.1, QGns.cau-6A.2, QGns.cau-6A.3, QGns.cau-6A.4*, and

QGns.cau-7A.2 (Cui et al., 2014; Jia et al., 2013; Kumar et al., 2007; Zhai et al., 2018). Based on these findings, our QTLs discovered in GNS may be novel genomic regions.

QTL Analysis: Yield

Due to its complex polygenic nature, YLD is often characterized by epistatic and pleotropic effects. Due to its complexity, it may be difficult to pinpoint the exact genomic region(s) involved in characterizing YLD. In our study, due to our small filtered robust SNP marker datasets in both reference maps, we identified a QTL on the 3BL on both maps. With ML-BLUP data, it was designated as *Qyld.hwwgYLD-3B.2*$_b$ (IWGSCv2.1) and *Qyld.hwwgYLD-3B.2*$_d$ (Jagger). At individual locations (MET-QTL analysis), the YLD QTLs were *Qyld.hwwgYLD-3B.2*$_a$ (IWGSCv2.1) and *Qyld.hwwgYLD-3B.2*$_c$(Jagger). From the low heritability (H^2 =0.19) and estimated variance responses, we can deduce that environmental factors influence YLD response more than genotypic factors. This aligns with previous findings (Jaenisch et al., 2022). We discovered that the environmental response of our YLD QTLs on 3BL was due to HZ19 which had very strong additive effects (HZ19: Qyld *hwwgYLD-3B.2*$_a$ = -71.3 kg ha^{-1}). Reports have indicated that YLD QTLs have been found on the 3BS around the centromeric and telomeric regions (Tura et al., 2020; Zhang et al., 2010). Additionally, our data shows that YLD is better defined by grain components than YLD alone based on their heritabilities, variance components, correlations, and respective significance levels. Yield trait components such as GWT, GN, and SN have QTLs distributed across all chromosomes at different frequencies (Cao et al., 2020; Saini et al., 2022b; Tura et al., 2020). Due to the lack of QTLs discovered on 3BL, our QTLs may be identifying novel genomic regions.

Conclusion

The scope of our study was to determine what genomic regions affect GY-related traits in the Overley x Overland population using the IWGSCv2.1 and Jagger maps that can explain the variation in YLD and its components in field trials. We evaluated different YLD and YLD-related traits and identified QTLs at various distributions for these traits across the wheat genome. Using both maps we identified QTLs for YLD (3BL), PHT (6AS, 4DL, 6AL, 4BS), GWT (6BL, 2AL, 4AL, 1AL), SNS (2BS, 7AS, 4AL, 3DL, 1AL), FT (5AL, 2BS, 3BL), number of GNS (2AL, 4AL, 2DS, 2BS, 5AL), TGW (2BL, 4AL), GDM (5AL, 1AL, 2BS), and PMAT (2BS, 4AL, 5AL). Overall, we identified more QTLs in total (ML-BLUP and MET analysis dataset) using the Jagger map (40 QTLs) than when using the IWGSCv2.1 map (30 QTLs). The IWGSCv2.1 map had more QTLs linked to GWT, SNS, PHT, and GNS, scanning both datasets. The Jagger map had more QTLs linked to FT, GNS, and TGW.

Both QTL analysis methods (ML-BLUPs and MET) identified QTLs with high phenotypic variation (PVE > 10%) using both reference maps. Some of the strongest QTLs for YLD and YLD components that were present in the first data set (ML-BLUP for IWGSCv2.1) were *Qyld.hwwgSNS-2B.1*$_a$ = 10.4%, *Qyld.hwwgGNS-4A.2*$_a$ = 18.4%, *Qyld.hwwgGWT-4A.2*$_b$ = 15%. Using the Jagger map, they were *Qyld.hwwgYLD-3B.2*$_d$ = 10.7%, *Qyld.hwwgGNS-4A.2*$_b$ = 25.4%, *Qyld.hwwgGWT-4A.2*$_c$ = 11.6%. Other factors (FT and PMAT) also showed strong effects on YLD in the ML-BLUP dataset for both maps *Qyld.hwwgPMAT-2B.1*$_b$ = 11.5%, *Qyld.hwwgPMAT-5A.2*$_a$ = 16.4%, *Qyld.hwwgFT-2B.1*$_c$ = 38.3%. In the second MET analysis the some of the strong QTLs identified were *Qyld.hwwgYLD-3B.2*$_a$ = 20.3%, *Qyld.hwwgGNS-4A.2*$_a$ = 18.3%, and *Qyld.hwwgGDM-1A.2*$_a$ = 26.6%; using the Jagger map they were *Qyld.hwwgGNS-4A.2*$_b$ = 27.6%, *Qyld.hwwgYLD-3B.2*$_c$ = 15.8%. Our results showed that the YLD and GNS

QTLs were mostly identified in the data from the Hays location for both maps. Other YLD component-related QTLs (e.g., SNS, GWT, and PHT) had varied contributions from different locations in both years. The future direction of this project will be to launch marker development which can aid breeders in developing selecting favorable alleles for crop yield improvement.

References

Avni, R., Oren, L., Shabtay, G., Assili, S., Pozniak, C., Hale, I., … Distelfeld, A. (2018). Genome based meta-QTL analysis of grain weight in tetraploid wheat identifies rare alleles of GRF4 associated with larger grains. *Genes*, *9*(12). https://doi.org/10.3390/genes9120636

Bokore, F. E., Cuthbert, R. D., Knox, R. E., Campbell, H. L., Meyer, B., N'Diaye, A., … DePauw, R. (2022). Main effect and epistatic QTL affecting spike shattering and association with plant height revealed in two spring wheat (Triticum aestivum L) populations. *Theoretical and Applied Genetics*, *135*(4), 1143–1162. https://doi.org/10.1007/s00122-021-03980-2

Brooking, I. R. (1990). Maize ear moisture during grain-filling, and its relation to physiological maturity and grain-drying. *Field Crops Research*, *23*(1). https://doi.org/10.1016/0378-4290(90)90097-U

Cao, S., Xu, D., Hanif, M., Xia, X., & He, Z. (2020). Genetic architecture underpinning yield component traits in wheat. *Theoretical and Applied Genetics*, *133*(6), 1811–1823. https://doi.org/10.1007/s00122-020-03562-8

Chen, Y., Carver, B. F., Wang, S., Cao, S., & Yan, L. (2010). Genetic regulation of developmental phases in winter wheat. *Molecular Breeding*, *26*(4), 573–582. https://doi.org/10.1007/s11032-010-9392-6

Chen, Z., Cheng, X., Chai, L., Wang, Z., Du, D., Wang, Z., … Ni, Z. (2020). Pleiotropic QTL influencing spikelet number and heading date in common wheat (Triticum aestivum L). *Theoretical and Applied Genetics*, *133*(6), 1825–1838. https://doi.org/10.1007/s00122-020-03556-6

Cheng, X., Chai, L., Chen, Z., Xu, L., Zhai, H., Zhao, A., … Ni, Z. (2015). Identification and characterization of a high kernel weight mutant induced by gamma radiation in wheat (Triticum aestivum L). *BMC Genetics*, *16*(1). https://doi.org/10.1186/s12863-015-0285-x

Cui, F., Zhao, C., Ding, A., Li, J., Wang, L., Li, X., … Wang, H. (2014). Construction of an integrative linkage map and QTL mapping of grain yield-related traits using three related wheat RIL populations. *TAG. Theoretical and Applied Genetics. Theoretische Und Angewandte Genetik*, *127*(3). https://doi.org/10.1007/s00122-013-2249-8

De Oliveira Silva, A., Slafer, G. A., Fritz, A. K., & Lollato, R. P. (2020). Physiological Basis of Genotypic Response to Management in Dryland Wheat. *Frontiers in Plant Science*, *10*. https://doi.org/10.3389/fpls.2019.01644

Díaz, A., Zikhali, M., Turner, A. S., Isaac, P., & Laurie, D. A. (2012). Copy number variation affecting the photoperiod-B1 and vernalization-A1 genes is associated with altered flowering time in wheat (Triticum aestivum). *PLoS ONE*, *7*(3). https://doi.org/10.1371/journal.pone.0033234

Duan, P., Xu, J., Zeng, D., Zhang, B., Geng, M., Zhang, G., … Li, Y. (2017). Natural Variation in the Promoter of GSE5 Contributes to Grain Size Diversity in Rice. *Molecular Plant*, *10*(5), 685–694. https://doi.org/10.1016/j.molp.2017.03.009

Duan, X., Yu, H., Ma, W., Sun, J., Zhao, Y., Yang, R., … Chen, J. (2020). A major and stable QTL controlling wheat thousand grain weight: identification, characterization, and CAPS marker development. *Molecular Breeding*, *40*(7). https://doi.org/10.1007/s11032-020-01147-3

Fritz, A., Martin, T. J., Shroyer, J. P., & Red, H. (2004). *Overley*. (April).

Gao, Y., Xu, X., Jin, J., Duan, S., Zhen, W., Xie, C., & Ma, J. (2021). Dissecting the genetic basis of grain morphology traits in Chinese wheat by genome wide association study. *Euphytica*, *217*(4). https://doi.org/10.1007/s10681-021-02795-y

Goffinet, B., & Gerber, S. (2000). Quantitative trait loci: A meta-analysis. *Genetics*, *155*(1), 463–473. https://doi.org/10.1093/genetics/155.1.463

Griffiths, S., Simmonds, J., Leverington, M., Wang, Y., Fish, L., Sayers, L., … Snape, J. (2009). Meta-QTL analysis of the genetic control of ear emergence in elite European winter wheat germplasm. *Theoretical and Applied Genetics*, *119*(3). https://doi.org/10.1007/s00122-009-1046-x

Jia, H., Wan, H., Yang, S., Zhang, Z., Kong, Z., Xue, S., … Ma, Z. (2013). Genetic dissection of yield-related traits in a recombinant inbred line population created using a key breeding parent in China's wheat breeding. *Theoretical and Applied Genetics*, *126*(8). https://doi.org/10.1007/s00122-013-2123-8

Kamran, A., Iqbal, M., & Spaner, D. (2014). Flowering time in wheat (Triticum aestivum L): A key factor for global adaptability. *Euphytica*, *197*(1), 1–26. https://doi.org/10.1007/s10681-014-1075-7

Krishnappa, G., Singh, A. M., Chaudhary, S., Ahlawat, A. K., Singh, S. K., Shukla, R. B., … Solanki, I. S. (2017). Molecular mapping of the grain iron and zinc concentration, protein content, and thousand kernel weight in wheat (Triticum aestivum L). *PLoS ONE*, *12*(4). https://doi.org/10.1371/journal.pone.0174972

Kulwal, P. L., Roy, J. K., Balyan, H. S., & Gupta, P. K. (2003). QTL mapping for growth and leaf characters in bread wheat. *Plant Science*, *164*(2). https://doi.org/10.1016/S0168-9452(02)00409-0

Kumar, N., Kulwal, P. L., Balyan, H. S., & Gupta, P. K. (2007). QTL mapping for yield and yield contributing traits in two mapping populations of bread wheat. *Molecular Breeding*, *19*(2), 163–177. https://doi.org/10.1007/s11032-006-9056-8

Kumari, S., Jaiswal, V., Mishra, V. K., Paliwal, R., Balyan, H. S., & Gupta, P. K. (2018). QTL mapping for some grain traits in bread wheat (Triticum aestivum L). *Physiology and Molecular Biology of Plants*, *24*(5), 909–920. https://doi.org/10.1007/s12298-018-0552-1

Kuzay, S., Lin, H., Li, C., Chen, S., Woods, D. P., Zhang, J., … Dubcovsky, J. (2022). WAPO-A1 is the causal gene of the 7AL QTL for spikelet number per spike in wheat. *PLoS Genetics*, *18*(1), 1–25. https://doi.org/10.1371/journal.pgen.1009747

Kuzay, S., Xu, Y., Zhang, J., Katz, A., Pearce, S., Su, Z., … Dubcovsky, J. (2019). Identification of a candidate gene for a QTL for spikelet number per spike on wheat chromosome arm 7AL by high-resolution genetic mapping. *Theoretical and Applied Genetics*. https://doi.org/10.1007/s00122-019-03382-5

Li, T., Deng, G., Su, Y., Yang, Z., Tang, Y., Wang, J., … Long, H. (2022). Genetic dissection of quantitative trait loci for grain size and weight by high-resolution genetic mapping in bread wheat (Triticum aestivum L). *Theoretical and Applied Genetics*, *135*(1), 257–271. https://doi.org/10.1007/s00122-021-03964-2

Li, T., Deng, G., Tang, Y., Su, Y., Wang, J., Cheng, J., … Long, H. (2021). Identification and Validation of a Novel Locus Controlling Spikelet Number in Bread Wheat (Triticum aestivum L). *Frontiers in Plant Science*, *12*(February), 1–14. https://doi.org/10.3389/fpls.2021.611106

Liu, H., Mullan, D., Zhang, C., Zhao, S., Li, X., Zhang, A., … Yan, G. (2020). Major genomic regions responsible for wheat yield and its components as revealed by meta-QTL and genotype–phenotype association analyses. *Planta*, *252*(4), 1–22. https://doi.org/10.1007/s00425-020-03466-3

Ma, J., Ding, P., Liu, J., Li, T., Zou, Y., Habib, A., … Lan, X. (2019). Identification and validation of a major and stably expressed QTL for spikelet number per spike in bread wheat. *Theoretical and Applied Genetics*, *132*(11), 3155–3167. https://doi.org/10.1007/s00122-019-03415-z

Maeoka, R. E., Sadras, V. O., Ciampitti, I. A., Diaz, D. R., Fritz, A. K., & Lollato, R. P. (2020). Changes in the Phenotype of Winter Wheat Varieties Released Between 1920 and 2016 in Response to In-Furrow Fertilizer: Biomass Allocation, Yield, and Grain Protein Concentration. *Frontiers in Plant Science*, *10*(January). https://doi.org/10.3389/fpls.2019.01786

Mcintosh, R. a, Dubcovsky, J., Rogers, W. J., Morris, C. F., Appels, R., Xia, X. C., … Hayden, M. (2013). Catalog of Gene Symbols for Wheat: 2013-2014 Supplement. *12th International Wheat Genetics Symposium*.

Miao, Y., Jing, F., Ma, J., Liu, Y., Zhang, P., Chen, T., … Yang, D. (2022). Major Genomic Regions for Wheat Grain Weight as Revealed by QTL Linkage Mapping and Meta-Analysis. *Frontiers in Plant Science*, *13*(February), 1–19. https://doi.org/10.3389/fpls.2022.802310

Muqaddasi, Q. H., Brassac, J., Koppolu, R., Plieske, J., Ganal, M. W., & Röder, M. S. (2019). TaAPO-A1, an ortholog of rice ABERRANT PANICLE ORGANIZATION 1, is associated with total spikelet number per spike in elite European hexaploid winter wheat (Triticum aestivum L) varieties. *Scientific Reports*, *9*(1), 1–12. https://doi.org/10.1038/s41598-019-

50331-9

Parvej, M. R., Hurburgh, C. R., Hanna, H. M., & Licht, M. A. (2020). Dynamics of corn dry matter content and grain quality after physiological maturity. *Agronomy Journal*, *112*(2). https://doi.org/10.1002/agj2.20042

Pearce, S., Saville, R., Vaughan, S. P., Chandler, P. M., Wilhelm, E. P., Sparks, C. A., … Thomas, S. G. (2011). Molecular characterization of Rht-1 dwarfing genes in hexaploid wheat. *Plant Physiology*, *157*(4), 1820–1831. https://doi.org/10.1104/pp.111.183657

Peng, J., Richards, D. E., Hartley, N. M., Murphy, G. P., Devos, K. M., Flintham, J. E., … Harberd, N. P. (1999). "Green revolution" genes encode mutant gibberellin response modulators. *Nature*, *400*(6741). https://doi.org/10.1038/22307

Qu, X., Liu, J., Xie, X., Xu, Q., Tang, H., Mu, Y., … Ma, J. (2021). Genetic Mapping and Validation of Loci for Kernel-Related Traits in Wheat (Triticum aestivum L). *Frontiers in Plant Science*, *12*. https://doi.org/10.3389/fpls.2021.667493

Quarrie, S. A., Pekic Quarrie, S., Radosevic, R., Rancic, D., Kaminska, A., Barnes, J. D., … Dodig, D. (2006). Dissecting a wheat QTL for yield present in a range of environments: From the QTL to candidate genes. *Journal of Experimental Botany*, *57*(11), 2627–2637. https://doi.org/10.1093/jxb/erl026

Saini, D. K., Srivastava, P., Pal, N., & Gupta, P. K. (2022). Meta-QTLs, ortho-meta-QTLs, and candidate genes for grain yield and associated traits in wheat (Triticum aestivum L). In *Theoretical and Applied Genetics* (Vol. 135). https://doi.org/10.1007/s00122-021-04018-3

Sala, R. G., Andrade, F. H., & Westgate, M. E. (2007). Maize kernel moisture at physiological maturity as affected by the source-sink relationship during grain filling. *Crop Science*, *47*(2). https://doi.org/10.2135/cropsci2006.06.0381

Slafer, G. A. (2003). Genetic basis of yield as viewed from a crop physiologist's perspective. *Annals of Applied Biology*, *142*(2), 117–128. https://doi.org/10.1111/j.1744-7348.2003.tb00237.x

Swamy, B. M., Vikram, P., Dixit, S., Ahmed, H. U., & Kumar, A. (2011). Meta-analysis of grain yield QTL identified during agricultural drought in grasses showed consensus. *BMC Genomics*, *12*. https://doi.org/10.1186/1471-2164-12-319

Tian, X., Wen, W., Xie, L., Fu, L., Xu, D., Fu, C., … Cao, S. (2017). Molecular mapping of reduced plant height gene Rht24 in bread wheat. *Frontiers in Plant Science*, *8*. https://doi.org/10.3389/fpls.2017.01379

Tura, H., Edwards, J., Gahlaut, V., Garcia, M., Sznajder, B., Baumann, U., … Fleury, D. (2020). QTL analysis and fine mapping of a QTL for yield-related traits in wheat grown in dry and hot environments. *Theoretical and Applied Genetics*, *133*(1), 239–257. https://doi.org/10.1007/s00122-019-03454-6

Tyagi, S., Mir, R. R., Balyan, H. S., & Gupta, P. K. (2015). Interval mapping and meta-QTL analysis of grain traits in common wheat (Triticum aestivum L). *Euphytica*, *201*(3), 367–380. https://doi.org/10.1007/s10681-014-1217-y

Wang, L., Ge, H., Hao, C., Dong, Y., & Zhang, X. (2012). Identifying loci influencing 1,000-kernel weight in wheat by microsatellite screening for evidence of selection during breeding. *PLoS ONE*, *7*(2). https://doi.org/10.1371/journal.pone.0029432

Wang, R. X., Hai, L., Zhang, X. Y., You, G. X., Yan, C. S., & Xiao, S. H. (2009). QTL mapping for grain filling rate and yield-related traits in RILs of the Chinese winter wheat population Heshangmai x Yu8679. *Theoretical and Applied Genetics*, *118*(2), 313–325. https://doi.org/10.1007/s00122-008-0901-5

Wintersteiger AG. (2018). *Laboratory preparation In the earth lies the seed of new growth.*

Wolf, S. Y. (1994). *Winter wheat variety characteristics*. 62.

Xin, F., Zhu, T., Wei, S., Han, Y., Zhao, Y., Zhang, D., … Ding, Q. (2020). QTL Mapping of Kernel Traits and Validation of a Major QTL for Kernel Length-Width Ratio Using SNP and Bulked Segregant Analysis in Wheat. *Scientific Reports*, *10*(1). https://doi.org/10.1038/s41598-019-56979-7

Xu, Y. F., Li, S. S., Li, L. H., Ma, F. F., Fu, X. Y., Shi, Z. L., … An, D. G. (2017). QTL mapping for yield and photosynthetic related traits under different water regimes in wheat. *Molecular Breeding*, *37*(3). https://doi.org/10.1007/s11032-016-0583-7

Yang, L., Zhao, D., Meng, Z., Xu, K., Yan, J., Xia, X., … Zhang, Y. (2020). QTL mapping for grain yield-related traits in bread wheat via SNP-based selective genotyping. *Theoretical and Applied Genetics*, *133*(3). https://doi.org/10.1007/s00122-019-03511-0

Yang, Y., Dhakal, S., Chu, C., Wang, S., Xue, Q., Rudd, J. C., … Liu, S. (2020). Genome wide identification of QTL associated with yield and yield components in two popular wheat cultivars TAM 111 and TAM 112. *PLoS ONE*, *15*(12 December). https://doi.org/10.1371/journal.pone.0237293

Zanke, C. D., Ling, J., Plieske, J., Kollers, S., Ebmeyer, E., Korzun, V., … Röder, M. S. (2014). Whole genome association mapping of plant height in winter wheat (Triticum aestivum L). *PLoS ONE*, *9*(11). https://doi.org/10.1371/journal.pone.0113287

Zhai, H., Feng, Z., Du, X., Song, Y., Liu, X., Qi, Z., … Ni, Z. (2018). A novel allele of TaGW2-A1 is located in a finely mapped QTL that increases grain weight but decreases grain number in wheat (Triticum aestivum L). *Theoretical and Applied Genetics*, *131*(3), 539–553. https://doi.org/10.1007/s00122-017-3017-y

Zhai, H., Feng, Z., Li, J., Liu, X., Xiao, S., Ni, Z., & Sun, Q. (2016). QTL analysis of spike morphological traits and plant height in winter wheat (Triticum aestivum L) using a high-density SNP and SSR-based linkage map. *Frontiers in Plant Science*, *7*(November 2016), 1–13. https://doi.org/10.3389/fpls.2016.01617

Zhang, J., Gizaw, S. A., Bossolini, E., Hegarty, J., Howell, T., Carter, A. H., … Dubcovsky, J. (2018). Identification and validation of QTL for grain yield and plant water status under contrasting water treatments in fall-sown spring wheats. *Theoretical and Applied Genetics*, *131*(8), 1741–1759. https://doi.org/10.1007/s00122-018-3111-9

Zhang, L. Y., Liu, D. C., Guo, X. L., Yang, W. L., Sun, J. Z., Wang, D. W., & Zhang, A. (2010). Genomic distribution of quantitative trait loci for yield and yield-related traits in common wheat. *Journal of Integrative Plant Biology*, *52*(11), 996–1007. https://doi.org/10.1111/j.1744-7909.2010.00967.x

Zhang, Y., Li, D., Zhang, D., Zhao, X., Cao, X., Dong, L., … Wang, D. (2018). Analysis of the functions of TaGW2 homoeologs in wheat grain weight and protein content traits. *Plant Journal*, *94*(5), 857–866. https://doi.org/10.1111/tpj.13903

Appendix A - Supplemental Data Chapter 1

Table 3.12. Primer sequences and amplification protocols of KASP markers that were used in this study.

A)

Marker Name	Chr	Position (Mb)	FAM Sequence	HEX Sequence	Common Sequence
Lr37-Yr17-Sr38_GBG-KASP	2AS	5,814,608	GGACGGCGTTTGCTCATGCTA	AGGACGGCGTTTGCTCATGCTG	AGCAGTATGTACACAAAA
IWB29391	2BS	166,612,997	GTCACAAGACCAGGGGATTG	GTCACAAGACCAGGGGATTT	CCTGGGGCCTTGTTACACTA
Ppd_D1_D2	2DS	36,206,276	CGAGCAGCTCCCGACG	GGGCGAGCAGCTCCAAC	GGTCTCCAATCAAGGCGGT
KS0617_287045	2DL	308,449,460	GGAGACAATTGAGGCCGTGT	GGAGACAATTGAGGCCGTGA	GGAGCCACCCCTCAACTTA
KS617_288635	2DL	388,514,681	CCGTCACTAAATTCGCGGC	CCGTCACTAAATTCGCGGT	CCTGTGATCCATCCCAGCAT
VrnA1E4	5AL	590,394,627	AGAGTTTTCCAAAAAGATAGATCAATGTAAAT	GAGTTTTCCAAAAAGATAGATCAATGTAAAC	GTTAGTAGTGATGGTCCAATAATGCCAAA
2B:53467101	2BS	60,567,502	GAATGCATACTTATTGCGGGTTTA	GAATGCATACTTATTGCGGGTTTC	ACACTGTTCGCTTTCGCATA

2B:57674889	2BS	65,211,983	AGAGGAATCCAAGGTCATCCC	AGAGGAATCCAAGGTCATCCA	ATGGTGGATCTTCTAATAGGTACG
2B:770650575	2BL	779,821,067	CAACACCACAATCACCTTCCC	CAACACCACAATCACCTTCGT	ATGTGCTGCGGTACATACGT
2D:638369560	2DL	652,727,251	GCTGGACCACAAAGAACATAGG	GCTGGACCACAAAGAACATAGT	CCTATACATCTTCAGCCACGC
2D:639534738	2DL	651,572,347	GGTAGTCAAGCTTATGATCTTCCTC	GGTAGTCAAGCTTATGATCTTCCTT	CTGACGTGGAAGGACGGG

*Primer sequences do not include tails.

B)

Cycle	PCR Conditions
1	94ºC, 15:00
2	94ºC, 0:20
3	60ºC, 1:00
4	Cycle 2, 49x
5	59ºC, 0:30, -1ºC/cycle
6	Step 5, 34x
7	10ºC, 5:00

Table 3.13. Linkage group formation summary for IWGSCv2.1 and Jagger reference sequences.

Procedure	IWGSCv2.1			Jagger		
	RILs$_A$[*]	**SNPs**	**No. Linkage Groups$_A$**	**RILs$_B$**[**]	**SNPs**	**No. Linkage Groups$_B$**
Form Linkage Groups[1]	162	878	22	162	1246	22
Split Linkage Groups[2]	162	878	69	162	1246	65
Drop Linkage Groups[3]	162	845	43	162	1209	36
Clustering of Markers	162	845	44	162	1209	35
Filtering Double-Crossovers	162	782	44	158	1134	38
Merging Linkage Groups[4]	162	782	36	158	1133	28
Restoration	162	802	36	158	1156	27

[1]Intial linkage groups from reading the unfiltered dataset
[2]Linkage groups split based on maximum recombination frequency = 0.35 and minimum LOD = 6
[3]Linkage groups with less than three markers were removed
[4]Markers were merged together in their respective chromosome group and first clustered at p-value =2. All markers in the genetic map were re-clustered at a more stringent threshold p-value = 1e-06 to split linkage groups.

*IWGSC v2.1 reference map
**Jagger reference map
[†]Number of SNPs for each respective reference map

Table 3.14. Estimated variance of random effects for stripe rust infection type and severity.

	Estimated variance	
Random Effect	**Infection type (1 to 9)**	**Severity (%)**
Rep(Environment)	0.084ns†	13.0ns
Genotype	0.727***	96.1***
Genotype x Environment	0.729***	72.4***
Residual	1.143	141.1

†ns, non-significant; *** designates p-value < 0.001 for Wald test.

Table 3.15. Marker statistics of the linkage maps constructed from Overley x Overland RIL population using the IWGSCv2.1 reference sequence genome.

Linkage Group	SNPs (#)	Length (cM)	Ave. Spacing (cM)	Max Spacing (cM)
Chr. 1A.1	28	143.2	5.3	25.8
Chr. 1A.2	16	73.1	4.9	12.8
Chr. 1B.1	45	182.4	4.1	16.6
Chr. 1B.2	3	10.2	5.1	6.8
Chr. 1D	26	68.6	2.7	20.3
Chr. 2A	76	270.7	3.6	25.2
Chr. 2B.1	17	33.7	2.1	7.1
Chr. 2B.2	64	207.9	3.3	28.0
Chr. 2D.1.1	4	14.6	4.9	8.5
Chr. 2D.1.2	25	134	5.6	16.8
Chr. 2D.2	13	52.8	4.4	24.7
Chr. 3A.1	44	199.5	4.6	20.2
Chr. 3A.2	13	57.7	4.8	9.4
Chr. 3B.1	9	19.8	2.5	3.2
Chr. 3B.2	60	266	4.5	33.5
Chr. 3D	6	5.7	1.1	3.1
Chr. 4A.1	2	37.6	37.6	37.6
Chr. 4A.2	16	125.4	8.4	15.6
Chr. 4A.3	6	21.9	4.4	10.3
Chr. 4B.1	7	35.5	5.9	17.4
Chr. 4B.2	17	103.4	6.5	18.5
Chr. 4D	3	9.4	4.7	5.1
Chr. 5A.1	45	322.4	7.3	26.9
Chr. 5A.2	6	31.1	6.2	8.3
Chr. 5B.1	7	41.4	6.9	11.0
Chr. 5B.2	16	119.4	8.0	17.3

Chr. 5D	7	28.9	4.8	17.5
Chr. 6A	59	282.4	4.9	22.2
Chr. 6B	58	179.1	3.1	13.1
Chr. 6D	3	28.4	14.2	28.4
Chr. 7A	39	210.3	5.5	18.2
Chr. 7B.1	28	118.9	4.4	14.3
Chr. 7B.1.2	19	97.7	5.4	20.6
Chr. 7D.1	7	21.2	3.5	4.7
Chr. 7D.1.2	8	59.1	8.4	24.8
Overall	**802**	**3613.2**	**4.7**	**37.6**

Table 3.16. Marker statistics of the linkage maps constructed from Overley x Overland RIL population using the Jagger reference sequence genome.

Linkage Group	SNPs (#)	Length (cM)	Avg. Spacing (cM)	Max Spacing (cM)
Chr. 1A	79	256.7	3.3	27.2
Chr. 1. B.1	56	179.5	3.3	19.6
Chr. 1. B.2	5	26.3	6.6	15.3
Chr. 1D.1	38	97.2	2.6	23.1
Chr. 1D.2	4	4.1	1.4	2.2
Chr. 2A.1	121	249.5	2.1	19.2
Chr. 2B	106	277.7	2.6	43.4
Chr. 2D.1	40	221.9	5.7	23.9
Chr. 2. D.2	14	44	3.4	24.9
Chr. 3A	68	295.8	4.4	52
Chr. 3B.1	88	289.7	3.3	23.5
Chr. 3B.2	11	14.3	1.4	2.2
Chr. 3D	9	10.6	1.3	2.9
Chr. 4A	40	245.2	6.3	22.2
Chr. 4B	25	156.8	6.5	20.5
Chr. 5A	83	397	4.8	25.2
Chr. 5B.1	13	48.8	4.1	10.9
Chr. 5B.2	28	132	4.9	14.4
Chr. 5D	11	39.2	3.9	16
Chr. 6A	78	269.5	3.5	20.7
Chr. 6B	80	168.2	2.1	10.5
Chr. 6D	7	38.1	6.3	9.4
Chr. 7A	60	230.1	3.9	17.3
Chr. 7B.1	46	119.1	2.6	11
Chr. 7B.2	30	121.7	4.2	16.3
Chr. 7D.1	7	14.3	2.4	4.9

Chr. 7D.2	9	34.8	4.4	10
Overall	**1156**	**3981.9**	**3.5**	**52**

Table 3.17. QTLs identified for stripe rust disease responses using multi-location best linear unbiased predictors (ML-BLUP) for Jagger.

The LOD thresholds are based on permutation tests 1000x and α = 0.05 for IT = 3.59 and SEV = 3.36 using the Jagger map. Abbreviations are LOD = log odds ratio; PVE = percentage of variance explained; A = Additive Effect; C.I. = Confidence interval (cM).

QTL	Response	Chr.	Marker Interval	LOD	PVE (%)	A	P.A.[1]	C.I.
QYr.hwwgIT–2A$_b$	IT	2AS	S2A_20860853 – S2A_6690360	9.58	14.88	-0.32 Score	OY	12.5 – 14.5
QYr.hwwgSEV–2A$_b$	SEV	2AS	S2A_20860853 – S2A_6690360	14.98	26.52	-4.67%	OY	12.5 – 14.5
QYr.hwwgIT–2B.1$_a$	IT	2BS	SUN_24253245 – S2B_70479277	7.04	11.04	0.28 Score	OD	110.5 –116.5
QYr.hwwgSEV–2B.1$_a$	SEV	2BS	SUN_24253245 – S2B_70479277	3.54	5.28	2.08%	OD	111.5 – 116.5
QYr.hwwgSEV–2B.2$_b$	SEV	2BL	S2B_767134652 – S2B_770782296	4.91	7.52	-2.49%	OY	246.5 – 248.5
QYr.hwwgIT–2D$_b$	IT	2DL	S2D_665681641 – S2D_666306598	10.9	18.6	0.36 Score	OD	36.5 – 43
QYr.hwwgSEV–2D$_b$	SEV	2DL	S2D_665681641 – S2D_666306598	8.49	14.68	3.49%	OD	32.5 – 43

[1]Favorable parental allele contributing to resistance; OY = Overley OD = Overland.
*Additive effect of the Overley allele.

Figure 3.6. Linkage maps of the Jagger map using ML-BLUPs for stripe rust infection type and severity.
Linkage maps of chromosome group 2 (2A, 2B, and 2D) using the Jagger map showing QTL peaks for A) IT and B) SEV using multi-location BLUPs (ML-BLUP).

A.) Stripe rust infection type, Jagger map

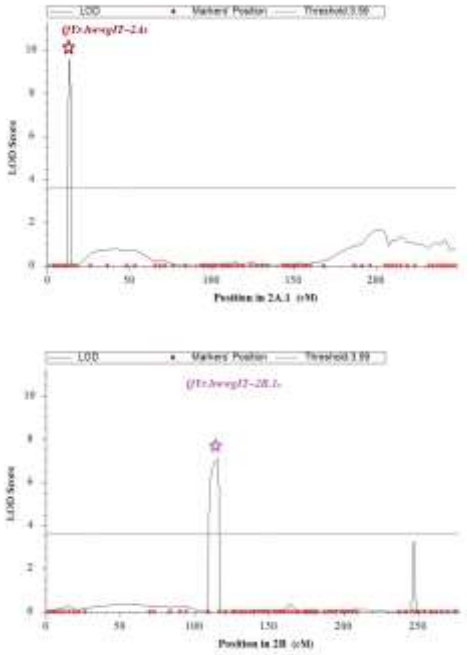

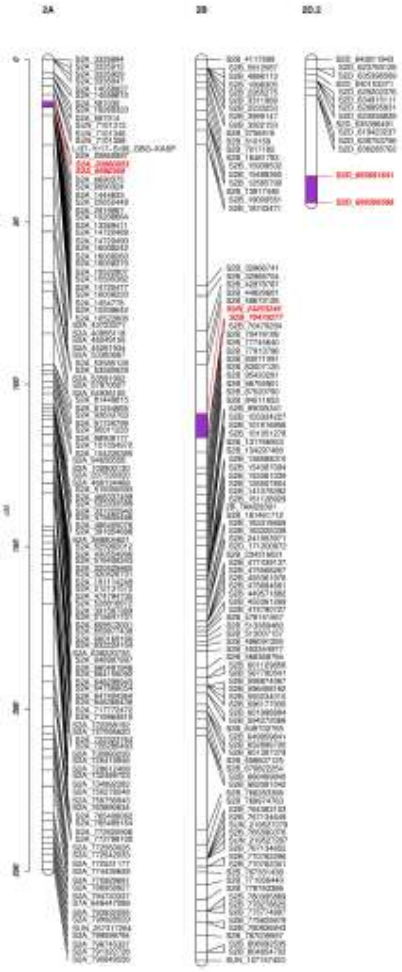

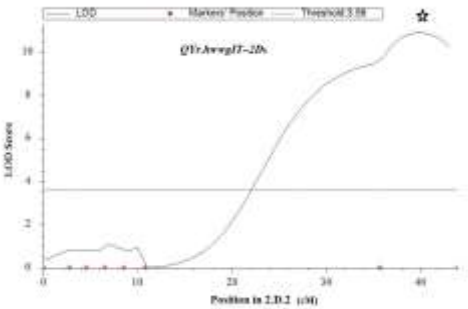

B.) Stripe rust severity, Jagger map

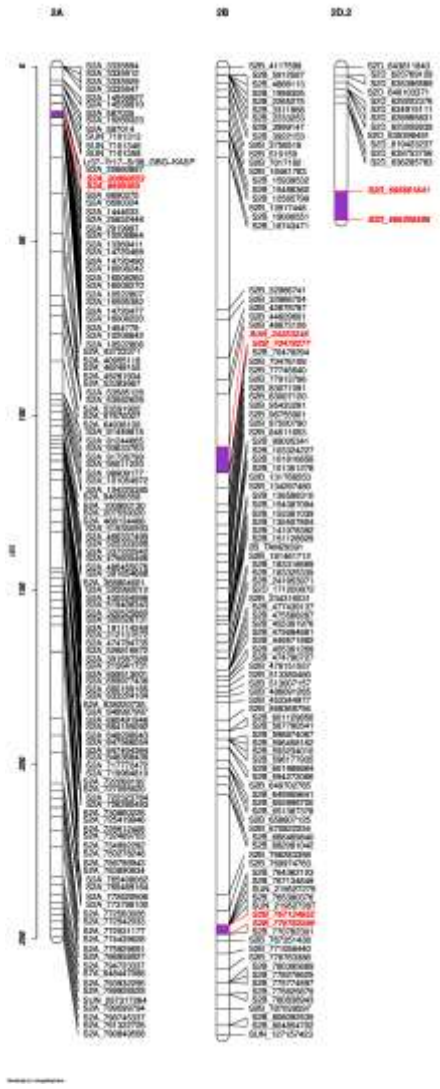
2A
2B
2D.2

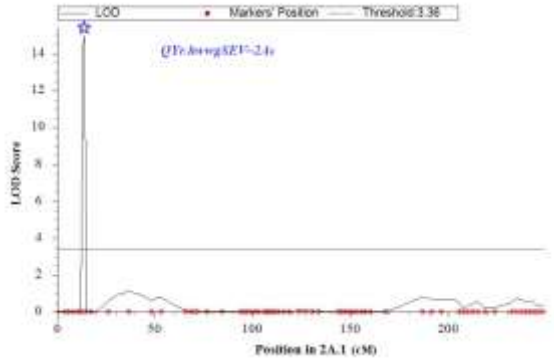
LOD
Markers' Position
Threshold:3.36
QTr.bwwgSEV-2A.1
LOD Score
Position in 2A.1 (cM)

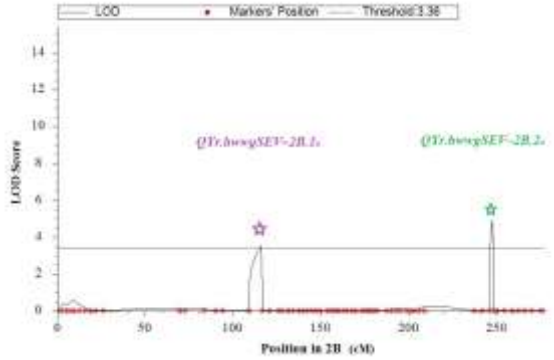
LOD
Markers' Position
Threshold:3.36
QTr.bwwgSEV-2B.1
QTr.bwwgSEV-2B.2
LOD Score
Position in 2B (cM)

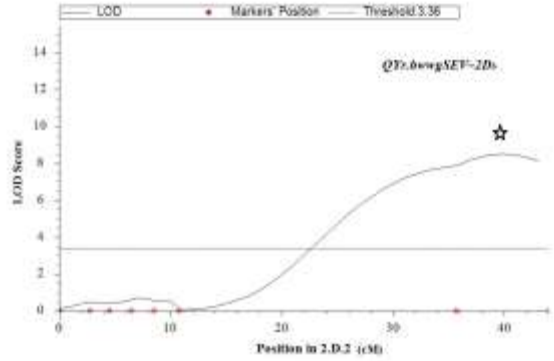
LOD
Markers' Position
Threshold:3.36
QTr.bwwgSEV-2D.2
LOD Score
Position in 2.D.2 (cM)

Table 3.18. QTLs identified using the multi-environment trial (MET)-QTL analysis across multiple environments using the Jagger reference map for stripe rust infection type and severity.

List of QTLs identified using the multi-environment trial (MET)-QTL analysis based on permutation LOD: IT (6.64) & SEV (6.41) for best linear unbiased predictors for stripe rust infection type (IT) and severity (SEV) in each of seven trials using the Jagger reference-derived map. Resp. = Response of disease trait, LOD = log odds ratio; PVE = percentage of variance explained. A = additive (main) effect of genotype, A × E = additive effect × environment interaction; C.I. = Confidence interval (cM).

QTL Name	*Resp.	Chr.	QTL Marker Interval	LOD	PVE (%)	PVE[1]	PVE[2]	A[3]	P.A.[4]	C.I.
QYr.hwwgIT–2A$_b$	IT	2AS	S2A_20860853 – S2A_6690360	35.1	15.97	7.1	8.9	-0.22 score	OY	13.5 – 14.5
QYr.hwwgSEV–2A$_b$	SEV	2AS	S2A_20860853 – S2A_6690360	19.5	5.31	2.1	3.2	-1.19%	OY	12.5 – 14.5
QYr.hwwgIT–2B.1$_a$	IT	2BS	SUN_24253245 – S2B_70479277	28.5	13.65	11.1	2.6	0.28 score	OD	114.5 –116.5
QYr.hwwgSEV–2B.2$_a$	SEV	2BL	S2B_769974763 – S2B_764362103	12.8	6.79	2.8	4.0	-1.37%	OY	243.5 – 246.5
QYr.hwwgIT–2D$_b$	IT	2DL	S2D_665681641 – S2D_666306598	51.5	21.54	20.8	0.8	0.38 score	OD	37.5 – 41.5
QYr.hwwgSEV–2D$_b$	SEV	2DL	S2D_665681641 – S2D_666306598	36.4	19.11	16.9	2.2	3.40%	OD	37.5 – 43
QYr.hwwgSEV–2A$_c$	SEV	2AS	S2A_3335947 – S2A_14558827	30.7	26.94	10.5	16.5	-2.65%	OY	2.5 – 3.5

[1]PVE due to additive effect of the Overley allele

[2]PVE due to A x E interaction

[3]Additive effect of the Overley allele

[4]Favorable parental allele contributing to resistance; OY = Overley OD = Overland.

Figure 3.7. Linkage maps of Jagger showing QTL peaks for IT and SEV across multiple environments.

A) Stripe rust infection type

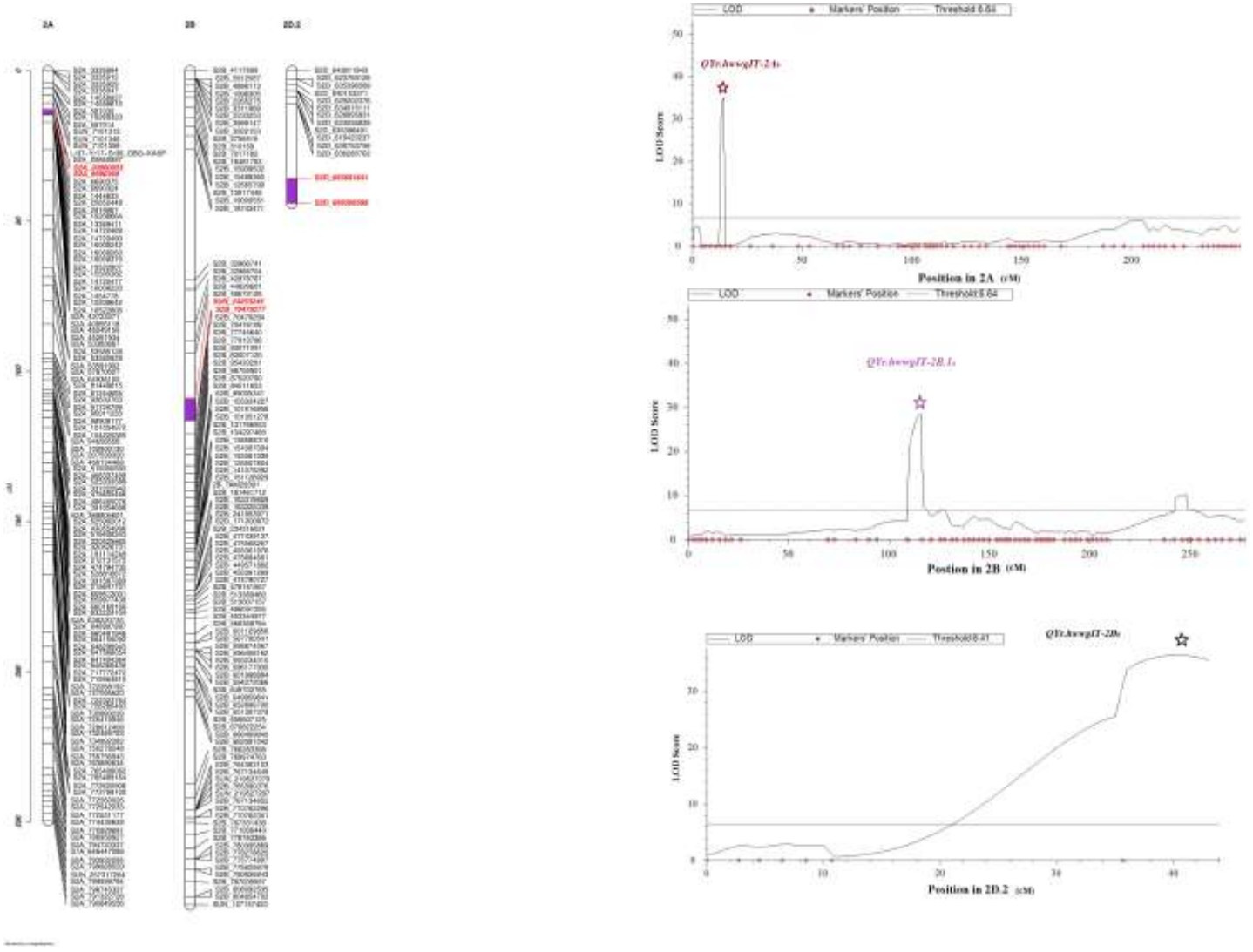

B) Stripe rust severity

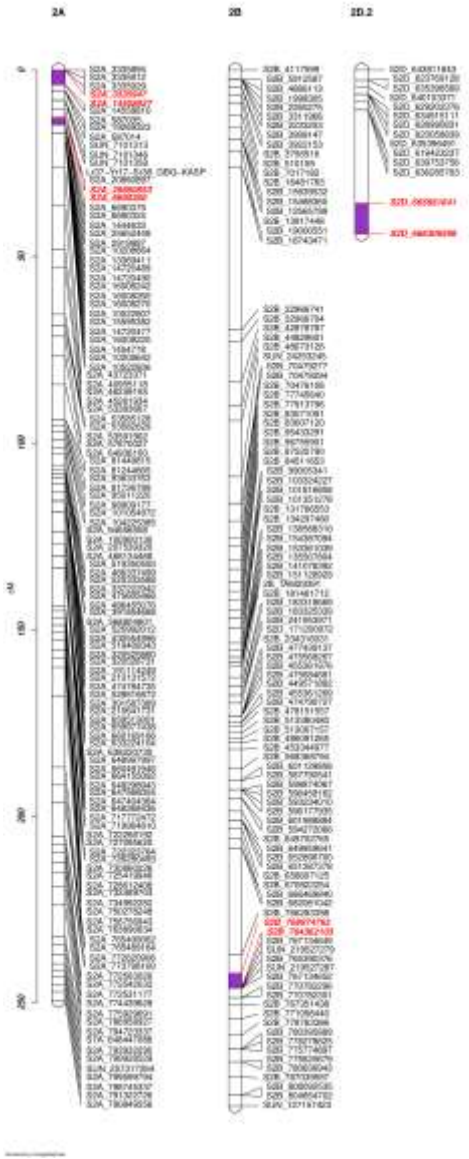

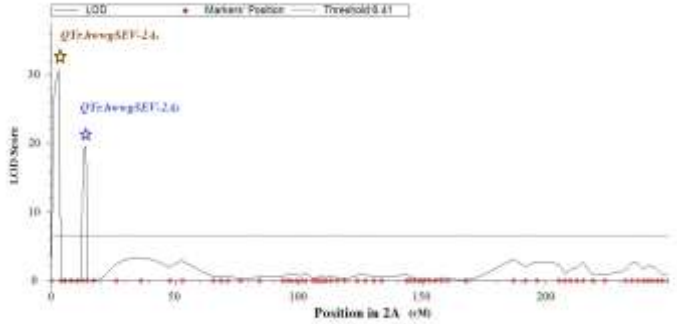

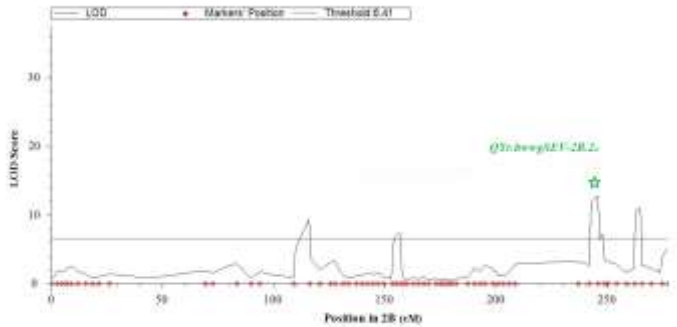

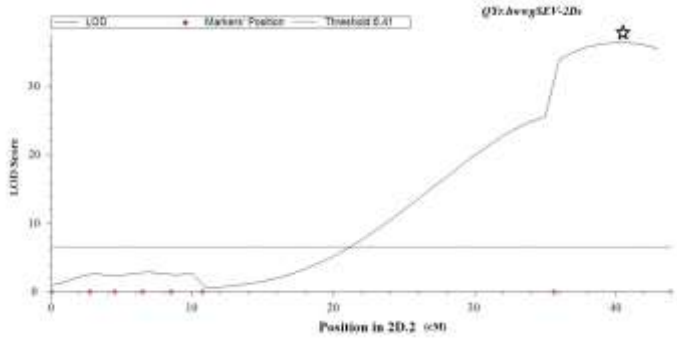

Table 3.19. AX E effects for stripe rust resistance across locations using the Jagger reference map.
The A x E effects for IT and SEV resistance across locations associated with QTLs on the Jagger reference map from MET analysis, from Table 1.5 and Table 3.18. C.I. =Confidence interval (cM).

				A x E							
QTL Name	**Chr.**	**Unit**	**A**	**CF19**	**CF20**	**HZ19**	**PL19**	**PL20**	**RS18**	**RS19**	**P.A.[1]**
QYr.hwwgIT–2A$_b$	2AS	score	-0.22	0.22	0.17	-0.08	-0.28	0.20	0.21	0.43	OY
QYr.hwwgSEV–2A$_c$	2AS	percent	-2.65	-2.75	-0.91	2.49	2.49	-6.56	2.72	2.52	OY
QYr.hwwgIT–2B.1$_a$	2BS	score	0.28	-0.08	-0.12	-0.0001	-0.10	-0.11	0.16	0.24	OD
QYr.hwwgSEV–2B.2$_a$	2BL	percent	-1.37	1.36	-0.61	1.10	1.10	-0.93	-3.38	1.36	OY
QYr.hwwgIT–2D$_b$	2DL	score	0.38	-0.14	-0.06	-0.01	0.02	0.04	0.12	0.02	OD
QYr.hwwgSEV–2D$_b$	2DL	percent	3.40	-1.12	0.57	-0.45	-0.45	2.54	0.34	-1.43	OD

[1]Favorable parental allele contributing to resistance; OY = Overley OD = Overland
*Additive effect of the Overley allele.

Appendix B - Supplemental Data Chapter 3

Figure 3.8. Distributions of best linear unbiased predictors (BLUPs) for additional yield and yield components in the Overley x Overland RIL population were measured in Ashland (2018 and 2019) and in Hays (2019).
Traits measured are A) PMAT, B) FT, C) TGW D) PHT. Multi-environmental trials indicate a comprehensive average across all trials. The parental means are colored green (Overley) and blue (Overland).

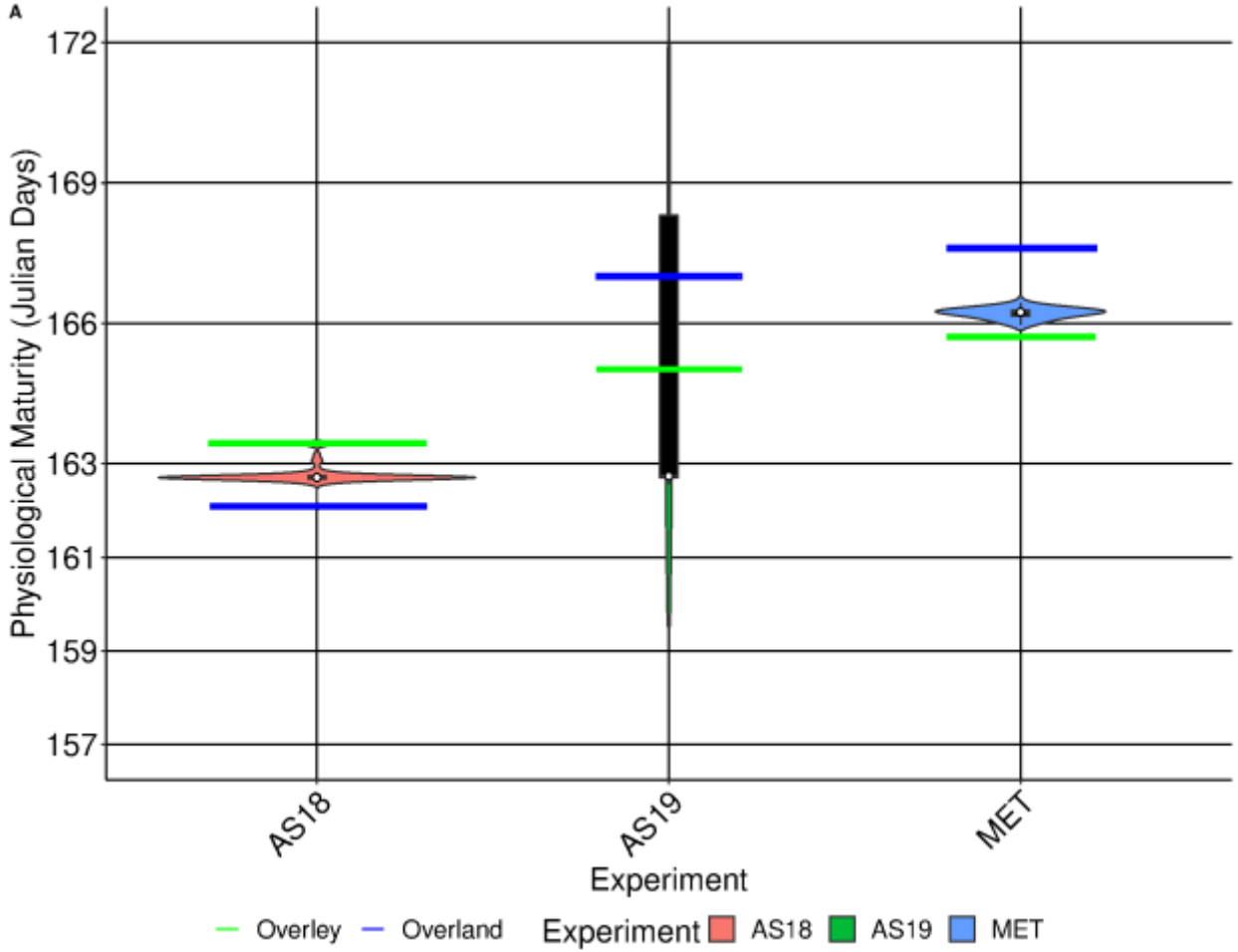

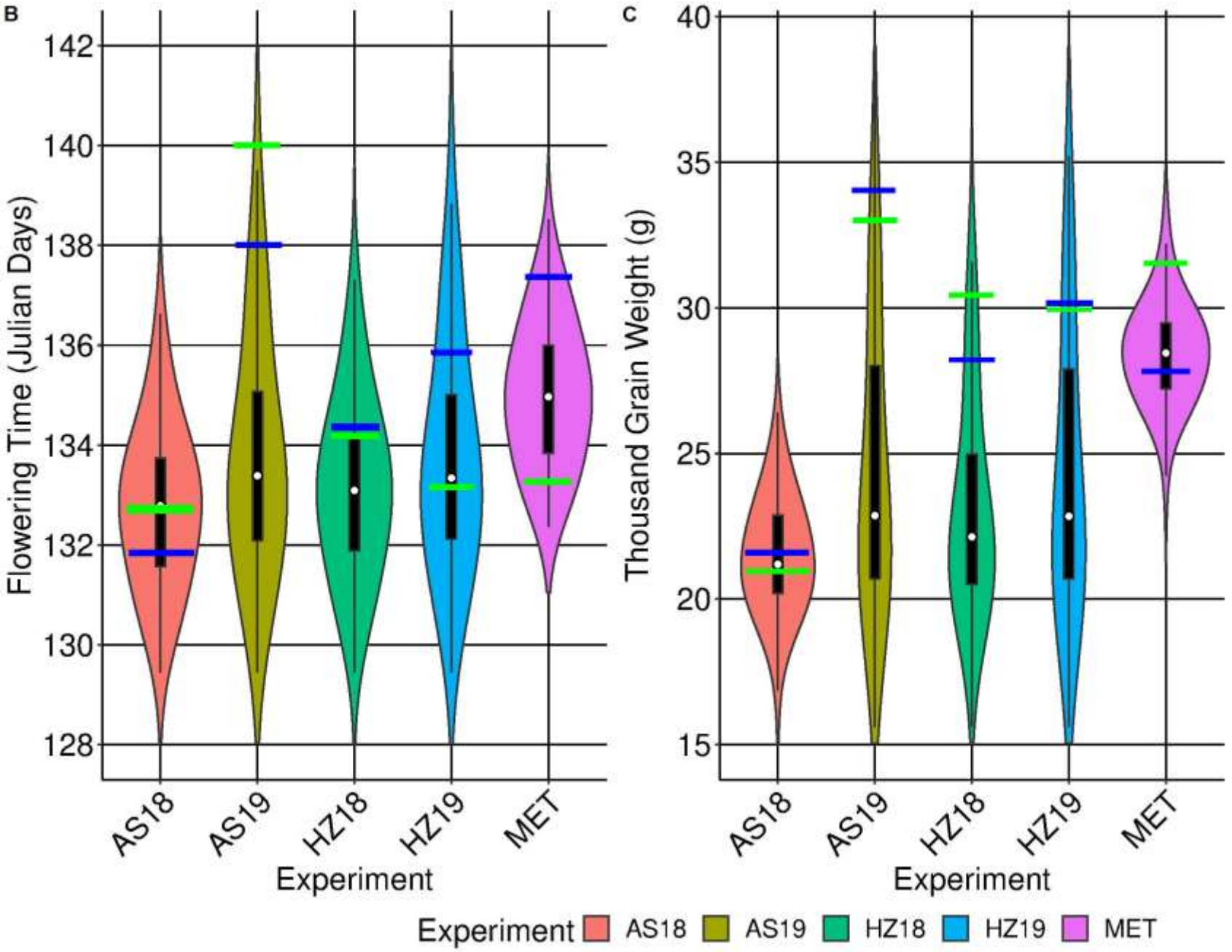
B
Flowering Time (Julian Days)
142
140
138
136
134
132
130
128
AS18
AS19
HZ18
HZ19
MET
Experiment
C
Thousand Grain Weight (g)
40
35
30
25
20
15
AS18
AS19
HZ18
HZ19
MET
Experiment
Experiment AS18 AS19 HZ18 HZ19 MET

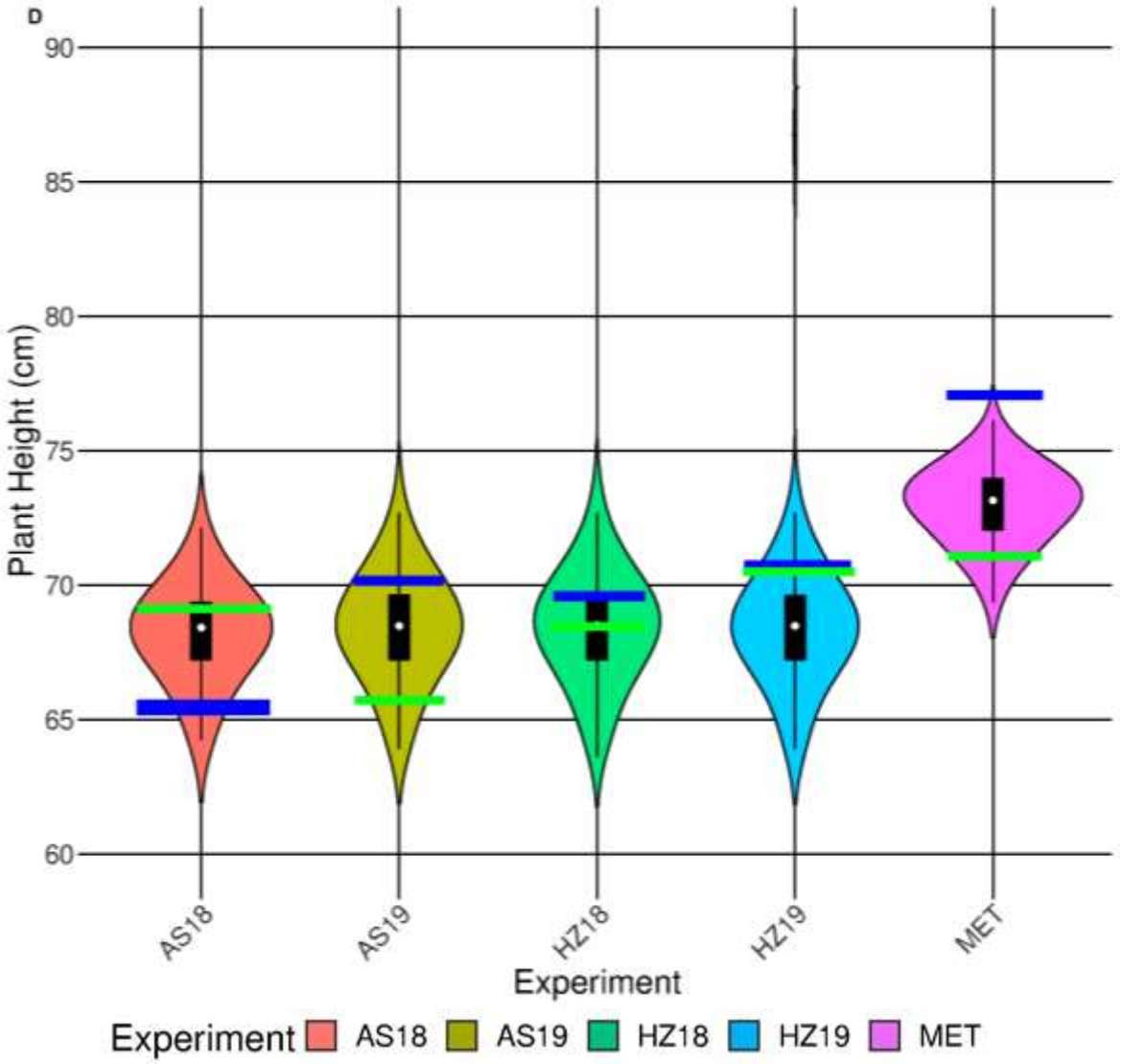
D
90
85
80
75
70
65
60
Plant Height (cm)
AS18
AS19
HZ18
HZ19
MET
Experiment
Experiment AS18 AS19 HZ18 HZ19 MET